Université de Lille

SCIENCES AND TECHNOLOGIES FACULTY

Doctoral School **ED SMRE**

Laboratory: **Unity of Catalysis and Solid State Chemistry**

THESIS

Defended by

Mayerly Juliana APARICIO QUINONEZ

In order to become a Doctor of the University Lille, Sciences and Technology

Academic Field **Molecules and Condensed Matter**

Speciality **Process Engineering**

Kinetic and thermodynamic study for the development of a separation process for acid products of glycerol oxidation via reactive distillation

Thesis supervised by: **Dr. HDR. Mickaël CAPRON** Director

Dr. Marcia ARAQUE Co-Supervisor

Thesis planned to be defended the 27th of November before the Committee Members:

Referees	Patrick COGNET	Professor at the INP-ENSIACET
	Álvaro ORJUELA	Professor at National University of Colombia.
Examiners	Pascal FONGARLAND	Professor at the Claude Bernard University Lyon 1
	Carole LAMONIER	Professor at the University Lille
	David EDOUARD	Associate professor at the Claude Bernard University Lyon 1
	Clémence NIKITINE	Associate professor at the Claude Bernard University Lyon 1
	Jérôme LE NÔTRE	R&D responsible SAS PIVERT

Université de Lille

FACULTÉ DES SCIENCES ET TECHNOLOGIES

École doctorale **ED SMRE**

Unité de recherche **Unité de Catalyse et Chimie du Solide**

THÈSE

Présentée par

Mayerly Juliana APARICIO QUINONEZ

En vue de l'obtention du grade de docteur de l'Université Lille

Discipline **Molécules et Matière Condensée**

Spécialité **Génie des procédés**

Étude cinétique et thermodynamique pour le développement d'un procédé de séparation des acides issus de l'oxydation du glycérol par distillation réactive

Thèse dirigée par :	**Dr. HDR. Mickaël CAPRON**	Directeur
	Dr. Marcia Araque	Co-Encadrante

La soutenance de la thèse est prévue le 27 Novembre 2019 devant le jury composé de :

Rapporteurs	Patrick COGNET	Professeur à INP-ENSIACET
	Álvaro ORJUELA	Professeur à l'Université nationale de Colombie
Examinateurs	Pascal FONGARLAND	Professeur à l'Université Claude Bernard Lyon 1
	Carole LAMONIER	Professeur à l'Université Lille
	David EDOUARD	Maître de conférences à l'Université Claude Bernard Lyon 1
	Clémence NIKITINE	Maître de conférences à l'Université Claude Bernard Lyon 1
	Jérôme LE NÔTRE	Responsable Recherche SAS PIVERT

It is my genuine gratefulness and warmest regard that to dedicate this work God Almighty, my creator and the source of my knowledge and understanding and to my strong pillar, my source of inspiration, wisdom and my biggest treasure the Aparicio Quinonez family.

Acknowledgment

Firstly, I would like to thank SAS PIVERT society and the CNRS for financing this work, LGPC LYON for being a great copartner in this in this investigation project group, Ester&Cat^2, and to the UCCS laboratory for welcome me since my very first time in France.

I would like to show especial gratitude to Prof. Mickael Capron for the continuous support of my Ph.D study and my hole research career, for his patience, motivation, all the good times and laughs together and for adopting me as a daughter and, I could not have imagined having a better advisor and mentor for my Ph.D. I would like to express my sincere gratitude to Dr. Marcia Araque whose expertise was invaluable in the formulating of the research and who always offered me a great support in the roughest moments and for that I will be grateful for the rest of my life. I would also like to Prof. Pascal Fongarland for his unconditional emotional support, guidance, motivation and trust and during this process and to Prof. Paola Maradei who was the first to believe in me, for being my role model and to whom I owe all my achievements.

My sincere thanks to Dr. Clemence and Prof. Adlane for their excellent cooperation, advice and guidance and with whom I managed to have scientific discussions which incented me to widen my research from various perspectives. Also, I would like to acknowledge Celine and Johan and in general to all my laboratory colleagues, for their wonderful collaboration and constant will to help, specially to Barbara, David, Sandrine, Olivier and Daniel for their kindness.

Finally, I would like to thank my family especially to my parents for their wise counsel, unconditional love, for having me constantly in their prayers and thoughts and for taking me back to Colombia every night with their calls. Last but not the least I want to show my gratitude to the people that became my extended family, my friends Anita, Carmen, Kifah, Laura, Mirella, Pedro, and Robert who were my biggest support giving me days and nights of fun, laughs and good times that I will keep in my heart wherever I go, thanks for all your encouragement!

Abstract

Several biomass conversion routes have been studied recently in order to obtain high value chemicals that ensure the long term sustainable management of carbon resources. In this context, glycerol oxidation reaction has been developed leading to selective catalysts and optimum conditions for the production of carboxylic acids such as glycolic, formic and glyceric. These organic acids derivatives have huge economic potential in the chemical field, mainly as precursors for synthesizing a variety of valuable chemicals. However, the carboxylic acids are produced in highly diluted mixtures, therefore the challenge is associated with the recovery and purification resulting in high production costs, polymerization and thermal degradation as some of the main problems. Several alternative separation processes have been proposed to overcome those problems. The protection of acid function by esterification reaction is one of the most promising alternatives through the reactive distillation in a divided wall column (RDWC), as one of the most promising alternatives in process intensification, allowing the removal of water and several acids simultaneously. RDWC requires accurate kinetic and thermodynamic information about multicomponent phase equilibrium in the reactive mixture for process design. To determine the viability of the technology, three alcohols were chosen: propanol, butanol and octanol. The glycolic acid was chosen as a representative acid of the mixture. The binary parameters of the existing couples in the three systems were determined. The NRTL model was selected as the most suitable to represent the binary behavior. The three systems were studied in the presence of homogeneous and heterogeneous catalyst. The kinetic study showed that the models based on Langmuir-Hinshelwood (L-H) and Eley-Rideal (E-R) adsorption were able to describe the kinetic behavior of the different systems. The LH demonstrated to be the most suitable one for propanol system whereas for the butanol and octanol systems it was the ER model. In the study to decrease the amount of water from the mixture prior to the acidification process it was found that the water can be reduced by up to 60% by distillation without affecting the acids. Additionally, the study to reduce the amount of water in the initial mixture prior to the acidification process showed that the amount of water can be reduced by up to 60% by simple distillation without affecting the acids present. Finally, a preliminary simulation of the reactive distillation process to determine its viability in terms of energy consumption it was carried out.

Key words: Kinetic, Thermodynamic, Reactive distillation, Process intensification, and glycolic acid.

..

Resumé

Plusieurs voies de conversion de la biomasse ont été étudiées récemment afin d'obtenir des produits chimiques à haute valeur ajoutée qui assurent la gestion durable à long terme des ressources en carbone. Dans ce contexte, la réaction d'oxydation du glycérol a été mise au point, conduisant à des catalyseurs sélectifs et à des conditions optimales pour la production d'acides carboxyliques tels que les acides glycoliques, formiques et glycériques. Les dérivés de ces acides organiques ont un énorme potentiel économique dans le domaine chimique, principalement en tant que précurseurs pour la synthèse d'une variété de produits chimiques stratégiques. Cependant, les acides carboxyliques sus mentionnés sont produits dans des mélanges fortement dilués. Le défi est donc associé à la récupération et à la purification, ce qui entraîne des coûts de production élevés. La polymérisation des produits entre eux et la dégradation thermique sont les principaux problèmes rencontrés. Plusieurs procédés de séparation ont été proposés pour surmonter ces problèmes. La protection de la fonction acide par réaction d'estérification est l'une des alternatives les plus prometteuses. Une fois intégrée au sein d'une distillation réactive dans une colonne à parois divisées (RDWC) par ex, cela représente une des alternatives les plus prometteuses dans l'intensification du procédé, permettant simultanément la récupération de plusieurs acides et l'élimination de l'eau. RDWC exige des informations cinétiques et thermodynamiques précises sur l'équilibre de phases multicomposantes dans le mélange réactif pour la conception du procédé. Pour déterminer la viabilité de la technologie, trois alcools ont été choisis : le propanol, le butanol et l'octanol. L'acide glycolique a été choisi comme acide représentatif du mélange car il peut être obtenu avec une sélectivité importante en utilisant des catalyseurs à base d'argent et qu'il présente un intérêt grandissant dans des domaines liés à l'industrie cosmétique. Les paramètres binaires des couples existants dans les trois systèmes ont été déterminés. Le modèle NRTL a été choisi comme étant le plus approprié pour représenter le comportement binaire. L'étude cinétique des trois systèmes en présence d'une catalyse homogène et hétérogène a également été réalisée. Les modèles cinétiques basés sur l'adsorption de Langmuir-Hinshelwood (L-H) et Eley-Rideal (E-R) ont permis de décrire le comportement cinétique des différents systèmes, L-H pour le système propanol et E-R pour les systèmes butanol et octanol. L'étude supplémentaire visant à réduire la quantité d'eau dans le mélange initial avant le processus d'acidification a montré que la quantité d'eau peut être réduite jusqu'à 60% par simple distillation sans affecter les acides présents. La dernière étape consistait en une simulation préliminaire du procédé de distillation réactive pour déterminer sa viabilité en termes de consommation d'énergie et de procédé.

Mots clés : Cinétique, Thermodynamique, Distillation réactive et intensification des processus.

Summary

Table index

Figure index

INTRODUCTION

Glycerol is usually used as an additive or as a raw material in a wide range of processes including the production of food additives, tobacco, pharmaceuticals, synthesis of trinitroglycerin, alkyd resins and polyurethanes. It is also used in the manufacture of lacquers, varnishes, inks, adhesives, synthetic plastics, regenerated cellulose, explosives and other diverse industrial products. Glycerol also is increasingly used as a substitute for propylene glycol [1].

Despite the versatility, new pathways for glycerol uses are being proposed, given the excess of glycerol available from the biodiesel production. Catalytic conversion processes are being carried out targeting the production of high value compounds with important applications in the industry. The processes developed so far can be divided into the following reactions: carboxylation, etherification, transesterification, esterification, pyrolysis, hydrolysis and oxidation [2]. The products obtained from the aforementioned reactions are of particular interest due to the commercial relevance of the oxygenated glycerol derivatives. During the last decades, different oxidation routes for glycerol have been explored, including chemical, electrochemical and biological [4].

Glycerol oxidation has been studied in our laboratory, UCCS, leading to selective catalysts and optimum conditions for the production of several carboxylic acids such as glycolic, tartronic and glyceric acid in dilute mixtures. These organic acids are of high interest for their applications, mainly as precursors for synthesizing a variety of valuable chemical derivatives *via* different chemical conversion pathways. Silver-based catalysts have been shown to be more selective to form glycolic acid, differentiating silver catalysts from other noble metals conventionally used in the oxidation of glycerol, such as Au, Pd and Pt, normally characterized by high glyceric acid selectivity. The production of the acids is carried out in a basic and highly diluted medium. The products of the reaction are obtained in salt form, thus an intermediate stage of acidification between the oxidation reaction and separation process should be included in order to convert them into acid form.

Nowadays, the production challenge of carboxylic acids, either by the biological or chemical route, is associated to the challenge involved in their separation and purification. The main problems with these steps are related to high purification costs, polymerization, thermal degradation of the

acids and water content usually higher than 90 wt%. Therefore, it is important before industrialization of the process to develop a purification technology that will require less energy to be both environmentally and economically attractive [2-7].

Conventional well-practiced physical separation methods are distillation and extraction; however, they present several drawbacks. For dilute aqueous streams, not only is distillation difficult and costly, the boiling points of the obtained acids are similar and only slightly higher than that of water. Separation *via* extraction is limited by phase separation and distribution of the components involved in the reacting system [8]. Therefore, the costs associated with products recovery, concentration and purification account for 60-70% of the product cost, making these chemical technologies impractical [7]. In the chemical industry, it is well known that conventional distillation systems are energy inefficient. Over the past few years, distillation research has focused on improving distillation efficiency and thus reducing operating costs. In our case, for dilute aqueous streams, not only is distillation difficult and costly, the boiling points of the obtained acids are similar and only slightly higher than the one of water. Separation *via* extraction is limited by phase separation and distribution of the components involved in the reacting system [8]. In view of these constraints, it is appropriate to explore alternative methods that allow the elimination of water while maintaining the integrity of the acids.

Several separation technologies are currently available which make the recovery and purification of carboxylic acids possible. These methods can be classified into three major categories: membrane processes, adsorption processes and chemical processes. However, the application of most of these technologies are limited to solutions containing only carboxylic acids. Membrane technology has emerged as one of the most sustainable separation processes, allowing selective permeation of a component from a multi-component mixture. Membrane processes like reverse osmosis, electrodialysis and filtration (nanofiltration and microfiltration) are currently being used for the recovery of carboxylic acids [2,7,9,10]. The adsorption technology is a simple technique with an electrostatic mechanism [11], in which the surface area and chemical nature of the adsorbent play an important role in acid recovery [8]. Chemical processes include distillation and conventional extraction.

However, the implementation of these technologies at the industrial level implies a challenge in terms of economic and technical feasibility. From these needs and limitations, the concept of

process intensification was created, aiming to improve the chemical processes in terms of energy efficiency, safety, cleanliness and economic profitability of the process. The strategies of process intensification consist of combining different operations in a single unit, its implementation allows cheaper processes, smaller equipment, safer process, lower energy consumption, reduction of waste or sub-products and better image of the company [4].

Within the range of existing chemical processes, an emergent technology has appeared where the reaction and separation occur in a single unit, also known as reactive separation. Several unit separation operations such as the distillation and extraction can be combined with the reaction step (Reactive Distillation and Reactive Extraction). Generally, when the reaction is combined with a separation step, the separation is improved by the reaction through improved mass transfer rates or, conversely, the separation drives the reaction at high conversions and/or selectivity. In addition, the combination of reaction and separation in a single operation is also appreciated for its simplicity and novelty, which results in saving in investment and operating costs obtained on a successful scale, right up to commercial operations [8,12].

Hence, this work focuses on the efficient implementation of separation technologies which are cost-effective and environmentally friendly in reducing the initial water content before the implementation of more complex technologies for the separation of acids. The implementation of the strategy of separation and reaction in a single unit has high potentials. Although reactive distillation is a good option in this case. The reactive distillation in a divided wall column is even more attractive since it considers two stages of separation and one of reaction, allowing a better separation and at the same time lowering production costs [5].

The present thesis is in the frame of a global project financially supported by the PIVERT SAS company that seeks to implement the glycerol oxidation process at industrial level. The previous part consisted in the development of the catalyst and reaction systems, the second one should address the separation and purification of the acids produced. For this reason, the aim of this work is to develop a methodology for purification and recovery of the carboxylic acids from the diluted mixture. This will be based on selective esterification through the application of reactive dividing wall column and allowing combination of reaction and separation in a single unit (see Figure 1).

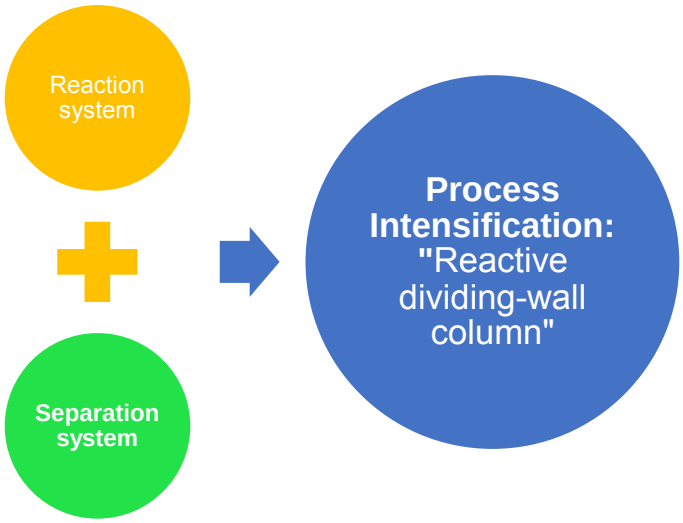

Figure 1. Process intensification strategy

In this work, the esterification reaction was studied for glycolic and formic acids using propanol, butanol and octanol, alcohols that can be obtained from bio routes [6]. Preliminary tests were performed with glycolic acid where the reaction was first carried out using H_2SO_4 as a bench mark and then a selection amongst Amberlyst 15, Amberlyst 16, Amberlyst 36, Dowex and Nafion as heterogeneous catalyst. For the studied systems, a kinetic study was also carried out to determine the suitable alcohol for the esterification reaction. For the chosen acid-alcohol system, a complete thermodynamic analysis is proposed, the corresponding parameters for the phase equilibria models were correlated in Aspen Plus®

In parallel, different water removal strategies were studied in order to minimize the energy consumption of the reactive divided wall column. Different process alternatives were evaluated: vacuum distillation, atmospheric distillation, crystallization and liquid-liquid extraction.

The last part consisted of evaluation by simulation of the implementation of the reaction system for reactive divided wall columns. In order to achieve this, a classical design method is used presented by Amminudin *et al.* [7]. The study considered the feasibility of the technology in the three proposed scenarios (*e.g.* propanol, butanol and octanol).

Chapter 1. STATE OF THE ART

1.1 Glycerol valorization via selective oxidation

The selective oxidation of glycerol using heterogeneous catalysis is one of the most promising routes considering the easy execution and implementation. The operating conditions required are mild, generally proceeding at temperatures below 100°C under moderate pressures, oxygen or air, between 1 and 10 bar. Given the reacting potential of the three hydroxyl groups of glycerol, the economic importance of this reaction is based on the wide range of interesting products which can be obtained such as 1,3-dihydroxyacetone, hydroxypiruvic acid, glyceric acid, tartronic acid, glycolic acid, mesoxalic acid and oxalic acid. Special interest was focused on the production of 1,3-dihydroxyacetone and glyceric acid, where Pt, Pd and Au catalysts have shown the best performances. As a support, carbon was mainly used in different structures such as activated carbon, graphite, nanofibers [2-4]. Studies have shown that factors such as particle size, the type of support and its porosity affect the performance of the reaction.[8] The pH is a key parameter in the reaction selectivity, *i.e.* in acidic conditions the oxidation of the secondary hydroxyl group is promoted, inclining the selectivity towards hydroxyacetone and hydroxypyruvic acid whereas under basic conditions, the glyceric acid is often the predominant product [9].

The main drawback of this type of catalysts is the high cost, due to the noble metals presence, catalytic deactivation and fluctuating selectivity. Recently, research has been oriented towards the use of catalysts with active phases such as Ag and Cu, which are readily available and resistant to deactivation. These new catalysts are selective towards glycolic, formic and tartronic acid, compounds which have received little attention as target products so far [7-8].

1.1.1 Selective oxidation of glycerol to glycolic acid

Most of the studies on selective oxidation of glycerol consider glycolic acid as a secondary product, a step which should be avoided. However, in recent years the applications (hence the economic potential) of glycolic acid have increased. The molecule has two functionalities: an alcohol group and a moderately strong acid group. These qualities make the glycolic acid perfect for a wide range of applications, for example, in the pharmaceutical industry, skin care products, the food industry -as a flavoring agent and preservative-, in adhesives and plastics and in the textile industry as dyeing and in organic synthesis [9-10]. Jiang *et al*. [12] presented an application for glycolic acid esters in the oil and gas industry, where they showed that glycolic acid esters have

great potential as bifunctional additives in the gasoline and methanol mixtures, since they function as phase stabilizers and vapor pressure depressors.

The current synthetic preparation of glycolic acid is generally carried out from chloroacetic acid or from formaldehyde hydrocyanation [13]. In biological synthesis, it can be produced from ethylene glycol by oxidation or glycolonitrile by hydrolysis using a variety of microorganisms. Chemolytotrophic iron oxidizing bacteria and sulphide were also used to produce glycolate. However, the previous methods required expensive and highly polluting precursors [14].

Table 1-1 presents a summary of glycerol oxidation studies using heterogeneous catalyst, which consider glycolic acid within the desired products. The most selective catalysts towards the production of glycolic acid are those reported by Skrzynska *et al.* [10] and Schünemann *et al.* [15] using as active phase Ag and Cu, respectively. In both cases, Al_2O_3 was used as support. Bianchi *et al.* [9] present a type of catalyst with high performance but one that involves metals such as Pt and Au which are easily deactivated. The work developed until now support the possibility of improvement in glycerol oxidation and aims towards greater production of glycolic acid.

Table 1-2. Catalyst and their catalytic performance in glycerol oxidation to glycolic acid reported since 2005

Catalyst	Glycerol [M]	Oxidant	NaOH/ glycerol	X [%]	S_{GlycA} [%]	S_{GlyA} [%]	S_{TartA} [%]	Researchs and year	Ref
1%Pd/C	0.3	3 bar O_2	4	100 (50°C)	26.9	21.4	38.7	Bianchi et al. 2005	[9]
(Au–Pd)/C-Pr.	0.3	3 bar O_2	4	100 (50°C)	27.0	47.1	22.6		
Au–Pt)/C-Pr.B	0.3	3 bar O_2	4	90 (50°C)	54.3	36.9	6.3		
3%Pt/C	1.08	1 bar O_2	1.5	98.8 (40°C)	19.7	30.1	29.8	Brainer et al. 2013	[16]
4.8wt%Pt/Fe_3O_4	0.3	1 bar O_2	1.5	56 (60°C)	53	36	2	Sproge et al. 2015	[17]
Ag/Al_2O_3	0.3	3 bar O_2	4	100 (60°C)	44.8	27.2	0	Skrzynska et al. 2015	[10]
Au/Al_2O_3	0.3	3 bar O_2	4	100 (60°C)	20.7	60.4	0		
4.8wt% Pt/NP–TiO_2	0.3	6 bar O_2	1.5	100 (60°C)	16	60	7	Chornaja et al. 2016	[10]
5wt%Cu–Al_2O_3	0.05	10 bar O_2	4	67 (90°C)	32	15	0	Schünemann et al. 2017	[18]

Vaalbio team, from the UCCS (Unité de Catalyse et de Chimie du Solide) laboratory, has worked in recent years on the process of glycerol oxidation for the production of glycolic acid. They found that an Ag-based catalysts are much more selective for glycolic acid. After 3 h of reaction at 60°C

under 5 bar of oxygen, 85% conversion of glycerol was achieved together with a selectivity of 57% to glycolic acid [19]. The effect of impurities on the catalytic activity was also studied by working with pure and crude glycerol. Ag catalysts showed good stability in continuous mode and very good resistance to impurities present in a crude glycerol fraction [20].

In order to continue with the glycerol valorization process, the carboxylic acids obtained must be separated and purified. The challenge for its valorization is associated to the complexity of the mixture and the thermal sensitivity of the produced derivatives. Table 1-3 presents a typical average composition of the glycerol oxidation reactor effluent and the respective boiling point of the acids present.

Table 1-3. Final conditions of glycerol oxidation reaction.

Acids	Mixing ratio [molar%]	Teb [°C]
Glycolic acid	50	100
Formic acid	25	101
Glyceric acid	15	272
Tartronic acid		471
Oxalic acid	<1	157
Lactic acid		122
Glycerol	≈ 9	290

To make the glycerol oxidation process viable using silver catalysts, the Vaalbio team proposed the design of a process where the carboxylic acids produced by oxidation will be recovered and separated. The existing separation technologies were then reviewed, and the most important remarks are summarized in this chapter.

1.2 Separation techniques of short-chain carboxylic acids

In the separation of short-chain carboxylic acids as lactic, acetic, formic, propionic, glycolic and succinic acids, several technologies have been used [21]. They can be generally classified in three large groups: membrane, adsorption, and chemical processes.

1.2.1 Membrane processes

Membrane separation processes are promising technologies, sometimes used to enhance the conversion of reactants for thermodynamically or kinetically limited reactions. Filtration, reverse osmosis and electro-dialysis are the most important sub-processes. The main limitations of membrane processes are their relatively high cost and energy consumption as well as the polarization and fouling problems. The summary of recent scientific studies using membrane processes are shown in Table 1-4.

Table 1-4. A summary sheet of membrane processes

ACIDS	CONDITIONS	RECOVERY	REF
Succinic acid	Type of membrane: Ceramic pH: 10-11 Low Feed concentration: 0.29-0.58 g L^{-1}, electrostatic repulsions are dominant (salts recovery increase)	85%	[22]
	The best membranes: NF270(1), NFDK(2), NFDL(3) Pressure: 30 bar Concentration : 10 g L^{-1}	88.9%(1) 89.6%(2) 79.0%(3)	[23]
	EDBM , 180 min, 120 A/m^2 and 200 g/L succinic acid	75.4%	[24]
	Sequential steps of ED and EDBM 0,67 kW h^{-1}	60%	[25]
Acetic acid	The best membrane: β-CD membrane, CD= cyclodextrine Optimum parameters: Feed concentration = < 36.7 g L^{-1} Pressure = 3.5 bar Flow rate of feed stock = no significant effect on retention Operation time = 3–4 months	99%	[26]
	The best membranes: DK, DL and NF270 Temperature: 30ºC Acid concentration: 50 mM pH= 7	87.3%	[27]
	Combination: activated carbon (AC), nanofiltration (NF) and reverse osmosis (RO). Reverse osmosis membrane: pH 4.3 and 500 psi pressure.	68%	[28]
	Lower pressure = 10 bar for NF and 20 bar for RO Higher temperature = 45°C for NF and RO Feed volume=10 and 9 times of the permeate volume in NF and RO process, respectively	Purity 65%	[29]
Lactic acid	EDBM, 1.32 mol L^{-1} lactate current density of 40 $mAcm^{-2}$	69.5%	[30]

1.2.1.1 Filtration

This technology uses different ranges of pressure-driven filtration membranes including microfiltration (MF), ultrafiltration (UF) and nanofiltration (NF) which use a size ranges of 0.1–10.0 μm, 1–100 nm and 0.5-1 nm, respectively [31]. Unlike MF and UF, NF separation is based on sieving and charge effects due to the presence of ionisable groups on the surface of the membrane. Hence, this technology is the most outstanding candidate for the recovery of carboxylic acids because of their negative charge (some cases) and low molecular weight, since it employs various mechanisms including steric based exclusions (namely size or molecular weight), shape and charge. NF offers several advantages such as great flexibility in the scale of production, high degree of separation and selectivity [30,26].

Recently, Staszak *et al.* [22] investigated the separation of succinic acid in the presence of glycerol, using a ceramic membrane. They showed a high recovery of acid (85%) at pH value of 11 and low feed concentration (0.29-0.58 g L^{-1}), which means that at these conditions, nearly all glycerol was successfully permeated through the membrane while organic acids in the form of salts were retained. In 2016, Sosa et al. [23] studied the recovery of succinic acid using six different membranes (*i.e.,* NF90, NFDK, NP030, NF270, NFDL, NP010). The best selected membranes, NF270, NFDK and NF-DL, showed similar performances, demonstrating very low and negative rejections for acetate and formate, while succinate recovery remained above 90% in most cases. Baruah *et al.* [26] studied the removal performance of acetic acid (AA) from dilute aqueous solution (≤ 3%) using α-, β-, and γ-Cyclodextrins (CD) membranes. Membrane separation performance was investigated as a function of feed concentration, operating pressure, flow rate and operation time. Among all the membranes tested, β-CD membrane achieved 99% recovery of AA from aqueous solution. Zacharof *et al.* [27] researched the feasibility of separation of AA using five nanofiltration membranes (NF270, HL, DL, DK and LF10), among them, DK, DL and NF270 were identified as the best candidates for AA separation and concentration from this effluent, both in terms of retention and permeate flux. With a pH and acid concentration values of 7 and 50 mM respectively, these membranes achieved retention ratio up to 75%. However, when sodium bicarbonate and sodium chloride were added, retention was improved drastically, reaching 87.3%. The former suggests that these salts can successfully be applied in the nanofiltration of carboxylic acid in order to concentrate and separate carboxylic acids from mixtures.

1.2.1.2 Reverse Osmosis (RO)

RO is a pressure-driven membrane technique. The pressure difference between the concentrated side and the diluted side is larger than a certain value that depends upon the difference of the respective concentrations and is called osmotic pressure difference. The rate at which water flows through the membrane is then proportional to the differential pressure. In order to overcome the feed side osmotic pressure, fairly pressure is required. NF membranes allow the passage of water and of relatively larger molecules. Ions are retained more than molecules of the same size, which indicates a potential for concentrating as well as purifying carboxylic acid or carboxylate solutions. RO membranes are characterized by having smaller pores, mainly allowing water permeation [32]. In harmony with these features, and for the recovery of organic acids, this latter technology can be complemented with NF in order to improve the process performance. This is particularly the case with Ahsan *et al.* [28], who researched the feasibility of recovering and concentrating sugars and AA from prehydrolysis liquor (PHL) of the Kraft-based dissolving pulp process prior to the fermentation of hemi-cellulosic sugars. The process combined reverse osmosis (RO) and nano-filtration (NF) by activated carbon adsorption (AC). Figure 1-1 shows the purification process.

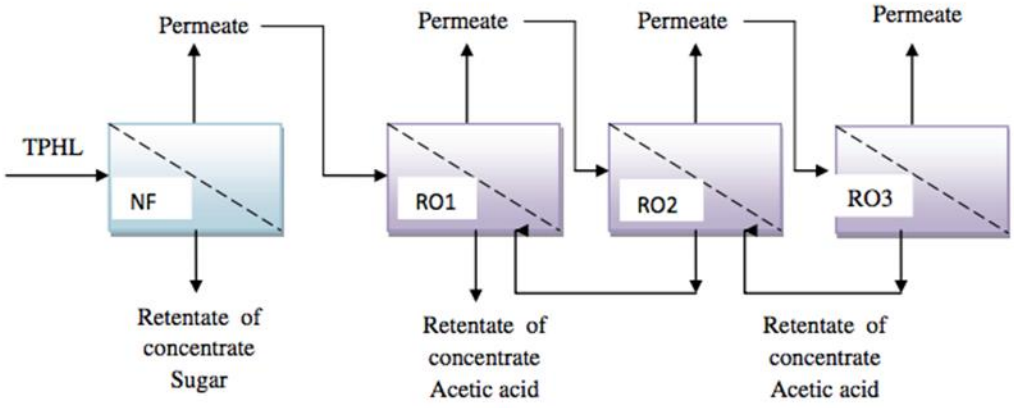

Figure 1-2. Multistage process of nanofiltration and reverse osmosis for recovering and concentrate hemicellulosic sugars and acetic acid [28].

First, the PHL is passed through an AC adsorption step and then through one step of NF and three steps of RO. A total of 80 to 90% of AA was permeated in the stage of NF, followed by a 68% of AA retention in RO membranes at pH 4.3 and 34.5 bar pressure. The AA concentration increased from 10 to 50 g L^{-1}. Lyu *et al.* [29] studied the feasibility of simultaneous separation of acids from sugar in modelling no cellulosic hydrolysate solution through two-stage nanofiltration (NF) and reverses osmosis (RO) process. Two-stage membrane process (DK NF-SE RO) was proven to

be a feasible way, where the glucose mass was 97.59% in the concentrate of NF, and in the permeate of RO, AA had a purity of 65.32 wt%.

1.2.1.3 Electrodyalisis with bipolar membranes (EDBM)

When charged compounds have to be separated from a solution, EDBM represents a powerful technology. EDBM is a variation of electrodialysis (ED) in which bipolar membranes (BM) are used. In both cases, an electric field is applied as the driving force for the separation of ions through ion exchange membranes. However, while ED uses only cation exchange membranes, anion exchanges membranes, and electrodes, EDBM uses bipolar membranes as the core of the technology. This difference optimizes the recovery process. In EDBM, the end results are the formation of an alkaline solution on the anion-exchange side and an acid solution on the cation exchange side, in contrast with ED, where a more concentrated solution and a more dilute solution of carboxylate salt are formed [32,34].

In recent years, EDBM has been widely used for the purification and recovery of organic acid solutions. Wang *et al.* [30] have reported recovery of lactic acid by continuous EDBM with glucose as a substrate, lactate recovery of 69.5% under a current density of 40 mA cm^{-2}. Szczygiełda *et al.* [24] studied the feasibility of separation and concentration of succinic acid through EDBM. According to their results, the highest acid concentration (75.4% after 180 min) in the concentrate chamber and the highest current efficiency were obtained when the current density and the initial concentration of succinic acid salt in the dilute chamber were equal to 120 A m^{-2} and 200 g L^{-1}, respectively. Therefore, the results have proved that it is possible to use the EDBM process as one of the steps of separation and concentration of succinic acid. Moreover, as already mentioned, the application of EDBM process allows the concentration of succinic acid and additionally the conversion from salts to the acidic form. On the other hand, ED can be used as a concentration step only, and then EDBM is used to treat concentrates from ED in order to obtain the acid solution. This is particularly the case of Glassner *et al.* [25]: they proposed a desalting electrodialysis combined with a water-splitting electrodialysis to achieve succinic acid with high purity. After water-splitting electrodialysis, a total purification yield of 60% was achieved. In order to yield a higher purity (>99%) of succinic acid, the aqueous solution was subjected to anionic and cationic ion exchangers to remove ionic impurities.

EDBM is an environmentally friendly alternative to the technology currently in use, however, this method presents several limitations, mainly, the low current efficiency, the high energy consumption, the material costs of the membranes, fouling and the low selectivity for one specific acid, *i.e.*, other organic acids such as AA, are isolated together with succinic acid [35].

1.2.2 Ion exchange/ adsorption

Ion exchange is a simple technique widely used in the demineralization and purification. Ion exchange resins are usually polymeric resins with a linked cation or anion exchange group. For carboxylic acid separation, the polymer adsorbent showed good selectivity and high adsorption capacity even in the presence of inorganic salts. The predominantly used resins are strong or weak base resins, which have tertiary or quaternary amines as the ion exchange group [36, 37]. The main adsorbents found in literature are shown in Table 1-5.

Table 1-5. Commercial Ion exchange resins used in the recovery of carboxylic acids. TA : Tertiary amine, SA: Secondary amine, QA: quaternary amine.

Type resin	Name	Functional groups	Ref
Weak Base resin	Amberlite IRA-67	TA	[38]
	Amberlite A21	TA	[39]
	Amberlite IRA-96	TA	[40]
	Amberlite IRA-35	TA	[41]
	Dowex MWA-1	TA (90%) and SA	[42]
	Indion 860	TA	[37]
	Duolite A7	SA in majority	[43]
Strong Base resin	Amberlite IRA-400	QA (Type I)	[44]
	Amberlite IRA-420	QA (Type I)	[45]
	Amberlite IRA-410	QA (Type II)	[46]
	Amberlite IRA-900	QA (Type I)	[47]
	Amberlite IRA-120	QA (Type I)	[40]
	Indion 810	QA (Type I)	[37]

As pH influence directly the protonation of the resins, loading capacity has a strong dependence on pH. The increase in pH decreases the availability of protons and therefore the possibility of ion pairing between the protonated amine group and the carboxylate. In general, the commercial weak base resins sustain most of their adsorption capacity up to the pKa of the acid and then undergo a sharp decrease up to neutral pH. The progressive decay in capacity with pH depends on the pKa of the acid and the basicity of the resin [31,42,43,48]. Thus, weak base resins become charged over a limited pH range and otherwise are not able to exchange anions whereas strong base resins exchange anions over a broad pH range [32].

Ion exchange processes have recently been studied in the recovery of short-chain carboxylic acids. The summary of experimental conditions is shown in Table 1-6. With respect to lactic acid recovery, Rampai *et al.* [49] studied their separation efficiency in aqueous solution using Amberlite IRA-400. The results showed that pH and temperature affected the adsorption process. Increasing the pH and temperature increased the adsorption capacity of lactic acid on the resins. The maximum adsorption capacity of 1.8 g of lactic acid per gram of wet resin was obtained at pH 6 and 70 °C. In order to elute lactic acid from the saturated resin, different eluents such as NaCl, DI water, and H_2SO_4 were studied. Among them, H_2SO_4 was more effective, NaCl and DI water unsuccessfully eluted lactic acid from the resins.

Table 1-6. Summary of recent reports in the recovery of short-chain carboxylic acid via Ion Exchange adsorption process

ACID	CONDITIONS	CAPACITY ADSORPTION [$mg.g^{-1}$]	REF
Lactic acid	Resin = Amberlite IRA-400 pH=6.0 T=70 ºC Eluent=0.1 M H_2SO_4	180	[49]
	Two resins = Amberlite IRA-96 and Amberlite IRA – 120 pH=7 T=25 ºC Eluent=0.1 N HCL	210	[40]
Lactic + acetic acid	Resin= Amberlite IRA-67 pH=3.3 T=25 ºC	60.10	[50]
Succinic acid	Resin= NKA-9 pH=2 T=10 ºC	155.9	[51]

For weak base resins (*e.g.*, amberlite IRA-67), acid adsorption decreases as pH increases, this result was obtained by Yousuf *et al.* [50] in lactic and AA recovery. In this case, a maximum acid removal of 74% was obtained from the aqueous solution. The adsorption capacity calculated was 60.1 mg g^{-1} resin. A study performed by Bishai *et al.* [40] showed that lactic acid recovery can be enhanced using two steps of purification. In the first stage, a weak anion exchange resin was used in order to separate lactic acid from other anions present in the solution. Afterwards, a strong cation exchanger was used which washes out the target molecule (*i.e.,* lactic acid) while trapped other cations present in the solution. The selected ion exchangers were Amberlite IRA 96 and

Amberlite IR 120, respectively. After the simple two-step purification process, the purity of lactic acid increases up to 99.2% with a recovery yield of 98.9%. This result shows that the recovery yield of lactic acid was significantly enhanced compared to the results obtained by Tong *et al.* [52], John *et al.* [47], Quintero *et al.* [48], who reported recovery yield percentages of 82.6, 92.5 and 73%, respectively. Hence, a system of columns packed with Amberlite IRA-96 and IR-120 could be a suitable technology for purification of lactic acid.

Succinic acid recovery from aqueous solution was reported by Sheng *et al* [51] using macroporous resins HPD-300, HPD-400, HPD-450, HPD-500, HPD-826, AB-8, and NKA-9. According to the adsorption capacity, NKA-9 was chosen as the most suitable resin for succinic acid purification, which resulted from suitable polarity and pore size. A maximum adsorption capacity of 155.9 mg g^{-1} resin was obtained at pH 2 and 10 ºC.

In general, ion exchange/adsorption process is a reliable technology, their main advantage is the ease of the auxiliary phase removal. Solid adsorbents confined in columns are effortlessly handled in comparison to liquid–liquid systems in which phase separation might require either large equipment or energy-demanding operations. However, the main drawback is the cost associated with regeneration of commercial adsorbents. In other words, adsorbents are prone to fouling which may limit the operational lifetime of the material, making adsorption operation very expensive.

1.2.3 Chemical processes

1.2.3.1 Reactive extraction (RE)

Reactive extraction (RE) has been proposed as a promising technique for the recovery of carboxylic acids. This technology is developed to intensify separation by solvent extraction and represents a connection between chemical (solute and extractant reaction) and physical phenomena (diffusion and solubilization of the components) [53]. Generally, RE represents a reaction between the acid (solute) and extractant at the interface of organic phase. The reaction complexes formed are then solubilized in the organic phase where transfers of molecules take place by the diffusion and solubilization mechanism. This technology strongly depends on various parameters such as the composition of the organic and aqueous phases, properties of the solvents (extractant and diluent), types of complexes formed, temperature and pH. The purpose of this technology is achieving a high distribution coefficient with higher selectivity. This can be achieved

by using an appropriate organic phase at optimum conditions [54].

Extractants used for the extraction of carboxylic acids are categorized as conventional oxygen-bearing hydrocarbon, phosphorus bonded oxygen bearing extractants, and high molecular weight aliphatic amines [53, 55, 56]. Since phosphorous and amine extractants have been mainly used in the recovery of carboxylic acids, only these extractants are discussed below.

1.2.3.1.1 Organo-phophorous compounds:

These extractants are characteristic due to the presence of a phosphoryl group that is a stronger Lewis base than conventional carbon-bonded oxygen donor extractants. The extractants belonging to this group are more water-immiscible and extractable than carbon-bonded oxygen donor extractants. Therefore, weak organic acids are extracted by organo-phosphorus compounds with a significantly higher distribution ratio than by carbon-bonded oxygen donor extractants under comparable experimental conditions. The distinction between these two categories is based on the strength of the solvation bonds and the specificity of solvation. Although the extractability of phosphorous compounds is lower than those of aliphatic amine extractants, their low toxicity allows their use in the fermentation process [53, 57]. Fahim *et al.* [58] found that the distribution coefficients for acetic and propionic acid are high in the reactive extraction by tri-octyl-phosphine oxide (TOPO) and tri-butyl-phosphate (TBP). Others reports [59, 60] showed that TOPO had a higher distribution coefficient than TBP in the extraction of acetic acid, glycolic acid, lactic acid, succinic acid.

1.2.3.1.2 High molecular weight aliphatic amines

Another method in separation technology is the extraction of organic compounds from aqueous media by amines dissolved in a water-immiscible organic solvent [57]. Long-chain aliphatic amines are found to be effective extractants for carboxylic acids, they have been favored because of a lower cost and generally higher distribution coefficient [61]. This latter feature is due to the strong amine interactions with the acid allow for the formation of acid-amine complexes [62].

Different amines have been studied. Ternary amines are generally favored over primary secondary and quaternary amines. Primary amines are characterized by a large mutual solubility of the aqueous and organic phase, hence, their use is not practical; secondary amines have the

highest reported distribution coefficient, but tend to form amides in the downstream regeneration by distillation; quaternary amines extract acid at both acidic and basic pH *via* an anion exchange mechanism, but are difficult to regenerate by back extraction with caustic. Consequently, tertiary amines are the most attractive for extraction from aqueous stream on the basis of their low aqueous solubility and intermediate basicity, providing reasonable extracting power along with the possibility of stripping [63]. The basicity of tertiary amines is proportional to their chain length. Nevertheless, the trend of extraction power is not always dictated by the basicity of a tertiary amine [53] [57]. Among all aliphatic amines, lauryl-trialkylmethylamine (Amberlite LA-2), tri-n-octylamine, tri-iso-octyl-amine, tri-n-(octyl-decyl)-amine (Alamine 336) and quaternary alkylammonium salt (Aliquat 336) have been shown to be effective extractants for separation of carboxylic acids from dilute aqueous solution [53, 64, 62].

Generally, the amine extractants are dissolved in a diluent (organic solvent) due to its viscous and corrosive nature. It controls the density, viscosity and surface tension of the organic phase. However, the chemical structure of a diluent may have various effects connected with the formation of acid-amine complexes in the organic phase [53]. The most diluents utilized are polar in nature (presence of functional groups). They are good solvating media for an ion-pair such as an acid-amine complex. The category includes chlorinated hydrocarbon, ketone, alcohol, and halogenated aromatic solvents. Nonpolar diluents provide very low distribution of the acid and poor solvation of the polar complexes, alkanes, benzene, alkyl substituted aromatics, and so forth fall in this category [54].

In the extraction of carboxylic acids, organophosphates compounds such as TOPO, TBP and aliphatic amines have large distribution coefficients [63],[65-69]. Aliphatic amines are slightly more effective and less expensive than phosphorus extractants. Also, they have significantly higher distribution coefficients than carbon-bonded oxygen donor extractants under comparable experimental conditions. This indicates that conventional extractants, *e.g.*, ketones, ethers, and alcohols, are not often able to fulfil the basic requirements because of their low distribution coefficients [62]. In other words, unlike aliphatic amines, hydrocarbon and phosphorous extractants are nonreactive in nature and extract the acid molecules by solvation. Distribution coefficients of various extractants of lactic acid in water systems are shown in Table 1-7.

Table 1-7. Distribution Coefficients of various extractants of Lactic Acid in Water Systems

Extractants pure	KD	Ref
Aliquat 336	2,17	[65]
Alamine 336	0,76	[67]
Try-hexylamine	1,27	[67]
Try-octylamine	0,63	[67]
Try-butyl-phosphate	0,71	[68]
Octanol	0,32	[63]
Decanol	0,13	[69]
MIBKa	0,14	[63]
Diethyl-ether	0,1	[63]
Di-isopropyl-ether	0,04	[63]
Hexane	0,0003	[66]
Chloroform	No extraction	[68]

[a]methyl-isobutyl-ketone

The reactive extraction of short-chain carboxylic acids from aqueous solution has recently been studied in the literature. The summary of experimental conditions is shown in Table 1-8. In respect of extraction of succinic acid, the work carried out by Eda *et al.* [70] has obtained very satisfactory results using tri-n-octylamine (TOA) in 1-decanol as extraction-diluent system.

Table 1-8. Summary of recent reports in the recovery of short-chain carboxylic acid via reactive extraction process

ACID	REMARKS	RECOVERY	REF
Succinic	Extractant solutions: 1) 30% tri-propyl-amine (TPA) in 1-octanol 2) 30% (v/v) TPA–TOA mixture mixture in a 2:8 weight ratio and dissolved in 1-Octanol. Feed flow rates (0.1, 0.2, and 0.3 L min^{-1}) T= 25ºC and pH= 3	95%	[71]
Succinic	Extractant= tri-n-octylamine (TOA) Diluent= supercritical CO2, Feed flow rate = 0,39 mol·dm^{-3}, T= 35°C, P=16 MPa, t=30 min	62%	[72]
Succinic	Extractant= tri-n-octylamine (TOA) Diluent= 1-Decanol, T=25ºC, Concentration =30%TOA. Feed flow rate = 0.1 kmol·m^{-3}	91%	[70]
Succinic	Extractant= tri-n-octylamine (TOA) Diluent= 1-Decanol, T=32.5 ºC, Concentration =33%TOA. Feed flow rate = 0.2 kmol·m^{-3}	93.7%	[73]
Glycolic	Extractant= mixture of 50% trioctylamine (TOA) and 50% tridodecylamine (TDA) (w/w) Diluent= dimethyl phthalate (DMP)[1], methyl isobutyl ketone (MIBK)[2], 2-octanone[3], 1-decanol[4], and cyclohexyl acetate (CHA)[5] Initial concentration= 1.163 mol kg^{-1} T= 25ºC.	81.61%[1] 80.36%[2] 79.10%[3] 77.81%[4] 73.05%[5]	[74]

Glycolic	Extractant= tri-n-octylamine (TOA) Diluent= cyclohexane and decan-1-ol Initial GA concentration (Cin)= 0,1707mol/L initial amine composition (CºTOA)= 22.31%v/v Temperature (T)= 23ºC.	91.83%	[75]
Propionic	Substrate: Glycerol, pH: < 4.5, T= 26ºC Feed flow rate: 1.13 kg h^{-1} Extractant-diluent system: Alamine 336 in cyclohexane (53:47 w/w)	76%	[76]
Propionic	Extractant= tri-n-octylamine (TOA) Diluent= supercritical CO2, Feed flow rate = 1.04 mol·dm^{-3}, T= 35 °C, P=16 MPa, t=60 min	94.7%	[77]
Acetic	Extractant= tri-n-octylamine (TOA) Diluent= supercritical CO_2 (2 g min^{-1}) Feed flow rate 85.8 g L^{-1} T= 45°C, P=14.8 MPa, t= 5h	93%	[78]

The results showed that distribution coefficient (K_D) increased with increasing TOA concentration from 10 to 30% (v/v) and extraction efficiency (E%) decreased to 40% with increasing temperature from 25 to 60 ºC. Thus, the highest reactive extraction efficiency of approx. 91% was obtained at 25 °C, 30% TOA and an initial acid concentration in aqueous phase of 0.1 mol L^{-1}. Then, an optimization study of reactive extraction of succinic acid was carried out by the same team using response surface methodology. An extraction efficiency of 93.75% was obtained with optimum values of parameters being: 0.2 kmol m^{-3} acid concentration, TOA composition of 33 (%v/v), at 32 ºC [73].

In a later publication, Agrahari *et al.* [71] researched the extraction of succinic acid using two different types of extractant solutions. The first solution was 30% tri-propyl amine (TPA) dissolved in 1-octanol, while the second solution was prepared by diluting a 30% (v/v) TPA—TOA mixture in the ratio 2:8 by weight in 1-octanol as diluent. The experimental conditions are shown in Table 1-8. Removal efficiency of succinic acid (SA) of more than 95% were obtained with both solutions, however, bearing in mind that the low cost of TPA in comparison with TOA, the authors selected the comparatively cheaper alternative, TPA. Afterwards, with this latter solution a SA removal efficiency of 99% was achieved using an initial concentration fewer than 59000 ppm. Subsequently, Granstrom *et al.* [76] studied the extraction of carboxylic acids such as propionic acid (PA), succinic acid (SA) and acetic acid (AA) from aqueous solution in a continuous process, using tri-n-(octyl-decyl)-amine (alamine 336) in cyclohexane (53:47 w/w) as extractant-diluent system. The experimental conditions are shown in Table 1-8. The results have shown extraction yields of 76, 21 and 53% of PA, SA and AA, respectively.

In respect of glycolic acid (GA), a mixture of 50% trioctylamine (TOA) and 50% tridodecylamine (TDA) (w/w) diluted in different solvents such as dimethyl phthalate (DMP), methyl isobutyl ketone (MIBK), 2-octanone, 1-decanol, and cyclohexyl acetate (CHA) was used as extractant-diluent systems to carry out the GA extraction. A substantial amount (73.05 to 81.61%) of glycolic acid is recovered by all the amine-diluent systems and at 1.163 $mol \cdot kg^{-1}$ initial concentration of (TOA + TDA) mixture. The order in which the solvents can recover glycolic acid is found to be DMP > MIBK > 2-octanone >1-decanol > CHA. Thus, the highest values of KD and extraction of glycolic acid are found to be 4.44 and 81.61%, respectively [74]. Then, an optimization study of reactive extraction of glycolic acid was carried out by the same team using response surface methodology (RSM) using TOA (amine) dissolved in organic solvents (cyclohexane and decan-1-ol) considering four design variables: initial GA concentration (C_{in}) in the aqueous phase, initial amine composition (C^{o}_{TOA}) in the organic phase, modifier composition (M), and equilibrium temperature (T). The optimized conditions were 0,1707mol/L, 22.31 %v/v, 73.28 %v/v, and 23ºC, respectively. At these conditions, the maximum experimental value of the degree of extraction was found to be 91.83% [75].

The application of supercritical CO_2 ($scCO_2$) as a solvent for the reactive extraction of carboxylic acids from aqueous solution is innovative and still under development. This method has potential as an effective and environmentally friendly alternative method to the traditional technology of carboxylic acid recovery [79]. The scheme of the reactive extraction process of carboxylic acid from aqueous solution using $scCO_2$ is shown in Figure 1-3. Where, $(H_2A)_a(G)_b$ is the complex formed between carboxylic acid (H_2A), and a suitable reactant or extractant (G). An increase in extraction efficiency can be achieved by adding suitable extractants (high molecular weight aliphatic amines, phosphorus-bonded oxygen bearing extractants) to the $scCO_2$ phase. Tertiary aliphatic amines are known to be effective extractants for carboxylic acids and they do not react with CO_2 [54],[63],[80-81].

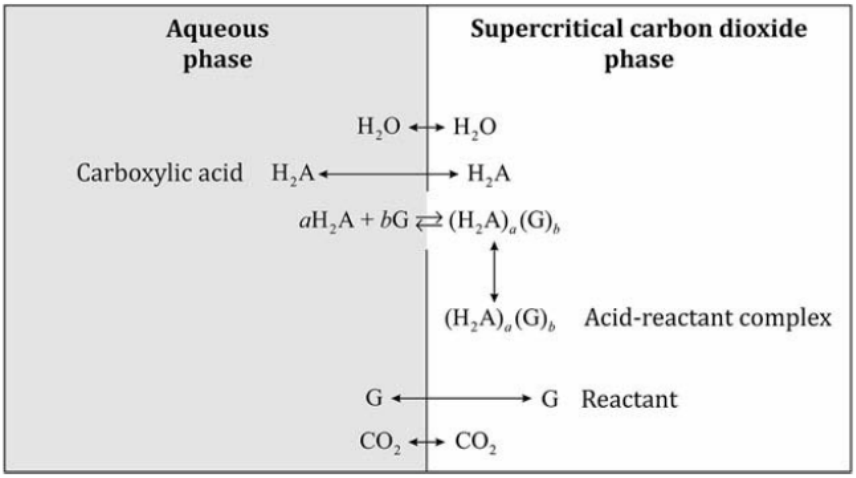

Figure 1-3. Scheme of the reactive extraction process of carboxylic acid from aqueous solution using supercritical carbon dioxide [71]

Henczka *et al.* [77] studied the reactive extraction of acetic and propionic acids from aqueous solutions using supercritical carbon dioxide ($scCO_2$) and tri-n-octylamine (TOA). It was shown that KD values for reactive extraction of propionic acid (0.26–0.75) were higher than for acetic acid (0.04–0.23), hence, the highest reactive extraction efficiency 94.7 and 79.5% was obtained for propionic acid and acetic acid, respectively, using supercritical CO_2 as diluent under the reaction conditions shown in the Table 1-8. Later, following the same methodology and extractant-diluent system described above, they researched the extraction of succinic acid from an aqueous solution. The highest reactive extraction efficiency of approx. 62% was obtained for the process conducted in semi-continuous mode at 35 °C and 16 MPa for the initial acid concentrations in aqueous phase of 0.39 mol dm^{-3} [72] . On the other hand, the recovery of acetic acid from aqueous solution via reactive extraction processes was improved by Garret *et al.* [78] using the same extractant-diluent system. Within the range of variables studied, maximum acetic acid recovery of 93% was predicted. Thus, the supercritical reactive extraction process is an efficient method of succinic acid, propionic and acetic acid separation from aqueous solutions. Besides the relatively high yield, this method is characterized by simplicity and competitiveness as compared to the other separation methods [72].

1.2.3.1.3 Solvent recovery by back extraction

The success of the reactive extraction process lies in the complete recovery of acid from the loaded organic phase. After extraction, the carboxylic acids have to be removed from the organic

phase to obtain pure carboxylic acid products. A simplified diagram of the extraction and regeneration processes is shown in Figure 1-4. When stripping the acids from the solvent, the solvent is recovered as well and can be re-used. Solvent extraction processes are often done at ambient temperature meaning that the majority of costs come from chemicals and mixing. The circulation of the extractant affects remarkably the economy of the process [82]. The acid can be back extracted from loaded organic phase using various regeneration methods: by temperature, by diluent swing, using NaOH, using trimethyl-amine and Gas-Antisolvent-Induced Regeneration. In temperature and diluent swing the extraction is based on the change in the extraction equilibrium caused by a change (increase) in the temperature and in the composition of the diluent, respectively, in order to produce a system that promotes distribution of the acid to the aqueous phase. Diluent swing has the disadvantage of diluting the extract stream and requiring distillation of large amounts of solvent (after the regeneration) [57,62,82-84].

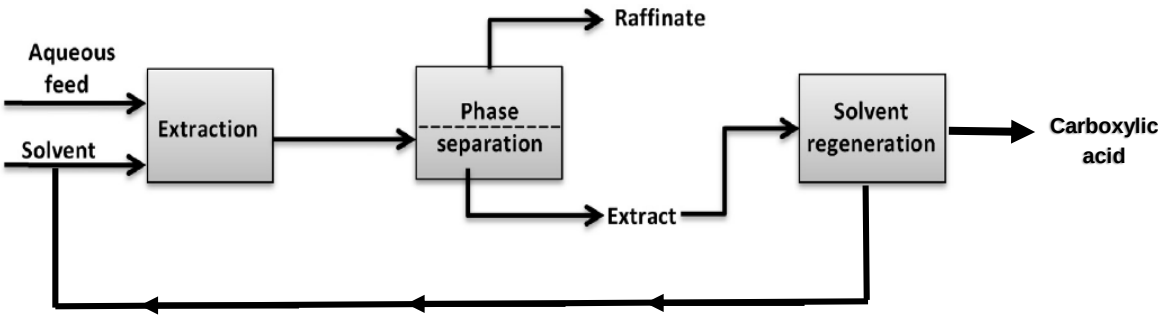

Figure 1-4. A simplified diagram of the extraction and regeneration processes [82].

Back extraction with NaOH and trimethyl-amine are based on the higher solubility of the acids in these substances compared to organic phase. Both NaOH and trimethyl-amine extractions can result in 100% regeneration [82, 83], however, unlike NaOH, the regeneration of acid extracted in the organic phase using a stronger volatile amine like trimethyl-amine (TMA) in aqueous phase is more cost-effective, *i.e*. this regeneration technique avoids consumption of chemicals and creation of salts byproducts. In general, the aqueous base, which is volatile, enables thermal decomposition of the acid–base complex in the aqueous back-extract. The decomposition forms carboxylic acid as a product and freebase as a vapor that can be reabsorbed in water and recycled for reuse in back-extraction. The most obvious water-soluble, volatile base is ammonia [57, 62,82-85].

Among all methods abovementioned, TMA regeneration allows a fast reaction and a nearly complete regeneration of the acid, which signifies that TMA could be successfully employed for the regeneration [83]. However, their main drawback is the toxicity and the need to use a distillation step to regenerate TMA. In this way, currently, a new technology is being studied. Gas-Antisolvent-Induced Regeneration technologies replace the inert liquid diluent with a gas antisolvent. Here, antisolvent is used to denote a substance that has a low capacity to solubilize the extracted acid. In this process, the diluent composition change will be affected by pressurizing it with a gas antisolvent (*e.g.*, propane). A benefit of this process over conventional recovery techniques is that the diluent components can be easily separated (*e.g.*, by a flash distillation) without using a distillation step [62, 86].

1.2.3.2 Reactive distillation (RD)

Reactive distillation (RD) holds dominance over conventional physical separation methods such as distillation and extraction. It is a unit operation that combines simultaneous chemical reaction and multi-component distillation in the same vessel. RD is applied specifically to reversible chemical reactions in the liquid phase, in which reaction equilibrium limits the conversion of the reactants [87].

Reactive distillation (RD) has been proposed as a promising technique for the recovery of short-chain carboxylic acid with high purity and high yield [88] for many reasons: improving selectivity, increased conversion, better heat control, effective utilization of reaction heat, scope for difficult separations and the avoidance of azeotrope are a few of the advantages that RD offers. As the products in RD are continuously separated from the reaction zone, no limiting chemical equilibrium can be established and thus the reaction velocity is maintained at a high rate, resulting in greater yields. Other benefits of RD can include the minimization of side reactions and the utilization of the heat of the reaction for the mass transfer within the same column. Therefore, affecting distillation and reaction simultaneously can reduce the capital costs and operating costs are significantly lower with RD than for conventional processes; and can yield benefits like reduction of recycle, separation optimization and lower requirements of pumps, instrumentation and piping [87, 89, 90]. Nevertheless, there are several disadvantages as a very complex process, nonreactive azeotropes may disappear under reactive distillation condition. In some processes,

the optimum conditions of temperature and pressure for distillation may be far from optimal for reaction and *vice-versa* [90].

Reactive distillation (RD) has been studied for the recovery of lactic acid from aqueous solution. In this process, the lactic acid recovery involves two reversible reactions, esterification (1) and hydrolysis (2), catalyzed by an acidic catalyst. This latter can be homogeneous or heterogeneous such as sulphuric acid and ion exchange resin, respectively. Different alcohols can be use in esterification, *e.g.*, ethanol, butanol, methanol and 2-propanol [34, 89].

$$Lactic\ acid + methanol \rightarrow methyl\ lactate + water \qquad (1)$$

$$methyl\ lactate + water \rightarrow lactic\ acid + methanol \qquad (2)$$

The reactive distillation columns for esterification and hydrolysis are shown in Figure 1-5. In esterification columns, lactic acid and alcohol are fed at the top and the bottom, respectively, and after the reaction, water is obtained in the distillate and lactate in the residue stream. The distillate and residue streams are fed in the hydrolysis column. Water is fed at the bottom and lactate at the top of the column. After hydrolysis, alcohol is recovered at the top and lactic acid is recovered in the residue [89].

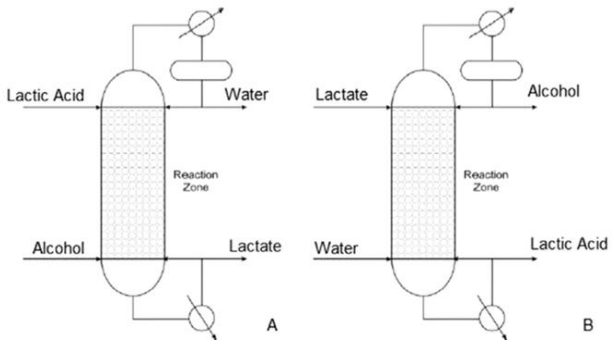

Figure 1-5. Reactive Distillation columns for esterification (A) and hydrolysis (B) [87]

Komesu *et al.* [91] researched lactic acid purification using reactive distillation system. The results showed that the process for lactic acid purification proposed in this work, provides large potential to achieve high yield of ethyl lactate (99.94%) and lactic acid with 3 times higher concentration (347.68 g L^{-1}) than the raw material at conditions shown in Table 1-9. Subsequently, Rao *et al.*

[32] studied the recovery of lactic acid in Batch RD, using n-butanol as reactive and Amberlite as catalyst. In this case, the results shown that Amberlite reduces about 15% the amount of formation of polylactic acid to a lower value than for without a catalyst. The yield of recovered lactic acid was estimated as high as 95%.

Table 1-9. Summary of recent reports in the recovery of short-chain carboxylic acid via reactive distillation process

Acid	conditions	YE [%]*	Ref.
Lactic acid	Semi-batch RD, t= 2 h T=125 ºC Catalyst= H_2SO_4 Ethanol	99,94	[91]
Lactic acid	Batch RD, t=140 min Catalyst= Amberlite n-buthanol	95	[32]
Acetic acid	Semi-batch RD, t= 100min T=70 ºC Catalyst= Organic polymer Methanol	About 80	[92]
Acetic + Formic acid	T=64,6 ºC 28 %FA + 62 %AA Methanol	-	[93]

*Y_E: Yield esterification reaction

The recovery of acetic acid by reactive distillation through esterification with methanol in the presence of ion-exchange resin as a catalyst has been investigated in detail by Singh *et al.* [92]. A recovery of 80% was obtained experimentally for feed concentrations of 30% (w/w) using a laboratory column at 70 ºC.

Reactive distillation (RD) provides an alternative approach for the separation of multicomponent azeotropic mixture. By changing substance properties through a chemical reaction with appropriate reactants, thermodynamic limitations can be avoided. Formic acid and acetic acid form an azeotrope in the following conditions: 49.8% FA and 11.2% AA and 39 mol% water at T= 105 ºC and P= 960 mbar. The separation of these acids mixture was studied by Painer *et al.* [93]. The esterification reaction was carried out in continuous RD, using methanol as reactant. Constituents separation by reactive extraction was confirmed, almost complete recovery of formic acid (>98%) was possible, acetic acid conversion of 69% was observed too. For separation and isolation of acetic acid either esterification or alternatively distillation separation can be applied.

Although yields in terms of separation and recovery using reactive distillation are good, energy

efficiency is not good in all cases. In some cases, when having multicomponent mixtures, in order to achieve high levels of purification of the desired product a series of additional distillations must be considered. Current energy costs are the main reason why the reduction of energy requirements is a necessity. Continuous improvements in reactive distillation intensification processes have considered design strategies such as thermally coupled distillation columns, heat integrated distillation columns and divided wall columns [94-95]. These strategies are based on modifications of the configuration inside the column allowing an improvement in the separation and recovery of products, which makes the technology more energy efficient and in turn improves its sustainability [96].

For the purposes of this research, the technology of reactive divided wall column (RDWC) was chosen considering its advantage in the separation of multicomponent mixtures. This technology is presented in the literature as one of the best options in terms of energy savings, between 15 and 75%, and at least 20% of capital cost reduction compared to conventional processes [5].

Though currently not widely used at industrial level, RDWC has captured the attention being the subject of various research work which has as its main objective its design, feasibility analysis and control. The RDWC is defined in the literature as a reaction device with a separation system included represented by central partitions. Weinfeld *et al.* [5] present the schematic that allows to identify the fundamental stages in the transition from conventional distillation process to the reactive divided wall column process (see Figure 1-6). The figure shows the separation of a mixture of three components with decreasing volatility from A to C. The yellow area represents the part where the reaction takes place. The partition wall divides a single column into two parts: a prefractionation section and a main column. It uses only one reboiler and one condenser.

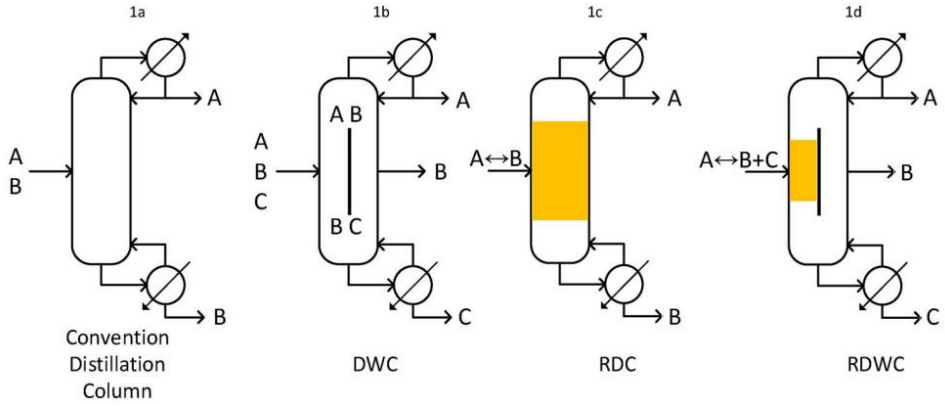

Figure 1-6. Overview of the development of the reactive divided wall column (RDWC). (a) Conventional, (b) dividing wall, (c) reactive, and (d) reactive dividing wall distillation columns [5].

The advantages that researchers have found with the RDWC implementation is the decrease in the initial capital investment because it requires a smaller number of equipment and the cost of operation due to lower energy consumption. The authors agree that by applying this technology, high purity products can be achieved, in the products recovered in the middle of the column and at the bottom of the column. Compared to multi-component distillation systems, the implementation of RDWC requires less construction volume [97, 98].

However, this technology has some disadvantages associated with the sizing of the column, higher height due to the increase in the number of stages and greater diameter by the inclusion of the wall inside the column. The greater number of stages makes the pressure drop along the column an important parameter especially at the time of design. In this type of compact system there is only one operating pressure in the whole unit, *i.e*. in the reaction zone as well as in the separation zone [94, 95, 97, 98].

1.2.4 Strengths and weakness of separation technologies

The production cost of carboxylic acids can be reduced by increasing the productivity and using the proper recovery method. Several alternatives separation technologies have been reviewed above. Their advantages and disadvantages are summarized in Table 1-10. From an economic standpoint, membrane processes and ion exchange/adsorption are not the most appropriate technologies in the recovery of carboxylic acids. Consequently, reactive extraction and reactive distillation have the highest chances of industrial implementation. Reactive distillation allows better

use of energy; however, their implementation is very complex and limited by the type of reaction and the reaction conditions. Furthermore, reactive extraction is a practical technique, which has strongly attracted the attention of researchers, its major drawbacks such as toxicity of back-extractants (TMA) and low pH of work affects mainly fermentation process.

Table 1-10. Summary of advantages and disadvantages of separation technologies of carboxylic acids [50][87][29][59][88].

SEPARATION TECHNIQUES	ADVANTAGES (+)	DISADVANTAGES (-)
Membrane Processes	- Great flexibility in scale production. - High selectivity. - High levels of purification. - Integration with conventional fermenters. - Enhance the conversion of reactants.	- High cost of membranes. - Membrane fouling. - High energy consumption.
Ion Exchange/Adsorption	- Reliable technology. - Ease of the auxiliary phase removal. - High selectivity. - High adsorption capacity.	- High cost associated with regeneration.
Reactive extraction	- Small volumes of solvents. - High degree of phase separation. - Lower water miscibility. - Smaller extraction equipment. - Recycle of solvents. - Low cost of extractants. - Proper choice of back - Extractants yields high productivity. - Practically all data needed for commercial design are available.	- Toxicity of back-extractants (TMA). - Most extractants work efficiently at low pH.
Reactive Distillation and Reactive divided wall column	- High levels of purification. - Lower energy consumption. - Improving selectivity. - Increased conversion. - Effective utilization of reaction heat. - Scope for difficult separations. - Prevents the formation of azeotrope.	- Process is complex. - Applied specifically to reversible chemical reactions in the liquid phase. - Corrosion by the use of homogenous catalyst. - The optimum conditions of temperature and pressure for distillation may be far from optimal for reaction. - In RDWC: One operating pressure and increased pressure drop.

1.3 Conclusion

Several techniques were reviewed as possible alternatives for the recovery of carboxylic acids from glycerol oxidation. The reactive divided wall column (RDWC) unit was chosen considering its advantages regarding conversion, selectivity and energy efficiency. The implementation of this

technology could allow the separation of carboxylic acids produced in a high degree of purity. However, its implementation requires detailed information concerning the thermodynamic and kinetic of the products involved in the separation reaction process. The intermediate stages between the output of the glycerol oxidation reactor and the reactive distillation column must also be studied. In this work, we will present the required studies to obtain the necessary information to carry out simulation and design of the process of recovery of carboxylic acids using reactive divided wall column. The preliminary feasibility study of the technology was made considering three scenarios, *i.e.* the use of three different alcohols (*i.e.,* propanol, butanol and octanol) and the most valuable acid present in the mixture, glycolic acid.

1.4 Bibliography

[1] B. M. Pagliaro, M. Rossi, and M. Pagliaro, “Glycerol : Properties and Production,” pp. 1–18, 2008.

[2] S. Veluturla, N. Archna, D. Subba Rao, N. Hezil, I. S. Indraja, and S. Spoorthi, “Catalytic valorization of raw glycerol derived from biodiesel: a review,” *Biofuels*, vol. 9, no. 3, pp. 305–314, 2018.

[3] J. M. Chem, “Selective Oxidation †,” no. c, pp. 337–340, 2012.

[4] D. Reay, C. Ramshaw, and A. Harvey, *Process Intensification*, 2nd Editio. 2013.

[5] A. Weinfeld, S. A. Owens, and R. B. Eldridge, “Reactive dividing wall columns : A comprehensive review,” *Chem. Eng. Process. Process Intensificatio*, vol. 123, no. September 2017, pp. 20–33, 2018.

[6] C. Weber, A. Farwick, and F. Benisch, “Trends and challenges in the microbial production of lignocellulosic bioalcohol fuels,” pp. 1303–1315, 2010.

[7] K. A. Amminudin, R. Smith, D. Y. Thong, and G. P. Towler, “DESIGN AND OPTIMIZATION OF FULLY THERMALLY Part 1 : Preliminary Design and Optimization Methodology,” vol. 79, no. October, 2001.

[8] B. Katryniok *et al.*, “Selective catalytic oxidation of glycerol: perspectives for high value chemicals,” *Green Chem.*, vol. 13, no. 8, p. 1960, 2011.

[9] C. L. Bianchi, P. Canton, N. Dimitratos, F. Porta, and L. Prati, “Selective oxidation of glycerol with oxygen using mono and bimetallic catalysts based on Au, Pd and Pt metals,” *Catal. Today*, vol. 102–103, pp. 203–212, 2005.

[10] E. Skrzyńska, S. Zaid, A. Addad, J.-S. Girardon, M. Capron, and F. Dumeignil,

"Performance of Ag/Al $_2$ O $_3$ catalysts in the liquid phase oxidation of glycerol – effect of preparation method and reaction conditions," *Catal. Sci. Technol.*, vol. 6, no. 9, pp. 3182–3196, 2016.

[11] S. Chornaja *et al.*, "Pt supported TiO2-nanofibers and TiO2-nanopowder as catalysts for glycerol oxidation," *React. Kinet. Mech. Catal.*, vol. 119, no. 2, pp. 569–584, 2016.

[12] X. Jiang and Y. Tang, "Preparation and application of Hydroxyacetic Acid Esters as Methanol-Gasoline additives," *Asian J. Chem.*, vol. 25, no. 15, pp. 8447–8450, 2013.

[13] C. H. Zhou, H. Zhao, D. S. Tong, L. M. Wu, and W. H. Yu, "Recent advances in catalytic conversion of glycerol," *Catal. Rev. - Sci. Eng.*, vol. 55, no. 4, pp. 369–453, 2013.

[14] Y. Deng, Y. Mao, and X. Zhang, "Metabolic engineering of E. coli for efficient production of glycolic acid from glucose," *Biochem. Eng. J.*, vol. 103, pp. 256–262, 2015.

[15] S. Schünemann, F. Schüth, and H. Tueysuez, "Selective Glycerol Oxidation over Ordered Mesoporous Copper Aluminum Oxide Catalysts," *Catal. Sci. Technol.*, vol. 7, pp. 5614–5624, 2017.

[16] J. E. N. Brainer, D. C. S. Sales, E. B. M. Medeiros, N. M. Lima Filho, and C. A. M. Abreu, "Wet oxidation of glycerol into fine organic acids: Catalyst selection and kinetic evaluation," *Brazilian J. Chem. Eng.*, vol. 31, no. 4, pp. 913–923, 2014.

[17] E. Sproge *et al.*, "Production of glycolic acid from glycerol using novel fine-disperse platinum catalysts," *IOP Conf. Ser. Mater. Sci. Eng.*, vol. 77, no. 1, pp. 2–6, 2015.

[18] S. Schünemann, F. Schüth, and H. Tueysuez, "Selective Glycerol Oxidation over Ordered Mesoporous Copper Aluminum Oxide Catalysts," *Catal. Sci. Technol.*, vol. 7, pp. 5614–5624, 2017.

[19] E. Skrzyńska, S. Zaid, A. Addad, J.-S. Girardon, M. Capron, and F. Dumeignil, "Performance of Ag/Al $_2$ O $_3$ catalysts in the liquid phase oxidation of glycerol – effect of preparation method and reaction conditions," *Catal. Sci. Technol.*, vol. 6, no. 9, pp. 3182–3196, 2016.

[20] E. Skrzyńska, S. Zaid, J. S. Girardon, M. Capron, and F. Dumeignil, "Catalytic behaviour of four different supported noble metals in the crude glycerol oxidation," *Appl. Catal. A Gen.*, vol. 499, pp. 89–100, 2015.

[21] Y. S. Talnikar, Vivek Digambar; Mahajan, "Recovery of acids from dilute streams: A review of process technologies," *Korean J. Chem. Eng.*, vol. 31, no. 10, pp. 1720–1731, 2014.

[22] K. Staszak, M. J. Wozniak, Z. A. Karas, J. Staniewski, and K. Prochaska, "Application of

nanofiltration in the process of the separation of model fermentation broths components," *Polish J. Chem. Technol.*, vol. 15, no. 4, pp. 1–4, 2013.

[23] P. A. Sosa, C. Roca, and S. Velizarov, "Membrane assisted recovery and purification of bio-based succinic acid for improved process sustainability," *J. Memb. Sci.*, vol. 501, pp. 236–247, 2016.

[24] M. Szczygiełda, J. Antczak, and K. Prochaska, "Separation and concentration of succinic acid from post-fermentation broth by bipolar membrane electrodialysis (EDBM)," *Sep. Purif. Technol.*, vol. 181, pp. 53–59, 2017.

[25] D. A. Glassner and R. Datta, "Proces for the production and purification of succinic acid," 1992.

[26] K. Baruah and S. Hazarika, "Separation of acetic acid from dilute aqueous solution by nanofiltration membrane," *J. Appl. Polym. Sci.*, vol. 131, no. 15, p. n/a-n/a, 2014.

[27] M. P. Zacharof, S. J. Mandale, P. M. Williams, and R. W. Lovitt, "Nanofiltration of treated digested agricultural wastewater for recovery of carboxylic acids," *J. Clean. Prod.*, vol. 112, pp. 4749–4761, 2016.

[28] L. Ahsan, M. S. Jahan, and Y. Ni, "Recovering/concentrating of hemicellulosic sugars and acetic acid by nanofiltration and reverse osmosis from prehydrolysis liquor of kraft based hardwood dissolving pulp process," *Bioresour. Technol.*, vol. 155, pp. 111–115, 2014.

[29] H. Lyu *et al.*, "Monophenols separation from monosaccharides and acids by two-stage nanofiltration and reverse osmosis in hydrothermal liquefaction hydrolysates," *J. Memb. Sci.*, vol. 504, pp. 141–152, 2016.

[30] X. Wang, Y. Wang, X. Zhang, H. Feng, and T. Xu, "In-situ combination of fermentation and electrodialysis with bipolar membranes for the production of lactic acid: Continuous operation," *Bioresour. Technol.*, vol. 147, pp. 442–448, 2013.

[31] N. K. Zaman, J. Y. Law, P. V. Chai, R. Rohani, and A. W. Mohammad, "Recovery of organic acids from fermentation broth using nanofiltration technologies: A review," *J. Phys. Sci.*, vol. 28, pp. 85–109, 2017.

[32] C. S. López-Garzón and A. J. J. Straathof, "Recovery of carboxylic acids produced by fermentation," *Biotechnol. Adv.*, vol. 32, no. 5, pp. 873–904, 2014.

[33] C. Fernandez-Gonzalez, A. Dominguez-Ramos, R. Ibañez, and A. Irabien, "Electrodialysis with Bipolar Membranes for Valorization of Brines," *Sep. Purif. Rev.*, vol. 45, no. 4, pp. 275–287, 2016.

[34] Q. Z. Li *et al.*, “Recovery processes of organic acids from fermentation broths in the biomass-based industry,” *J. Microbiol. Biotechnol.*, vol. 26, no. 1, pp. 1–8, 2015.

[35] J. B. McKinlay, C. Vieille, and J. G. Zeikus, “Prospects for a bio-based succinate industry,” *Appl. Microbiol. Biotechnol.*, vol. 76, no. 4, pp. 727–740, 2007.

[36] M. I. Gonzalez, S. Alvarez, F. A. Riera, and R. Alvarez, “Purification of Lactic Acid from Fermentation Broths by Ion-Exchange Resins,” pp. 3243–3247, 2006.

[37] M. J. Dethe, K. V Marathe, and V. G. Gaikar, “Adsorption of Lactic Acid on Weak Base Polymeric Resins,” *Sep. Sci. Technol.*, vol. 41, no. 2, pp. 2947–2971, 2007.

[38] B. G. Garrett, K. Srinivas, and B. K. Ahring, “Performance and stability of Amberlite TM IRA-67 ion exchange resin for product extraction and pH control during homolactic fermentation of corn stover sugars,” *Biochem. Eng. J.*, vol. 94, pp. 1–8, 2015.

[39] S. Rebecchi, D. Pinelli, L. Bertin, F. Zama, F. Fava, and D. Frascari, “Volatile fatty acids recovery from the effluent of an acidogenic digestion process fed with grape pomace by adsorption on ion exchange resins,” *Chem. Eng. J.*, vol. 306, pp. 629–639, 2016.

[40] M. Bishai, S. De, B. Adhikari, and R. Banerjee, “A platform technology of recovery of lactic acid from a fermentation broth of novel substrate Zizyphus oenophlia,” *3 Biotech*, vol. 5, no. 4, pp. 455–463, 2015.

[41] B. Davison, N. Nghiem, and G. Richardson, “Succinic Acid Adsorption from Fermentation Broth and Regeneration,” *Appl. Biochem. Biotechnol.*, vol. 113, 2004.

[42] S. M. Husson and C. J. King, “Multiple-Acid Equilibria in Adsorption of Carboxylic Acids from Dilute Aqueous Solution,” *Ind. Eng. Chem. Res.*, vol. 425, pp. 502–511, 1999.

[43] L. A. Tung and C. J. King, “Sorption and Extraction of Lactic and Succinic Acids at pH > pKa1 . Factors Governing Equilibria,” *Ind. Eng. Chem. Res.*, pp. 3217–3223, 1994.

[44] M. Piassi, L. Fontes, D. Cristina, and J. Contiero, “L-(+)- Lactic acid production by Lactobacillus rhamnosus B103 from dairy industry waste,” *Brazilian J. Microbiol.*, vol. 2, no. 2, pp. 4–10, 2016.

[45] P. G. Æ. T. Jamroz and Æ. B. S. Æ. S. Ledakowicz, “Equilibrium and dynamic investigations of organic acids adsorption onto ion-exchange resins,” pp. 185–190, 2004.

[46] C. S. López-garzón, L. A. M. Van Der Wielen, and A. J. J. Straathof, “Green upgrading of succinate using dimethyl carbonate for a better integration with fermentative production,” *Chem. Eng. J.*, vol. 235, pp. 52–60, 2014.

[47] K. Zhang and S. Yang, “In situ recovery of fumaric acid by intermittent adsorption with IRA-900 ion exchange resin for enhanced fumaric acid production by Rhizopus oryzae,” *Biochem. Eng. J.*, vol. 96, pp. 38–45, 2015.

[48] Q. Li, J. Xing, W. Li, Q. Liu, and Z. Su, “Separation of Succinic Acid from Fermentation Broth Using Weak Alkaline Anion Exchange Adsorbents,” *Ind. Eng. Chem. Res.*, vol. 63, pp. 3595–3599, 2009.

[49] T. Rampai, S. Thitiprasert, W. Boonkong, K. Kodama, V. Tolieng, and N. Thongchul, “Improved lactic acid productivity by simultaneous recovery during fermentation using resin exchanger,” *Ind. Eng. Chem. Res.*, vol. 21, no. 1, pp. 193–199, 2016.

[50] A. Yousuf, F. Bonk, J. R. Bastidas-Oyanedel, and J. E. Schmidt, “Recovery of carboxylic acids produced during dark fermentation of food waste by adsorption on Amberlite IRA-67 and activated carbon,” *Bioresour. Technol.*, vol. 217, pp. 137–140, 2016.

[51] Z. Sheng, B. Tingting, C. Xuanying, W. Xiangxiang, and L. Mengdi, “Separation of Succinic Acid from Aqueous Solution by Macroporous Resin Adsorption,” *J. Chem. Eng. Data*, vol. 2, no. 21, p. 9, 2016.

[52] W. Tong *et al.*, “Purification of L(+)-lactic acid from fermentation broth with paper sludge as a cellulosic feedstock using weak anion exchanger Amberlite IRA-92,” *Biochem. Eng. J.*, vol. 18, pp. 89–96, 2004.

[53] S. Kumar and B. Babu, “Separation of carboxylic acids from waste water via reactive extraction,” *Int. Conv. Water*, pp. 1–9, 2008.

[54] D. Datta, S. Kumar, and H. Uslu, “Status of the Reactive Extraction as a Method of Separation,” *J. Chem.*, vol. Volume 201, no. i, pp. 1–16, 2014.

[55] D. Verser and T. Eggeman, “Recovery of organic acids.” 2009.

[56] S. J. KLEIBER Michael, GNABS Ulrike, “Method for purifying carboxylic acids from fermentation broths,” 2016.

[57] Y. K. Hong, W. H. Hong, and D. H. Han, “Application of reactive extraction to recovery of carboxylic acids,” *Biotechnol. Bioprocess Eng.*, vol. 6, pp. 386–394, 2001.

[58] A. Qader and M. A. Hughes, “Extraction equilibria of acetic and propionic acids from dilute aqueous solution by several solvents,” *Sep. Sci. Technol.*, vol. 27, no. 13, pp. 1809–1821, 1992.

[59] W. Cai, S. Zhu, and X. Piao, “Extraction equilibria of formic and acetic acids from aqueous solution by phosphate-containing extractants,” *J. Chem. Eng. Data*, vol. 46, no. 6, pp. 1472–

1475, 2001.

[60] T. Hano, M. Matsumoto, T. Ohtake, K. Sasaki, F. Hori, and Y. Kawano, “Extraction equilibria of organic acids with tri-n-octylphosphineoxide,” *Journal of Chemical Engineering of Japan*, vol. 23, no. 6. pp. 734–738, 1990.

[61] J. M. Wardell and C. J. King, “Solvent Equilibria for Extraction of Carboxylic Acids from Water,” *J. Chem. Eng. Data*, vol. 23, no. 2, pp. 144–148, 1978.

[62] K. L. Wasewar, A. A. Yawalkar, J. A. Moulijn, and V. G. Pangarkar, “Fermentation of Glucose to Lactic Acid Coupled with Reactive Extraction: A Review,” *Ind. Eng. Chem. Res.*, vol. 43, no. 19, pp. 5969–5982, 2004.

[63] A. S. Kertes and C. J. King, “Extraction chemistry of fermentation product carboxylic acids,” *Biotechnol. Bioeng.*, vol. 28, no. 2, pp. 269–282, 1986.

[64] S. Kumar and B. V Babu, “Process Intensification for Separation of Carboxylic Acids from Fermentation Broths using Reactive Extraction,” *J. Futur. Eng. Technol.*, vol. 3, no. 3, pp. 19–26, 2008.

[65] S. T. Yang, S. A. White, and S. T. Hsu, “Extraction of Carboxylic Acids with Tertiary and Quaternary Amines: Effect of pH,” *Ind. Eng. Chem. Res.*, vol. 30, no. 6, pp. 1335–1342, 1991.

[66] S. Uenoyama, T. Hano, M. Hirata, and S. Miura, “Extraction Kinetics of Organic Acids with Tri-n- octylphosphine Oxide,” *J. Chem. Technol. Biotechnol.*, vol. 67, pp. 260–264, 1996.

[67] H. Honda, Y. Toyama, H. Takahashi, T. Nakazeko, and T. Kobayashi, “Effective lactic acid production by two-stage extractive fermentation,” *J. Ferment. Bioeng.*, vol. 79, no. 6, pp. 589–593, 1995.

[68] D. H. Han and W. H. Hong, “Water-Enhanced Solubilities of Lactic Acid in Reactive Extraction Using Trioctylamine / Various Active Diluents Systems,” *Sep. Sci. Technol.*, no. December 2014, pp. 271–281, 1998.

[69] K. L. Wasewar, A. B. M. Heesink, G. F. Versteeg, and V. G. Pangarkar, “Equilibria and kinetics for reactive extraction of lactic acid using Alamine 336 in decanol,” *J. Chem. Technol. Biotechnol.*, vol. 1075, no. January, pp. 1068–1075, 2002.

[70] S. Eda, P. Rajarathinam, and P. Kumar, “Reactive Extraction of Succinic Acid from Aqueous Solutions using Tri-N- Octylamine (TOA) in 1-Decanol : Equilibria and Effect of temperature,” *Int. J. Chem. Sep. Technol.*, vol. 2, no. 24, p. 11, 2015.

[71] G. K. Agrahari, N. Pandey, N. Verma, and P. K. Bhattacharya, “Membrane contactor for

reactive extraction of succinic acid from aqueous solution by tertiary amine," *Chem. Eng. Res. Des.*, vol. 92, no. 11, pp. 2705–2714, 2014.

[72] M. Henczka and M. Djas, "Reactive extraction of succinic acid using supercritical carbon dioxide," *Sep. Sci. Technol.*, vol. 1, no. 49, pp. 1–7, 2017.

[73] S. Eda, "Recovery of Succinic acid by Reactive Extraction using using Tri-n-Octylamine in 1-Decanol : Equilibrium Optimization Using response surface method and kinetic studies," *Int. J. Chem. Sep. Technol.*, vol. 2, no. 2, p. 13, 2016.

[74] D. Datta, Y. S. Aşçı, and A. F. Tuyun, "Extraction Equilibria of Glycolic Acid Using Tertiary Amines: Experimental Data and Theoretical Predictions," *J. Chem. Eng. Data*, p. acs.jced.5b00497, 2015.

[75] D. Datta and S. Kumar, "Modeling Using Response Surface Methodology and Optimization Using Differential Evolution of Reactive Extraction of Glycolic Acid," *Chem. Eng. Commun.*, vol. 2, no. 1, pp. 37–41, 2014.

[76] T. Granstrom, J. Ahola, J. Hietala, and E. Tirronen, "Method for recovering and purifying propionic acid." 2015.

[77] M. Henczka and M. Djas, "Reactive extraction of acetic acid and propionic acid using supercritical carbon dioxide," *J. Supercrit. Fluids*, vol. 110, pp. 154–160, 2016.

[78] B. G. Garrett, K. Srinivas, and B. K. Ahring, "Design and optimization of a semi-continuous high pressure carbon dioxide extraction system for acetic acid," *J. Supercrit. Fluids*, vol. 95, pp. 243–251, 2014.

[79] N. Kapucu, A. Guvenc, A. Mehmetoglu, and A. Calimli, "REACTIVE EXTRACTION OF ORGANIC ACIDS BY SUPERCRITICAL CO2," *Rev. Chem. Eng.*, vol. 15, no. 4, pp. 233–244, 1999.

[80] A. Rahmanian and H. S. Ghaziaskar, "Selective extraction of maleic acid and phthalic acid by supercritical carbon dioxide saturated with trioctylamine," *J. Supercrit. Fluids*, vol. 46, pp. 118–122, 2008.

[81] H. S. Ghaziaskar and M. Kaboudvand, "Solubility of trioctylamine in supercritical carbon dioxide," *J. Supercrit. Fluids*, vol. 44, pp. 148–154, 2008.

[82] S. Kesonen, "Recovery of carboxylic acids from aqueous streams by extraction and back extraction," Lappeenranta university of technology, 2013.

[83] K. L. Wasewar, "Reactive Extraction : An Intensifying Approach for Carboxylic Acid Separation," *Int. J. Chem. Eng. Appl.*, vol. 3, no. 4, 2012.

[84] A. Keshav and K. L. Wasewar, “Back extraction of propionic acid from loaded organic phase,” *Chem. Eng. Sci.*, vol. 65, no. 9, pp. 2751–2757, 2010.

[85] L. J. Poole and C. J. King, “Regeneration of Carboxylic Acid-Amine Extracts by Back-Extraction with an Aqueous Solution of a Volatile Amine,” vol. 336, pp. 923–929, 1991.

[86] J. Mcmorris and S. M. Husson, “Gas antisolvent-induced regenaration of lactic acid-laden extractants,” *Sep. Sci. Technol.*, vol. 36, no. 6, pp. 1129–1148, 2007.

[87] V. D. Talnikar and Y. S. Mahajan, “Recovery of acids from dilute streams : A review of process technologies,” *Korean J. Chem. Eng.*, vol. 31, no. 10, pp. 1720–1731, 2014.

[88] R. Kumar, S. M. Mahajani, H. Nanavati, and S. B. Noronha, “Recovery of lactic acid by batch reactive distillation,” vol. 1150, no. June 2005, pp. 1141–1150, 2006.

[89] A. Komesu, M. R. Wolf Maciel, J. A. Rocha de Oliveira, L. H. da Silva Martins, and R. Maciel Filho, “Purification of Lactic Acid Produced by Fermentation: Focus on Non-traditional Distillation Processes,” *Sep. Purif. Rev.*, vol. 46, no. 3, pp. 241–254, 2017.

[90] K. D. Patil and B. D. Kulkarni, “Review of Recovery Methods for Acetic Acid from Industrial Waste Streams by Reactive Distillation,” *J. Water Pollut. Purif. Res.*, vol. 1, no. 2, pp. 13–18, 2014.

[91] A. Komesu, P. F. M. Martinez, B. H. Lunelli, R. M. Filho, and M. R. W. Maciel, “Lactic acid purification by reactive distillation system using design of experiments,” *Chem. Eng. Process. Process Intensif.*, vol. 95, pp. 26–30, 2015.

[92] A. Singh, A. Tiwari, S. M. Mahajani, and R. D. Gudi, “Recovery of Acetic Acid from Aqueous Solutions by Reactive Distillation,” pp. 2017–2025, 2017.

[93] D. Painer, S. Lux, and M. Siebenhofer, “Recovery of Formic Acid and Acetic Acid from Waste Water Using Reactive Distillation,” *Sep. Sci. Technol.*, vol. 50, no. 18, 2015.

[94] L. Zheng, W. Cai, X. Zhang, and Y. Wang, “Process Intensi fi cation Design and control of reactive dividing-wall column for the synthesis of diethyl carbonate,” *Chem. Eng. Process. Process Intensif.*, vol. 111, pp. 127–140, 2017.

[95] M. M. Donahue, B. J. Roach, J. J. Downs, T. Blevins, M. Baldea, and R. B. Eldridge, “Process Intensification Dividing wall column control : Common practices and key findings,” *Chem. Eng. Process. Process Intensif.*, vol. 107, pp. 106–115, 2016.

[96] T. D. Nguyen, “Conceptual design, simulation and experimental validation of divided wall column: application for nonreactive and reactive mixture,” Institut national polytechnique de Toulouse, 2015.

[97] L. O. Z. Dejanovic,I; Matijasevic, “Dividing wall column — A breakthrough towards sustainable distilling,” *Chem. Eng. Process. Process Intensificatio*, vol. 49, pp. 559–580, 2010.

[98] N. Asprion and G. Kaibel, “Dividing wall columns : Fundamentals and recent advances,” *Chem. Eng. Process. Process Intensif.*, vol. 49, no. 2, pp. 139–146, 2010.

Chapter 2. Experimental and Analytical methods

The development of the strategy of separation and purification of carboxylic acids produced from glycerol oxidation was carried out in four main stages. Figure 2-1 presents the main blocks of this research carried out throughout this thesis. The selection and analysis of the process implementation was made considering three scenarios in which different alcohols are used. Throughout this chapter, we will present the methodology in details applied for the case of the model system, esterification reaction of glycolic acid and butanol.

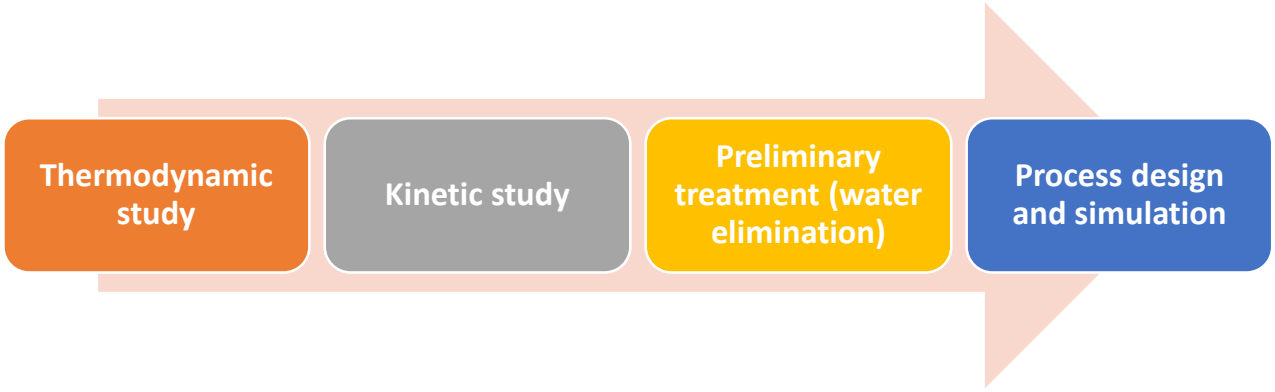

Figure 2-1. Overview of thesis development

2.1 *Thermodynamic study*

The thermodynamic study was carried out for the different binaries that are part of the reaction systems between glycolic acid with propanol, butanol and octanol.

2.1.1 Vapor-liquid and Liquid- liquid equilibrium

2.1.1.1 Materials

Butyl glycolate (BG, >95%, Sigma-Aldrich), n-butanol (BuOH, Alpha Aeser), water (W, HPLC grade) and acetonitrile (ACN, HPLC grade, EMD) were used to conduct the experiments. The purity of the products was confirmed by gas chromatography to determine the presence of impurities. Traces of impurities were presented in butyl glycolate. KF Hydranal-coulomat E (Riedel-de Haën) solution to determine the presence of impurities in acetonitrile. Traces of water were the only impurities detected in acetonitrile.

BG was further purified by vacuum distillation up to 99% purity. Only 85-90% of the pre-distilled volume was used for the experiments, discarding the first fraction (5-10%) and the reboiler residue (5%).

Due to the non-availability of the propyl glycolate and octyl glycolate, they were produced using the following process: the first stage consisted of the synthesis of esters using homogeneous catalysis following the procedure below:

- The reactants are placed in a 250 mL three-necked flask. The three-necked flask; open to the atmosphere and equipped with a cooling system, is placed in an oil bath under magnetic stirring. First, both reactants are solubilized at temperature between 50 and 60 °C, depending on the alcohol. After the sulfuric acid is added, the reaction is stirred overnight (16h) under reflux at constant temperature. The reaction temperature was fixed at 80°C. Once the solution is recovered, it is transferred into a flask and treated. Figure 2-2 presents the process of recovery and purification of esters. To neutralize the sulfuric acid, 5.00 mL of 2M NaOH solution must be added. The pH of the solution to be treated is measured (generally, between 1 and 2). The addition is complete when the pH is between 5 and 7. The additional volume of NaOH solution, higher than the calculated value (5.00 mL), corresponds to the volume necessary to neutralize the amount of remaining glycolic acid. The solution is transferred to a decanter. About 20 to 30 mL of ethyl acetate are added. Ethyl acetate is added to the flask in order to extract the organic phase in which the product is present. The solution is allowed to decant and both the aqueous phase (bottom) and the organic phase (top) are recovered. When the esterification reaction is carried out with propanol, dichloromethane was used as extraction solvent, and the order of the phases in the decanter is reversed. The organic phase was dried by adding $MgSO_4$ and then filtered in order to remove the solvent and excess alcohol. The evaporation was carried out under the vacuum and with moderate heating. To confirm purity, the products were further purified by vacuum distillation up to 99% purity. Only 85-90% of the pre-distilled volume was used for the experiments, discarding the first fraction (5-10%) and the reboiler residue (5%). The purity of the products was confirmed by gas chromatography and mass spectroscopy.

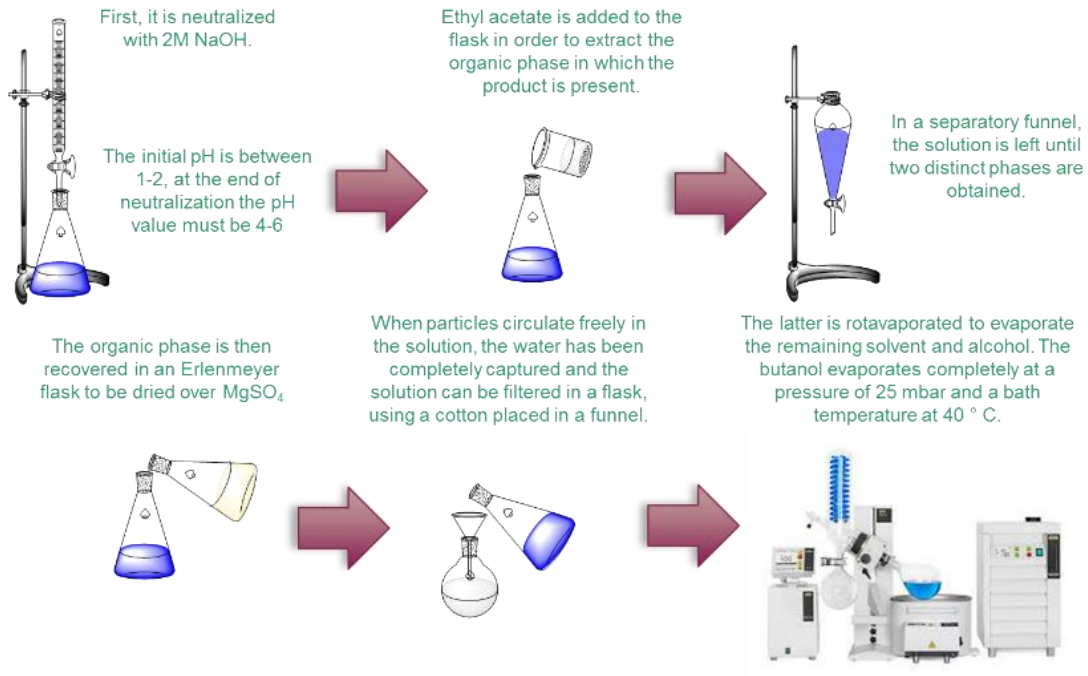

Figure 2-2. Purification and recovery process of esters.

To monitor the reaction, thin layer chromatography (TLC) with silica gel was used. The mobile phase consisted of ethyl acetate and petroleum ether in the ratio of 30:70 (v/v). The spots were detected using a potassium permanganate solution ($KMnO_4$) and the subsequent heating of the sheet.

2.1.1.2 Experimental procedures

2.1.1.2.1 Vapor pressure measurement

T-P data for the propyl glycolate, butyl glycolate and octyl glycolate were measured in the VLLE602 FISCHER® LABODEST® unit. The accuracy of the temperature measurements was ± 0.05°C and the pressure control ± 0.1mbar. 80 to 90 mL of the sample were used for the measurements. The measurements were made in ascending order of pressure from 100 to 1013.25 mbar. Before taking the measurements, the system was purged with helium. The validation of the vapor pressure determination technique was done with water.

2.1.1.2.2 Vapor-liquid equilibrium experiments

T-x-y equilibrium data for the BG and the BuOH systems were measured in the VLLE602 FISCHER® LABODEST® unit operating on the recirculation principle. The accuracy of the

temperature measurements was ± 0.05 °C and the pressure control ± 0.1 mbar. For the validation of the equipment, the ethanol-water equilibrium for which there are numerous data in the literature, was initially measured. Once the equipment was successfully validated, the other experiments were started. The total volume of the mixture must be at least 80 mL. Once the mixture is loaded, the system is purged with helium. 40 µL were taken from each sample and diluted with 1 mL of 42-58% volume of W-ACN.

2.1.1.2.3 Liquid-liquid equilibrium experiments

BG-W liquid-liquid equilibrium data for binary mixtures were determined using magnetically agitated (30 cm^3) vials. The vials were placed in an isothermal oil bath equipped with a temperature control system. The liquid mixtures were stirred at a constant temperature for 1 hour. After reaching equilibrium, the temperature inside the vial was measured with an electronic thermocouple (± 0.1°C). The samples were centrifuged for 2 minutes at 4000 rpm. The lower phase was recovered with a syringe and the weight of each phase was recorded. The difference between the total initial mass and that of the two phases was checked and was less than 1% (mass) for all experiments. A sample of 400 µL was taken and weighed from each phase for analysis. The samples were diluted in 10 mL volumetric balloons with a solution of 42-58 % volume W-ACN.

The tie lines were obtained by the preparation of ternary mixtures of known global composition within the region of the two phases. Traces of methyl red were added to improve the visualization of the interface. The organic phase preferentially dissolves methyl red causing the ester rich phase to be orange and the aqueous phase to remain colorless or slightly red. The liquid mixtures were stirred at a constant temperature for 12 hours. After balancing the equilibrium, it was centrifuged for 20 minutes at 4000 rpm and returned to the isothermal bath for a further 12 hours.

The lower phase was recovered with a syringe and the weight of each phase was recorded. The difference between the total initial mass and that of the two phases was checked and was less than 1% (mass) for all experiments. From each phase, a sample of 400 µL was withdrawn and weighed for analysis. The samples were diluted in 10 mL volumetric balloons with a solution of 42-58 % volume W-ACN.

2.1.1.3 Parameter adjustment

The binary parameters of the different systems studied were determined following the methodology presented in Figure 2-3.

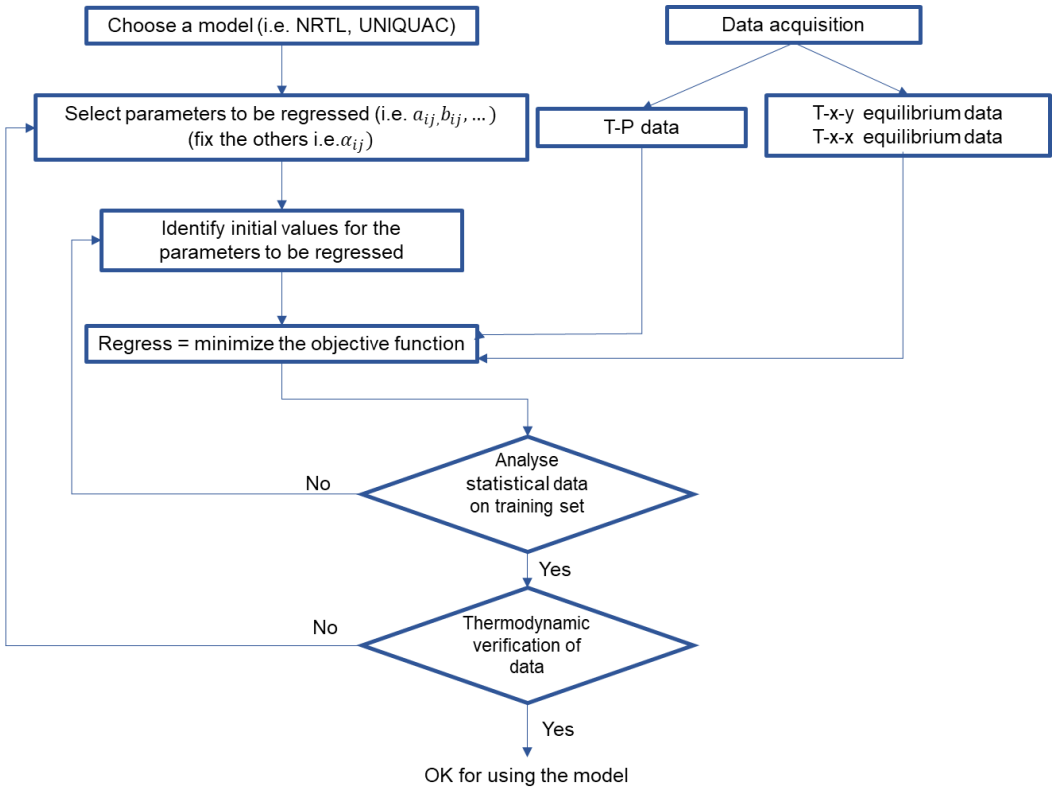

Figure 2-3. Methodology for regressing and validating a model using experimental data. Modified scheme[1]

In order to adjust the parameters of the different existing thermodynamic models and experimental data, Aspen Plus® uses different types of objective functions which depend on the type of information supplied to the software and the information required. For VLE, regression normally considers the bubble pressure or bubble temperature as the target variable (eq 2.1) [1].

$$F_{Obj} = \frac{1}{n_{exp}} \sum_i^{n_{exp}} \left(\frac{P_i^{cal}(C,p) - P_i^{exp}}{P_i^{exp}} \right)^2 \quad (2.1)$$

Where P_i^{cal} and P_i^{exp} are the pressure values determined from the regression and the measured value, respectively, and n_{exp} is the number of experiments performed.

The analysis of the results obtained, and the verification of their validity were carried out considering variance and standard deviation. However, the most commonly used are the average

absolute deviation in percentage (eq 2.2) that corresponds to the unbiased measurement of the same variable (the number of experimental points with weights other than zero) and the Root mean square error in percentage (eq 2.3), which is the maximum likelihood estimate when the population is normally distributed.

$$AAD = \frac{1}{k}\sum_{i=1}^{k}\left|\frac{Z_i - ZM_i}{ZM_i}\right| \tag{2.2}$$

$$RMSE = \left[\frac{1}{k}\sum_{i=1}^{k}\left(\frac{Z_i - ZM_i}{ZM_i}\right)^2\right]^{1/2} \tag{2.3}$$

Where Z is a regressed property value, ZM is the corresponding experimental value from the data set, and k is the number of data points.

When data regression is carried out with aspen, statistical verification of the entire process is carried out by means of value analysis of weighted sum-of-squares error, it is defined as:

$$\sum_{l=1}^{g} wl\left[\sum_{i=1}^{k}\sum_{j=1}^{m}\left(\frac{Z_{ij} - ZM_{ij}}{\sigma_{ij}}\right)^2\right]_l \tag{2.4}$$

Where ZM is the measured (experimental) value, Z is the calculated value, σ is the standard deviation, w is the weighting factor for a data group, l is the data group number in the regression case, g is the total number of data groups used, i is the data point number within a data group, k is the total number of points in a data group, j is measured variable for a data point (such as temperature, pressure, or mole fraction) and m is number of measured variables for a data point.

And with residual root-mean-square error, it is defined as:

$$RRMS = \sqrt{\frac{weighted\ sum\ of\ squares}{K-n}} \tag{2.5}$$

Where K is the total number of data points in all groups an n is the total number of parameters.

2.1.2 Solid - liquid equilibrium

2.1.2.1 Materials

Glycolic acid (GA, 98%, Alpha Easer), Butyl glycolate (BG, >95%, Sigma-Aldrich), n-butanol (BuOH, >99.5%, Alpha Easer), water (W, HPLC grade) and acetonitrile (ACN, HPLC grade, EMD) were used to conduct the experiments. The purity of the products was tested by gas chromatography. Traces of impurities were presented in butyl glycolate. Karl-Fisher (Hydranal-coulomat E (Riedel-de Haën) solution) was applied to determine water presence in acetonitrile. Traces of water were the only impurities detected in acetonitrile. BG was further purified by

vacuum distillation up to 99% purity. Only 85-90 % of the pre-distilled volume was used for the experiments, discarding the first fraction (5-10 %) and the reboiler residue (5 %).

2.1.2.2 Experimental procedures

2.1.2.2.1 Solubility

The determination of GA solubility in BG, BuOH and W was carried out in a closed glass vial (30 cm^3) and agitated with a magnetic bar for a period of 1h. The amount of GA in each vial had to exceed the solubility limits as a function of temperature in order to ensure the saturation of the liquid phase. These vials were placed in an isothermal oil bath equipped with a temperature control system. The temperature was measured with an electronic thermocouple (± 0.1 °C) inside the vial after agitation. The liquid phases were recovered and subjected to a centrifugation process at 4000 rpm for 2 minutes to precipitate the suspended crystals. A sample of 400 µL was withdrawn and weighed for analysis. The samples were diluted in 10 mL volumetric balloons with a solution of 42-58 % volume W-ACN. The samples were analyzed by HPLC.

2.1.2.2.2 Calorimetric Analysis

The calorimetric measurements were done using differential scanning calorimetry at atmospheric pressure (Discovery DSC, Thermal Analyzers). Prior to analysis, samples of about 8 mg were weighed (Sartorius Analytical Balances) and heated to remove residual water from the sample. This was achieved using hermetically sealed aluminum crucibles at 2 °C.min^{-1} under nitrogen flow (20 cm^3.min^{-1}) within a temperature range of -50.00 to 250.00 °C. The equilibrium time at the initial and final temperature of 4 minutes was used. The procedure was repeated at least twice to observe changes in the sample during calorimetric analysis.

The calorimetric analysis was carried out after a vacuum drying process of glycolic acid at 50.00 °C for approximately 4h. The verification of the equipment was validated from the calorimetric analysis carried out on the medium. The deviation of the fusion temperature was ±1 °C. The first calorimetric data of the DSC at atmospheric pressure presented dispersion mainly at high temperatures, so it was only decided to preheat the sample and reduce the rate of heating.

2.1.2.3 Parameter adjustment

The determination of the binary parameters of the NRTL model was carried out using MATLAB 9.4. Figure 2-4 presents the block diagram of the MATLAB 9.4 program (see ANNEX D).

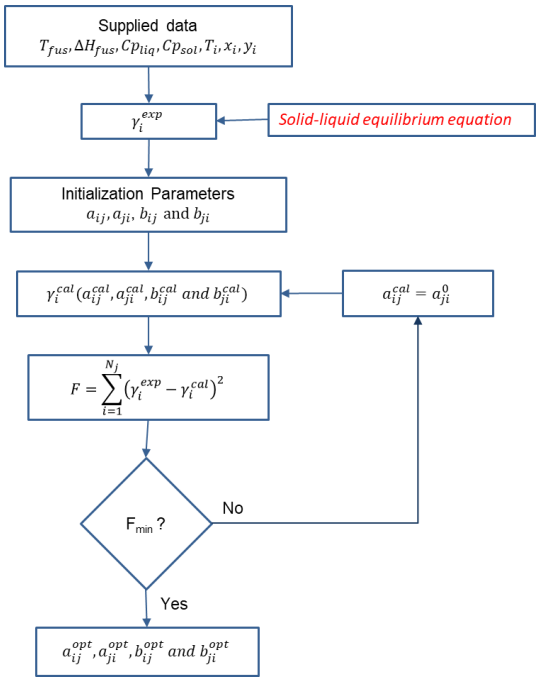

Figure 2-4. Regression process of binary parameters using the NRTL model for solid-liquid equilibrium.

2.2 *Kinetic study*

The kinetic study of the esterification reaction of glycolic acid with different alcohols (*i.e.* propanol, butanol and octanol) in the presence of homogeneous and heterogeneous catalysis was carried out following the methodology presented in section number 2.1.

2.2.1 Homogeneous and heterogeneous catalysis

2.2.1.1 Materials

Glycolic acid (GA, 98%, Alpha Easer), formic acid (FA, 99%, Alpha Easer), n-propanol (PrOH, >99.5%, Alpha Aeser), n-butanol (BuOH, >99.5%, Alpha Aeser), Octanol (OcOH, >99.5%, Alpha Aeser), water (W, HPLC grade) and acetonitrile (ACN, HPLC grade, EMD) were used to conduct the experiments. The purity of the products was tested by gas chromatography. Karl-Fisher Hydranal-coulomat E (Riedel-de Haën) solution was applied to determine the presence of impurities in acetonitrile. Traces of water were the only impurities detected in acetonitrile.

As a homogeneous catalyst, sulfuric acid (95-98 % purity, Sigma Aldrich) was chosen and as heterogeneous catalysts, some ion exchange resins available in the market were chosen. In total, five cation-exchange resins were used for comparing the homogenous with heterogeneous catalysts. Amberlyst 15, Amberlyst 16, Amberlyst 36, Nafion and Dowex, acid cation-exchange

resin, were manufactured by Sigma Aldrich. The resins were dried at 80.00 °C before use. Nafion, acid cation-exchange resin, was manufactured by Alfa Aesar.

2.2.1.2 Experimental procedures

2.2.1.2.1 Catalytic test

The kinetics of glycolic acid esterification was carried out in a three-necked flask of 250 mL capacity, open to the atmosphere and equipped with a cooling system, and placed in an oil bath under magnetic stirring. The reaction temperature was controlled within ±0.50 °C by locating the flask in an oil bath. First, both reactants were solubilized at a temperature between 50 and 60 °C, depending on the alcohol. The sampling "t0" is carried out just before the reaction begins, meaning that when the temperature of the reactant mixture is slightly lower, the reaction temperature (± 2.00 °C) and the catalyst is added. After which, the reaction is stirred at least for 4h under reflux at constant temperature. The samples are taken at 10, 20 and 30 minutes after t0 and then every hour for 4 hours.

2.2.1.2 Analytical techniques

Several techniques were used for the quantification of the reactants and products of the reaction in aqueous and organic phase.

2.2.1.2.1 High-performance liquid chromatography (HPLC)

High performance liquid chromatograph (HPLC- SHIMADZU) with refractive index detector (RID) was used as the main analytical technique. The HPLC was equipped with a column Luna Omega C18 (octadecyl, inverse phase), 250 mm in length,4.6 mm as an internal diameter, and a particle size of 5 µm. The mobile phase was acetonitrile/water 58-42 (%v/v) acidified 0.06 g L^{-1} with respect to water, at a constant flow rate of 0.5 $mL.min^{-1}$. The column oven temperature was kept constant at 30°C. The volume injected for each analysis was 10 µL. The samples were diluted in a solution of equal concentration of the mobile phase, without acidifying. The calibration of the products was carried out in triplicates to obtain the repeatability within 0.5 % in moles. Table 2-1 presents the different mobile phases and the time of analysis according to the type of alcohol used.

Table 2-1. Mobile phase according to the type of alcohol

	Glycolic acid	Formic acid
Propanol	50-50 % (v/v) W-ACN (15 min)	50-50 % (v/v) W-ACN (20 min)
Butanol	42-58 % (v/v) W-ACN (15 min)	42-58 % (v/v) W-CAN (25 min)
Octanol	35-65 % (v/v) W-ACN (20 min)	35-65 % (v/v) W-CAN (30 min)

2.2.1.2.2 Karl fischer

The coulometric water measurement technique Karl-Fisher (KF) was used to measure the water content in reagents and reaction samples. The equipment 831 KF Coulometer Metrohm was used, injecting a mass between 40 and 60 mg.

2.2.1.3 Mass balance

HPLC was chosen to follow the progress of the reaction, quantifying alcohols, acids and esters. On the other hand, KF was used for water quantification. For the quantification, a sample is taken and then diluted in a solution of equal concentration to the mobile phase. The results allowed the determination of the molar distribution during the reaction, from which the conversion, selectivity and yield were calculated.

The calculations were established following the equations:

$$Acid\ conversion\ (\%) = \frac{N_{iacid} - N_{acid}}{N_{iacid}} * 100 \quad (2.6)$$

$$Selectivity\ [\%]: \frac{N_{ester}}{N_{iacid} - N_{acid}} * 100 \quad (2.7)$$

$$Yield\ [\%]: \frac{N_{ester}}{N_{iacid}} * 100 \quad (2.8)$$

Where N_{iacid} and N_{acid}represent the moles of acid at the beginning and after the beginning of the reaction, and N_{ester} corresponds to the moles of formed ester.

The mass balance was determined by calculating the mass fraction of the products quantified in HPLC, this fraction corresponds to the dry base. The water content calculated by KF is added to the calculation of the dry base fraction, and subsequently a normalization is conducted. In this way, the mass distribution of the four products in the mixture was obtained.

Additionally, the carbon balance was established in the following way:

(2.8)

$$Carbon\ balance\ (\%) = \frac{(N_{iacid} * 2) + (N_{iBuOH} * 4) - (N_{acid} * 2) + (N_{BuOH} * 4) + (N_{ester} * 6)}{(N_{iacid} * 2) + (N_{iBuOH} * 4)} * 100$$

The essential criteria were the closure of the total mass and carbon balances, with a permitted variance of ± 5 %.

2.2.1.4 Parameters adjustment of the kinetic model

The adjustment of the kinetic parameters was carried out using MATLAB 9.4. Figure 2-5 presents the flow diagram of the MATLAB 9.4 program for the adjustment of the kinetic model. The program considers as starting point the moles of each of the species i in the different experiments j, and their respective reaction conditions. This information is used together with the activity coefficient data of each of the species to calculate the activities. From the mass balance and the initial values of Ea and $k0$ the values of molar fractions are estimated, these are the values to consider in the objective function. Once the function is minimized, it is considered that the optimal parameters have been obtained.

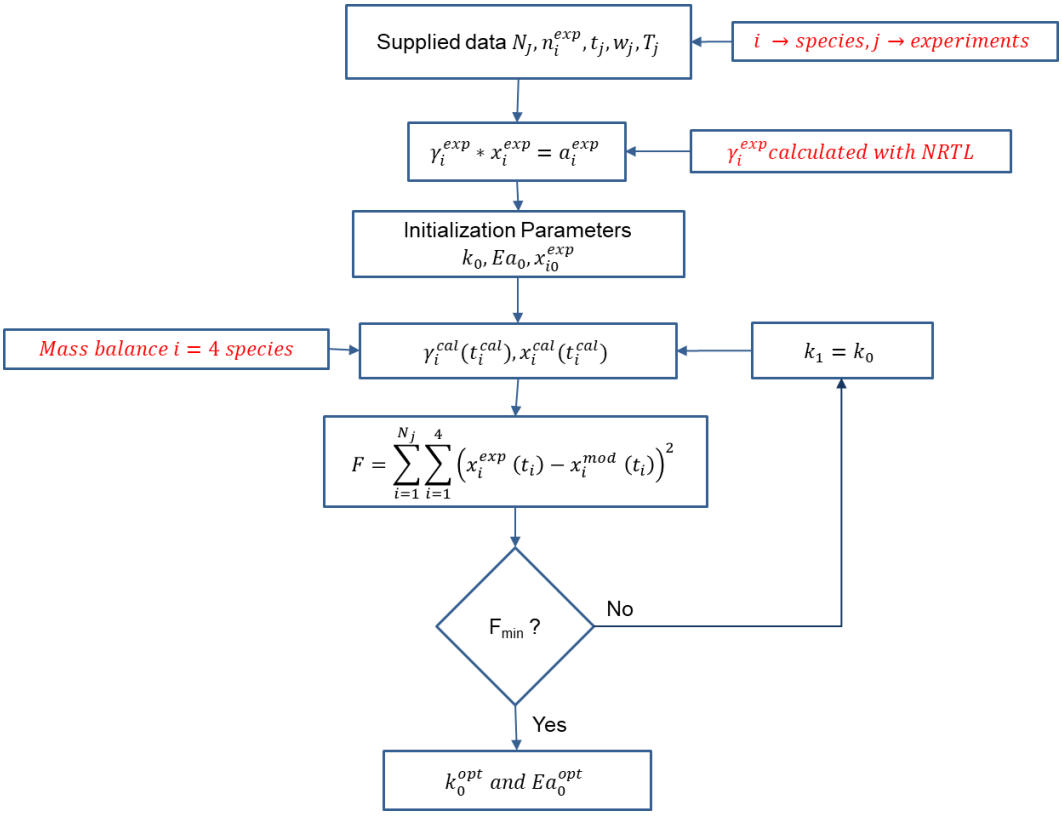

Figure 2-5. Flow diagram for the adjustment of the kinetic model.

2.3 Preliminary treatment (water elimination)

The preliminary treatment was carried out through two experimental stages. First, the preparation of carboxylic acids mixture (initial mixture) *via* glycerol oxidation. Second, the implementation of different separation techniques such as vacuum distillation, simple distillation, and liquid-liquid extraction to reduce the high quantity of water (initially >95wt%) in the carboxylic acid mixture.

2.3.1 Preparation of model mixture

Initial mixture preparation was carried out via glycerol oxidation reaction. Initially, an aqueous solution was prepared using glycerol (purity 99.5% w/w from Alfa Aesar) 0.3 M, the NaOH (reagent grade, purity ≥ 98% procured from Sigma- Aldrich) was adjusted to provide a NaOH/glycerol molar ratio of 4 in a volumetric flask of 200 cm^3.Then, this solution was added to the reactor and 0,5g of the catalyst 5%Ag/$Ce_{0.75}Zr_{0.25}O_2$ prepared in UCCS Laboratory were flushed into the reactor and pressurized with oxygen (5 bar). Glycerol oxidation reaction was prepared in the semi-batch stainless steel reactor at a constant temperature of 100 °C for 5 h at 1000 rpm. For having the same initial conditions in each experiment, a total of 20 batches were mixed in order to obtain a homogeneous distribution of the initial acids.

2.3.2 Analytical method

High-performance liquid chromatography (HPLC- SHIMADZU) with refractive index detector (RID) was used as an analytical method in all techniques mentioned above. For acids quantification, the HPLC was equipped with a column Phenomenex ROA-Organic H^+ (8%) of 300mm in length and an internal diameter of 78mm. The mobile phase was acidified H_2SO_4 (2.5mM) and the flow rate was set at 0.5 mL min^{-1}. The column oven temperature was kept constant at 35 °C. For solvent analysis, Luna Omega C18 (octadecyl, inverse phase) was used in this experiment, length 250mm, the internal diameter of 4.6mm and particle size of 5 µm. The mobile phase was acetonitrile/water 58-42 (%v/v) acidified 0.06 g L^{-1} with H_2SO_4 respect to water, at a constant flow rate of 0.5 mL.min^{-1}. The column oven temperature was kept constant at 30 °C. The injection volume was 10 µL for each analysis. The samples were diluted in a solution of water/acetonitrile 42–58 (%v/v) for 1-butanol and water/acetonitrile 30–70 (%v/v) for 1-octanol of an equal concentration of the mobile phase, without acidifying. The calibration of the products was performed in triplicates to obtain the repeatability within 0.5% in moles.

2.3.3 Experimental procedures

2.3.3.1 Simple distillation

Considering that the initial mixture obtained *via* glycerol oxidation reaction contains a mixture of salts, the corresponding acids are therefore in salt form. Two sample types were tested with this technique in salt and in acid form. Both sample types were tested with a water removal of 30 wt% and 60 wt% using 240mL of mixture respectively. To obtain the initial mixture in acid form, 9,40g of sulfuric acid (95–98% purity, Sigma Aldrich) was added. The operation conditions were 105 °C and 101°C in temperature on the top and bottom of the column, respectively.

2.3.3.2 Vacuum distillation

The vacuum distillation experiments were carried out in the same way as simple distillation. This means, using the same initial mixture, the same types of samples as well as the same water removal percentage. The operation conditions were 80 °C and 100 mbar.

2.3.3.3 Liquid-Liquid Extraction

The Liquid-Liquid extraction experiments were carried out using the starting mixture and two different types of alcohols such as 1-butanol (purity 99 % w/w from Alfa Aesar) and 1-octanol (purity 99 % w/w from Alfa Aesar) as solvents. The molar ratio between mixture and alcohol was 1:2 and 1:4 respectively. The extraction was carried out for samples in salt and acid form, separately. The initial mixture was acidified with 8.26g of sulfuric acid 0.8M (95–98 % purity, Sigma Aldrich). Liquid-liquid extraction was carried out in the semi-batch stainless steel reactor at a temperature, extraction time and stirring rate of 35°C, 20 min and 1000 rpm, respectively. After that a funnel was used in order to separate the two phases formed.

On the other hand, distribution coefficient (K_D) was calculated using the ratio of the concentration of the compound in the organic and aqueous phase, in the equilibrium state at 13,47 pH value. For the evaluation of the experiments, Ahsan *et al.* [2] defined an extraction efficiency given in equation 2.

$$K_D = \frac{([A]_1 * V_{org})}{([A]_2 * V_{aq})} \quad (2.9)$$

$$E = \frac{n_{AA,aq,in} - n_{AA,aq,out}}{n_{AA,aq,in}} 100\% \quad (2.10)$$

Where $K_D$is the process equilibrium constant,$[A]_1$the concentration in the organic phase V_{org} the volume of organic phase, $[A]_2$ represents the concentration in the aqueous phase and V_{aq} volume of aqueous phase. As clearly defined in the IUPAC definition, when any chemical reaction occurs, the concentration of a particular species will change, the distribution ratio will change, but the distribution constant (partition ratio or partition coefficient) of this particular species does not change [3-4]. Where E is the extraction efficiency ,$n_{AA,aq,in}$ is the mol of acid in the aqueous phase (input) ,$n_{AA,aq,out}$is the mol of acid in the aqueous phase (output).

2.3.3.4 Reactive Extraction

The experiments of reactive extraction were carried out using the starting mixture and 1-butanol (purity 99 % w/w from Alfa Aesar) as a solvent and Tri-n-octylamine (TOA, Sigma Aldrich, purity >98%) was used as an extractant, a straight-chain tertiary amine, TOA is usually used in the form of a solution in organic diluent due to high viscous and corrosive properties. The molar ratio between mixture and alcohol was 1:2. The extraction was carried out for samples in salt and acid form, separately. The initial mixture was acidified with 1.12 g of sulfuric acid 0.8 M (95–98 % purity, Sigma Aldrich). Reactive extraction was carried out in the semi-batch stainless steel reactor at a 35 °C temperature, extraction time and stirring rate of 6h and 1000 rpm, respectively. After that, a funnel was used in order to separate the aqueous and organic phases formed after 2h and their temperature was maintained at 25 °C.

2.3.3.5 Precipitation

A precipitation test was carried out after the vacuum distillation step, with the sample after water removal of 80 wt%, using 150 mL of the initial mixture. The operation conditions in vacuum distillation were 80°C and 100 mbar. And subsequently, a precipitation test was performed at 0 °C and 6000 rpm for 10 min. The concentration of acids was determined by a mass balance of carboxylic acids in the system. In addition, in order to complement the analysis of this stage, neutralization test for the initial mixture was carried out using a solution of NaOH of concentration 1 M.

2.4 Bibliography

[1] P. Hemptinne, Jean-Charles. BARREAU, Alain, LEDANOIS, Jean-Marie , MOUGIN, *SELECT THERMODYNAMIC MODELS FOR PROCESS SIMULATION A Practical Guide using a Three Steps Methodology*, Editions T. PARIS, FRANCE, 2012.

[2] L. Ahsan, M. S. Jahan, H. Liu, and Y. Ni, “Recovery of acetic acid from pre-hydrolysis liquor of a kraft-based dissolving pulp production process by reactive extraction with triisooctylamine,” *J-for*, vol. 2, no. 4, pp. 38–43, 2012.

[3] A. Berthod and S. Carda-Broch, “Determination of liquid-liquid partition coefficients by separation methods,” *J. Chromatogr. A*, vol. 1037, no. 1–2, pp. 3–14, 2004.

[4] A. Andrés *et al.*, “Setup and validation of shake-flask procedures for the determination of partition coefficients (log D) from low drug amounts,” *Eur. J. Pharm. Sci.*, vol. 76, pp. 181–191, 2015.

Chapter 3. Thermodynamic study: phase equilibrium for the esterification of glycolic acid with butanol, propanol and octanol system

As already mentioned in chapter 1, in order to continue with the valorization of the different carboxylic acids obtained during the glycerol oxidation reaction, process strategies must be developed that allow their recovery and purification from the highly diluted medium in which they are produced, overcoming high production costs, polymerization and thermal degradation as some of the main problems. The different carboxylic acid recovery strategies presented in chapter 1 show that the protection of the acid function by esterification reaction is one of the most promising alternatives through reactive distillation (RD), where several acids can be recovered, and water eliminated simultaneously. Reactive distillation requires precise thermodynamic and kinetic information about the multicomponent phase equilibrium in the reactive mixture for process design. In the particular case of glycolic acid, the most abundant and interesting acid, there is a lack of information on equilibrium phases when considering the implementation of using RD as a recovery and purification process.

In process engineering, thermodynamics is an essential part to understand the modifications a system undergoes due to heating, compression, expansion, mixing, separation or chemical reactions. It is important to understand the changes that can occur in multi-component mixtures due to variations in temperature, pressure and composition.

In general, phase equilibrium, physical and thermodynamic properties of both pure fluids and mixtures are ultimately governed by intermolecular forces. The greater the intermolecular forces, the more the behavior of the mixture moves away from the ideal, making it more difficult to model.

In this chapter, the methodology applied to determine the different thermodynamic equilibria for the system of esterification of glycolic acid with butanol, chosen as model reaction (See Rxn.1), will be presented, in addition to the data obtained for propanol and octanol systems.

$$\underset{Glycolic\ acid}{C_2H_4O_3} + \underset{Butanol}{C_4H_{10}O} \leftrightarrow \underset{Butyl\ glycolate}{C_6H_{12}O_3} + \underset{Water}{H_2O} \qquad Rxn.1$$

The methodology used to determinate the binary interaction parameters of the existent couples in the model system is presented in Figure 3-1. The first step was the experimental determination of vapor-liquid, liquid-liquid and solid-liquid equilibrium data for the different systems.

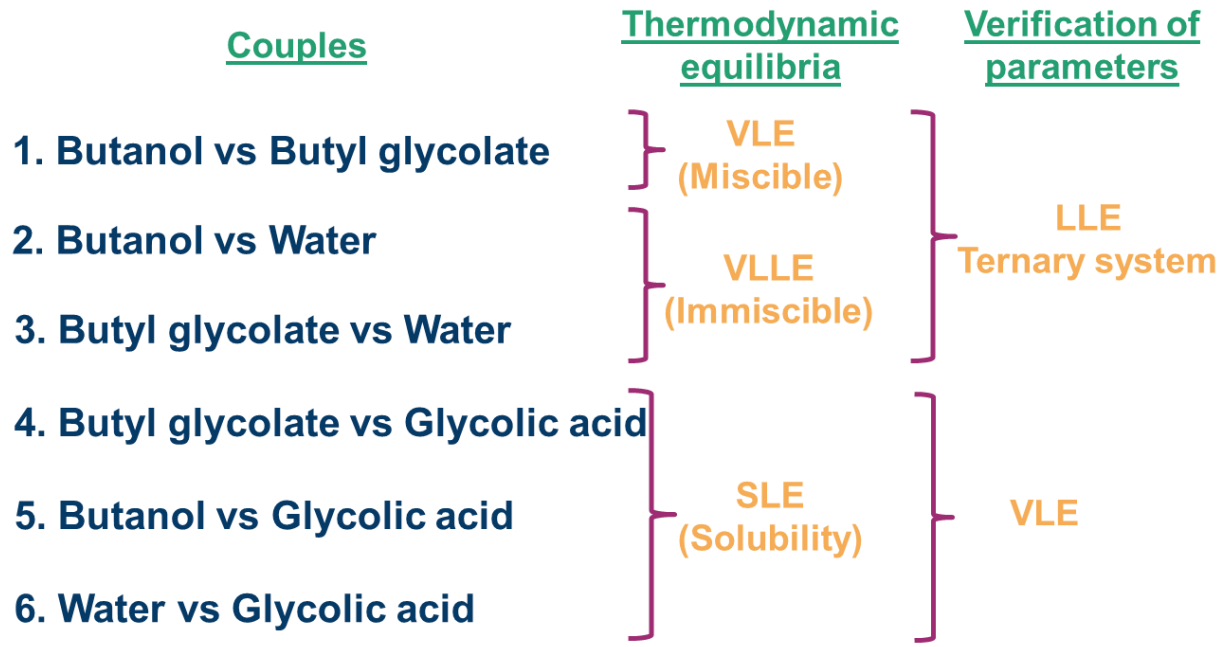

Figure 3-1. Binary systems in the esterification of glycolic acid and butanol system.

The importance of being able to determine thermodynamic models from experimental data is to be able to reliably represent both liquid-liquid equilibrium (LLE) and vapor-liquid equilibrium (VLE). Several authors use models based on the generalized group contribution (UNIFAC) [1]. However, in many cases; especially when the nature of the molecules is different (*e.g.*, polar versus non-polar), the prediction is unreliable. Although the experimental determination of many equilibria is challenging, especially when the systems are not miscible, the above justifies the need for experimental measurements and correlations. Determined binary coefficients must be able to predict VL and LL equilibria in multicomponent systems. For the glycolic acid system with the different alcohols studied in this project, there are no data available in the literature.

Vapor-liquid equilibria were determined under isobaric conditions using an apparatus VLLE602 FISCHER® LABODEST®. T-x-y data at 300.00, 700.00 and 1013.25 mbar for the binary couples were obtained. Liquid-liquid equilibria were determined for the binary system of butyl glycolate-water and ternary system of butanol-butyl glycolate-water. The equilibrium data were correlated with different equations such as NRTL (Non-Random-Two-Liquid) and UNIQUAC to obtain the

binary interaction parameters using a regression tool included in Aspen Plus®. Solid-liquid equilibria were determined using the data obtained from the solubility of glycolic acid with different solvents used to adjust binary parameters for the NRTL equation.

3.1 Glycolic acid and butanol system

The determination of the activity coefficients of binary systems requires experimental information on phase equilibrium but also the information on the vapor pressure to carry out the different calculations. For each of the systems studied, vapor pressure measurements were carried out for the compounds that are not available in the literature of in the Aspen database.

3.1.1 Vapor pressure

The vapor pressures of pure compounds, P_{sat}, and their corresponding correlations with temperature, have an important influence on the calculation of the magnitudes that define the vapor-liquid equilibrium, such as the activity coefficients or the Gibbs energy function, and therefore on the treatment and reduction of thermodynamic data of the equilibrium of each system (consistency test, fit to models, prediction, etc.) [1, 3].

The P_{sat} of the pure components was determined experimentally, using the same equipment described in section Vapor pressure measurement 2.1.1.2.1. Figure 3-2 presents the P-T diagrams for butyl glycolate obtained from the data regression using the Antoine equation and from the NRTL prediction. The measurements were carried out in a pressure range from 100.00 to 1013.25 mbar.

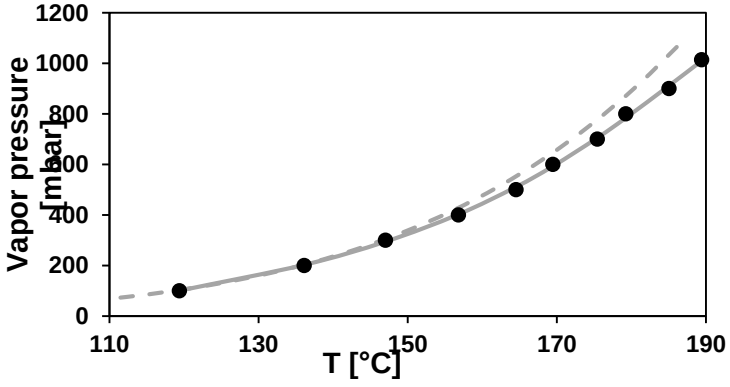

Figure 3-2. P-T diagram of butyl glycolate (●) this work, (-) Regression with Antoine equation and (- - -) NRTL prediction.

Owing to these data, the determination of the extended Antoine equation coefficients was achieved using the Aspen Plus® regression tool. In the case of butyl glycolate the equation 3.1. the parameters obtained fit favorably to the experimental data.

$$lnP^{sat,l} = 43878.5 + \frac{-1.37951\text{e}{+06}}{T-5.48209\text{e}{-07}} + 10.345\text{T} - 7435.11\text{lnT} - 5.48209\text{e} - 15T^6 \qquad (3.1)$$

$$119.39\ ^\circ\text{C} > \text{T} > 189.44\ ^\circ\text{C}$$

The boiling point of butyl glycolate at atmospheric pressure reported in the literature by Anderse in 1998 is 184.00 °C [4], while in the Aspen Plus® database the reported 187.15 °C. However, in this work the value is above both cases at 189.44 °C. Figure 3-2-2 shows that from 500.00 mbar of pressure the difference between the curve obtained from the regression of experimental data and by prediction is greater, this may indicate that using predictive models for the calculation of vapor pressure is not a favorable strategy.

3.1.2 Vapor-Liquid equilibrium

Deviations from ideality have been studied from the first and second principles of thermodynamics, where they are determined from relationships of the state properties such as temperature, pressure, volume and entropy, Gibbs energy in any closed or open system. The partial derivative of this last system with respect to the number of moles of species i, at constant conditions of T, P and the number of moles of the rest of species n_j, allow the definition of chemical potential of species i in the mixture:

$$\mu_i \equiv \left[\frac{\partial(nG)}{\partial n_i}\right]_{T,P,n_j} \qquad (3.2)$$

Applying the concept of chemical potential to a closed system with two phases in equilibrium, it can be considered that each of the phases is like an open system that exchanges matter with the other phase. Using equation 3.2 to each of the phases, and considering that the equilibrium P and T are uniform throughout the system, the conclusion is reached:

$$\mu_i^\alpha = \mu_i^\beta = \cdots = \mu_i^\pi \ (i = 1, 2, 3, \dots, N) \qquad (3.3)$$

The expression 3.3 can also be expressed in terms of fugacity as shown in equation 3.4.

$$f_i^\alpha = f_i^\beta = \cdots = f_i^\pi \ (i = 1, 2, 3, \dots, N) \qquad (3.3)$$

For more details, see **ANNEX C**

The complexity and nature of the mixture determines the thermodynamic models to be used for the study of each system. The systems of less complexity or homogeneous mixtures can be represented from the models of ideal gas, ideal dissolution and Raoult's Law (Eq. 3.4). Where x_i is the molar fraction of the component i in the solution and y_i is its molar fraction in gaseous phase.

$$y_i P = x_i P^{\sigma} \tag{3.4}$$

More complex systems or heterogeneous mixtures cannot be represented in the same way. These systems have deviations from the ideality, which are often of great magnitude and do not allow the ideal model to be used for design and control purposes. Indeed, by introducing two auxiliary thermodynamic properties related to Gibbs' energy: fugacity coefficient (φ_i) and activity coefficient γ_i, it is possible to transform the ideal models and Raoult's Law into a general expression suitable for the treatment of liquid-vapor equilibrium of non-ideal real systems (Eq. 3.5).

$$y_i \varphi_i P = \gamma_i x_i P^{\sigma} \tag{3.5}$$

These expressions make it possible to relate the experimental data obtained from the vapor-liquid equilibrium with the activity coefficients and fugacity coefficients.

The choice of thermodynamic models for determining the fugacity and activity coefficients depends on the compounds and the pressure and temperature range of the process. For this, one can choose between equations of state, to model the vapor phase and models of activity coefficients, to model the liquid phase, or, the combination of the two.

Within the existing methods for the determination of the activity coefficients that consider the definition of local composition, Wilson's method [4] (1964) shows that Gibbs' energy in excess could be conveniently expressed through an algebraic function of the local composition and developed the equation that bears his name, using local volumetric fractions for the adjustment of two parameters. This equation is useful for dissolutions of polar or associated components (*e.g.*, alcohols) dissolved in non-polar solvents, mainly miscible mixtures. However, this model is not able to predict immiscibility and cannot represent maximums and minimums in the activity coefficients versus composition. Therefore, it is not applicable in immiscibility case.

Other models that use local compositions are Renon's NRTL [5] (1968), Abrams' UNIQUAC (Universal Quasichemical) and Prausnitz [6] (1975), the Heil equation that modifies the Wilson

equation to represent equilibrium in polymeric solutions and UNIFAC, developed by Fredenslund, Jones and Prausnitz[1] (1975), which calculates the activity coefficients from the contributions of the functional groups that are part of the molecules in solution, assuming, as Smith, Van Ness and Abbott (2001) say: "a liquid mixture can be considered as a solution of the structural units from which molecules are formed, rather than a solution of the molecules themselves" [7].

According to the properties of the molecules involved in the esterification of glycolic acid and butanol reaction, the reference system, the mentioned models were used to determine the binary coefficients of the mixtures studied in this chapter.

The experimental data $T - x - y$ for the butanol and butyl glycolate (BuOH-BG) system were determined at three different pressure conditions 300.00, 700.00 and 1013.25 mbar. Figure 3-3 presents the $T - x - y$ data for the BuOH-BG system at 1013.25 mbar. The results at 300.00 mbar and 700.00 mbar are summarized in **ANNEX E**.

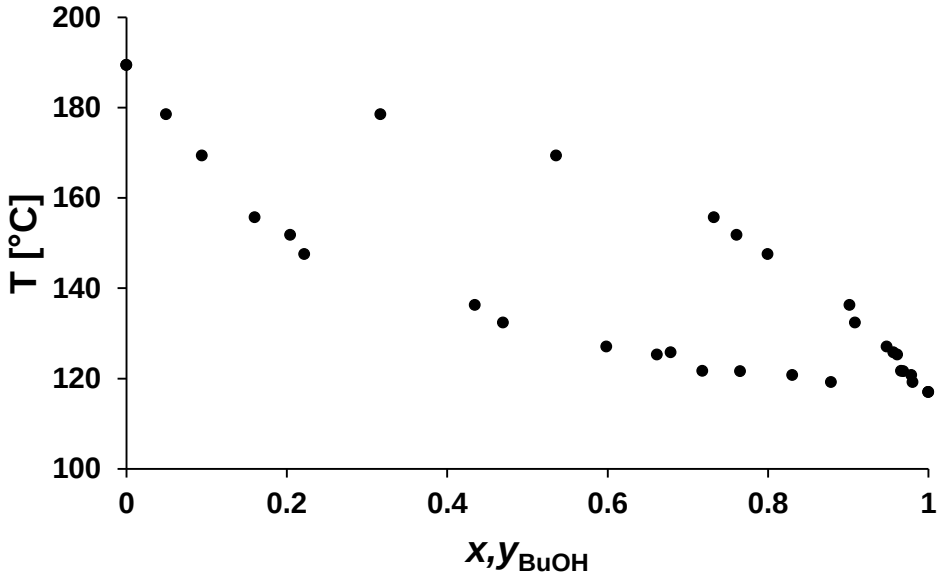

Figure 3-3. VLE for the binary BuOH + BG. at 1013.25 mbar. Exp (●)

The first study carried out was the comparison of using an ideal model and an equation of state for the modelling of the vapor phase. The determination of the binary parameters of the BuOH-BG system was performed using the Aspen Plus® regression tool. The experimental data in this chapter were correlated using the algorithm of maximum-likelihood objective function [8]. The binary parameters a_{ij} and b_{ij} were determined for the NRTL for the liquid phase. The vapor phase was considered ideal, taking into account that the data were obtained at low pressures. However, the vapor phase modeling was also performed with the Hayden-O'Connell equation (HOC) [9]. The association parameters that require the use of the equation are not available in the Aspen Plus® database for the mixture butanol and butyl glycolate. To perform the regression we considered the data available for the butanol and butyl acetate system, strategy also employed by Orjuela *et al*. [10], the author used the same values for vapor phase modeling for couples containing diethyl succinate.

Figure 3-4 represents the fitting of the experimental data of the BuOH-BG system at 1013.25 mbar using the NRTL model and the NTRL-HOC model. The vapor phase is represented in the same way either using an ideal model or using an additional state equation. The results show that in this case it is suitable to use an ideal model for the adjustment of the vapor phase data since graphically no considerable differences are observed.

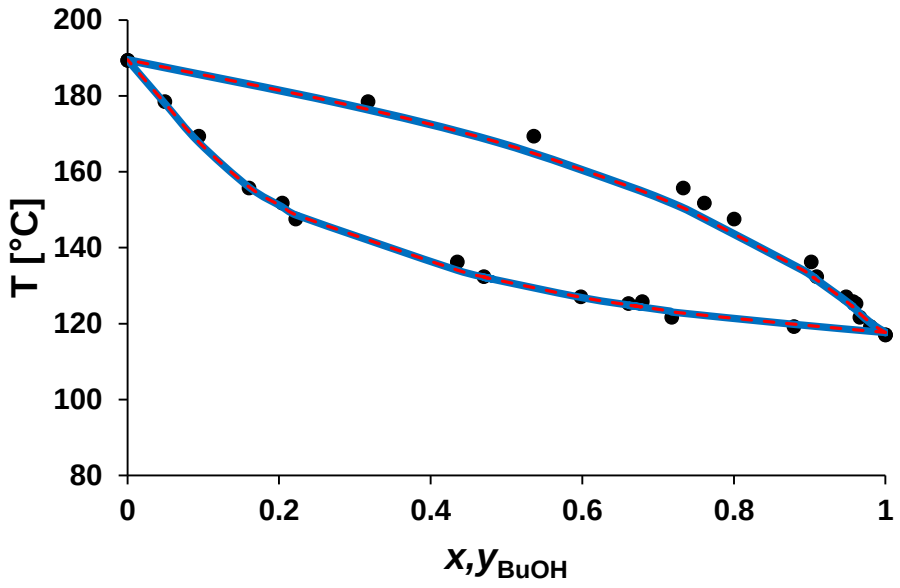

Figure 3-4. VLE for the binary BuOH + BG. at 1013.25 mbar. Exp (●), NTRL-HOC adjustment (▬▬) and NRTL adjustment (▬▬)

Table 3-1 presents the binary parameters obtained from regression with the NRTL model used the ideal gas equation and the Hayden-O'Connell equation for vapor phase prediction for liquid vapor equilibrium at pressure 1013.25 mbar.

Table 3-1. Binary parameter for NRTL and NRTL-HOC models

HOC Association Parameters		
	BuOH	**BG**
BuOH	2.2	1.3
BG	1.3	0.53
NRTL		
Component i	**BuOH**	**BuOH**
Component j	**BG**	**BG**
	Ideal gas	HOC
AIJ	-18.359	-19.982
AJI	8.5633	9.368
BIJ	8273.0	9034.3
BJI	-3848.5	-4205.7
CIJ	0.3	0.3

The total differences between the values predicted by the NRTL or NRTL-HOC model and the values observed is 1.1%. This evidences that at the conditions used in this study the vapor phase can be modeled considering its behavior as ideal. The difference in the data can be associated with the fact that the parameters considered for the Hayden-O'Connell equation do not correspond to the molecules in question, they are an approximation. However, it can be considered that the modeling of the vapor phase with the ideal gas equation and Hayden-O'Connell is approximately the same. In both cases, it shows that the experimental data compared to those obtained theoretically by the model have a low standard deviation, indicating that the experimental values are largely consistent with those calculated theoretically.

In all cases, the consistency of the vapor-liquid equilibrium data was verified by following the area test of Redlich-Kister; this test consists in the verification of the thermodynamic consistency of the experimental data. This method results from the integration of the Gibbs-Duhem equation into isobaric conditions and is represented by the expression 3.6.

$$\int_0^1 ln\frac{\gamma_1}{\gamma_2}dx = \int_{x=0}^{x=1}\frac{H^E}{RT^2}dT \qquad (3.6)$$

the tolerance interval for this test was 10%. For all the data analyzed, the test was approved in both cases, which indicates that the parameters determined, accurately describe the behavior of the liquid phase and the vapor phase. For further calculations, the ideal gas equation for vapor phase modelling will be considered.

To evaluate the sensitivity of the activity coefficients as a function of pressure variation, three different pressures were studied: 300.00, 700.00 and 1013.25 mbar. NRTL models was considered for modeling the experimental data obtained. The binary parameters a_{ij} and b_{ij} were determined with this model.

Figure 3-5 shows the binary diagram of BuOH-BG system at 300.00, 700.00 and 1013.25 mbar correlated with NRTL with the experimental data. The determined binary parameters fit the data obtained experimentally with great precision at three different pressures. The thermodynamic verification of the thermodynamic data in the three cases was favorable. Sanz *et al.* [11] and Duran *et al.* [12] have reported similar studies for alcohol-ester and alcohol-alcohol, respectively. In both cases, the authors measure the equilibrium at three different pressure conditions. Sanz *et al.* [11] indicated from their measurements that relative volatility increases slightly as pressure decreases, thereby favoring separation. Similar results were observed in this investigation, the change in the boiling point is more sensitive to low pressures than to high pressures.

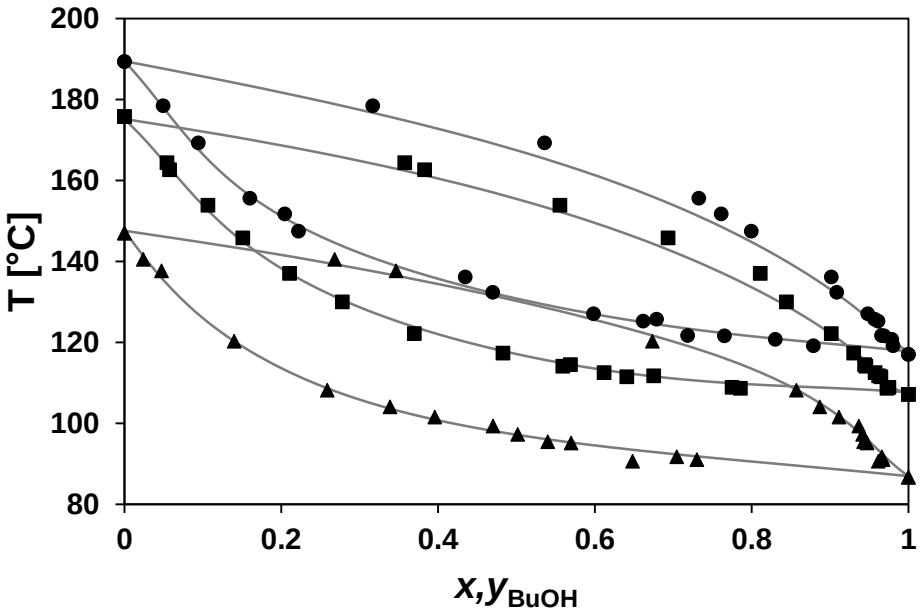

Figure 3-5. VLE for the binary BuOH+BG 300 (▲), 700 (■), 1013.25 (●) experimental and mbar NRTL adjusted (---).

The effect of the pressure variation on the activity coefficient is almost negligible for butanol, at high concentration conditions the activity coefficients are slightly similar, however at high dilution conditions, the decrease from 1013.25 to 300.00 mbar, an increase of 0.73 to 1.12 is observed. The activity coefficients are kept close to the change of pressure. The activity coefficients of the second component, butyl glycolate, are more sensitive to pressure changes. This coincides with what is published in the literature reported by Sanz *et al* [11] and Duran *et al* [12].

Two thermodynamic models were considered for modeling the experimental data obtained, NRTL and UNIQUAC models, the binary parameters α_{ij} and b_{ij} were determined and compared using both models. For being molecules with a similar chemical nature, the coefficient present in the NRTL model was established in $\alpha_{ij} = 0.3$ $(\alpha_{ij} = \alpha_{ji})$, and the parameters r and q presented in UNIQUAC model, necessary for the regression of the binary parameters with this model, were taken from the Aspen Plus® data base.

Figure 3-6 shows the adjustment of the thermodynamic data at 1013.25 mbar using the NTRL and UNIQUAC models. The models fit the data properly, this case with both models the same behavior is observed.

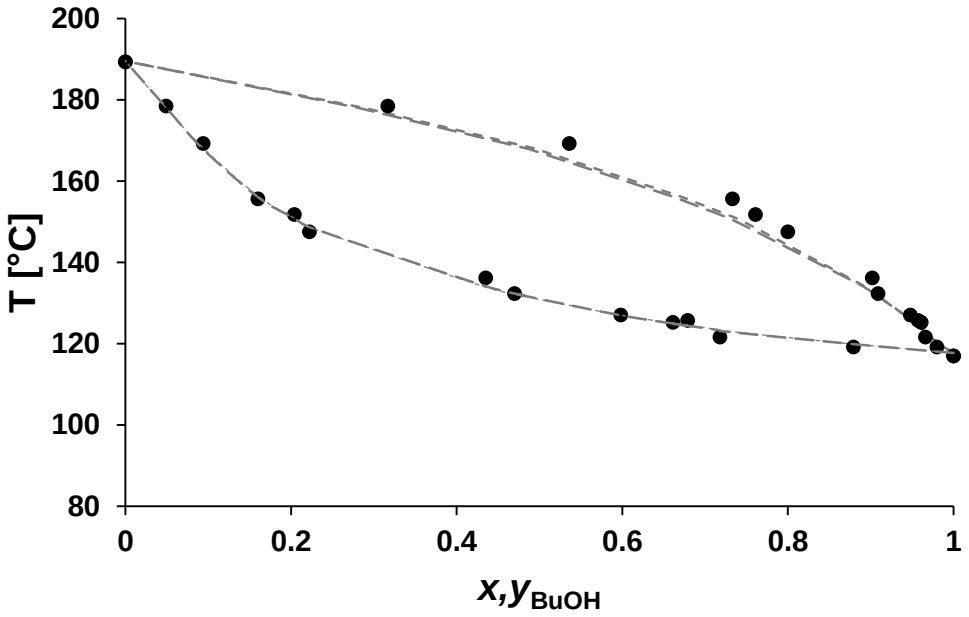

Figure 3-6. VLE for the binary BuOH+BG at 1013.25 mbar. Exp (●), NRTL (-- -- --), UNIQUAC (- - - -)

The parameters obtained for both equations are presented in Table 3-2. The standard deviation obtained with both models is the same. This indicates that the prediction of the liquid phase with either model can be achieved properly.

Table 3-2. Binary parameter for NRTL and UNIQUAC models for the system BuOH-BG

NRTL			
Component i	**BuOH**	**BuOH**	**BuOH**
Component j	**BG**	**BG**	**BG**
Pressure [mbar]	300.00	700.00	1013.25
AIJ	-17.2469	-17.246	-18.359
AJI	-1.311	3.140	8.563
BIJ	1547.6	7819.3	8273.0
BJI	470.8	-1596.1	-3848.5
CIJ	0.3	0.3	0.3

UNIQUAC			
Component i	**BuOH**	**BuOH**	**BuOH**
Component j	**BG**	**BG**	**BG**
Pressure [mbar]	300.00	700.00	1013.25
AIJ	1.183	6.505	6.729
AJI	-0.138	-2.078	-3.938

BIJ	-433.2	-3004.0	-3064.6
BJI	-37.3	1030.7	1789.2

Figure 3-7 presents the comparison of the phase equilibrium using the NRTL model with binary parameters correlated with the experimental data and the UNIFAC as predictive model. This study was carried out in order to verify if the results obtained experimentally coincide with the results obtained by prediction. It is observed that both the UNIFAC and NRTL models are able to accurately predict the behavior of the vapor phase. Figure 3-7 shows that the behavior of the liquid phase predicted by the UNIFAC and NRTL models does not coincide. The difference in the prediction of the behavior of the liquid phase when using UNIFAC as predictive model and NRTL model evidence that the same results are not achieved when considering a predictive method and a method based on experimental data.

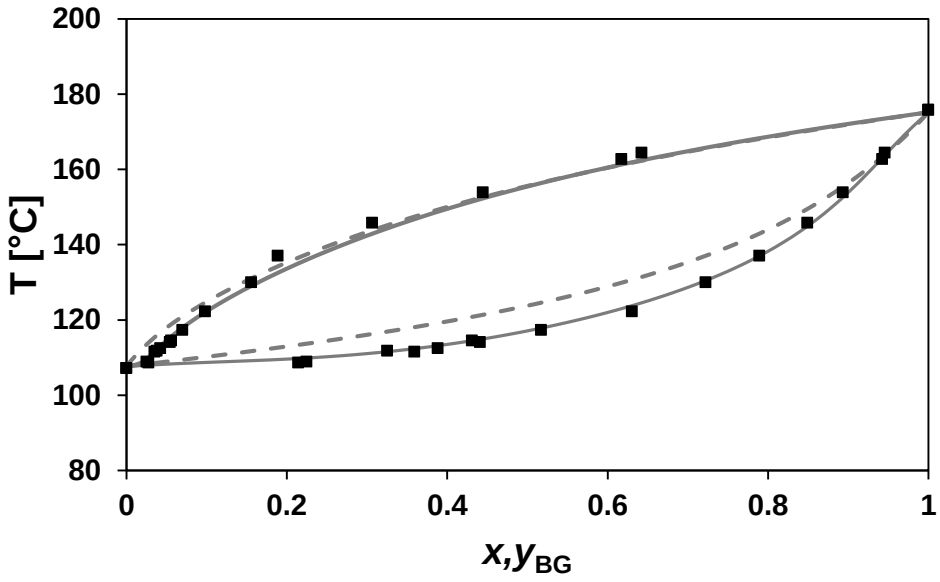

Figure 3-7. VLE for the binary BuOH+BG at 700 (▲) mbar, UNIFAC (- - -), NRTL (———).

Figure 3-8 presents the activity coefficients of the BuOH-BG system as a function of the concentration calculated from the NTRL and UNIFAC models. The comparison of the activity coefficients obtained with the UNIFAC and NRTL models shows more easily the error when considering the predictive model. Sans *et al* [11] studied the alcohol-ester system of methanol and methyl lactate, they indicated that the deviation from Raoult's law or non-ideality evidenced in the activity coefficients, indicates the different molecular interactions between equal and different molecules. Both molecules, ester and alcohol, have an OH group that can form hydrogen bonds

with similar or different molecules. The observed deviations from ideality may be due to the tendency of alcohol to self-associate at high concentrations, while at low concentrations the tendency for hydrogen to bind to the ester would be predominant. This phenomenon, which occurs due to the difference in size or a significant difference between the boiling points of the two molecules, would explain the observed reversal in deviations from Raoult's law.

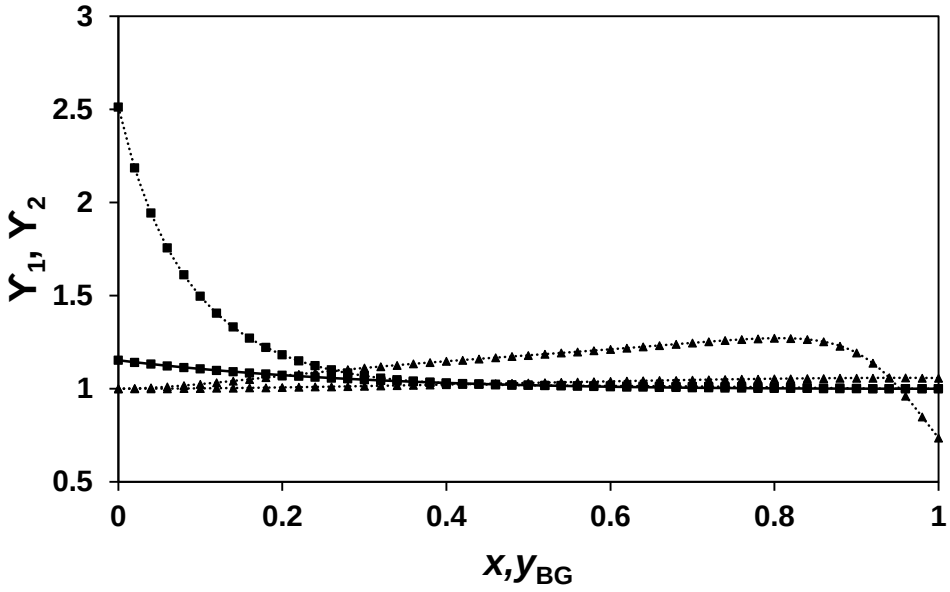

Figure 3-8. Activity coefficient BG (■) + BuOH (▲) at 1013.25 mbar. UNIFAC (——), NRTL (……).

3.1.3 Liquid-Liquid equilibrium

The esterification systems of glycolic acid (GA) and butanol (BuOH) also consist of water (W) and butyl glycolate (BG), the presence of these new substances requires a different treatment than that presented before because it is a mixture of non-miscible compounds. The BG produced from the esterification reaction of GA and BuOH will form a second liquid phase because of his limited solubility in the presence of water. In order to determine the thermodynamic parameters of a non-miscible system, information about both, the vapor-liquid equilibrium and the liquid-liquid equilibrium. Liquid-liquid equilibrium consists of the measurement of solubility as a function of the temperature in each of the phases. In this study the NRTL and UNIQUAC models were initially considered for the adjustment of the parameters, models suggested in the opening for these cases [13]. These models have the ability to describe systems with these types of the behaviors. In the case of the NRTL model, the modification of the α_{ij} parameter allows to infer the immiscibility of the system before performing the regression of the parameters. In this research the α_{ij} value

was set at 0.2. This parameter was set to improve the prediction. Some authors such as Orjuela *et al.* [4, 6] prefer to include this parameter within the parameters to be calculated by regression, while others simply adjust it according to the criteria reported in the literature from the nature of the molecules [15].

Figure 3-9 shows the liquid-liquid equilibrium data of the BG-W system within a temperature range of 32.05 to 61.15°C, at atmospheric pressure. From these data and using the Aspen Plus® regression tool, the binary parameters for the NRTL and UNIQUAC models were determined. In this study the NRTL and UNIQUAC models were initially considered for the adjustment of the parameters, models suggested in the opening for these cases.

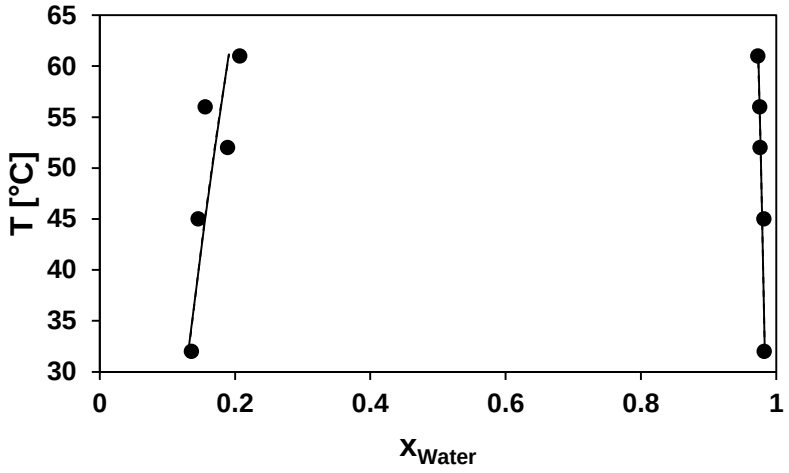

Figure 3-9. LLE for the binary BG + W at 1013.25 mbar. Exp (●), NRTL (-), UNIQUAC (--)

The parameters determined for NRTL and UNIQUAC, presented in the Table 3-3, adjust the experimentally obtained data with great precision as shown in Figure 3-9.

Table 3-3. LLE Binary parameter for NRTL and UNIQUAC models.

	NRTL	**UNIQUAC**
Component i	**W**	**W**
Component j	**BG**	**BG**
AIJ	1,792	0,852
AJI	-2.643	-1,105
BIJ	563.40	-204,19
BJI	1013.13	-310,07
CIJ	0.2	---

The root means square error (RMSE) percentage using the NRTL and UNIQUAC models for temperature prediction is 0.4 % for both models. The models predict the W compositions better than the BG compositions.

In order to predict the liquid-liquid equilibrium for the BG+W+BuOH system, the binary parameters were taken from the Aspen Plus® database for the BuOH-W system. Therefore, sufficient information was available to predict the LLE. Several authors have reported similar studies for involved systems in reactive distillation processes by esterification [3,10,15,16].

In order to corroborate the prediction, the tie lines were determined by preparing solutions at known concentration within the non-miscible zone. At a given temperature, the point where the tie lines cross the composition of two phases (conjugated) in equilibrium, represents the composition at the miscibility limit. In this zone. For this reason, there is the formation of two phases (inorganic and organic phase) in which the concentration of each of the compounds will be determined after reaching equilibrium.

The experimental data of the tie lines for the BG + W + BuOH system are listed in Table 3-4, where w_i represents the mass fraction of each component.

Table 3-5. LLE tie line data for BG + W + BuOH at 25°C.

INORG			**ORG**		
W_W	W_{BG}	W_{BuOH}	W_W	W_{BG}	W_{BuOH}
0,898	0,082	0,021	0,115	0,772	0,113
0,903	0,065	0,032	0,148	0,657	0,195
0,906	0,049	0,044	0,171	0,527	0,302
0,909	0,027	0,063	0,181	0,298	0,521

There are different correlations in the literature that allow to identify errors in the tie lines [13]. The correlation of Othmer-Tobias presented for the first time in 1942, was derived from an empirical equation proposed by Bachman in 1940 to include systems containing non-miscible liquids [17]. Today this correlation is one of the most used strategies to identify random errors in tie lines [10, 14, 18].

The consistency of the LLE data was verified with the Othmer-Tobias method and a linear relationship was obtained for the system as shown in Figure 3-10.

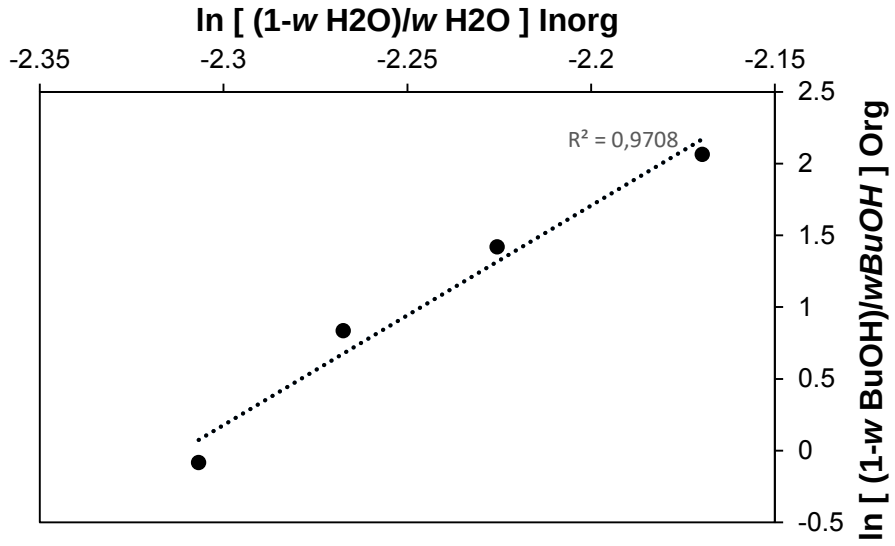

Figure 3-10. Othmer-Tobias plots for the BG + W + BuOH ternary system.

From the binary parameters obtained using the NRTL and UNIQUAC model, it should be possible to predict the behavior of mixtures with more than two components of those studied. In the case of the ternary system BG + W + BuOH, the binary parameters that better represented the LLE are those obtained from the adjustment of the NRTL model. Figure 3-11 presents the ternary system prediction using the binary data from the NRTL model and the experimental data. The extreme of the tie lines for the BG + W + BuOH system, although not in perfect agreement with the prediction obtained with the NRTL model, follow nevertheless the same trend.

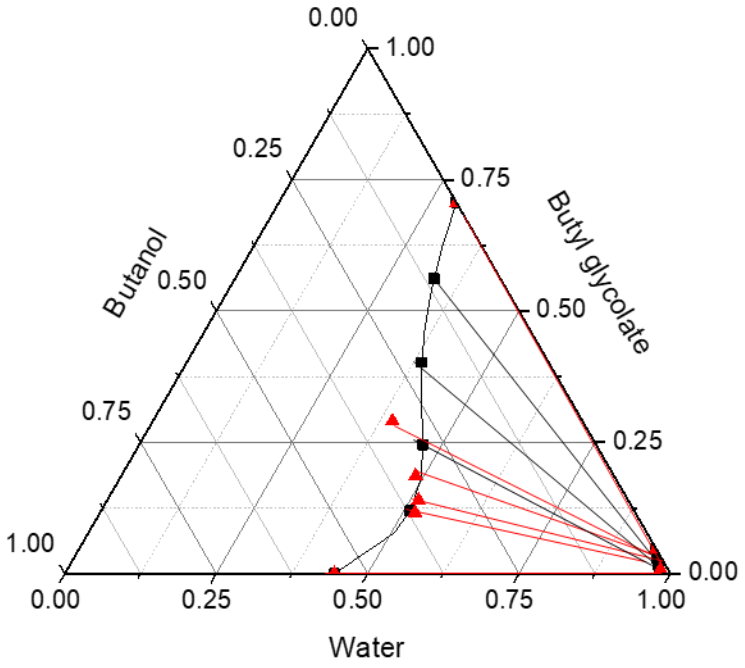

Figure 3-11. LLE for the ternary BuOH+ BG+ W at 1013.25 mbar. Tie lines: This work (----), NRTL(——)

The advantages of the NRTL model is that it allows to consider the non-miscibility. The diagrams obtained with the binary parameters regressed with the UNIQUAC and UNIFAC models do not coincide with the experimental data. For this reason, NRTL modeling was chosen as the most appropriate model for the simulation and design of the reactive distillation process.

3.1.4 Solid-liquid equilibrium

In the reaction system between glycolic acid and butanol, solid-liquid equilibrium must be determined. The binary systems formed by glycolic acid must be determined from their solubility in the presence of the different solvents. Solubility represents the intermolecular forces between solute and solvent. In thermodynamic terms, it is represented by the increase or decrease of the solution enthalpy. Solubility depends not only on the activity coefficient of the solute but also on the fugacity of the standard state used to evaluate the activity coefficient and the fugacity of the pure solute [19]. The variation between the two fugacities is evidenced as a change in the Gibbs free energy, this property can be determined from the fundamental properties of enthalpy and entropy [20].

The solid-liquid equilibrium equation is widely used in the literature to determine the activity coefficients of a solute [21]–[23]:

$$ln(a_{GA}) = \ln(x_{GA}\gamma_{GA}) = \frac{\Delta H_{fus}}{R}\left[\frac{1}{T_{fus}} - \frac{1}{T}\right] + \left(\frac{1}{RT}\right)\int_{T}^{T_{fus}} (C_{pL} - C_{pS})dT \; - \; \left(\frac{1}{R}\right)\int_{T}^{T_{fus}} \frac{(C_{pL} - C_{pS})dT}{T} dT - \lambda_{PT} \quad (3.7)$$

Glycolic acid is assumed as solid in the binary mixtures in which this compound is present and the triple point temperature is equal to the fusion temperature (T_{fus}). a_{GA}, x_{GA}, and , γ_{GA} are activity, molar fraction and activity coefficient of glycolic acid in saturated solution respectively. ΔH_{fus} is the fusion enthalpy, and C_{pL} and C_{pS} are the specific heat per mol of liquid and solid phase. The hygroscopic character of glycolic acid and its easy thermal degradation at temperatures above 100.00°C can make calorimetric measurements difficult.

The compilation of the values of glycolic acid obtained from the literature and calculated using Aspen Plus® are presented in the Table 3-6.

Table 3-6. Properties of glycolic acid collected.

Property		Value	Reference
$\boldsymbol{T_{fus}}$ **[°C]**		78.15	[24]
$\boldsymbol{\Delta H_{fus}}$ **[J/mol]**		19300	
$\boldsymbol{C_{pL}}$ **[J /mol K]**	A_L	302.01	Aspen
$\boldsymbol{C_{pL} = A_L + B_L T}$	B_L	-0.2122	
[90 to 100 °C]			
$\boldsymbol{C_{pS}}$ **[J /mol K]**	A_S	26.615	
$\boldsymbol{C_{pS} = A_S + B_S T}$	B_S	0.3251	
[30 to 50 °C]			

In order to determine the activity coefficients of glycolic acid using the solid-liquid equilibrium (equation 3.7), it is also required the solubility of glycolic acid in different solvents. The activity coefficients determined with the solid-liquid equilibrium model can be correlated to determine the binary parameters of both the UNIQUAC and NRTL models. For the purpose of this study, the model selected was the NRTL model, which exhibited a better prediction of liquid-liquid equilibrium. MATLAB 9.4 tool was used to determine the binary parameters by minimizing of the objective function between the calculated activity coefficients and experimental values (MATLAB 9.4 (see **ANNEX F**).

3.1.4.1 Calorimetric analysis

Previously to the calorimetric analysis, a thermogravimetric analysis (TGA) was performed in order to establish the maximum temperature at which glycolic acid can be heated without degradation. The temperature observed was 100.00°C. Once the maximal heating temperature was fixed, the calorimetric analysis (DSC) of glycolic acid was performed and the results are presented in Figure 3-12. The graph shows a single peak corresponding to the solid-liquid transition or fusion temperature of the glycolic acid. The integration allows calculated the heat required to achieve the transition, in this case is an endothermic transition.

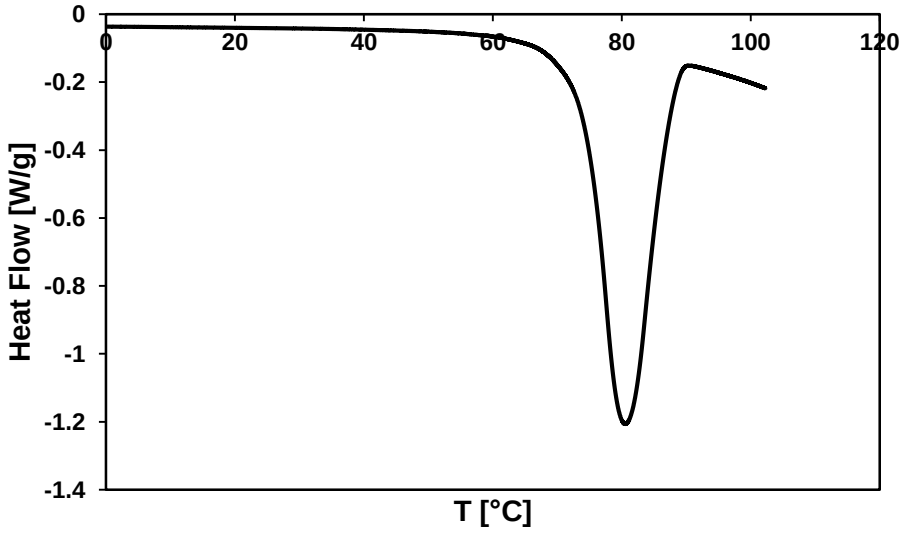

Figure 3-12. Calorimetric curves obtained by DSC at 2 K/min at 1.01325 bar.

The fusion enthalpy and fusion temperature values were reported in the NIST database by Emel'yanenko *et al.* [24], being 19300 J.mol^{-1} and 78.15 °C, respectively. In this work, the same values of fusion enthalpy and fusion temperature were found before subjecting the glycolic acid to a vacuum drying process to eliminate the amount of water present.

In the DSC analysis of glycolic acid after vacuum drying, no peaks associated with a solid transition state were observed. Only one cycle could be carried out on the sample, since the loss of mass was greater than 20 % after the first cycle. The results of T_{fus}, and ΔH_{fus} varied according to what was reported by Emel'yanenko et al. [24]. T_{fus} was 80.15°C, slightly higher than the reported value (78). ΔH_{fus} was 14923 J.mol^{-1} changed in 22% below the reported value. This confirms that the amount of water present in the glycolic acid can cause an endothermic event associated with the evaporation of the water produced during glycolic acid melting.

The calorimetric analysis of the sample was carried out at atmospheric pressure (Figure 3-12). The scanning at high pressures where degradation is avoided could not be carried out due to equipment limitations. At atmospheric pressure, it was observed that after fusion, the mass loss is important, indicating the beginning of a thermal decomposition process.

In order to measure the solid heat capacity, the heating process was carried out according to the machine limitations, the lowest possible speed was 2 °C.min^{-1}. To minimize solid decomposition during heat capacity measurements, a scan of up to 100 °C was performed.

Figure 3-13 presents the heat capacity of the solid phase of glycolic acid as a function of temperature compared to the curve obtained at the same conditions by the Aspen Plus® property prediction tool. The solid heat capacity was considered between the temperature range of 30.00 to 50.00 °C, the difference increases with the increase in temperature in approximate 27%.

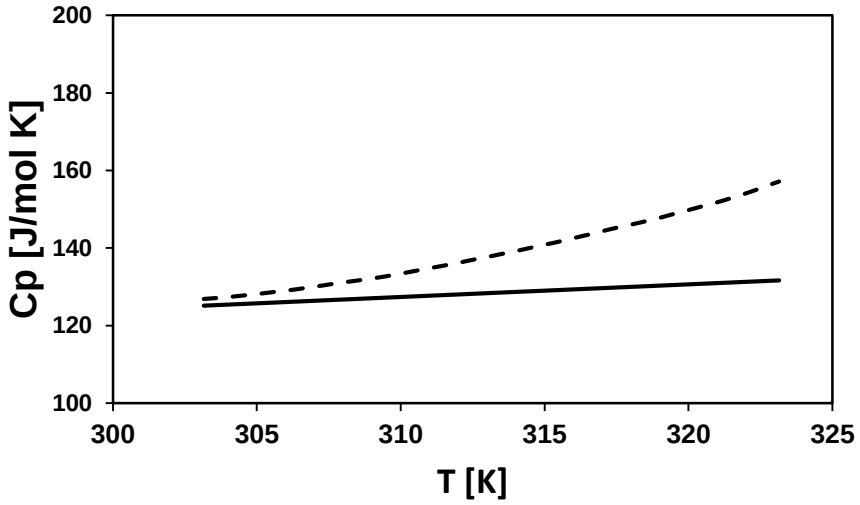

Figure 3-13. Solid phase heat capacity of glycolic acid at 1.01325 mbar (This work) **(- - -)**. Aspen prediction (**—**).

Figure 3-14 presents the heat capacity of the liquid phase of glycolic acid as a function of temperature compared to the curve obtained at the same conditions by the Aspen Plus® property prediction tool. The liquid heat capacity was considered in the temperature range between 92.00 to 98.00 °C. The difference decreases with the temperature increase in around 3%.

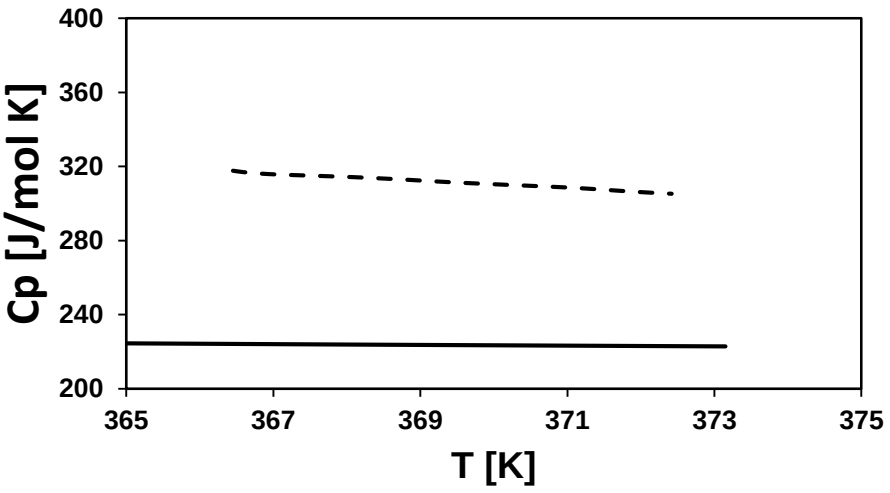

Figure 3-14.Liquid phase heat capacity of glycolic acid at 1.01325 mbar (This work) (- - -). Aspen prediction (—).

The change of the calorific capacities with respect to the predicted values is up to 30% different. The biggest difference is observed in the case of the calorific capacity of the liquid phase where the calorific capacity increases. This could be the result of the beginning of the solid decomposition process. Since the heat capacity of the solid phase coincides reasonably with the heat capacity predicted by Aspen, for thermodynamic study purposes, the heat capacity values for both phases will be taken from the Aspen Plus® prediction. Table 3-7 presents the data used to adjust the binary parameters in Matlab.

Table 3-7. Properties of glycolic acid determinate.

Property		Value
T_{fus} [°C]		80
ΔH_{fus} [J/mol]		14923
C_{pL} [J /mol K]	A_L	1034.4
$C_{pL} = A_L + B_L T$	B_L	-1.9569
[30 to 50 °C]		
C_{pS} [J /mol K]	A_S	331.67
$C_{pS} = A_S + B_S T$	B_S	1.5035
[90 to 100 °C]		

3.1.4.2 Binary Parameter Determination

The determination of the binary parameters for a system composed of liquid and solid requires as initial information the solubility data. In the literature there is only solubility information available for the GA and W systems. Figure 3-15 presents the solubility determined in this study and the

solubility reported from the literature. The solubility data of GA-W obtained in this work do not coincide with the values reported by Apelblat *et al.* [25]. The difference can be associated with the techniques of quantification, the author employs an in situ infrared technique and in this work liquid chromatography is used. In both cases the solubilization process was the same.

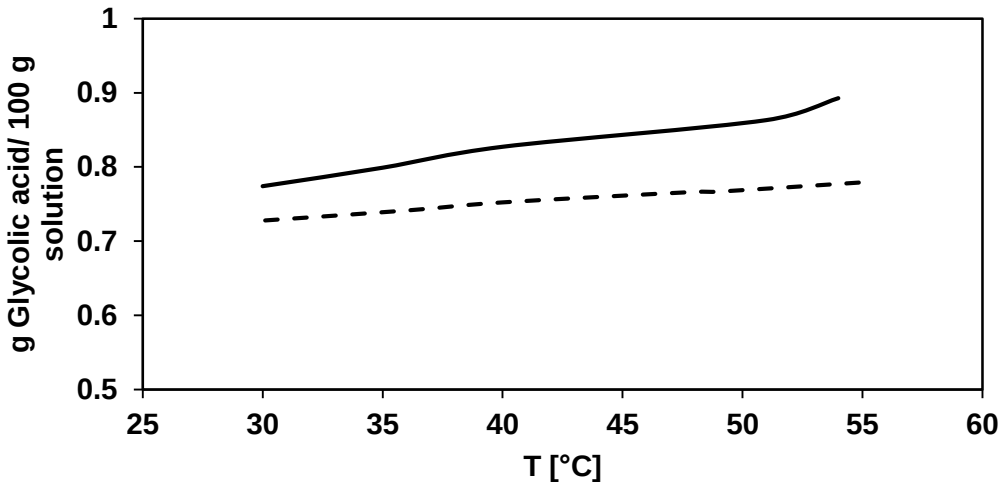

Figure 3-15. Glycolic acid Solubility in Water this work(▬) and Apelblat *et al* [25] (- - -).

To verify the reliability of the experimental method, measurements were performed twice in some cases, where the deviation was less than 5%. Both, solubility data reported in the literature and experimental for the GA-W system were correlated using the solid-liquid equilibrium (equation 3.30) to determine the binary parameters of the NRTL model. The solubility of glycolic acid was determined BuOH, BG and W, as shown in Figure 3-17.

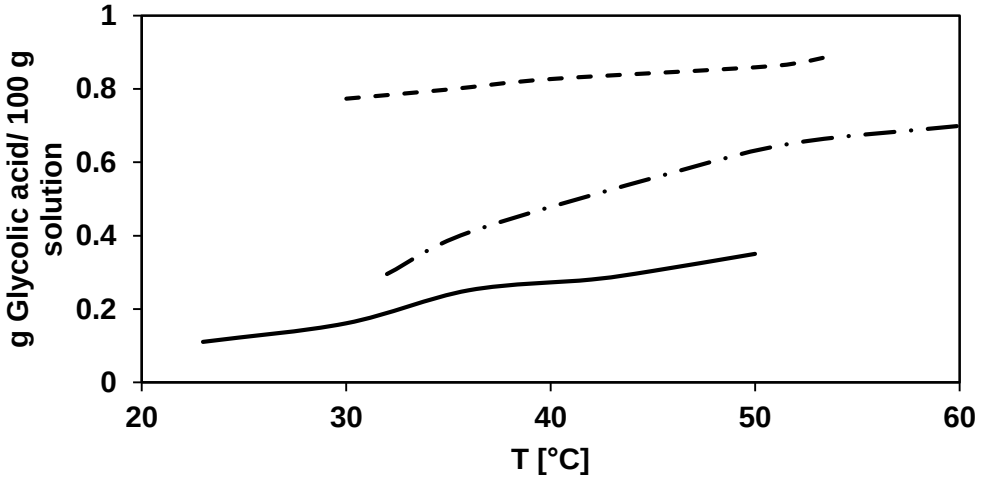

Figure 3-16. Glycolic acid Solubility in Water (- - -), Butyl glycolate (-- - --), and Butanol (▬).

The binary parameters of the NRTL model were used to confirm its reliability and the ability to model the liquid and vapor phases of the GA-W system as shown in Figure 3-17.

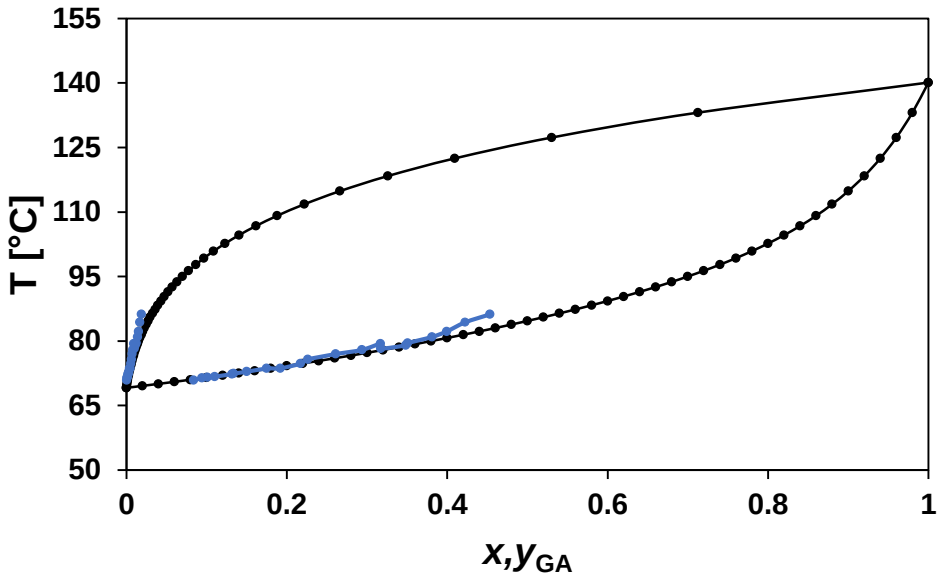

Figure 3-17. VLE for the binary GA + W at 300 mbar. VLE exp (-----) and NRTL adjusted (- - -).

The binary parameters obtained according to the values reported by Apelblat *et al.* [25] were not able to predict the vapor-liquid equilibrium data for the GA-W system. Instead, the binary parameters obtained using the experimental data of this project were able to predict the behavior of the liquid phase of the vapor-liquid equilibrium of the GA-W system determined at isobaric conditions (300.00 mbar). The vapor-liquid equilibrium for the GA-W system was only determined for a range of fractions due to solubility limitations.

Table 3-8 presents the binary parameters obtained for the GA-W, GA-BuOH, and GA-BG systems.

Table 3-9. Binary parameters for the NRTL model.

NRTL			
Component i	**GA**	**GA**	**GA**
Component j	**W**	**BG**	**BuOH**
AIJ	0	0	0
AJI	0	0	0
BIJ	536.8455	-181.3178	57.337
BJI	-298.0107	1317.198	554.8973
CIJ	0.3	0.3	0.3

3.2 Glycolic acid and Propanol system

The thermodynamic parameters of the reaction system formed by glycolic acid and propanol were determined following the methodology presented in section 3.1. For this system there is also no information available in the literature either. Propyl glycolate is an ester that is not currently available in the market, to carry out this part of the study, the first stage consisted in the production and purification of the ester.

3.2.1 Vapor pressure

The P_{sat} of the pure components was determined experimentally, the purity of 98% was verified by GCMS (see ANNEX G.I). Figure 3-18 presents the P-T diagrams for the experimentally data obtained for the propyl glycolate, the graph also includes the curve obtained from the regression of the data using the Antoine equation and the NRTL prediction. Measurements were made in a pressure range of 100.00 to 1013.25 mbar.

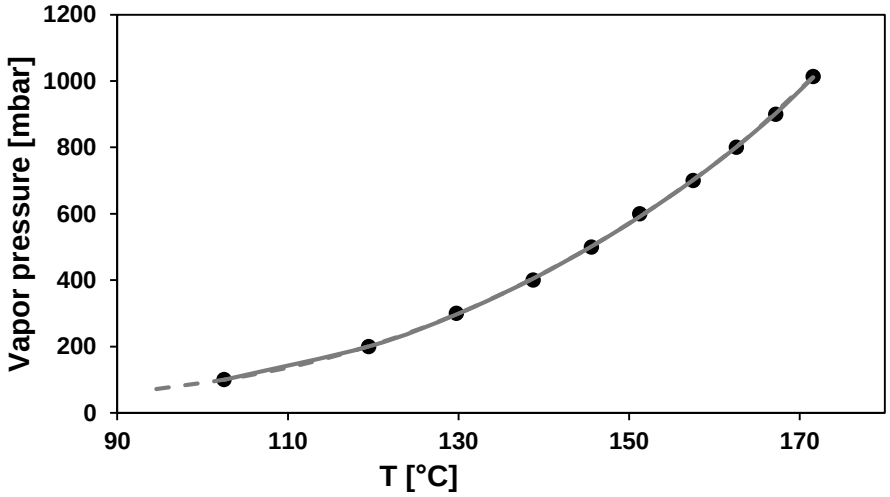

Figure 3-18. P-T diagram of propyl glycolate (●) this work, (---) Regression with Antoine equation and (- - -) NRTL prediction.

In the case of propyl glycolate, the Antoine equation (3.8) was reached using the Aspen Plus® regression tool, the parameters obtained fit favorably to the experimental data.

$$lnP^{sat,l} = -27291.7 + \frac{8.11e{+}05}{T \pm 1.18e{+}05} - 6.85127 + 4670.8\ln T + 4.54e - 15T^{6} \qquad (3.8)$$

$$102.51\ ^{\circ}\mathrm{C} > T > 171.58\ ^{\circ}\mathrm{C}$$

The boiling point of propyl glycolate at atmospheric pressure reported in the literature by Anderse in 1998 is 170.10 °C [4]. This compound is not found in the database of Aspen Plus® and the measured value of this work is close to the reported value 171.58 °C. The difference in the measure is part of the deviation from the measure.

3.2.2 Vapor-Liquid equilibrium

The VLE measurement for the propanol propyl glycolate (PrOH-PG) system was carried out at 1013.25 mbar. The vapor phase was assumed ideal considering the results previously obtained. The NRTL and UNIQUAC models were used to describe the liquid phase.

The experimental data $T - x - y$ for the PrOH-BG system were determined 1013.25 mbar (see Figure 3-19).

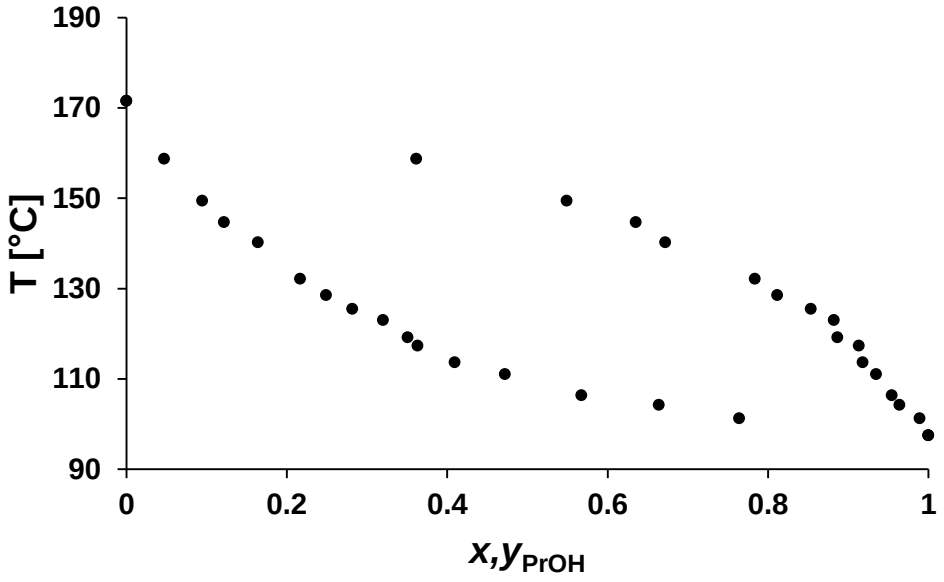

Figure 3-19. VLE for the binary PrOH + PG. at 1013.25 mbar. Exp (●)

Figure 3-20 shows the adjustment of the experimental data using the NRTL and UNIQUAC models. It can be seen graphically that the system corresponds to an ideal system, the models used are able to represent the system studied with the same precision. Although it is a homogeneous system and with an ideal behavior, in both cases, model NRTL and UNIQUAC, the verification test of the thermodynamic data failed, Duran *et al*. [12] report the same inconvenience,

the authors indicate that a possible cause for not passing the test may be due to a limited number of experimental data at the infinite dilution zones.

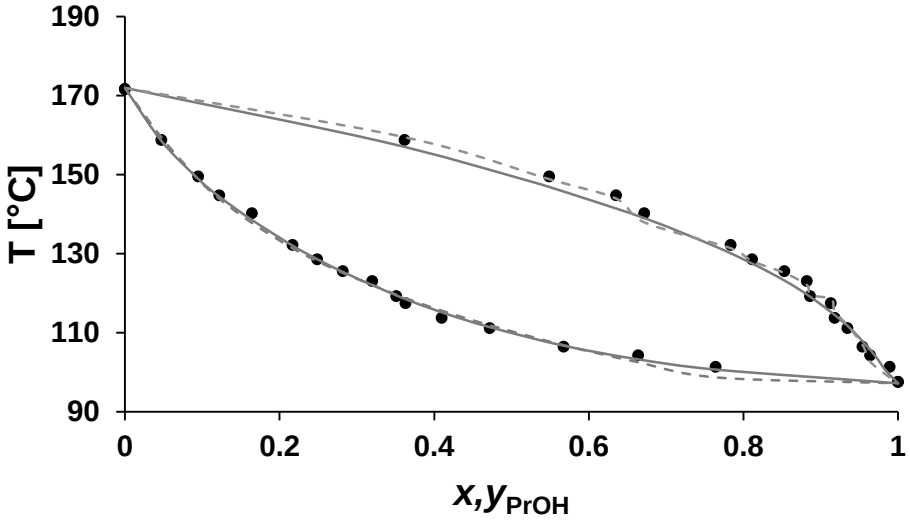

Figure 3-20. VLE for the binary PrOH+PG at 1013.25 mbar. Exp (●), NRTL (-), UNIQUAC (- - - -)

The parameters obtained for both equations are presented in Table 3-10. The thermodynamic parameters are able to describe the system adequately.

Table 3-10. Binary parameter for NRTL and UNIQUAC models for the system PrOH-PG

1013.25 mbar		
Component i	**PrOH**	**PrOH**
Component j	**PG**	**PG**
Model	NRTL	UNIQUAC
AIJ	30.808	11.238
AJI	4.981	-1.281
BIJ	-10000	-5379.99
BJI	-2486.92	851.31
CIJ	0.3	0.3

3.2.3 Solid-liquid equilibrium

The binary parameters of the glycolic acid - Propanol (GA-PrOH) and glycolic acid-propyl glycolate (GA-PG) systems were carried out following the same strategy presented in section 3.1.4. Figure 3-21 presents the solubility curve for the GA-PrOH and GA-PG systems.

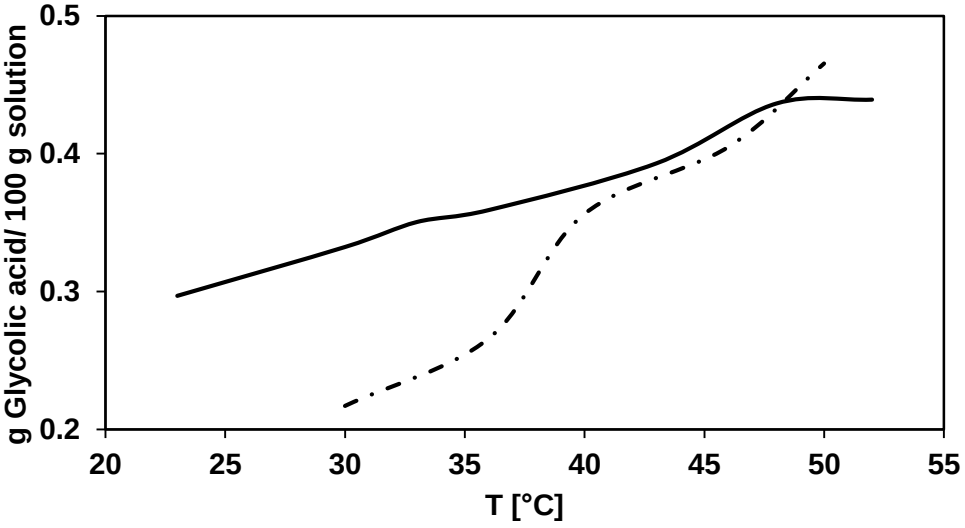

Figure 3-21. Glycolic acid Solubility in Propyl glycolate (-- - --), and Propanol (—).

Table 3-11 presents the binary parameters of the NRTL model for the GA-PrOH and GA-PG systems.

Table 3-12. Binary parameters for the NRTL model for GA-PrOH and GA-PG

	NRTL	
Component i	**GA**	**GA**
Component j	**PrOH**	**PG**
AIJ	0	0
AJI	0	0
BIJ	1015.08	-90.351
BJI	-192.60	693.907
CIJ	0.3	0.3

3.3 Glycolic acid and Octanol system

The thermodynamic parameters were also determined for the system conformed by the products of the esterification reaction between glycolic acid and octanol.

3.3.1 Vapor pressure

The P_{sat} of octyl glycolate was experimentally determined, the purity was verified by GCMS at the end of several stages of vacuum distillation (98%) (see ANNEX G.II). Figure 3-22 presents the P-T diagrams for the data obtained for octyl glycolate, the graph also includes the curve obtained

from the regression of the data using the Antoine equation and the NRTL prediction. The measurements could only be carried out up to 500 mbar pressure, at higher pressure conditions a yellowish change in the liquid was observed. Analyses of this substance indicated the presence of new peaks impossible to identify with the existing database. It should be noted that these measurements of this compound performed at operating limit conditions of the equipment. The difference between the curve obtained from the regression of experimental data and the prediction using the NRTL model increases progressively as the temperature increases, however this difference can be considered negligible as it is less than 1% in the experimentally evaluated range.

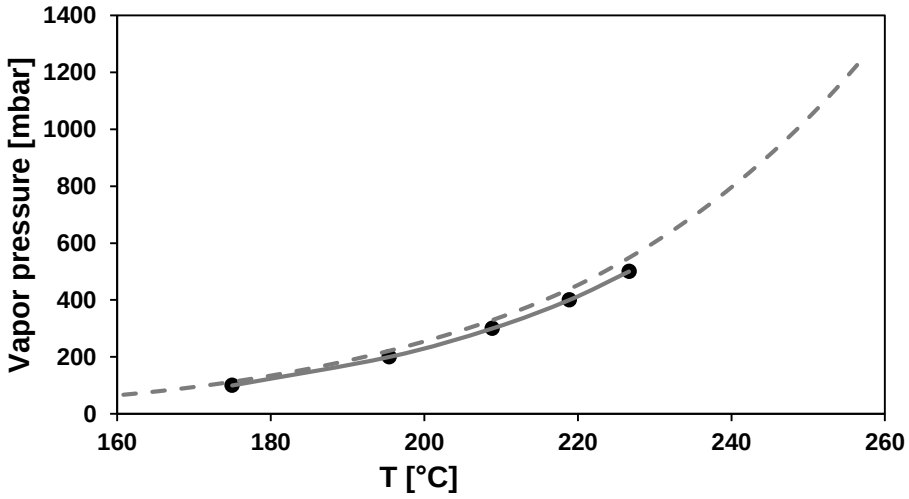

Figure 3-22. P-T diagram of octyl glycolate (●) this work, (---) Regression with Antoine equation and (- - -) NRTL prediction.

Antoine's equation for octyl glycolate is presented in equation 3.9. In the literature no experimental values of the boiling point of octyl glycolate are reported.

$$lnP^{sat,l} = -25715.97 + \frac{8.45e+5}{T} - 5.6031 + 4312.62\mathrm{lnT} + 2.0665\mathrm{e} - 15T^{6} \qquad (3.9)$$

$$174.95\ ^{\circ}\mathrm{C} > \mathrm{T} > 226.67\ ^{\circ}\mathrm{C}$$

3.3.2 Solid-liquid equilibrium

The binary parameters of the NRTL model for the glycolic acid - Octanol (GA-OcOH) and glycolic acid - octyl glycolate (GA-OG) systems were determined following the same methodology presented in section 3.1.4. Figure 3-23 presents the solubility curve for the GA-OcOH and GA-OG systems, these data were used for parameter regression.

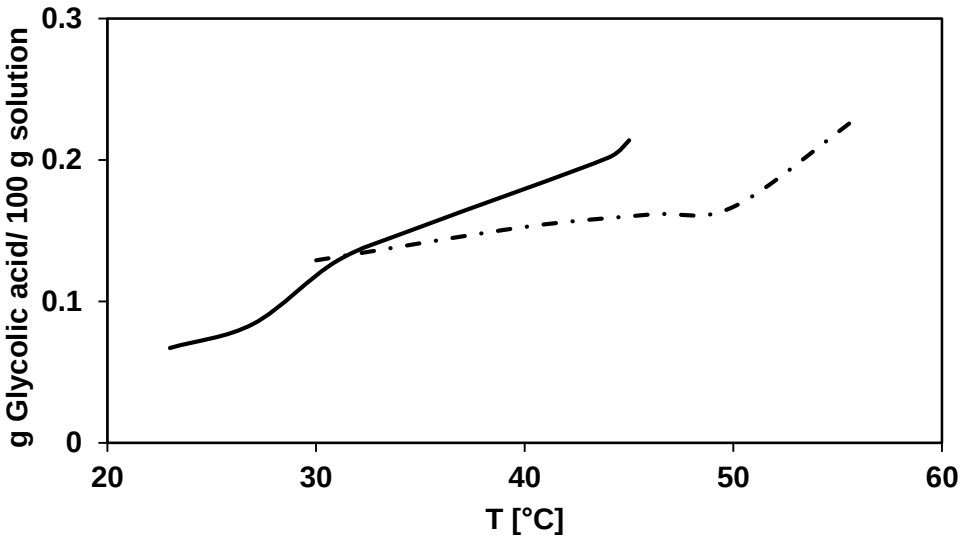

Figure 3-23. Glycolic acid Solubility in Octyl glycolate (-- - --), and Octanol (—).

Table 3-13 presents the binary parameters of the NRTL model for the systems

Table 3-13. Binary parameters for the NRTL model for GA-OcOH and GA-OG

	NRTL	
Component i	**GA**	**GA**
Component j	**OcOH**	**OG**
AIJ	0	0
AJI	0	0
BIJ	-6.461	1036.3
BJI	660.57	-158.67
CIJ	0.3	0.3

3.4 Conclusion

The main objective of the thermodynamic study was to determine the appropriate thermodynamic model to describe the behavior of the different binary systems studied. Two models were initially considered, UNIQUAC and NRTL model. The choice of the model was made from the validation of the binary parameters to describe the ternary system. NRTL model was chosen as the model that best fits and represents the experimental data. From this choice, the binary parameters of the solid-liquid systems were determined for this same model. The binary parameters of the NRTL model were used in chapter 4 to calculate the activity coefficients needed to determine the activities of the kinetic model.

3.5 Bibliography

[1] A. Fredenslund, R. L. Jones, and J. M. Prausnitz, “Group- contribution estimation of activity coefficients in nonideal liquid mixtures,” *AIChE J.*, vol. 21, no. 6, pp. 1086–1099, 1975.

[2] P. Susial, “Vapour-Liquid Equilibrium with a New Ebulliometer : Ester + Alcohol System at 0 . 5 MPa,” *Chinese J. Chem. Eng.*, vol. 18, no. 6, pp. 1000–1007, 2010.

[3] M. T. Sanz, S. Beltra, B. Calvo, and J. L. Cabezas, “Vapor Liquid Equilibria of the Mixtures Involved in the Esterification of Lactic Acid with Methanol,” pp. 1446–1452, 2003.

[4] F. A. Andersen, “FINAL REPORT ON THE SAFETY ASSESSMENT OF GLYCOLIC ACID, AMMONIUM, CALCIUM, POTASSIUM, AND SODIUM GLYCOLATES, METHYL, ETHYL, PROPYL, AND BUTYL GLYCOLATES, AND LACTIC ACID, AMMONIUM, CALCIUM, POTASSIUM, SODIUM, AND TEA-LACTATES, METHYL, ETHYL, ISOPROPYL, AN,” *Int. J. Toxicol.*, vol. 1717(1_sup, pp. 1–241, 1998.

[5] H. Renon and J. M. Prausnitz, “Local Compositions in Thermodynamic Excess Functions for Liquid Mixtures,” vol. 14, no. 1, pp. 135–144.

[6] J. M. Prausnitz, “Statistical Thermodynamics of Liquid Mixtures : A New txpression for the Excess Gibbs Energy of Partly or Completely Miscible Systems,” vol. 21, no. 1, 1975.

[7] M. Herrera-Calderón and J. C. Beltrán-Herrera, “Uso de coeficientes de actividad experimentales a dilución infinita para validar simulaciones de proceso Use of experimental activity coefficients at infinite dilution to validate process simulations,” *Cienc. Ed.*, vol. 27, no. 20, pp. 69–79, 2012.

[8] J. P. . Prausnitz, J. M.;Eckert, C. A.; Orye; R. V. , and O’Connell, *Computer Calculations for Multicom- ponent Vapor-Liquid and Liquid-Liquid Equilibria; Prentice Hall: Englewood Cliffs, NJ, 1980.*, Englewood. New Jersey, 1962.

[9] J. G. Hayden and J. P. O. Connell, “A Generalized Method for Predicting Second Virial Coefficients,” vol. 14, no. 192, pp. 209–216, 1975.

[10] A. Orjuela, A. J. Yanez, D. T. Vu, D. Bernard-brunel, D. J. Miller, and C. T. Lira, “Fluid Phase Equilibria Phase equilibria for reactive distillation of diethyl succinate Part I . System diethyl succinate + ethanol + water,” *Fluid Phase Equilib.*, vol. 290, no. 1–2, pp. 63–67, 2010.

[11] M. T. Sanz, B. Calvo, S. Beltra, and J. L. Cabezas, “Vapor-Liquid Equilibria at (33.33, 66.66, and 101.33) kPa and Densities at 298.15 K for the System Methanol + Methyl Lactate,” *J. Chem. Eng. Data*, vol. 47, no. 4, pp. 1003–1006, 2002.

[12] J. A. Duran, F. P. Córdoba, I. D. Gil, G. Rodríguez, and A. Orjuela, “Fluid Phase Equilibria,” *Fluid Phase Equilib.*, vol. 338, pp. 128–134, 2013.

[13] P. Hemptinne, Jean-Charles. BARREAU, Alain, LEDANOIS, Jean-Marie , MOUGIN, *SELECT THERMODYNAMIC MODELS FOR PROCESS SIMULATION A Practical Guide using a Three Steps Methodology*, Editions T. PARIS, FRANCE, 2012.

[14] A. Orjuela *et al.*, “Fluid Phase Equilibria Phase equilibria for reactive distillation of diethyl succinate . Part II : Systems diethyl succinate + ethyl acetate + water and diethyl succinate + acetic acid + water,” *Fluid Phase Equilib.*, vol. 290, no. 1–2, pp. 68–74, 2010.

[15] M. Toikka, D. Tro, and A. Samarov, “Fluid Phase Equilibria Liquid-liquid equilibrium and critical states for the quaternary system propionic acid e n -butanol e n -butyl propionate e water at 303 . 15 K,” vol. 460, 2018.

[16] B. A. Mandagaran and E. A. Campanella, “Modeling of phase and chemical equilibrium on the quaternary system acetic acid, n-butanol, water and n-butylacetate,” *Chem. Prod. Process Model.*, vol. 4, no. 1, 2009.

[17] P. Carniti, L. Cori, and V. Ragaini, “A critical analysis of the hand and Othmer-Tobias correlations,” *Fluid Phase Equilib.*, vol. 2, no. 1, pp. 39–47, 1978.

[18] J.-K. Kim and D.-W. Park, “Liquid-liquid equilibrium for the ternary systems of solvents+water+propionic acid at 25 ‡C and atmospheric pressure,” *Korean J. Chem. Eng.*, vol. 22, no. 2, pp. 256–263, 2005.

[19] E. Prausnitz, John M. Rudiger N, Lichtenthaler. Gomes de Azevedo, *Termodinamic molecular de los equilibrios de fases*. 2000.

[20] E. Mclaughlin, “Effect of a phase transition on the solubility solid,” vol. 29, no. 1, pp. 150–153, 1983.

[21] K. Bitchikh, A.-H. Meniai, W. Louaer, and J. P. Grolier, “Experimental and Modelling of liquid –solid equilibria,” vol. 00011, p. 00011, 2009.

[22] A. Orjuela, “Separation of Succinic Acid From Fermentation Broths and,” 2010.

[23] L. Negadi, M. Wilken, and J. Gmehling, “Solid-liquid equilibria for binary organic systems containing 1-methoxy-2-propanol and 2-butoxy ethanol,” *J. Chem. Eng. Data*, vol. 51, no. 5, pp. 1873–1876, 2006.

[24] V. N. Emel’yanenko, S. P. Verevkin, E. N. Stepurko, G. N. Roganov, and M. K. Georgieva, “Thermodynamic properties of glycolic acid and glycolide,” *Russ. J. Phys. Chem. A*, vol. 84, no. 8, pp. 1301–1308, 2010.

[25] A. Apelblat and E. Manzurola, “Solubility of suberic , azelaic , and diglycolic acids in water,” *J. Chem. Thermodyn.*, pp. 289–292, 1990.

Chapter 4. Kinetic study of the esterification of glycolic acid with butanol, propanol and octanol using homogeneous and heterogeneous catalysis

In the recent years, the production of glycolic acid has had great interest because it is a platform molecule with various industrial applications, including the rehabilitation of water wells, the leather industry, the oil and gas industry, the textile and laundry industry, and as a component in personal care products such as skin creams [1]. However, the most important application is to synthesize new biodegradable polymers, *e.g.* Polyglycolide and Poly(lactic acid-co-glycolic acid), which are raw materials for the reconstruction and transplantation of biological tissue organs [2].

Different alternatives have been found for the production of glycolic acid, through biological routes and from fermentation using nitrilase [1], by the enzymatic conversion of glycolonitrile [3], or by chemical routes through the selective oxidation of glycerol [4]. For all cases, acid recovery should be made from a highly diluted aqueous mixture formed by other components, mainly acids (e.g., formic acid, glyceric acid, tartronic acid, etc…). Given these conditions, the separation and recovery processes of glycolic acid involve a high process complexity, energy consumption and problems associated with contamination due to the use of different reagents.

According to recent studies, the glycolic acid recovery can be carried out by crystallization, ion exchange (cationic and/or anionic), electrolysis, liquid-liquid extraction, alcoholysis, and distillation. However, these techniques are underperforming. Though, the reactive distillation technique has been found to be an efficient, economical and environmentally friendly method of separating carboxylic acids, such as acetic acid, from wastewater streams [5]. In the literature, there is no evidence of processes using this technique for the recovery of glycolic acid.

The simulation and design of a reactive distillation process require information on reaction kinetics, the thermodynamic equilibrium of the mixtures involved, the mass transfer characteristics and information on the pure products involved in the process. The glycolic acid recovery in ester form implies the study of the esterification reaction, however in the literature few works have studied this acid. Mahajani [6] studied the reactions of glyoxylic acid with different aliphatic alcohols in the presence of ionic exchange resins both gelular and macroporous as catalysts. He demonstrated

that alcohol can react either with the acid or with the aldehyde group of glyoxylic acid to form ester and acetal of the ester, respectively. At lower temperatures, the selectivity towards the corresponding ester was more important, and at elevated temperatures, substantial formation of acetal of the ester was realized. The acetal of the ester can be selectively obtained by almost complete removal of water from the reaction mixture and conversion is favored as an equilibrium reaction. Jiang *et al.* [7] studied the synthesis of different esters from glycolic acid for using as phase stabilizers and depressants of vapor pressure of the methanol-gasoline mixture. The results show that the reaction performance can reach 80 to 87%, depending on the alcohol.

Implementing a strategy of separation by reactive distillation overcomes the disadvantages that can occur in the esterification reaction of glycolic acid. The limitations or low yields associated with chemical equilibrium are overcome through the continuous and selective elimination of water, as well as the obtaining of high purity products.

This part of the work focuses on determining the kinetics of the esterification reaction of the main acids present in the mixture after the glycerol reaction presented in chapter 1 (*e.g.* glycolic and formic acid), with the aim of being able to develop the strategy of reactive distillation for the separation and recovery of the acids.

The esterification of glycolic acid with butanol was chosen as model reaction (See Rxn.1) to develop the synthesis protocol and evaluate the efficiency of the different reaction techniques, thus to determine the optimum conditions for esterification reaction. Initially, the reactions were carried out using homogeneous catalysis in order to determine the maximum yields for each condition. Furthermore, a heterogeneous catalysis was also employed expecting to reach similar performances.

$$\underset{Glycolic\ acid}{C_2H_4O_3} + \underset{Butanol}{C_4H_{10}O} \leftrightarrow \underset{Butyl\ glycolate}{C_6H_{12}O_3} + \underset{Water}{H_2O} \qquad Rxn.1$$

The use of a solid catalyst allows the mechanical separation of the catalyst from the reagent-products mixture, in addition to reducing capital and processing costs. The distillation column reactor, packaged with ion exchange resin, offers clear advantages over the conventional approach of sequential reaction and separation. From the results of the literature, the solid

catalysts used in the esterification reaction can be classified into polymer-supported sulfonic acid resins, sulfonated silica gels, inorganic solid-supported acid catalysts and acid-treated clays [8]. However, it is the ion exchange resins that have shown the best results; for this work, a series of commercially available resins were selected.

Regarding the proper modeling of the esterification reaction kinetics, several works are reported in the literature with ion exchange resins where kinetic models of the pseudo-homogeneous type (PH) and heterogeneous models (Langmuir-Hinshelwood (L-H) and Eley-Rideal (E-R)) that have been commonly used to describe the reactions are considered [2, 8-24]. In order to validate the implementation of the different heterogeneous kinetic models, the absence of any intraparticle diffusion limitation was studied.

The effect of using kinetic models based on molar concentrations or fractions and on activities has also been studied, the latter additionally considering deviations from the ideality by adding the activity coefficients. Delgado *et al.* [25] have demonstrated, by studying the esterification of lactic acid with ethanol, that assuming ideal behavior of the liquid phase gives rise to large errors. Kinetic models were best adjusted when considering the non-ideality of the liquid mixture.

Chapter 3 presented the result of the thermodynamic study of the model reaction system between glycolic acid and butanol. These results will be used in the present chapter, where it was determined that the NRTL model can predict most of the binary systems involved in the model system.

4.1 Glycolic acid and butanol system

4.1.1 Homogeneous catalyst

For the reaction kinetics study, the first approach was made using homogeneous catalysis. In the literature, commonly mineral acids, such as H_2SO_4, HCl, HI, and strong organic acids, such as HCOOH, can be used as homogeneous catalysts [26]. The disadvantage of homogeneous catalysts is their miscibility with the reaction medium, which causes separation problems. In addition, at higher catalyst concentrations corrosion of equipments may occur. However, the information obtained is considered as a reference in terms of performance. H_2SO_4 was chosen as

a homogeneous catalyst for this study, it is one of the most widely used homogeneous catalysts in the industry.

4.1.1.1 Effect of reaction temperature

The effect of temperature on the model reaction of butanol and glycolic acid for the synthesis of butyl glycolate was studied at 50, 60 and 70 °C. Figure 4-1 shows the effect of temperature on the acid conversion. The reactions were carried out using 1 mol% of H_2SO_4 as a catalyst and a molar ratio glycolic:butanol acid of 1:3. It is observed that reactions at 60 and 70 °C reached the equilibrium between 60 and 120 minutes, while the equilibrium was reached after 240 minutes at 50 °C. After 240 minutes of reaction, the conversion was similar to the three temperatures, varying between 81% at 50 °C and 86% at 70 °C. This indicates that the heat effect is minor for the reaction system.

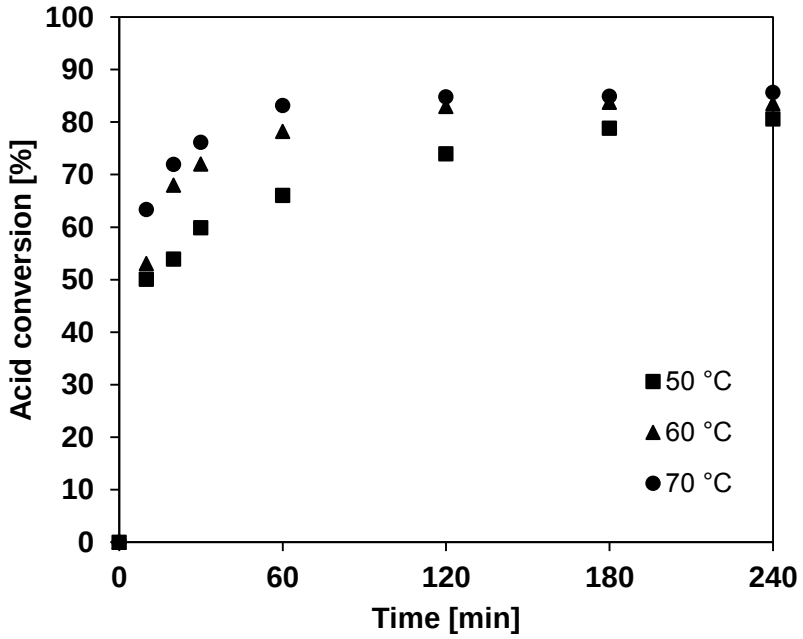

Figure 4-1. Effect of temperature on the conversion of glycolic acid.
Conditions: 1.3 molar ratio and 1 mol % of H_2SO_4

The initial reaction rate is defined as:

$$r_0 = \frac{C_{A_0} X_A}{t} \quad (4.1)$$

Where C_{A_0} and X_A are the initial concentration and the conversion of glycolic acid at t_1=10 min,

and $X_A = \frac{n_{A_0} - n_A}{n_{A_0}}$, the conversion X_A is calculated from the initial moles n_{A_0} and final moles n_A of acid. Figure 4-2 presents the relationship between temperature (T) and the initial reaction rate (r_0). The effect of temperature variation directly influences the initial reaction speed (r_0).

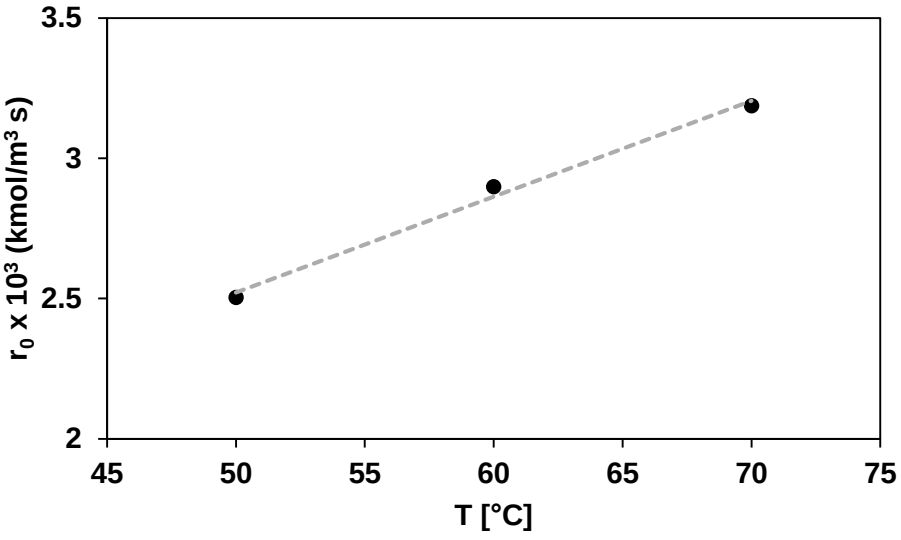

Figure 4-2. Reaction rate under different reaction temperatures

This behavior as a function of the change in temperature indicates that it is an endothermic reaction. This result will be confirmed later with the determination of the enthalpy of reaction.

Mekala *et al.* [27] studied the esterification reaction of acetic acid with methanol in the presence of H_2SO_4. The results showed that the increase in temperature and catalyst concentration is related to the increase in reaction rate. The effect of the variation of these parameters on the equilibrium is hence negligible.

4.1.1.2 Effect of alcohol:acid molar ratio

To study the effect of the butanol:glycolic acid molar ratio on the esterification reaction, 3 ratios were proposed: 1:1; 1:3 and 1:6. Stoichiometrically, the esterification reaction for the synthesis of butyl glycolate requires one mole of butanol for each mole of glycolic acid. Industrially, the strategy of operating with an excess of alcohol is well known and used to achieve higher conversions of acids according to the Le Chatelier's principle and considering that terms of availability and costs.

The study of the molar ratio effect was carried out at 70°C and 1 mol % of H_2SO_4 as a catalyst. Figure 4-3 shows the effect of the molar ratio on the conversion.

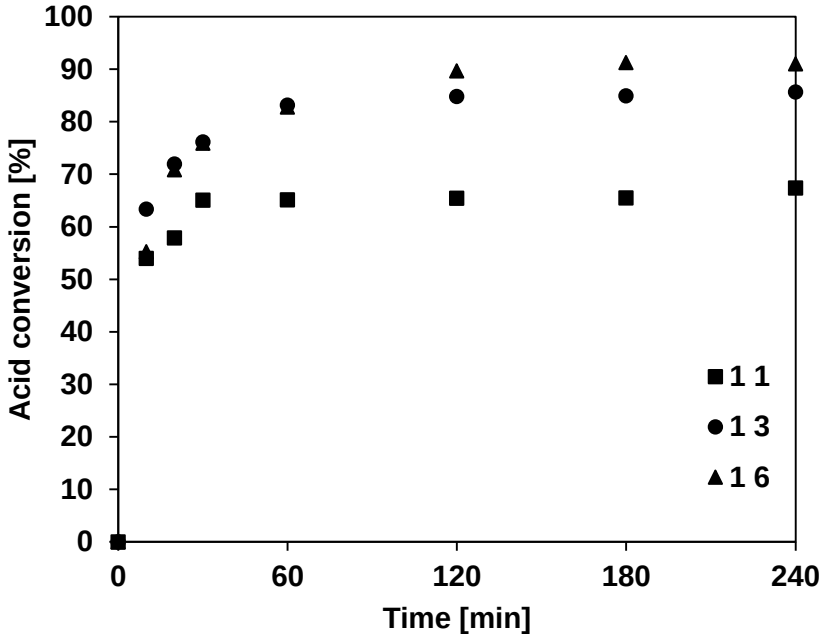

Figure 4-3. Effect of alcohol: acid ratio on the conversion of glycolic acid.
Conditions: 70 °C and 1 mol % of H_2SO_4

In general, the results reveal that the conversion increases with an increase in the molar ratio. After 120 min, the conversion is 65 % for the 1:1 molar ratio, 85 % for the 3:1 molar ratio and 91 % for the 6:1 ratio.

Lilja *et al.* [16] investigated the esterification reaction between propanoic acid and ethanol, 1-propanol and butanol, they have noticed that the initial reaction rate increases linearly with the acid concentration. On the other hand, for alcohol, such an increase is linearly only at low alcohol concentration but is nearly independent of it at high levels. Mekala *et al.* [27] also found that when carrying out the reaction of excess alcohol, the maximum conversion that can be achieved is 91% with a four-time excess of alcohol over the acid. In this work, a similar conversion rate was achieved.

4.1.1.3 Effect of the amount of catalyst

The variation of catalyst amount was carried out using H_2SO_4 varying in the range of 0.2-1.0 mol% with respect to the glycolic acid quantity. The temperature was fixed at 70 °C and the butanol:glycolic acid molar ratio at 1:3.

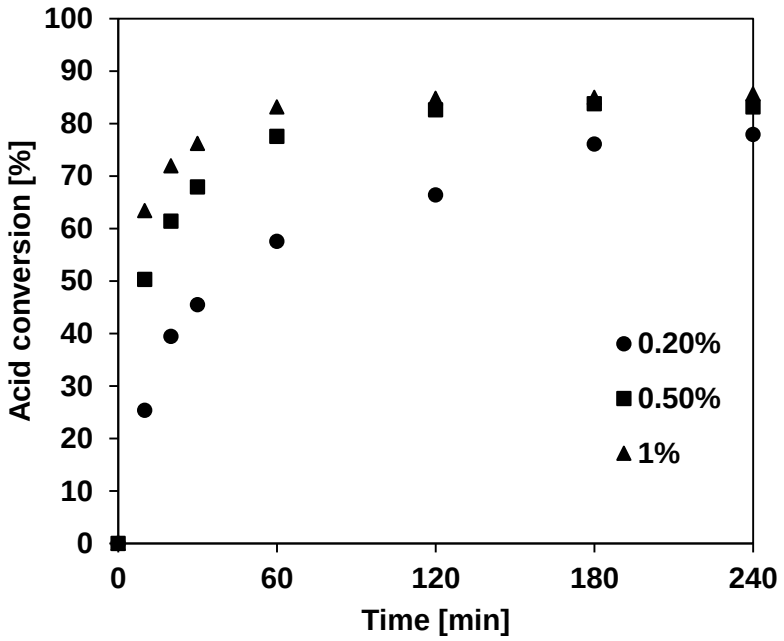

Figure 4-4. Effect of the H_2SO_4 amount in the glycolic acid conversion during the esterification with butanol. Conditions: 70 °C and 1:3 molar ratio.

Figure 4-4-4 shows the effect of the catalyst amount on the glycolic acid conversion. The initial reaction rate is increased considerably with the increase in the catalyst amount. The highest difference was observed for the 0.2 mol% test, where the four hours of reaction were not enough to reach the equilibrium. The tests with 0.5 and 1 mol% reach the equilibrium conversion after 60 minutes and 120 minutes, respectively. The amount of catalyst does not vary the final conversion, between 83 and 86 %, for the three reactions.

The variation of the amount of catalyst has a considerable effect on the initial reaction rate using the equation 4.1. Figure 4-5 shows the relationship between the amount of catalyst (w_{Cat}) and the initial reaction rate (r_0), it shows a linear relation between the interrelated parameters (r_0 and w_{Cat})

thus confirming that the experimental data used to calculate the reaction rate take into account the variation of the amount of catalyst.

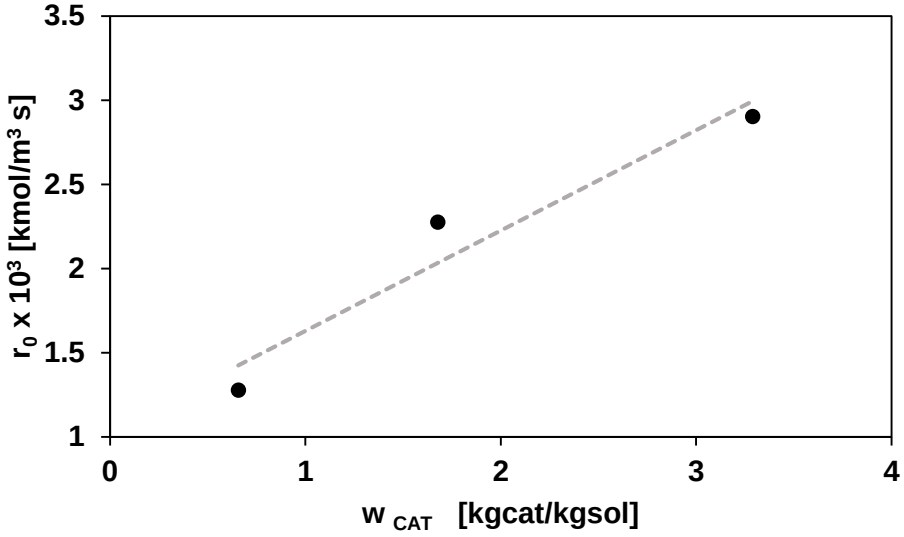

Figure 4-5. Evolution of reaction rates using different amounts of catalyst.

4.1.1.4 Equilibrium Constant and Kinetic Model

For each of the studied systems, the equilibrium constants (K_{eq}) were determined. A series of additional long experiments (reaction time greater than 20 h) were performed. The K_{eq} was determined at different temperatures from the equilibrium compositions of all endpoints using the equation 4.2. The activity coefficients of the components of the reaction mixture were calculated by the NRTL method presented in Chapter 3, as shown by the expression:

$$K_{Eq} = K_x K_\gamma = \frac{(x_{Eq_C} * x_{Eq_D})}{(x_{Eq_A} * x_{Eq_B})} * \frac{(\gamma_{Eq_C} * \gamma_{Eq_D})}{(\gamma_{Eq_A} * \gamma_{Eq_B})} \quad (4.2)$$

In equation 4.2, K_x represents the ratio of the molar fractions of the mixture at the equilibrium and K_γ represents the relation of the activity coefficients calculated at the same conditions (see Table 4-1).

Table 4-1. Equilibrium constants of glycolic acid esterification with butanol.

Temp [°C]	Kx	Keq
50	1.60	1.73
60	1.80	2.39
70	1.96	2.90

Figure 4-6 presents the Van't Hoff plot for the equilibrium constants calculated at different temperatures. The constants were calculated for the case where they are only a function of the molar fractions (▲) and the case where the constants are corrected with the activity coefficients (●).

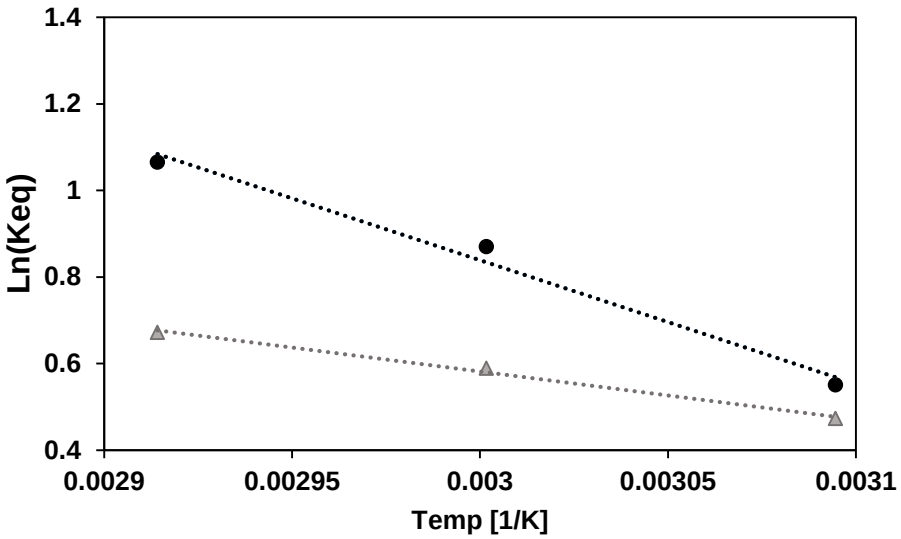

Figure 4-6. Van't Hoff plot for glycolic acid esterification with butanol from experimental data. Mole fraction (▲) Kx and activity (●) Keq

The comparison between the slopes of the curve concludes that at low temperatures, the system tends to follow an ideal behavior. However, when the temperature increases there is a significant difference between the ideal and non-ideal system. By including the effect of non-ideality in the calculation of the equilibrium constant, an increase in the total value is observed. These results are in agreement with that presented by Orjuela *et al.* [28] who found, for the succinic acid and ethanol system, an increase of a factor of 4 for the equilibrium constant, in this study the increase of factors was between 1 and 1.5. However, they consider that for their reaction, the effect of temperature was negligible. In the present study, however, the effect of temperature was

considered in order to reduce possible sources of error as much as possible and to achieve the best possible adjustment. Considering the equilibrium constant as a function of the activities the curve corresponded to an endothermic reaction [29].

The standard enthalpy of reaction ($\Delta_r H°$) can be calculated from the Van't Hoff equation 4.3:

$$\frac{dLn\ K_{eq}}{dT} = \frac{\Delta_r H°}{RT^2} \tag{4.3}$$

The expression of the equilibrium constant as a function of temperature was obtained, as indicated in equation 4.4:

$$Ln\ K_{eq} = -\frac{2858.5}{T} + 9.4143 \quad R^2 = 0.9852 \tag{4.4}$$

Using this equation, the obtained value of $\Delta_r H°$ turned out to be 23.76 kJ mol^{-1}. In the literature, there are no works similar to our case study, the closest result is the value reported by Xu *et al*. [2] who worked on the hydrolysis of methyl glycolate (reverse reaction of the esterification). They found a standard reaction enthalpy of -15.52 kJ mol^{-1} which is in accordance with our calculated value.

The objective of the kinetic study using homogeneous catalysis was to provide reference kinetic data to compare the yields obtained using heterogeneous catalysis. For the particular case of the esterification reaction, the kinetic model is widely known in the literature, it considers the reversible reaction what makes it a second-order model. At the operating conditions no secondary reactions were observed in any of the experiments [3, 6, 23, 25], [30–34]. As already mentioned, some authors have used the model in terms of mole fractions while others have used it in terms of activity. For this study, the final objective is to use the information gathered from the simulation of a reactive separation process, either employing the conventional reactive distillation strategy or by implementing a divided walled column. In order to obtain reliable results, our kinetic model was developed in terms of activity. Equation 4.5 represents the homogeneous kinetic model:

$$r = k_1^0 exp\left(-\frac{E_A}{RT}\right)\left(a_{GA}a_{BuOH} - \frac{a_{BG}a_W}{K_{eq}}\right) \tag{4.5}$$

Where k_1^0 and E_A represent the pre-exponential factor and the activation energy of the forward reaction, respectively. The equilibrium constant of the reaction, K_{eq}, is the ratio of the constants of the forward and reverse rates and the activity, a_i, is the product between the activity coefficient and the molar fraction. The experimental reaction rate was calculated considering the design equation of a batch reactor, assuming an ideal solution and constant solution volume (experiments were performed with pure products). The two adjustable parameters, k_1^0 and E_A, were determined from the analytical solution of the reaction rate (r) based on the mass balances of the known amount of catalyst as represented in equation 4.6:

$$r = \frac{n_0}{W}\frac{dX}{dt} \tag{4.6}$$

Equation 4.6 represents the reaction rate (r) as a function of the change of initial moles (n_0), expressed in terms of conversion to a given amount of catalyst (W). The methodology used to develop the kinetic study was based on the work done by Orjuela *et al.* [28]. The fourth-order Runge-Kutta method was used to numerically integrate the kinetic model 4.5 [35], using the ordinary differential equations solver ode45 in MATLAB 9.4 (The MathWorks, Inc., Natick, Massachusetts, United States). The optimization of the kinetic parameters was performed by minimizing the sum of residuals squares (SRS) between experimental (x_{exp}) and calculated (x_{cal}) species mole fractions using the following objective function in MATLAB 9.4 (see ANNEX H), represented in a general way in the equation 4.7:

$$SRS = \frac{1}{n}\sum_{All\ samples}^{Nc}\left(x_{exp} - x_{cal}\right)^2 \tag{4.7}$$

Where n is the number of experimental samples taken from the batch reactors in all experiments performed and NC is the number of components considered in each sample.

To confirm that the parameters found correspond to global optimum, the Multistart function in MATLAB 9.4 was used generating different combinations of initial points. For the adjustment of the variables the thermodynamic consistency was considered forcing positive values of the kinetic and adsorption constants.

As the last stage of verification, the absolute and relative error or mean relative deviation of the optimized constants was determined as presented in equations 4.8 and 4.9:

$$E_{Abs} = \frac{1}{n}\sum_{All\ samples}^{Nc}\left|x_{exp} - x_{cal}\right| \quad (4.8)$$

$$E_{Rel} = 100 * \frac{1}{n}\sum_{All\ samples}^{Nc}\frac{\left|x_{exp} - x_{cal}\right|}{x_{exp}} \quad (4.9)$$

4.1.1.5 Kinetic model results

For the kinetic study in the presence of homogeneous catalysis, a series of 8 experiments were carried out. The parameters modified were the temperature, the amount of catalyst and the molar ratio between acid: alcohol, the conditions are given in Table 4-2.

Table 4-2. Experimental conditions of forward reaction esterification.

RUN	Temp [°C]	Mole Ratio [BuOH/GA]	Catalyst amount [g]	Time [min]
1	50	3	0.257	240
2	60	3	0.257	240
3	70	3	0.257	240
4	70	6	0.257	240
5	70	1	0.257	240
6	70	3	0.257	240
7	70	3	0.051	240
8	70	3	0.129	240

For the calculation of the inverse reaction constant, different experiments were carried out using the water and ester reagents as the starting mixture. A total of 7 experiments were performed, the modified parameters were the same as for the forward reaction, the conditions are given in Table 4-3.

Table 4-3. Experimental conditions of inverse reaction esterification.

RUN	Temp [°C]	Mole Ratio [W/BG]	Catalyst amount [g]	Time [min]
1	50	3	0.257	360
2	60	3	0.257	360
3	70	3	0.257	360
4	70	6	0.257	360
5	70	1	0.257	360
6	70	3	0.051	360
7	70	3	0.129	360

The homogeneous kinetic model expresses in terms of activities predicts reasonably well the behavior of the esterification reaction mixture. Figure 4-7 presents an example of the predictive profile of the molar fractions obtained based on the activity model and the molar fractions obtained experimentally.

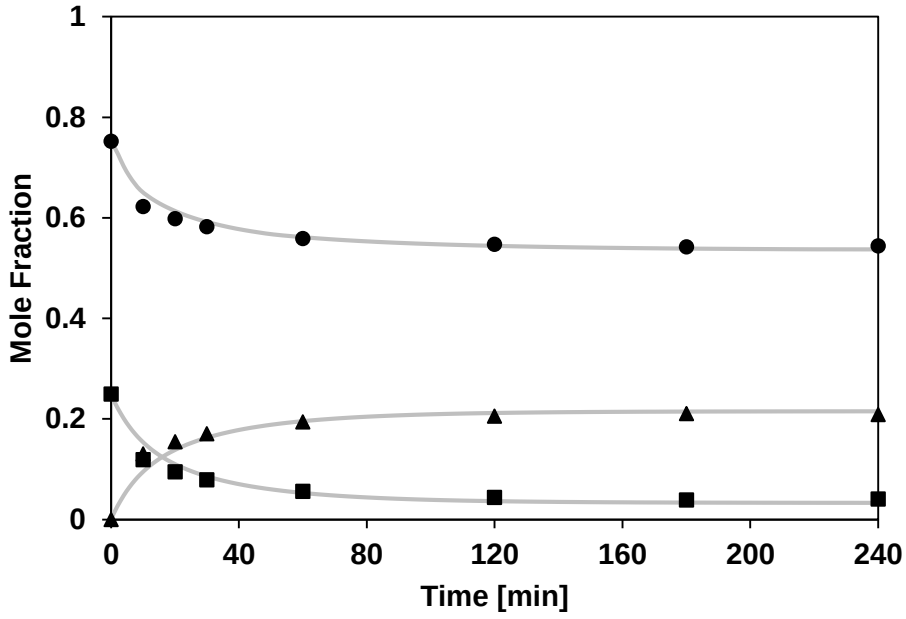

Figure 4-7. Experimental and predicted mole fraction profiles of glycolic acid esterification with butanol using second-order model. Exp 6: T = 70 °C, $W_{cat} = 0.1285\ g\ H_2SO_4$; Mole fraction: (■) Glycolic acid; (●) Butanol; (▲) Butyl glycolate.

The determination of the adjustable parameters is carried out considering all the experiments. Table 4-4 presents k_1^0 and E_A for the glycolic acid and butanol reaction system.

Table 4-4. Homogeneous kinetic model - Estimated Parameters for butanol and glycolic acid system

Parameters	Estimated Values	Standard deviation
E_A [J mol^{-1}]	90.05	13%
k_1^0 [mol (g*min)$^{-1}$]	7.45e12	<0.1%
SRS_N	1.09	
E_{Rel} [%]	7.54	

The parameter values obtained agree well with the values reported in the literature for similar acids such as acetic and propionic acids for the direct reaction [20], [26], [28], [36]–[38]. Considering just the direct reaction, the activation energy is 49.58 kJ mol^{-1}, this is an evidence that forward reaction is favored over reverse reaction. In general, the energy parameters of the esterification reaction of carboxylic acids are similar and range from 45.00 to 55.00 kJ mol^{-1}, using homogeneous catalysis. The fit of the kinetic model with the experimental data is quite good, which allows inferring that for the studied conditions there are no limitations associated with the solubility of the acid in the alcohol.

4.1.2 Heterogeneous catalyst

The second stage of the kinetic study consisted of the choice of the most suitable heterogeneous catalyst in the case of the model reaction. Prior to the kinetic study using heterogeneous catalysis, the existence of diffusion limitations was verified. Then several kinetic models that consider the presence of the heterogeneous catalyst were used to represent the experimental data.

4.1.2.1 Effect of the catalyst (Heterogeneous catalysis)

To compare the results obtained with the homogeneous catalyst (*i.e.*, H_2SO_4), five ion exchange resins widely used industrially and commercially were tested. This type of ion exchange resins first appeared in the 1960s, when the results of the research carried out on the mechanism of formation of macroreticular styrene (St) –divinylbensene (DVB) copolymers were reported [39]. In

general terms, the morphological characteristics of this porous material can be modified depending on the concentration of the cross-linking agent, the concentration of the diluents and the reaction temperature [40]. These materials have undergone structural modifications and additional processes such as sulfonation (SO_3H) that have given rise to ion exchange resins. Among the most widely and commercially available materials are Amberlyst 15 [6], [12], [13], [22], [30], [31], [36], [37], [41], [42] Amberlyst 16 [11], [43]–[45] , Amberlyst 36 [36], [46], [47], [48] Dowex [14], [31] and Nafion. These are differentiated among each other by the matrix type, e.g., type St-DVB, resine type, e.g., macroporous strong acidic cation, standard ionic form, e.g., H^+ and functional group, e.g. $–SO_3^-$.

For the purposes of this investigation, the choice of the catalyst was done considering the appropriate chemical and structural characteristics for the esterification reaction of the model reaction (*i.e.,* butanol + glycolic acid). Table 4-5. Properties of catalysts Presents the five different types of resins used in this study and their main characteristic parameters. The ion exchange resins have different characteristics including: morphological, *e.g.* surface area, average pore diameter, pore volume, and catalytic, *e.g.*, concentration of acid sites, this last parameter refers to the number of acid sites available per catalyst mass. The catalytic activity of the resin is related not only to the capacity but also to the strength of the acid site. Siril *et al.*[49] investigated the differences between four different types of Amberlyst, *e.i.,* 15, 35, 36 70, in terms of acidity, catalytic activity and thermal stability. They indicated that catalytic activity depends on the accessibility of acid sites through the polymeric matrix. In a general way, for the authors, the three parameters studied; acids, catalytic activity and thermal stability, are related to the presence of sulfonic groups in the resin, *i.e.* the resins with better catalytic performance and stability are the super-sulfonated, Amberlyst 35 and 36, as a result of the activation of sulfonic acid groups by having more than one group of acids in at least some of the benzene rings. This characteristic was also found in the Amberlyst 70. This type of catalyst in contact with highly polar solvents tend to change their morphology, the ion exchange resin swells completely, which allows the active sulfonic acid group to be completely dissociated and the dissolved protons to be distributed evenly in the polymer phase [2]. As a result, the chemical species involved in the reaction could easily penetrate the network of cross-linked polymer chains and come into contact with the dissolved protons. In this way, reactions can be said to be kinetically controlled.

Table 4-5. Properties of catalysts

	Amberlyst®15	Amberlyst®16	Amberlyst®36	DOWEX DR-2030	Nafion
Ionic form as shipped	Hydrogen	Hydrogen	Hydrogen	Hydrogen	
Average pore diameter	300 Å	250 Å	240 Å		
Total pore volume	0.40 mL g^{-1}	0.2 mL g^{-1}	0.2 mL g^{-1}	0.33 mL g^{-1}	
Surface area	53 m^2 g^{-1}	30 m^2 g^{-1}	33 m^2 g^{-1}	30 m^2 g^{-1}	
Concentration of Acid Sites	≥ 4.7 eq kg^{-1}	≥ 4.8 eq kg^{-1}	≥5.40 eq kg^{-1}	4.7 eq kg^{-1}	0.9 eq kg^{-1}
Maximum operating temperature	120 °C	130 °C	150 °C	150 °C	200 °C
Moisture holding capacity	52 to 57 % (H+ form)	52 to 58 %(H+ form)	51 to 57 %(H+ form)		

The reactions were carried out applying the following conditions: 70°C, molar ratio butanol:glycolic acid of 3 and a catalyst amount of 1.32 wt.%. Figure 4-8 compares the evolution of the glycolic acid conversion using different commercial ion exchange resins as catalysts. The test performed using H_2SO_4 at the same conditions is also presented in the Figure 4-8 as a benchmark.

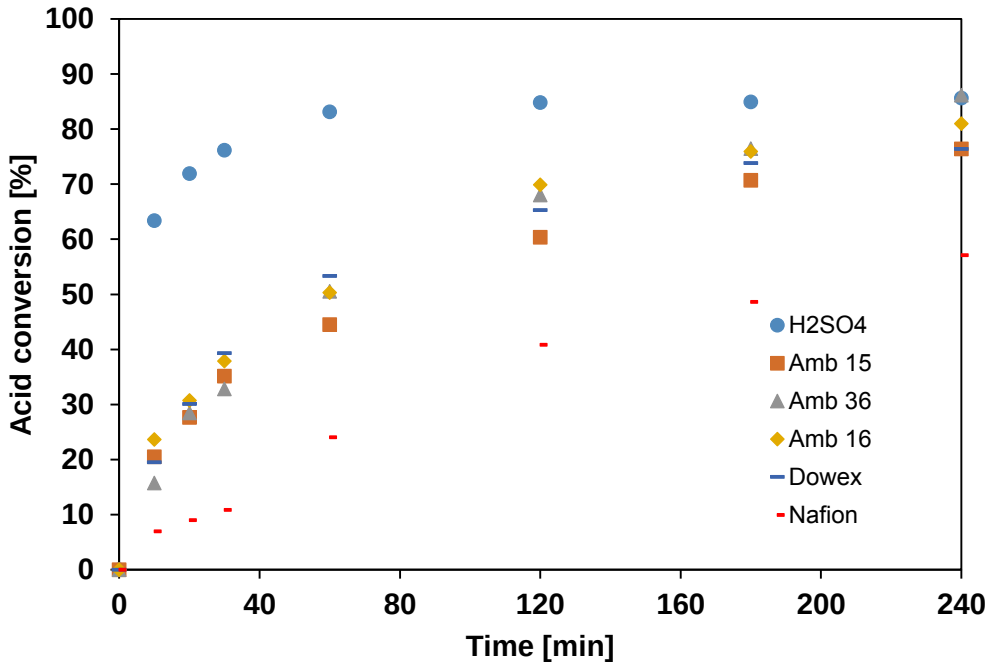

Figure 4-8. Effect of catalyst type on glycolic acid conversion.
Conditions: 70 °C and 1:3 molar ratio.

Nafion proved to be the catalyst with the lowest activity, possibly related to the low exchange capacity compared to the other selected catalysts (see Table 4-5. Properties of catalysts). Liu *et al.* [20] showed that for the Nafion activity to be comparable to the activity of H_2SO_4, the polymeric structure must be modified, the authors also found that the activity of this catalyst is strongly inhibited by the presence of water. The other resins showed similar catalytic behavior, with high activities and slower kinetics compared to H_2SO_4. After 240 minutes, only the Amberlyst 36 achieved a conversion equal to the one obtained with H_2SO_4 (*i.e*., 86 %). Amberlyst 16 also showed high activity with a conversion only 5 % lower compared to that obtained with the H_2SO_4. In this case, it is noticed that the activity does not depend on the morphology of the catalyst but it can be directly related to its capacity. Dowex and Amberlyst 15 despite having a capacity superior or equal to 4.7 eq kg^{-1} have similar conversions, both having 10 activity points less compared to Amberlyst 36. Amberlyst 36 has been widely used for esterification reactions due to its advantages in terms of catalytic activity and thermal stability, as already mentioned, product of its over sulfunation [36], [46], [47], [48] . Amberlyst 36 could be considered as a possible option for the implementation of the process at an industrial level.

4.1.2.2 Diffusional limitations

The study to determine diffusion limitations using Amberlyst 36 was performed for the esterification reaction of glycolic acid and butanol. This catalyst was selected for its excellent performances. Different stirring rates were evaluated to determine the effect of external mass transfer resistance. The stirring rate ranged from 300 to 700 rpm, keeping the other operating parameters constant. At the same reaction time, the conversion remained constant despite the change in the stirring rate suggesting that the external mass transfer resistance is not the speed-controlling step (see Figure 4-9). This result agrees with the work carried with Amberlyst 36 by Akyalcin *et al.* [46], pointed out that external diffusion in the case of esterification reaction between acetic acid and octanol does not affect conversion despite the viscosity of octanol. All other experiments in this work were performed at 600 rpm to ensure the measured reaction speed without external diffusion influences. Once the resistance to external mass transfer has been excluded, it is confirmed the overall rate is controlled by the internal diffusion of the reactants or the chemical reaction on the surface of the catalyst.

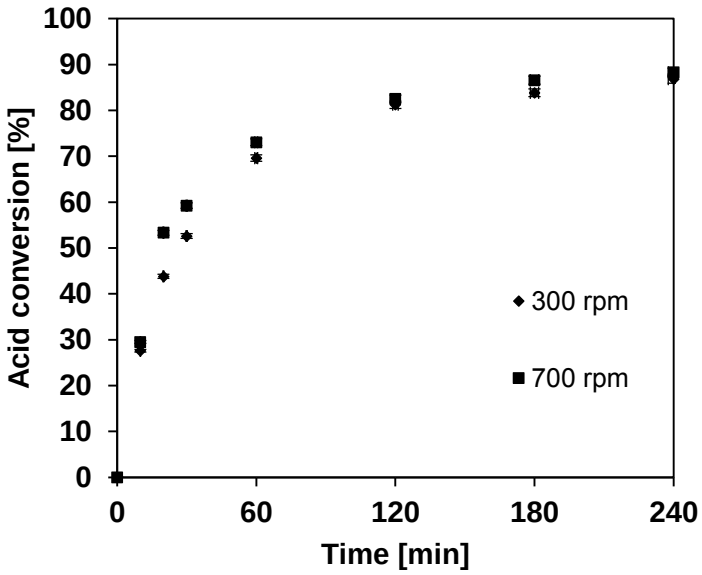

Figure 4-9. Stirring rate effect on glycolic acid conversion.

The effect of intra-particle diffusion in the reaction was studied for the Amberlyst 36. Two different particle sizes were screened, between 250-500 μm and greater than 500 μm. The same reaction conditions were used for both tests. Through the experiments, it was observed that there were no evident differences in reaction rates with change in particle sizes, which shows that internal resistance to mass transfer can be neglected (see Figure 4-10). Therefore, the commercial resins were used directly in the kinetic experiments.

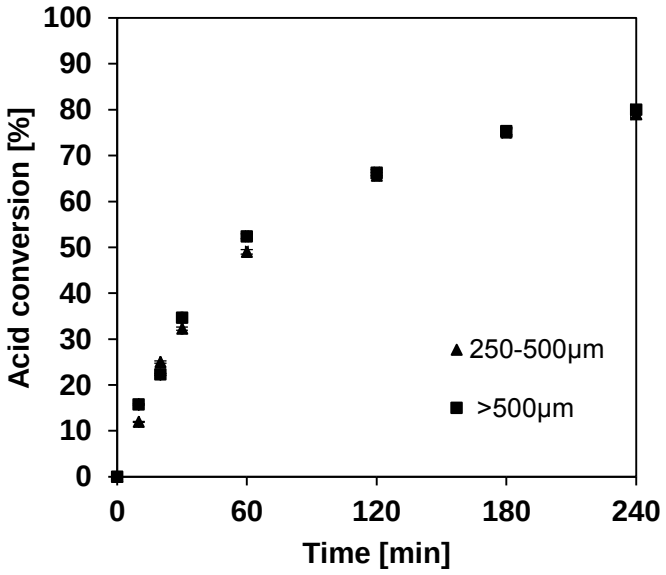

Figure 4-10 . Particle size effect on glycolic acid conversion.

These results agree with the results reported in the literature which state that external diffusion and intraparticle resistances are usually negligible for most reactions catalyzed by Amberlyst-type resins[28], [30], [34], [36], [41], [46], [47], [50]–[52]. This allows the kinetic study to be carried out with the certainty of working in a kinetic regime.

4.1.2.3 Kinetic Model (Heterogeneous catalysis)

Reactive separation systems require the use of heterogeneous catalysts capable of facilitating product separation, avoiding the damage associated with the use of homogeneous catalysts, such as corrosion, and ensuring the best reaction performance. Amberlyst 36 was chosen as the ideal catalyst for the model reaction. The studies presented so far indicate that the catalyst can be conveniently used because there are no diffusion limitations.

For the kinetic study using Amberlyst 36, a total of 27 experiments were carried out, in which parameters such as temperature, molar ratio, and catalyst quantity were varied (see Table 4-6).

Table 4-6. Experimental conditions of reaction esterification with Amberlyst 36.

RUN	Temp [°C]	Mole Ratio [BuOH/GA]	Catalyst amount [g]	Time [min]
1	50	1	0.625	4
2	70	1	0.625	4
3	50	6	0.625	4
4	70	6	0.625	4
5	50	3.5	0.25	4
6	70	3.5	0.25	4
7	50	3.5	1	4
8	70	3.5	1	4
9	50	3.5	0.625	3
10	70	3.5	0.625	3
11	50	3.5	0.625	5
12	70	3.5	0.625	5
13	60	1	0.25	5
14	60	6	0.25	5
15	60	1	1	4
16	60	6	1	4
17	60	1	0.625	3
18	60	6	0.625	3

19	60	1	0.625	5
20	60	6	0.625	5
21	60	1	0.25	3
22	60	6	1	3
23	60	3.5	0.25	5
24	60	3.5	1	5
25	60	3.5	0.625	4
26	60	3.5	0.625	4
27	60	3.5	0.625	4

For the kinetic study using heterogeneous catalysis, the methodology followed corresponds to the same study presented in the case of homogeneous catalysis. All the models studied were evaluated in terms of activity. However, in this case, the data was adjusted using a pseudo-homogeneous (PH) model and adsorption-based models as presented in the literature. Among the authors who used the PH model, Steinigeweg *et al.* [53] demonstrated that this model is sufficient to describe the profiles of the reactive distillation columns if there are small or medium amounts of water in the system. Orjuela *et al.* [28] also demonstrated that the PH model can describe the esterification reaction between succinic acid and ethanol, they also considered the dehydration reaction of ethanol, a secondary reaction in the studied conditions.

The model most used in the literature to describe the kinetic behavior of the esterification reaction in the presence of heterogeneous catalysts is the Langmuir-Hinshelwood (LH) model, this model considers that all compounds are absorbed on the surface of the catalyst [54]. Initially the molecules of acid and alcohol are absorbed on the surface, and finally the mechanism considers the desorption of the two products, ester and water [22]. In terms of activity, the LH model represents the reaction rate as in the equation 4.10:

$$r = \frac{k_1^0 exp\left(-\frac{E_A}{RT}\right)\left(a_{GA}a_{BuOH} - \frac{a_{BG}a_W}{K_{eq}}\right)}{(1+K_{GA}a_{GA}+K_{BuOH}a_{BuOH}+K_{BG}a_{BG}+K_W a_W)^2} \quad (4.10)$$

For this model, the number of parameters to be determined is 6. Where k_1^0 is the pre-exponential factor, E_A is the activation energy and $K_{GA}, K_{BuOH}, K_{BG}, K_W$ are the absorption coefficients of each of the molecules present in the solution. Some authors perform additional absorption experiments

to reduce the number of parameters to be calculated [52]. However, in this work all parameters were determined from the MATLAB 9.4 optimization tool.

De Silva *et al.* [22] investigated the heterogeneous kinetics of acetic acid esterification with ethanol using Trilite SCR-B ion exchange resin as catalyst. The heterogeneous reaction mechanism is closer to the LH model, compared the three kinetic models used, being the other two models the Eley-Rideal (ER) model and the PH model. The reaction rate is not significantly affected by variations in initial concentrations.

Gangadwala *et al.* [54] studied the kinetic behavior of the reaction between acetic acid and butanol using Amberlyst 15 as catalyst. The authors observed that the PH model, and modifications of it, explain the successful data on a wide range of catalyst loads and temperatures. The authors found that all molecules are absorbed in the same way on the catalyst surface. Delgado *et al.* [25] used the same catalyst to study the esterification reaction of lactic acid and ethanol, although the differences between the results obtained with the LH model and the PH model are relatively similar, due to the high polarity of the reaction medium, the PH model also provides a good agreement with experimental kinetic data. However, for the latter the strongly absorbed molecules were water and ethanol.

Tsai *et al.* [52] used Amberlyst 36 as a catalyst for the esterification reaction between propionic acid and methanol. The best results were obtained using the Langmuir-Hinshelwood-Hougen-Waston (LHHW) model. The authors carried out the absorption study of the different compounds on the surface of the catalyst. The results showed that the water and ester molecule were strongly absorbed.

Another model also mentioned and studied in the literature is the ER model. This model considers that the esterification reaction occurs between the adsorbed alcohol and the acid, only one reactant adsorbs on to the catalyst surface, to obtain the non-absorbed ester and adsorbed water molecules [14], [54]. Considering the above, the model can be expressed by equation 4.11:

$$r = \frac{k_1^0 exp\left(-\frac{E_A}{RT}\right)\left(a_{GA}a_{BuOH} - \frac{a_{BG}a_W}{K_{eq}}\right)}{(1+K_{GA}a_{GA}+K_{BuOH}a_{BuOH}+K_{BG}a_{BG}+K_W a_W)} \quad (4.11)$$

For this model, the number of parameters to be determined is 6, as in the previous model, even if it is known that only one of the reactants is adsorbed. Where k_1^0 is the pre-exponential factor, E_A is the activation energy and $K_{GA}, K_{BuOH}, K_{BG}, K_W$ are the absorption coefficients of each of the molecules present in the solution. Akyalc *et al.* [46] investigated the kinetic behavior of the acetic acid and octanol system in the presence of Amberlyst 36, the authors observed that the ER model precisely adjusts the kinetic experimental data obtained, however, for the authors the strongly absorbed molecules were acetic acid and water.

The mentioned models were used to describe the kinetic behavior of the system studied in the presence of Amberlyst 36. The activity-based kinetic model predictions overlap the profiles obtained from experiments. The last series of parameters obtained after the optimization process are presented in the Table 4-7, summarizes the parameters determined for each of one the models, these parameters represent a good agreement between the model and the experimental data in different conditions for esterification. In general, it is observed that with an excess of butanol and high catalyst loads, an almost complete conversion of glycolic acid is obtained after 2 h of reaction.

Table 4-7. Comparison of Kinetic Parameters Employed pseudo-homogeneous model (PH) and adsorption-based models (LH and ER) for the butanol and glycolic system.

Model	k_1^0 [mol (g*min)$^{-1}$]	E_A [kJ mol^{-1}]	K_{BuOH}	K_{GA}	K_{BG}	K_W	SRS_N	E_{Rel} [%]
PH	2.94e6	53.04	-	-	-	-	0.99	5.07
LH	5.32e10	56.81	1.00e2	2.22e-14	2.22e-14	3.08e1	0.52	3.66
ER	5.36e8	56.00	1.00e2	2.22e-14	2.22e-14	2.22e-14	0.62	4.02

The results of the adjustment show that the error decreases when the adsorption-based models are considered, although the difference between the results obtained using the PH model and those adsorption-based models vary by a maximum of 1.4%. This coincides with the conclusion of the studies carried out by Steinigeweg *et al.* [53] and Orjuela *et al.* [28] in which it is shown that the PH model can describe with great precision this type of reaction in the presence of ion exchange resins like Amberlyst type. Figure 4-11 presents the comparison between the fit with the different models to describe the kinetic behavior of the experiment 8, the adsorption-based models coincide with the experimental behavior while the PH model evidences a slight deviation.

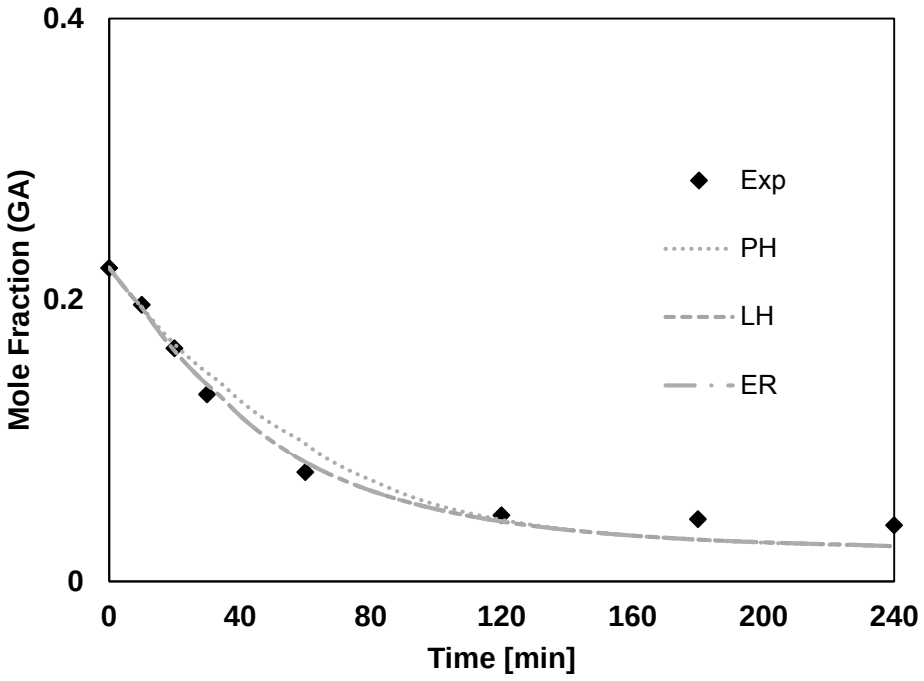

Figure 4-11. Comparison of different kinetic models in the prediction of the conversion of glycolic acid. Exp 8

Considering the models that represent the absorption phenomenon, there is a slight increase in the activation energy from 53 to 56 kJ mol^{-1}. The activation energy of the esterification reaction using Ambelyst 36 is 56 kJ mol^{-1}, the value is similar regardless of the model used for the adjustment. However, when considering the adsorption-based models, the activation energy increase, although on this particular reaction no information is available in the literature, the values obtained are within the range of values using the same type of catalyst, type of alcohol, primary, and carboxylic acids as carbon numbers between C2 and C4. Steinigeweg *et al.* [53] reported the activation energy value of 56.65 kJ mol^{-1} for the system between acetic acid and butanol in the presence of Amberlyst 15 as catalyst, this value could be compared with the values obtained in this study since in both cases it is a carboxylic acid with two carbons. Additionally, the glycolic acid contains an OH group. No secondary reaction associated with the presence of this OH group was observed at the studied conditions. It is worth noting that the activation energy increases by approximately 20% when switching from a homogeneous catalyst to a heterogeneous catalyst.

Considering the adsorption-based models, it is observed that the molecules are absorbed in the following decreasing order $K_{BuOH} > K_W > K_{GA} = K_{BG}$, which allows to eliminate the absorption parameters of the acid (K_{GA}) and ester (K_{BG}). These model modifications; assuming that alcohol

and water molecules are strongly absorbed, coincide with what was reported by Da Silva *et al.* [22]. The values of the adjusted absorption parameters showed that butanol and water are the most strongly absorbed molecules. However, the butanol absorption parameter is more important than the water absorption parameter, the difference is approximately 4 to 5 times greater.

The pre-exponential factor (k_1^0) represents the collision frequency between the molecules. From the values obtained, it is observed that for adsorption-based models, the value of the pre-exponential factor increases with respect to the value obtained from the regression using the pseudo-homogeneous model. For the models that consider a greater number of intermediate stages in the kinetic model, the pre-exponential factor is more important.

The best fit of the experimental data was achieved using the ER model, the adjustment of the experimental data demonstrate that it is only the butanol the only molecule that strongly adsorbed from the reagents, and the water molecule in the products. However, the results obtained with the HP model and the LH model are also accurate. Figure 4-12 presents the fit using the ER model.

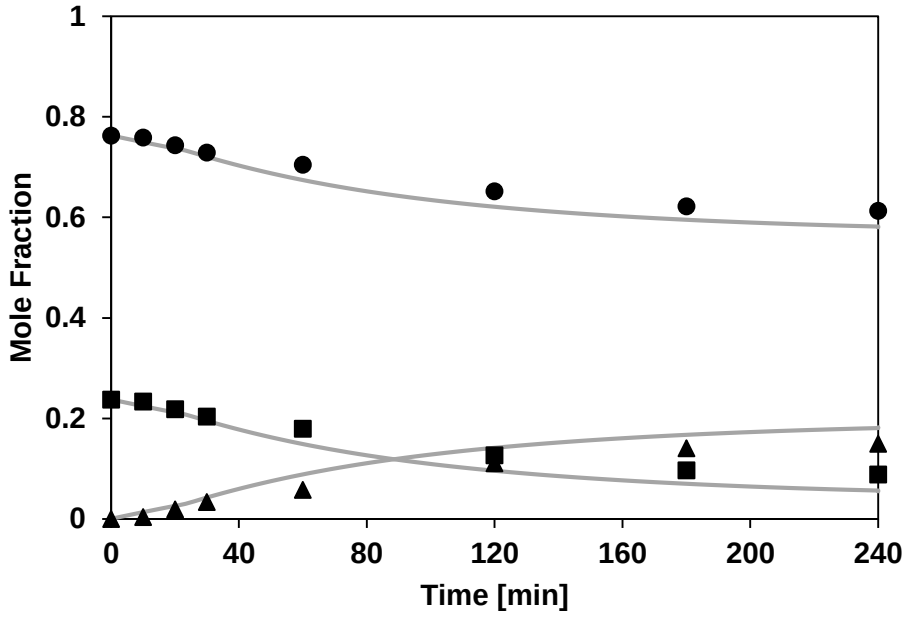

Figure 4-12. Experimental and predicted mole fraction profiles of glycolic acid esterification with butanol using ER model. Exp 7: T = 50 °C, $W_{cat} = 1\ g\ Amb\ 36$; Mole fraction: (■) Glycolic acid ; (●) Butanol; (▲) Butyl glycolate.

4.2 Glycolic acid and propanol system

The methodology implemented for the kinetic study of the propanol system and glycolic acid was the same as that presented in the section 4.1 for the butanol and glycolic acid system. Propanol was chosen as one of the short-chain alcohols between group C1 and C3 that is currently produced by bio routes. The catalysts used for the kinetic study were H_2SO_4, as a homogeneous catalyst, and Amberlyst 36, as a heterogeneous catalyst. The number of experiments was similar to the previous case, 8 experiments in the presence of the homogeneous catalyst and 27 experiments in the presence of the heterogeneous catalyst. As for the previous system there is no information available in the literature for the propanol system and glycolic acid.

4.2.1 Homogeneous catalyst

4.2.1.1 Equilibrium Constant and Kinetic Model

The equilibrium constant K_{eq} of the propanol and glycolic acid system was determined with the same method as the one presented in section 4.1.1.4.Table 4-8 presents the calculated values of K_{eq}.

Table 4-8. Equilibrium constants of glycolic acid esterification with propanol.

Temp [°C]	Kx	Keq
50	1.57	4.57
60	1.66	6.65
70	1.79	8.88

Figure 4-13 represents the equilibrium constant for the glycolic acid and propanol reaction system as a function of temperature. The figure shows the difference between ideal and non-ideal behavior.

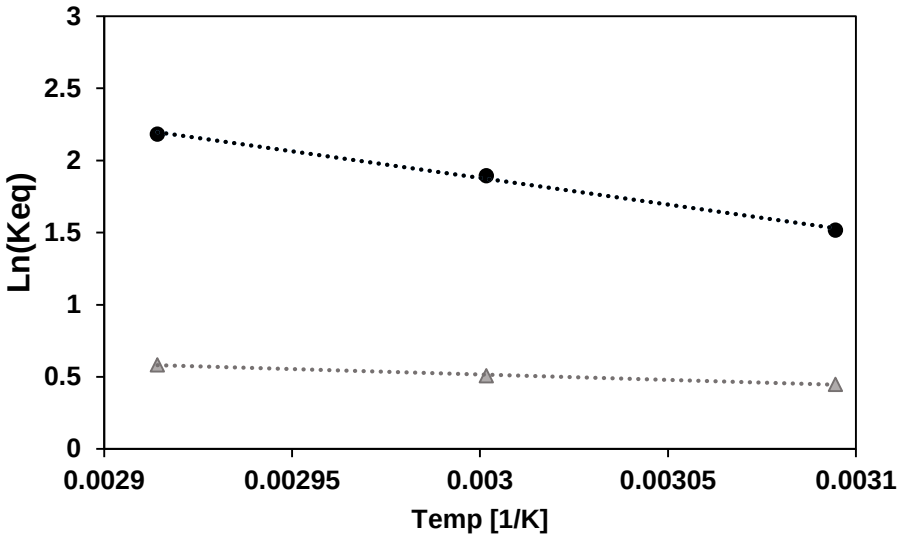

Figure 4-13. Van 't Hoff plot for glycolic acid esterification with propanol from experimental data. Mole fraction (▲) Kx and activity (●) Keq.

In the case of propanol, the slopes showed the same tendency observed with the butanol system, where the increase temperature increases the deviation between ideal and non-ideal system. For this system, the equilibrium constant as a function of the activities corresponded to an endothermic reaction according to curve.

The expression of the equilibrium constant as a function of temperature was obtained:

$$Ln\, K_{eq} = -\frac{3696.2}{T} + 12.968 \quad R^2 = 0.9967 \tag{4.11}$$

The value of $\Delta_r H°$ considered in this work was 30.73 kJ mol^{-1}. The value in this case is greater than the value obtained for the butanol system (23.76 kJ mol^{-1}).

The kinetic study for this system was made using the code developed with MATLAB 9.4 considering the respective thermodynamic information. Table 4-9 presents k_1^0 and E_A, for the glycolic acid and propanol reaction system. In this case only forward reactions were considered, due to the unavailability of the starting components of the reaction.

Table 4-9. Homogeneous kinetic model - Estimated Parameters for propanol and glycolic acid system

Parameters	Estimated Values	Standard deviation
E_A [kJ mol-1]	42.90	40%
k_1^0 [mol (g*min)$^{-1}$]	8.90e6	>0.1%
SRS_N	0.83	
E_{Rel} [%]	9.01	

The second-order model fits the experimental data considerably well. The activation energy obtained for this system is less than that obtained for the butanol system (49.58 kJ mol^{-1}). This is due to the fact that short chain alcohols are more active compare to long chain alcohols. Figure 4-14 shows the adjustment made with the kinetic model for one of the experiment number 7.

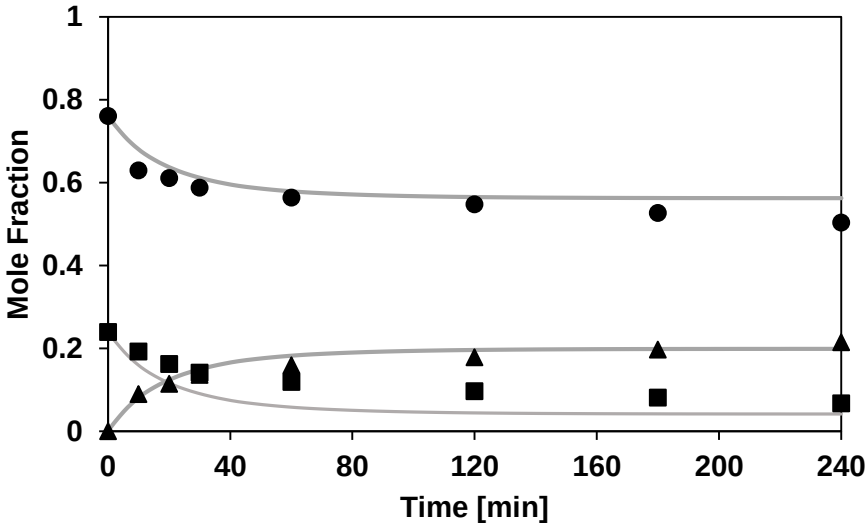

Figure 4-14. Experimental and predicted mole fraction profiles of glycolic acid esterification with propanol using second-order model. Exp 7: T = 50 °C, $W_{cat} = 0.257\ g\ H_2SO_4$; Mole fraction: (■) Glycolic acid ; (●) Propanol; (▲) Propyl glycolate.

4.2.2 Heterogeneous catalyst

The kinetic study using heterogeneous catalysis for the propanol and glycolic acid system was performed using pseudo-homogeneous (PH) and adsorption-based models, as presented in the previous section. Table 4-10 presents the results of the adjustment of the different parameters in each case. As in the case of butanol, when the esterification data of propanol and glycolic acid are adjusted to the PH model the activation energy is lower than when the absorption-based

models, LH and ER, are considered. The results obtained from this system show that there are still two strongly absorbed molecules but in this case, it is propanol and glycolic acid. The absorption parameter is higher for glycolic acid. The molecules are absorbed in the following decreasing order $K_{GA} > K_{POH} > K_W = K_{PG}$.

Table 4-10. Comparison of kinetic parameters employed pseudo-homogeneous model (PH) and adsorption-based models (LH and ER) for the propanol and glycolic acid system.

Model	k_1^0 [mol (g*min)$^{-1}$]	E_A [kJ mol^{-1}]	K_{PrOH}	K_{GA}	K_{PG}	K_W	SRS_N	E_{Rel} [%]
PH	1.59 e7	50.82	-	-	-	-	0.82	4.60
LH	1.04 e8	52.49	1.60	2.06	3.94e-14	3.94e-14	0.69	4.24
ER	4.38e8	52.42	26.71	33.64	2.58e-14	2.58e-14	0.69	4.22

The criteria for selecting the model that best describes the experimental data was made according to the error percentage. In this case the error of both adsorption-based models is similar, in spite of this, it is observed that in this case both reagents are adsorbed, this phenomenon is characteristic of the LH model. The best fit of the experimental data was achieved using the LH model, however, the results obtained with the PH model and the ER model also have good accuracy. Figure 4-15 presents the fit using the LH model.

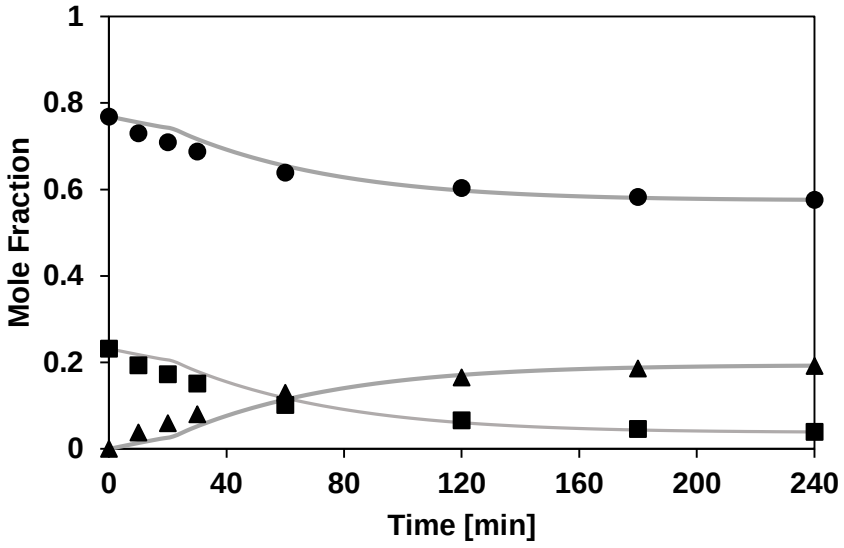

Figure 4-15. Experimental and predicted mole fraction profiles of glycolic acid esterification with propanol using LH model. Exp 23: T = 60 °C, $W_{cat} = 1\ g\ Amb\ 36$; Mole fraction: (■) Glycolic acid ; (●) Propanol; (▲) Propyl glycolate

Lilja *et al* [16] studied the esterification kinetics of propanoic acid with three different alcohols, ethanol, 1-propanol and butanol, in the presence of a fibrous heterogeneous catalyst. They reported an activation energy value of 52.6 kJ mol^{-1}, 49.9 kJ mol^{-1} and 47.3 kJ mol^{-1} for ethanol, 1-propanol and butanol, respectively. Even if it is not the same carbon number for carboxylic acid, this value is close to the values determined in this study of 52.9 kJ mol^{-1}. For the authors, it is also the LH model that best represents the experimental data.

4.3 Glycolic acid and octanol system

Other kinetic system studied was the octanol and glycolic acid system. Octanol is a long chain alcohol that is currently produced by bio routes. As with the study carried out with propanol, for this system the method applied for its analysis is the same as that applied for the glycolic acid butanol system. The catalysts used for the kinetic study were H_2SO_4 as a homogeneous catalyst, and Amberlyst 36 as a heterogeneous catalyst. The number of experiments was 8 in the presence of the homogeneous catalyst and 27 experiments in the presence of the heterogeneous catalyst. As for the previous system, there is no information available in the literature for the octanol system and glycolic acid.

4.3.1 Homogeneous catalyst

4.3.1.1 Equilibrium Constant and Kinetic Model

The equilibrium constant K_{eq} of the octanol and glycolic acid system was determined using the same method as presented in section 4.1.1.4. Table 4-11 presents the calculated values of K for the octanol and glycolic acid system.

Table 4-11. Equilibrium constants of glycolic acid esterification with octanol.

Temp [°C]	Kx	Keq
50	1.50	4.18
60	1.79	4.97
70	2.18	5.96

Figure 4-16 represents the equilibrium constant for the glycolic acid and octanol reaction system as a function of temperature. In this case, the non-ideal behavior is similar to the ideal one, with similar slope values for the range of temperature studied.

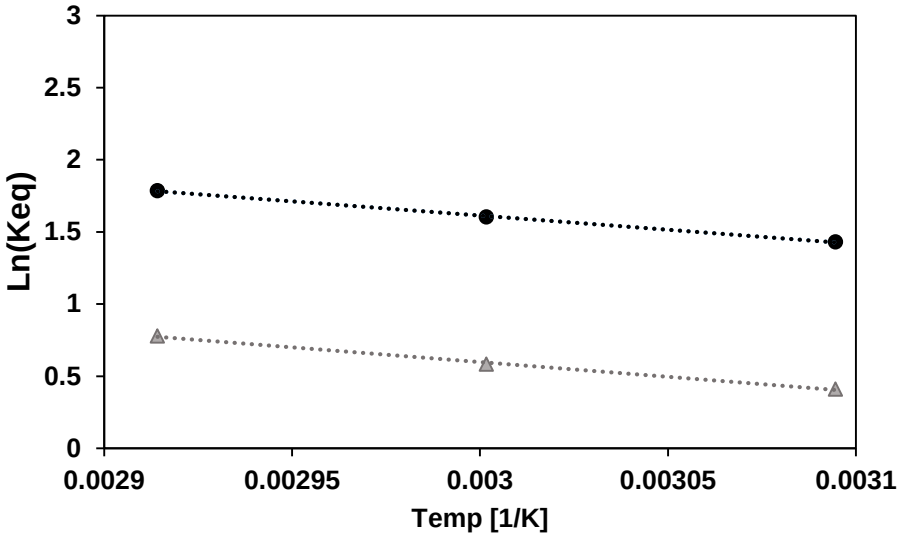

Figure 4-16. Van 't Hoff plot for glycolic acid esterification with octanol from experimental data. Mole fraction (gray delta) Kx and activity (black circle) Keq.

For this system, the curve corresponded to an endothermic reaction. However, it is observed that the reaction is less sensitive to thermal effects than that observed in the propanol and butanol system.

The expression of the equilibrium constant as a function of temperature was obtained:

$$Ln\ K_{eq} = -\frac{1968.4}{T} + 7.5192 \quad R^2 = 0.9989 \tag{4.12}$$

The value of $\Delta_r H°$ considered in this work was 16.36 kJ mol^{-1}. The value obtained in this case is lower than the value obtained for the butanol and propanol systems, 23.76 kJ mol^{-1} and 30.73 kJ mol^{-1}, respectively.

The kinetic study was carried out using the code developed with MATLAB 9.4 considering the respective thermodynamic information. Table 4-12 presents k_1^0 and E_A, for the glycolic acid and octanol reaction system. Only forward reactions were considered.

Table 4-12. Second-order kinetic model - Estimated Parameters for octanol and glycolic acid system

Parameters	Estimated Values	Standard deviation
E_A [kJ mol-1]	51.06	0.254
k_1^0 [mol (g*min)$^{-1}$]	1.20e6	82
SRS_N	0.30	
E_{Rel} [%]	5.42	

The activation energy determined for this case is the highest in comparison with the energies reported in the previous systems. Figure 4-17 presents the comparison between the experimental data and the results obtained with the homogeneous model. The model represents a suitable fit to the experimental data.

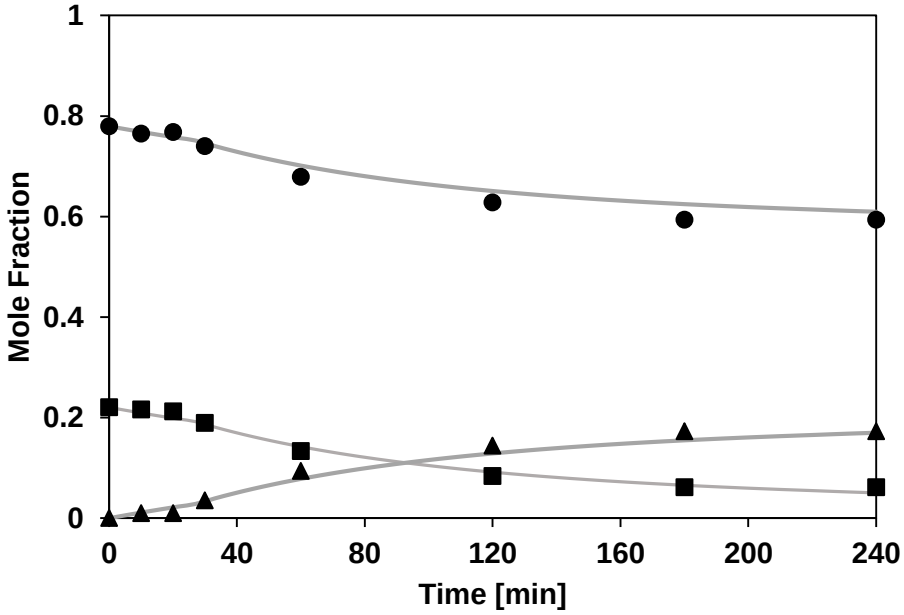

Figure 4-17. Experimental and predicted mole fraction profiles of glycolic acid esterification with octanol using second-orden model. Exp 1: T = 70 °C, $W_{cat} = 0.257\ g\ H_2SO_4$; Mole fraction: (■) Glycolic acid; (●) Octanol; (▲) Octyl glycolate

4.3.2 Heterogeneous catalyst

The kinetic study using heterogeneous catalysis showed in the case of octanol, that the ER model was able to represent with greater precision the experimental data obtained. For this system, only a strong absorption on the octanol molecule is observed for both the LH and the ER model. Table 4-13 presents the results of the parameter adjustment with the different models.

Table 4-13. Comparison of kinetic parameters employed pseudo-homogeneous model (PH) and adsorption-based models (LH and ER) for the octanol and glycolic acid system.

Model	k_1^0 [mol (g*min)$^{-1}$]	E_A [kJ mol^{-1}]	K_{OctOH}	K_{GA}	K_{OG}	K_W	SRS_N	E_{Rel} [%]
PH	6.05e3	36.93	-	-	-	-	1.54	6.19
LH	4.11e6	30.94	1.00e2	2.22e-14	6.05e-12	1.28e-11	0.91	4.74
ER	1.69e5	34.14	1.00e2	2.22e-14	2.22e-14	2.22e-14	1.18	5.42

The obtained value of activation energy of 34.14 kJ mol^{-1} is in agreement with the value reported by Akyalcin *et al* (24.90 kJ mol^{-1}) [55] in the esterification of a carboxylic acid C2, acetic acid, such as glycolic acid, and octanol. The authors found that Amberlyst 36 favors the esterification reaction between octanol and acetic acid, comparing the results obtained by Balakrishnan *et al* (58.89 kJ mol^{-1}) [55] in the presence of a polymer supported titanium tetrachloride complex, represented by the decrease of the activation energy. In this research it was also observed that the activation energy for the glycolic acid and octanol system (34.14 kJ mol^{-1}) is lower compared to the system with propanol (52.49 kJ mol^{-1}) and butanol (56.00 kJ mol^{-1}). However, as in the case of butanol, only the octanol molecule is strongly absorbed on the surface. Figure 4-18 presents the adjustment of the experimental data.

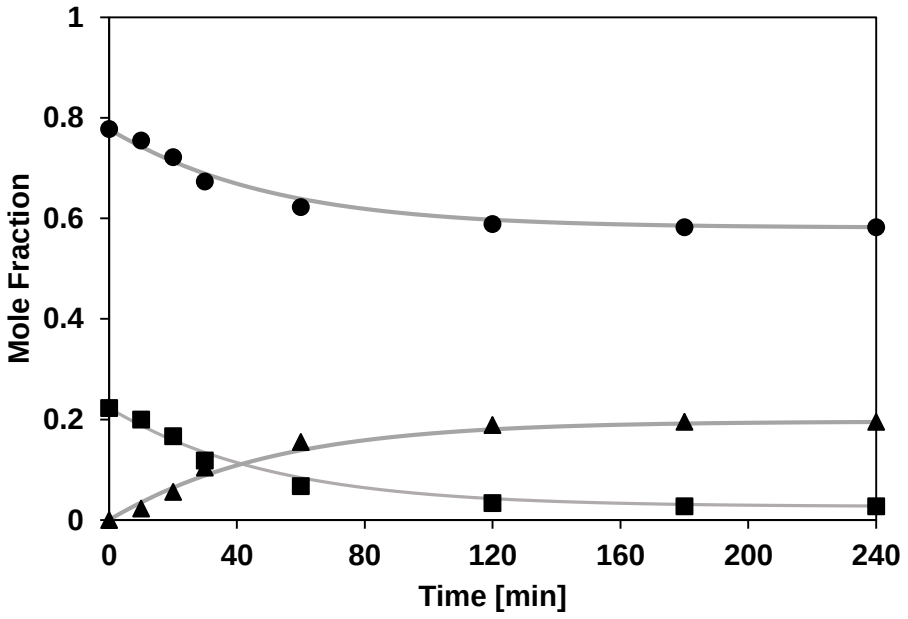

Figure 4-18. Experimental and predicted mole fraction profiles of glycolic acid esterification with octanol using ER model. Exp 25: T = 80 °C, $W_{cat} = 0.625\ g\ Amb\ 36$; Mole fraction: (■) Glycolic acid ; (●) Octanol; (▲) Octyl glycolate

4.4 Results and Discussion

The results obtained for each system allow to deduce some generalities according to the increase of the aliphatic chain length of the alcohol. The thermodynamic parameters study for the esterification reaction of glycolic acid with the three alcohols (*i.e.,* propanol, butanol and octanol) showed that the reaction in all cases is endothermic. Figure 4-19 shows the evolution of the enthalpy of reaction in function of aliphatic chain length obtained from experimental thermodynamic study. For comparison purposes, a theoretical study based on Density Functional Theory (DFT) was carried out to determine the reaction enthalpy for each system (see **ANNEX B.**). The calculations were performed for isolated molecules taking into account the effect of the solvent media using polarizable continuum model (PCM). In this method, the solvent is treated as a continuum dielectric medium, where the solute is considered as trapped molecules in a cavity surrounded by solvent. As the alcohol is in excess in our mixtures and for simplicity, it was considered for each system the dielectric constant value of the studied alcohol to represent the solvent media. Thus, it considered ε= 20.1 for propanol, ε= 17.8 for butanol and ε= 10.3 for octanol [56]. It is worth noting that there is no available data in the literature concerning our systems, thus DFT results can be useful to corroborate the thermodynamic results.

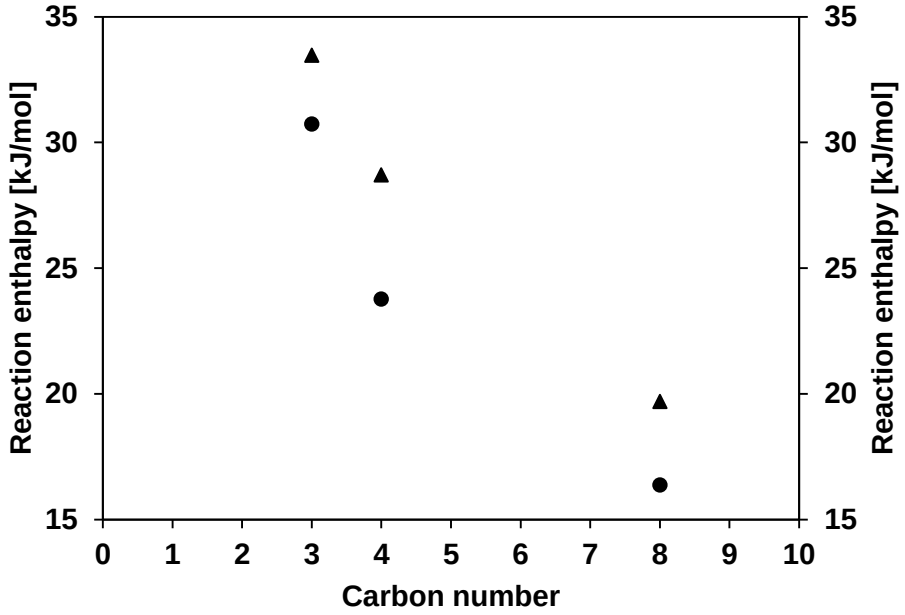

Figure 4-19. Evolution of the enthalpy of reaction in function of aliphatic chain length from: experimental (left) ● and DFT calculation (right) ▲.

Both experimental and DFT calculations show a same behavior, *i.e.,* a decrease of the reaction enthalpy with the increase of the carbon chain length of the alcohol. In the case of enthalpy, the values not only follow the same trend of decrease of enthalpy with the increase of the carbon chain length of the alcohol, but also the values obtained experimentally and by simulation vary only between 9 to 20% (see Table 4-14).

Table 4-14. Reaction enthalpy experimental and DFT calculated.

System	K_{Exp} [kJ mol^{-1}]	K_{DFT} [kJ mol^{-1}]
Propanol	30.73	33.47
Butanol	23.76	28.70
Octanol	16.36	19.69

Figure 4-20 shows the evolution of the entropy of the esterification reaction as a function of the length of the aliphatic chain obtained from the experimental thermodynamic study. As with enthalpy, a theoretical DFT study was performed to determine the reaction entropy of each system (see **ANNEX B.**). Following the same methodology as in the determination of the enthalpy. Experimental as well as DFT calculations show the same behavior, *i.e.* a decrease of the reaction entropy with the increase of the length of the carbon chain of the alcohol. However, the difference between the simulated values and the values obtained experimentally is very large, this can be explained from compression of the principle of calculations. The thermodynamic functions such as molar entropy, heat capacity, and enthalpy content, can be computed easily from the molecular partition function $q\ (V,T)$.

The rigid rotator-harmonic oscillator approximation to describe the motion of the nuclei in molecules is likely the weakest part of quantum methods for calculating entropy and heat capacity. In this model, the vibrations of nuclei in a molecule are treated as independent harmonic oscillators. Under this assumption, the high frequency and low amplitude vibrations in which the nuclei remain close to the equilibrium position are described relatively accurately. Problems arise when there are low barrier torsion potentials, large amplitude motions, or anharmonic vibrations, all of which are difficult to describe harmonically and as a result their contribution to the thermodynamics functions is difficult to evaluate. The errors associated with anharmonicity become significant at temperatures where the anharmonic modes become excited when the molecule leaves the harmonic potential surface.

The anharmonic contribution mainly affects the entropy and isochorous heat capacity thermodynamics functions, while its related contributions to the enthalpy of formation only amount to a few percent of the total vibrational contribution. It should be noted that the previous results were obtained from the thermodynamic parameters obtained throughout the study.

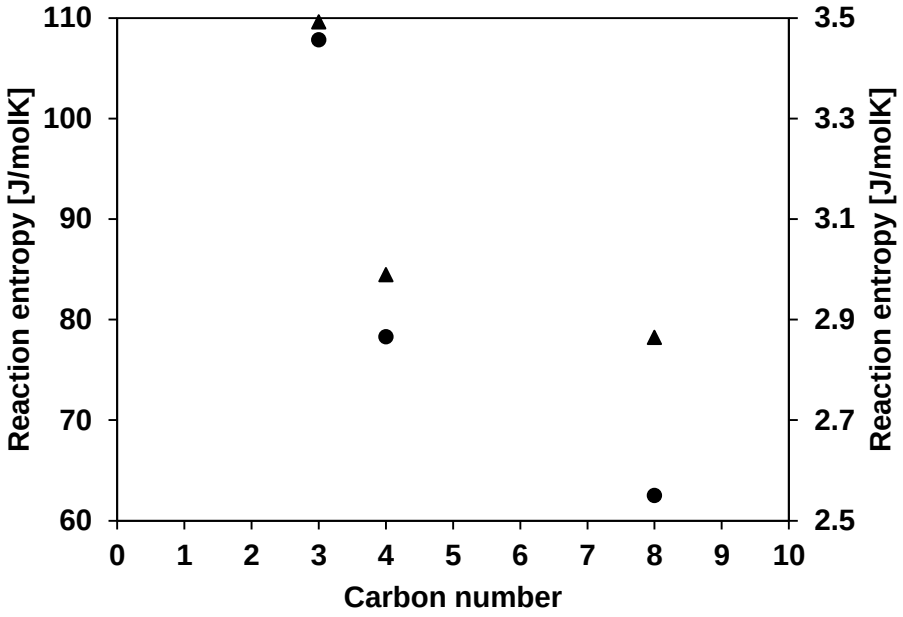

Figure 4-20. Evolution of the entropy of reaction in function of aliphatic chain length from: experimental (left) ● and DFT calculation (right) ▲.

The observed behavior of enthalpy and entropy can also be explained from the thermodynamics of binary systems. A mass spectrometric analysis of the 1-butanol/water system was performed by Wakisaka *et al.* [57], the authors report that at high alcohol concentrations in the system, the structure is governed mainly by H-bonds interactions, but at high water concentrations, the structure is dominated by the tetrahedral structure of the water. However, in the particular case of the butanol-rich solution, the first partially miscible low chain alcohol in water, the molecules exist largely as self-association groups, and monomeric water molecules are saturated in the solution. In other words, water molecules can remain in the butanol-rich phase by promoting butanol self-association, which counteracts the destabilization resulting from contact between butanol and water molecules. On the other hand, a Raman study [58] shows that the 1-octanol liquid structure is, in contrary to the low-chain alcohols, essentially unchanged after the addition of water. Hence, the decrease of degree of self-association of the alcohol with the increase of the aliphatic chains

length, explains how at short aliphatic chains the presence of water promotes deviation from the ideality.

The adjustment of the kinetic data of the homogeneous system using the second-order model is fairly satisfactory. However, it was observed a decrease error of the model with the increase of the carbon chain length of the alcohol. In the presence of the homogeneous catalyst H_2SO_4, the activation energy increases with the increase in the number of carbon in the aliphatic alcohol chain (*i.e.,* propanol: 42.9 kJ mol^{-1}, butanol: 49.50 kJ mol^{-1} and octanol: 51.06 kJ mol^{-1}).

The kinetic study of the esterification reaction of glycolic acid using heterogeneous catalyst, Amberlyst 36, in presence of three different alcohols showed that the activation energy tends to increase slightly with the increase of aliphatic chain length, C3 to C4. However, the activation energy decreases in the presence of octanol, this coincides with works reported in the literature employing Amberlyst 36 in the presence of octanol [46]. This indicates that for the systems studied, the octanol system is favored in particular.

The analysis of the kinetic study in the presence of heterogeneous catalysis using different kinetic models showed that the PH, LH and ER models can describe the behavior of the experimental data with great precision. However, there are few changes in the statistical data and the parameters determined that can be considered to carry out a better choice of the most appropriate model. From the analysis of the absorption-based models, LH and ER, it was observed that the absorption phenomenon of the molecules on the surface of the catalyst varies depending on the system. The propanol system was best represented by the LH model, while the ER model better represents the butanol and octanol systems. Lilja *et al.*[16] presented the esterification scheme where initially the proton is donated to the carboxylic acid, after the transfer of the proton, the carboxylic acid is accessible for the nucleophilic attack or the hydroxylic group of alcohol. The authors confirm that in this process the water molecules interact with the sulfonic acid through the equilibrium of protólysis, in the same way, the alcohol molecules can act as weak bases and receive the proton of the sulfonic acid. However, this latter type of interactions or equilibrium are not possible with the ester molecule. This may explain why in some cases both the molecule of carboxylic acid and the molecule of alcohol are adsorbed on the surface of the catalyst. These new considerations give rise to the consideration that the mechanism of the esterification reaction in the presence of heterogeneous catalysis is not the same as using homogeneous catalysis. Chu

et al [59] concluded from their investigation of the esterification reaction of acetic acid with ethanol and n-butanol catalyzed by SiW_{12} supported in activated carbon that the surface reaction is the apparent rate controlling step, but due to the difference in the structure of alcohol, the mechanism changes from a dual site mechanism for ethanol (model LH) to a single site mechanism for n-butanol (model ER). A possible interpretation that explains this change is that steric hindrance by n-butanol prevents the adsorption of acid, which changes the apparent mechanism and lowers the reaction rate. These results coincide with the findings of this research where it may indicate that there is a dual-site mechanism for propanol and a single-site mechanism for butanol and octanol. It can be considerate that the butanol and octanol systems have the same steric impediment that prevents the adsorption of glycolic acid. The long alkyl chain of alcohol blocked surface sites, hindering the adsorption of glycolic acid. Figure 4-21 presents a graphical representation of two systems, propanol and octanol, with glycolic acid on the surface of the catalyst. In this graph the active sites of the catalyst are represented as isolated molecules of benzene sulfonic acid.

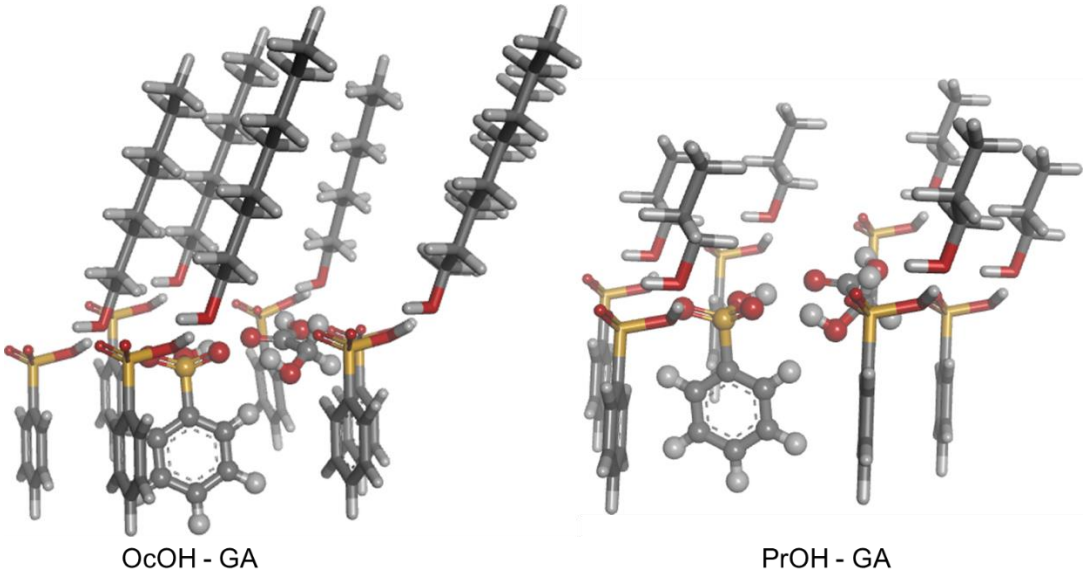

Figure 4-21. Graphical representation of two systems, propanol and octanol, with glycolic acid on the surface of the catalyst (Amberlyst type)

To verify the hypotheses put forward so far, the adsorption energies (E_{Ads}) of the three alcohols and glycolic acid were determined by DFT calculations with B3LYP functional and cc-pVTZ basis set using Gaussian 09 package, methodology presented by Kim *et al* [60] and Miao *et al* [61]. Figure 4-22 shows the geometry-optimized minimum energy configurations of the adsorbed model structure complexes (octanol, butanol, propanol and glycolic acid) in Amberlyst 36 (benzene

sulfonic acid) together with their zero point energy corrected adsorption energies. The results of the theoretical calculation revealed that the E_{Ads} of the alcohols in the functional groups of the sulfonic acid are comparable energies. However, an increase is observed with the increase of the aliphatic chain length of the alcohol (*i.e.,* E_{Ads}: propanol: 50.92 kJ mol^{-1}, butanol: 51.76 kJ mol^{-1} and octanol: 51.91 kJ mol^{-1}). The calculated adsorption energy values are close to those reported by Miao *et al* [61] for methanol (59 kJ mol^{-1}). The glycolic acid has higher adsorption energy (59.41 kJ mol^{-1}).

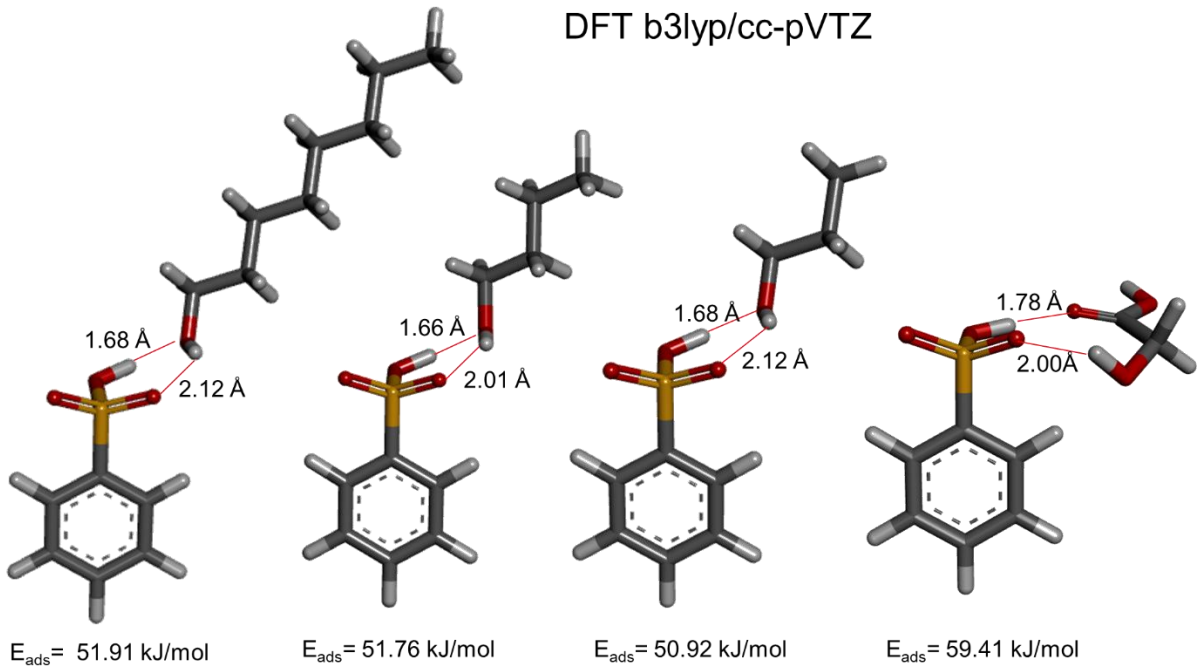

Figure 4-22. Geometric of octanol, butanol, propanol and glycolic acid adsorbed on benzene sulfonic acid site as optimized by B3LYP/cc-pVTZ.

The results of these energy absorption calculations show that alcohol can be adsorbed onto propilsulfonic acid groups and that the adsorption of glycolic acid is stronger than that of alcohols. These results are in complete qualitative agreement with the adsorption behavior found in the experimental and kinetic modeling results in the case of propanol being consistent with the LH model. This analysis coincides with that performed by Kim *et al.* [60] for the acetic acid and methanol system catalyzed by propylsulfonic acid-functionalized SBA-15. They demonstrated that esterification of their system followed a dual-site LH type reaction mechanism. The systems that present problems associated with the geometry and size of the molecules are well represented by the ER model, as in the case of butanol and octanol, none of our system includes the water molecule as an adsorbed molecule.

4.5 Conclusion

The kinetic study of the esterification reaction of glyceric acid with the different alcohols (propanol, butanol and octanol) led to the conclusion that adsorption-based kinetic model are capable of describing the behavior of experimental data. However, when considering models based on absorption, the behavior varies from one alcohol to another as mentioned. For acid and alcohol molecules that have similar dimensions, the LH model fits properly. When the difference in the size of the molecules is more important, the ER model is able to better represent the behavior of the experimental data. Activation energy increases with increasing aliphatic alcohol chain.

4.6 Bibliography

[1] J. E. Gavagan and M. S. Payne, “Method for producing glycolic acid from glycolonitrile using nitrilase,” 2002.

[2] Y. Xu, W. Dou, Y. Zhao, G. Huang, and X. Ma, “Kinetics study for ion-exchange-resin catalyzed hydrolysis of methyl glycolate,” *Ind. Eng. Chem. Res.*, vol. 51, no. 36, pp. 11653–11658, 2012.

[3] D. Datta and S. Kumar, “Reactive Extraction of Glycolic Acid Using Tri- n -Butyl Phosphate and Tri- n -Octylamine in Six Different Diluents : Experimental Data and Theoretical Predictions,” pp. 3041–3048, 2011.

[4] B. Katryniok *et al.*, “Selective catalytic oxidation of glycerol: perspectives for high value chemicals,” *Green Chem.*, vol. 13, no. 8, p. 1960, 2011.

[5] K. D. Patil and B. D. Kulkarni, “Review of Recovery Methods for Acetic Acid from Industrial Waste Streams by Reactive Distillation,” *J. Water Pollut. Purif. Res.*, vol. 1, no. 2, pp. 13–18, 2014.

[6] S. M. Mahajani, “Reactions of glyoxylic acid with aliphatic alcohols using cationic exchange resins as catalysts,” vol. 43, pp. 253–268, 2000.

[7] X. Jiang and Y. Tang, “Preparation and Application of Hydroxyacetic Acid Esters as Methanol-Gasoline Additives,” *Asian J. Chem.*, vol. 25, no. 15, pp. 8447–8450, 2013.

[8] R. Sirsam, D. Hansora, and G. A. Usmani, “A Mini-Review on Solid Acid Catalysts for Esterification Reactions,” *J. Inst. Eng. Ser. E*, vol. 97, no. 2, pp. 167–181, 2016.

[9] M. Kuzminska, “Heterogeneous acid catalysts for esterification in oleochemistry Maryna Kuzminska L ’ UNIVERSITÉ DE BORDEAUX,” 2016.

[10] B. M. Antunes, S. P. Cardoso, C. M. Silva, and I. Portugal, “Kinetics of ethyl acetate synthesis catalyzed by acidic resins,” *J. Chem. Educ.*, vol. 88, no. 8, pp. 1178–1181, 2011.

[11] A. R. Zahedipoor, S. Daneshyari, A. Malekzadeh, and S. Eslami, “Kinetic Study of Esterification of Lactic Acid with Ethanol using Ion Exchange Resin,” *Mod. J. Lang. Teach. Methods*, vol. 6, no. 4.3, pp. 017–033, 2016.

[12] W.-T. Liu and C.-S. Tan, “Liquid-Phase Esterification of Propionic Acid with *n* -Butanol,” *Ind. Eng. Chem. Res.*, vol. 40, no. 15, pp. 3281–3286, 2001.

[13] Z. Zeng, L. Cui, W. Xue, J. Chen, and Y. Che, “Recent Developments on the Mechanism and Kinetics of Esterification Reaction Promoted by Various Catalysts,” *Chem. Kinet.*, no. 2, pp. 256–282, 2011.

[14] I. B. Ju, H. W. Lim, W. Jeon, D. J. Suh, M. J. Park, and Y. W. Suh, “Kinetic study of catalytic esterification of butyric acid and n-butanol over Dowex 50Wx8-400,” *Chem. Eng. J.*, vol. 168, no. 1, pp. 293–302, 2011.

[15] Y. Liu, E. Lotero, and J. G. Goodwin, “Effect of carbon chain length on esterification of carboxylic acids with methanol using acid catalysis,” *J. Catal.*, vol. 243, no. 2, pp. 221–228, 2006.

[16] J. Lilja, J. Wärnå, T. Salmi, and L. J. Pettersson, “Esterification of propanoic acid with ethanol, 1-propanol and butanol over a heterogeneous fiber catalyst,” *Chem. Eng. J.*, vol. 115, no. 1–2, pp. 1–12, 2005.

[17] Y. Zhang, L. Ma, and J. Yang, “Kinetics of esterification of lactic acid with ethanol catalyzed by cation-exchange resins,” *React. Funct. Polym.*, vol. 61, no. 1, pp. 101–114, 2004.

[18] R. Maggi, N. R. Shiju, V. Santacroce, G. Maestri, F. Bigi, and G. Rothenberg, “Silica-supported sulfonic acids as recyclable catalyst for esterification of levulinic acid with stoichiometric amounts of alcohols,” *Beilstein J. Org. Chem.*, vol. 12, pp. 2173–2180, 2016.

[19] M. Minakawa, H. Baek, Y. M. A. Yamada, J. W. Han, and Y. Uozumi, “Direct dehydrative esterification of alcohols and carboxylic acids with a macroporous polymeric acid catalyst,” *Org. Lett.*, vol. 15, no. 22, pp. 5798–5801, 2013.

[20] Y. Liu, E. Lotero, and J. G. Goodwin, “A comparison of the esterification of acetic acid with methanol using heterogeneous versus homogeneous acid catalysis,” *J. Catal.*, vol. 242, no. 2, pp. 278–286, 2006.

[21] Shagufta, I. Ahmad, and R. Dhar, “Sulfonic Acid-Functionalized Solid Acid Catalyst in Esterification and Transesterification Reactions,” *Catal. Surv. from Asia*, vol. 21, no. 2, pp.

53–69, 2017.

[22] E. C. L. De Silva, B. A. N. N. Bamunusingha, and M. Y. Gunasekera, “Heterogeneous Kinetic Study for Esterification of Acetic Acid with Ethanol,” vol. XLVII, no. 01, pp. 9–16, 2014.

[23] A. K. Kolah, N. S. Asthana, D. T. Vu, C. T. Lira, and D. J. Miller, “Reaction Kinetics for the Heterogeneously Catalyzed Esterification of Succinic Acid with Ethanol,” pp. 5313–5317, 2008.

[24] G. Jyoti, S. Bhoi, and D. K. Sahu, “Production and Isolation of n -Butyl Acrylate Using Pervaporation-Aided Esterification Reaction : Kinetics and Optimization,” no. 3, pp. 617–627, 2019.

[25] P. Delgado, T. Sanz, and S. Beltr, “Kinetic study for esterification of lactic acid with ethanol and hydrolysis of ethyl lactate using an ion-exchange resin catalyst,” vol. 126, pp. 111–118, 2007.

[26] J. Lilja, D. Y. Murzin, T. Salmi, J. Aumo, P. Maäki-Arvela, and M. Sundell, “Esterification of different acids over heterogeneous and homogeneous catalysts and correlation with the taft equation,” *J. Mol. Catal. A Chem.*, vol. 182, no. 183, pp. 555–563, 2002.

[27] M. Mekala and V. R. Goli, “Kinetics of esteri fi cation of methanol and acetic acid with mineral homogeneous acid catalyst,” *Chinese J. Chem. Eng.*, vol. 23, no. 1, pp. 100–105, 2015.

[28] A. Orjuela, A. J. Yanez, A. Santhanakrishnan, C. T. Lira, and D. J. Miller, “Kinetics of mixed succinic acid/acetic acid esterification with Amberlyst 70 ion exchange resin as catalyst,” *Chem. Eng. J.*, vol. 188, pp. 98–107, 2012.

[29] P. Hemptinne, Jean-Charles. BARREAU, Alain, LEDANOIS, Jean-Marie , MOUGIN, *SELECT THERMODYNAMIC MODELS FOR PROCESS SIMULATION A Practical Guide using a Three Steps Methodology*, Editions T. PARIS, FRANCE, 2012.

[30] V. C. Nguyen *et al.*, “Esterification of aqueous lactic acid solutions with ethanol using carbon solid acid catalysts: Amberlyst 15, sulfonated pyrolyzed wood and graphene oxide,” *"Applied Catal. A, Gen.*, no. 2010, pp. 184–191, 2017.

[31] A. Tiwari, A. Keshav, S. Bhowmick, and O. Sahu, “Liquid-liquid Equilibria (LLE) of the quaternary mixture (acetic acid + ethanol + ethyl acetate + water) arising out of esteri fi cation reaction : Optimization studies,” *J. Mol. Liq.*, vol. 231, pp. 86–93, 2017.

[32] Y. Qu, S. Peng, S. Wang, Z. Zhang, and J. Wang, “Kinetic Study of Esterification of Lactic

Acid with Isobutanol and," *Chinese J. Chem. Eng.*, vol. 17, no. 5, pp. 773–780, 2009.

[33] A. M. Ostaniewicz-cydzik, C. S. M. Pereira, E. Molga, and E. Rodrigues, "Reaction Kinetics and Thermodynamic Equilibrium for Butyl Acrylate Synthesis from n - Butanol and Acrylic Acid," 2014.

[34] A. P. Toor, M. Sharma, G. Kumar, and R. K. Wanchoo, "Kinetic Study of Esterification of Acetic Acid with n- butanol and isobutanol Catalyzed by Ion Exchange Resin," *Bull. Chem. React. Eng. Catal.*, vol. 6, no. 1, pp. 23–30, 2011.

[35] A. Ralston, "Runge-Kutta Methods with Minimum Error Bounds," *Am. Math. Soc.*, vol. 16, no. 80, pp. 431–437, 1962.

[36] V. K. Pappu, V. Kanyi, A. Santhanakrishnan, C. T. Lira, and D. J. Miller, "Butyric acid esterification kinetics over Amberlyst solid acid catalysts: the effect of alcohol carbon chain length," *Bioresour Technol*, vol. 130, pp. 793–797, 2013.

[37] T. Pöpken, L. Götze, and J. Gmehling, "Reaction kinetics and chemical equilibrium of homogeneously and heterogeneously catalyzed acetic acid esterification with methanol and methyl acetate hydrolysis," *Ind. Eng. Chem. Res.*, vol. 39, no. 7, pp. 2601–2611, 2000.

[38] P. Dupont and F. Lefebvre, "Esterification of propanoic acid by butanol and 2-ethylhexanol catalyzed by heteropolyacids pure or supported on carbon," *J. Mol. Catal. A Chem.*, vol. 114, no. 1–3, pp. 299–307, 1996.

[39] K. A. Kun and R. Kunin, "Macroreticular Resins. III Formation of Macroreticular Styrene-Divinylbenzene Copolymers," *J. Polym. Sci.*, vol. 6, pp. 2689–2701, 1968.

[40] W. L. Sederel and G. J. D. E. Jong, "Styrene-Divinylbenzene Copolymers. Construction of Porosity in Styrene Divinylbenzene Matrices," *J. Appl. Polym. Sci.*, vol. 17, pp. 2835–2846, 1973.

[41] J. Lilja *et al.*, "Kinetics of esterification of propanoic acid with methanol over a fibrous polymer-supported sulphonic acid catalyst," *Appl. Catal. A Gen.*, vol. 228, no. 1–2, pp. 253–267, 2002.

[42] M. Ehteshami, N. Rahimi, A. A. Eftekhari, and M. J. Nasr, "Kinetic study of catalytic hydrolysis reaction of methyl acetate to acetic acid and methanol," *Iran. J. Sci. Technol. Trans. B Eng.*, vol. 30, no. 5, pp. 595–606, 2006.

[43] S. Bagheri, N. M. Julkapli, and W. A. Yehye, "Catalytic conversion of biodiesel derived raw glycerol to value added products," *Renew. Sustain. Energy Rev.*, vol. 41, pp. 113–127, 2015.

[44] J. Lin, A. H. Zaki, H. Wu, H. Lin, and M. Lee, “Kinetics study on esterification of acrylic acid and ethanol over acidic cation-exchange resin b eads Amb erlyst 35,” *J. Taiwan Inst. Chem. Eng.*, no. xxxx, pp. 1–7, 2019.

[45] C. H. Zhou, H. Zhao, D. S. Tong, L. M. Wu, and W. H. Yu, “Recent advances in catalytic conversion of glycerol,” *Catal. Rev. - Sci. Eng.*, vol. 55, no. 4, pp. 369–453, 2013.

[46] S. Akyalçin and M. R. Altiokka, “Kinetics of esterification of acetic acid with 1-octanol in the presence of Amberlyst 36,” *Appl. Catal. A Gen.*, vol. 429–430, pp. 79–84, 2012.

[47] Y. Tsai, H. Lin, and M. Lee, “Kinetics behavior of esterification of acetic acid with methanol over Amberlyst 36,” *Chem. Eng. J.*, vol. 171, no. 3, pp. 1367–1372, 2011.

[48] V. Marques *et al.*, “Sulfonated poly(divinylbenzene) and poly(styrene-divinylbenzene) as catalysts for esterification of fatty acids,” *Renew. energy*, vol. 114, pp. 725–732, 2017.

[49] P. F. Siril, H. E. Cross, and D. R. Brown, “New polystyrene sulfonic acid resin catalysts with enhanced acidic and catalytic properties,” *J. Mol. Catal. A Chem.*, vol. 279, pp. 63–68, 2008.

[50] A. P. Toor, M. Sharma, G. Kumar, and R. K. Wanchoo, “Ion-exchange Resin Catalyzed Esterification of Lactic Acid with Isopropanol: a Kinetic Study,” *Bull. Chem. React. Eng. Catal.*, vol. 6, no. 1, pp. 39–45, 2011.

[51] N. Calvar, B. González, and A. Dominguez, “Esterification of acetic acid with ethanol: Reaction kinetics and operation in a packed bed reactive distillation column,” *Chem. Eng. Process. Process Intensif.*, vol. 46, no. 12, pp. 1317–1323, 2007.

[52] Y.-T. Tsai, M. Lee, and H. Lin, “Kinetics of Catalytic Esterification of Propionic Acid and n -Butanol over Amberlyst 35,” *Ind. Eng. Chem. Res.*, vol. 41, no. 12, pp. 2882–2887, 2011.

[53] S. Steinigeweg and J. Gmehling, “*n* -Butyl Acetate Synthesis via Reactive Distillation: Thermodynamic Aspects, Reaction Kinetics, Pilot-Plant Experiments, and Simulation Studies,” *Ind. Eng. Chem. Res.*, vol. 41, no. 22, pp. 5483–5490, 2002.

[54] J. Gangadwala, S. Mankar, S. Mahajani, A. Kienle, and E. Stein, “Esterification of acetic acid with butanol in the presence of ion-exchange resins as catalysts,” *Ind. Eng. Chem. Res.*, vol. 42, no. 10, pp. 2146–2155, 2003.

[55] T. Balakrishnan and V. Rajendran, “Polymer Supported Reagents . III . Kinetic Study of Synthesizing n-Octylacetate Using Insoluble,” pp. 2075–2080, 2000.

[56] E. Maryott, Arthur; Smith, *Table of dielectric constants of pure liquids*. Washington D.C., 1951.

[57] A. Wakisaka, S. Mochizuki, and H. Kobara, “Cluster Formation of 1-Butanol – Water Mixture Leading to Phase Separation,” vol. 33, no. July, pp. 721–732, 2004.

[58] M. E. Gallina, P. Sassi, M. Paolantoni, A. Morresi, V. Elce, and S. Catania, “Vibrational Analysis of Molecular Interactions in Aqueous Glucose Solutions . Temperature and Concentration Effects,” pp. 8856–8864, 2006.

[59] W. Chu, X. Yang, X. Ye, and Y. Wu, “Vapor phase esterification catalyzed by immobilized dodecatungstosilicic acid (SiW12) on activated carbon,” vol. 145, pp. 125–140, 1996.

[60] I. Kim, J. Kim, and D. Lee, “A comparative study on catalytic properties of solid acid catalysts for glycerol acetylation at low temperatures,” *"Applied Catal. B, Environ.*, vol. 148–149, pp. 295–303, 2014.

[61] B. Miao, Shaojun; Shanks, “Mechanism of acetic acid esterification over sulfonic acid-functionalized mesoporous silica,” *J. Catal.*, vol. 279, no. 1, pp. 136–143, 2011.

Chapter 5. Preliminary treatment: study of different strategies for the water elimination

In the present chapter, the recovery of glyceric, glycolic and formic acids from a diluted aqueous mixture was studied. The mixture was obtained *via* glycerol oxidation using 5% $Ag/Ce_{0.75}Zr_{0.25}O_2$ catalyst which was prepared in UCCS laboratory[1]–[3]. Different ratios of water removal strategies were studied in order to minimize the energy consumption and determine the order of the intermediate stages of suitability of the mixture considering two types of initial sample: in salt form and in acid form. Different process alternatives were evaluated: vacuum distillation, atmospheric distillation, precipitation, and liquid-liquid extraction (see Figure 5-1).

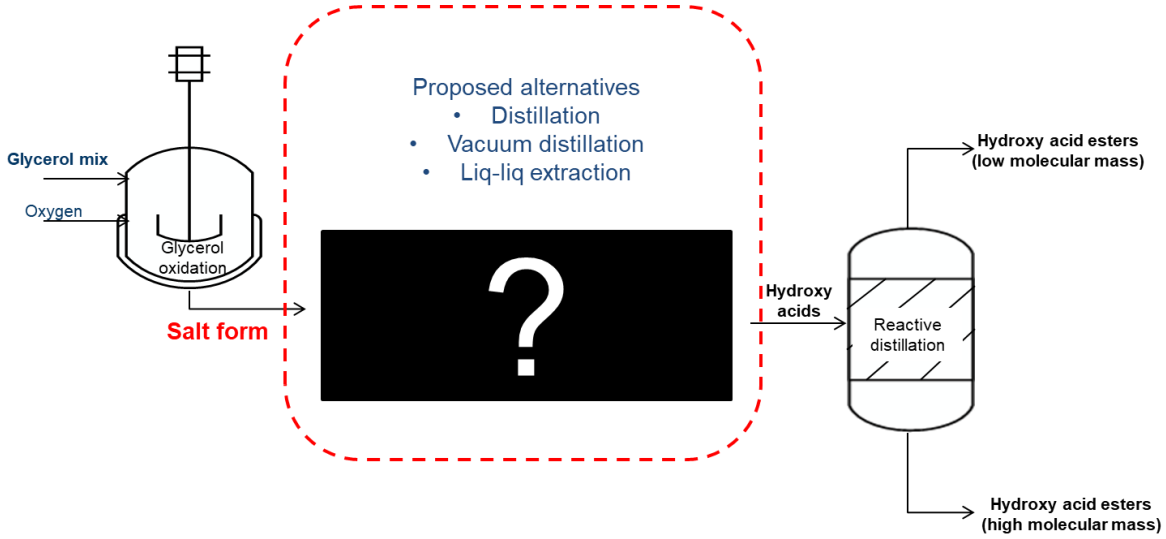

Figure 5-1. Different alternatives for the water elimination in the process of recovery of carboxylic acids.

5.1 Glycerol oxidation: Initial mixture obtained

The catalytic oxidation of glycerol leads to the formation of several products such as glyceric, formic, glycolic, tartronic and oxalic acids. One of the main problems concerns to the selectivity, through this process the products can be formed. Nevertheless, if these may be formed selectively, they have value as chemical intermediates in the fine chemicals industry [4]. The glycerol oxidation was investigated by Zaid and co-workers, at UCCS laboratory, by using materials based on Cerium/Zirconia support and silver as active phase (5% $Ag/Ce_{0.75}Zr_{0.25}O_2$) [5]. A glycerol conversion of 90% was obtained with selectivities of 15, 25 and 50% towards the

formation of glyceric, formic and glycolic acids, respectively, making this acids mixture an interesting alternative to design and scale-up the separation process.

Table 5-1 shows the concentration of the mixture obtained after glycerol oxidation using the catalyst at 100 °C, 5 bars for 5h at 1000 rpm. The conversion of glycerol was 85% and the selectivity obtained were 13, 41 and 39% towards the formation of glyceric, formic and glycolic acids respectively. Taking into account that the NaOH is present in the reaction, this mixture is made up of the organic salts of their corresponding acids, labeled in this work as the initial mixture in salt form. This mixture was acidified with H_2SO_4 to transform the organic salts in their corresponding acid. Separation/recovery of this mixture in salt and acid form was studied.

Table 5-1. Concentrations of initial mixture compounds obtained from glycerol oxidation.

Compounds	% mol wet base	%mol dry base
Formic	0.43	41
Glycerol	0.06	6
Glycolic	0.41	39
Glyceric	0.14	13
Water	98.96	0
Total	100	100

5.2 Separation techniques for recovery of carboxylic acids

In recent years, separation/recovery of carboxylic acids from aqueous solution has been studied in the literature [6][7][8]. Several techniques have been implemented including atmospheric and vacuum distillation, liquid-liquid and reactive extraction. In this chapter we will present the results obtained from subjecting the glycerol oxidation mixture to simple distillation and vacuum distillation.

5.2.1 Simple distillation

A simple distillation was carried out at 100 °C, to achieve two different percentages of water removal, 30 and 60 wt%. These tests were implemented in two types of mixtures, *i.e.*, in salt and

in acid form. The stability of acid mixtures was studied considering the molar percentage of each acid after the evaporation in the bottom of the column (see Figure 5-2).

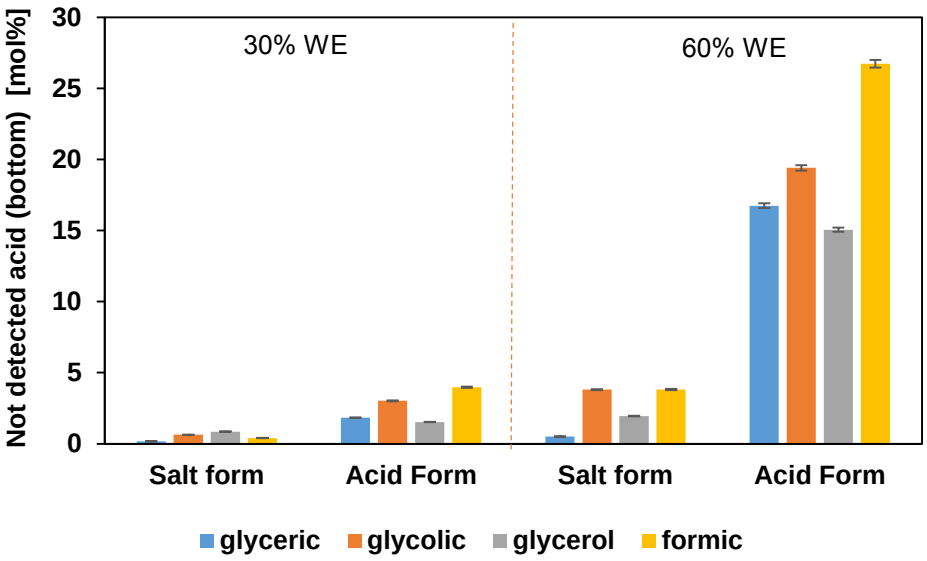

Figure 5-2. Results of simple distillation for a non-acidified and acidified mixture recovering 30 and 60 wt% of initial water content. Temp: 100 °C and Pres: 1 bar.

When the mixture was used in salt form, acid molar percentages detected were higher than 95%, indicating stability of acids in the mixture for most acids, losses up to than 5% were obtained by eliminating 60% of the initial amount. Formic acid, as the most volatile acid in the group, tends to evaporate more easily in less diluted media. In contrast, using the mixture in acid form, the loss of acids is higher, from 5 to 25% when eliminating 60% of the water, indicating an instability in this type of mixture.

This behavior can be explained due to the decreasing of the volatility of organic acids in presence of Na^+ ions. This effect has been investigated by Hakkinen *et al.* [9] using organic acids such as oxalic and succinic in aqueous mixtures. The volatility was clearly lower for the salt mixtures compared to oxalic acid and succinic acid, *i.e.*, the evaporation of these organic acids from salt mixtures continues after the temperature reaches complete volatilization for organic acids. Based on the results of the literature [9, 10], organic salt formation due to evaporation of HCl involve low-volatility material formation within aqueous mixtures of organic acids and NaCl. Chong *et al.* [11]

studied the recovery on acetic acid using a neutralization pre-treatment with NaOH, KOH, and $Ca(OH)_2$ before distillation. Without neutralization, acetic acid was detected in the distillate.

The results show that the water elimination is unfavorable when the compounds are in their acid form, on the contrary with salt compounds up to 60% of the water can be eliminated without problem.

5.2.2 Vacuum distillation

The vacuum distillation was carried out at 80°C and 100 mbars, to achieve two different percentages of water removal, 30 and 60 wt%. As well as for atmospheric distillation, the tests were implemented in two types of mixtures, *i.e*., in salt and acid form. Figure 5-3 shows the molar percentage of each acid not detected after vacuum distillation.

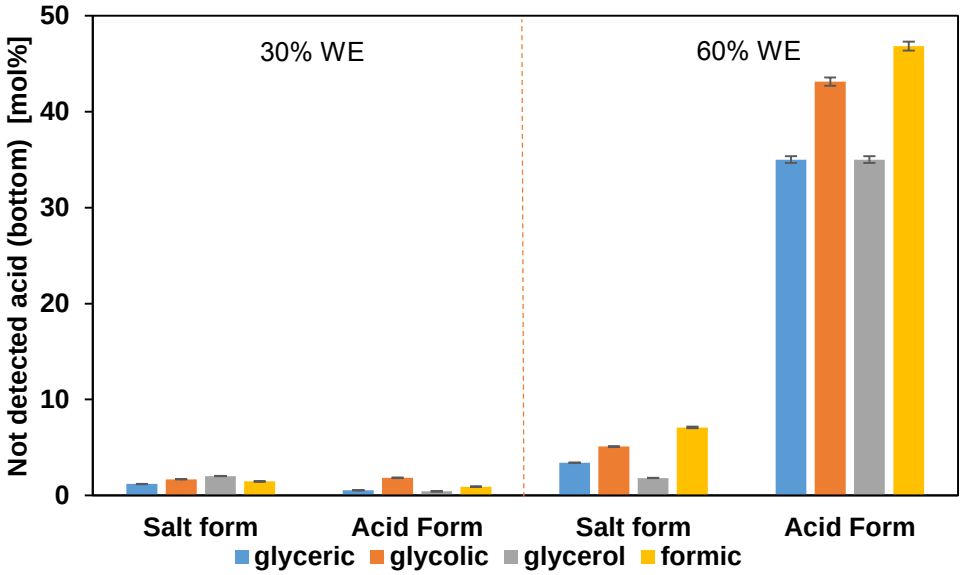

Figure 5-3. Results of vacuum distillation for a non-acidified and acidified sample recovering 30 and 60 wt% of initial amount of water. Temp: 80°C and Pres: 100 mbar.

When the mixture in salt form was tested, acid molar percentages detected after the vacuum distillation was higher than 98% in both water removal percentages, indicating stability of acids in the mixture and slightly higher than simple distillation (*i.e.,*95%). Comparable results were obtained with the mixture in acid form at 30% where no loss of acid content was observed. However, when a removal percentage of 60% was implemented, acid molar percentages detected in the bottom reduced by 45%. More instability was observed at these conditions in comparison with simple distillation (*i.e.,* 25%). Thus, the decreasing of evaporation pressure plays an important

role in the volatility of components, mainly, those with low volatility since the decreasing of boiling point temperature involves a quick evaporation [12].

Figure 5-4 shows the stability of the mixture in salt form to a water removal percentage of 80 wt%, and the comparison with tests of 30 and 60 wt%. A dewatering percentage higher than 60wt% involve a decrease in the acids amount in the aqueous solution residual in the bottom of the column due to the formation of a precipitated of salts. Consequently, the removal water percentage is limited by solubility of salts, latter depends on the affinity of compounds and temperature of the solution [13].

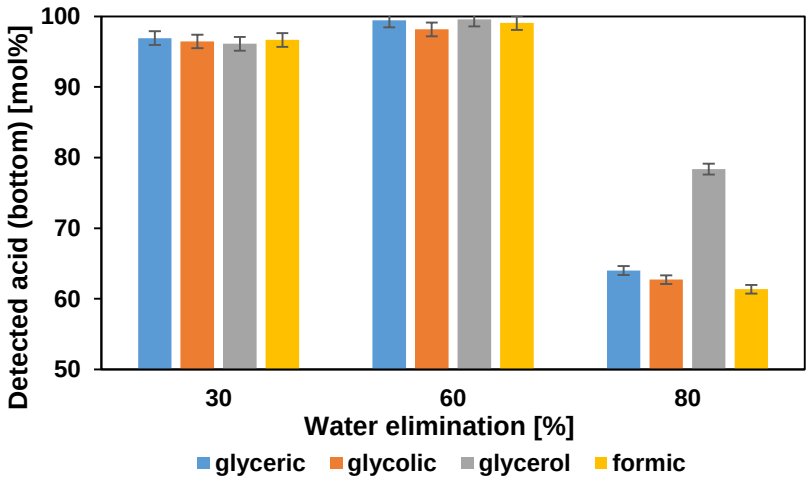

Figure 5-4. Results of vacuum distillation for non-acidified mixture sample recovering 30, 60 and 80 wt% of initial water content. Temp: 80 °C and Pres: 100 mbar.

5.2.3 Salt precipitation after water removal.

Precipitation is a classical method for the recovery and separation of carboxylic acids. This technique can recover organic acids from a bulk of fermentation broths efficiently, which makes it more competitive. It is well established and mature technique though it is energy intensive and not eco-friendly [14]. However, finding proper precipitants for the products is the key factor for this method. Some organic acids have been recovered by precipitation with calcium hydroxide (lactic and citric). Yedur *et al.* [15] concluded that the principals advantages of the integrated precipitation with ammonia are the lower amount of waste by-products and the possibility of recycling base and acid. The major disadvantage is the low selectivity of the precipitation with ammonia, *i.e.*, other

organic acids present in the fermentation broth will be precipitated together with succinic acid simultaneously [15,17-19].

The precipitation test *via* centrifugation was carried out for the remaining solution obtained after the vacuum distillation tests in order to identify the precipitate formed during the evaporation. Table 5-2 shows the percentage of salts precipitated in accordance with each water removal percentage. A low percentage of acids precipitated (<1%) were obtained when water removal of 30 and 60 % were carried out. In contrast, in the case of 80 wt% water removal, around 8.5% of acids were recovered in the precipitate, confirming that the decrease of acid molar percentages (surrounding 45%) in the vacuum distillation is due to the maximum solubility in water of the corresponding salts.

Table 5-2 Results of precipitation for a non-acidified sample recovering 30-60- 80 wt.% of initial water content. WE: Water Elimination.

ACIDS	PRECIPITATION		
	30% WE	60% WE	80% WE
Glyceric	<1	<1	8.4
Glycolic	<1	<1	8.5
Glycerol	<1	<1	9.1
Formic	<1	<1	9.1

Figure 5-5 shows the titration curve of initial mixture (glycolic, formic and glyceric acids) using a NaOH concentration of 1M, similar method used by Ibarra *et al.* [17]. The shape of acids mixture titration curve is that expected for monoprotic acids.

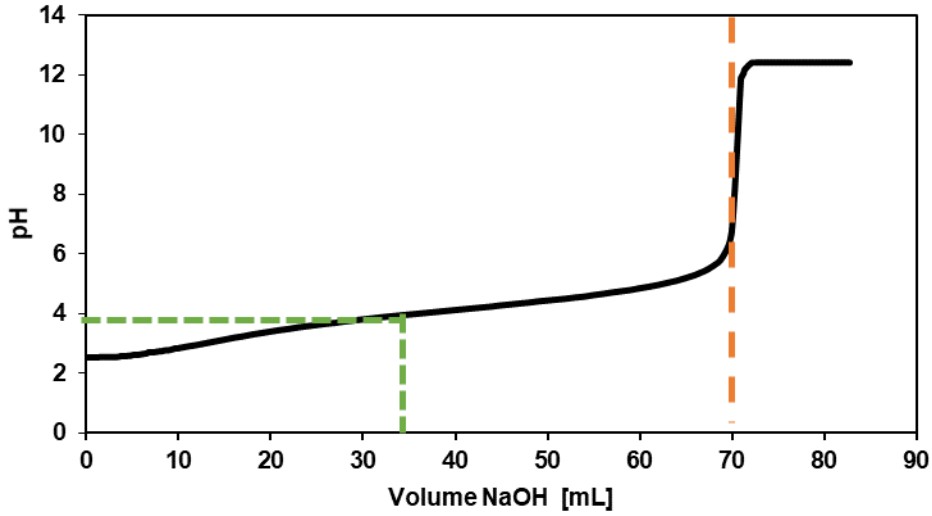

Figure 5-5. Titration curve of initial mixture (glycolic, glyceric and formic acids) using 1M NaOH solution at room temperature. Equivalence point (70mL)

The points used for pKa determination were the 1/2 equivalence point. A value of 3,9 was obtained, this one was similar to the values of each one reported in the literature at room temperature. Table 5-3, shows that the neutralization of these acids occurs simultaneously [18].In this sense, precipitation, the classical recovery method for carboxylic acids using a base for the acids neutralization, is not effective [16].

Table 5-3. pKa values of glycolic, glyceric and formic acids at room temperature.

Carboxylic acids	pKa Values	Ref.
Glycolic	3,83	
Glyceric	3,52	[19]
Formic	3,75	

5.2.4 Liquid-Liquid extraction

Liquid–liquid extraction itself is a well and extensively used method in the chemical industry. It is a promising method for the carboxylic acids recovery since is considered to be an efficient, economical and environmentally friendly method. Its main challenge is to develop a solvent that allows for high distribution and selectivity in the extraction, and an effective method to regenerate the solvent and recover the product [21,23]. Its application on an industrial scale has been limited because most conventional extraction agents show very unfavorable distribution coefficients for

organic acids. It appears only to have considered when more conventional methods such as distillation have failed.

Two broad categories of extraction system can be distinguished depending on the origins of this differential solubility. In the first, it arises from purely physical difference such as polarity, *i.e.*, the process depends only on the physical effects of difference in molecular structure. In the second category, the differential solubility is due to one of the solutes interacting chemically with the solvent to form a complex.

The recovery of glyceric, glycolic and formic acids was carried out *via* liquid-liquid extraction using two types of initial mixtures, in acid and salt form. For this technique, two organic solvents were used butanol and octanol, labeled as BuOH and OcOH. Two volume ratios between mixture/solution and solvent were used 1:2 and 1:4 in order to consider the effect of the amount of solvent. Figure 5-6 and Figure 5-7 show the extraction percent obtained using the mixtures in salt and acid form, respectively. Their use as extraction solvent is favored for both types of mixtures, despite the increase in the polarity resulting from the absence of protons, each carboxylic acid and its carboxylate remain relatively soluble; high extraction percentages were obtained (> 70%), this is due to the type of polarity of solvents.

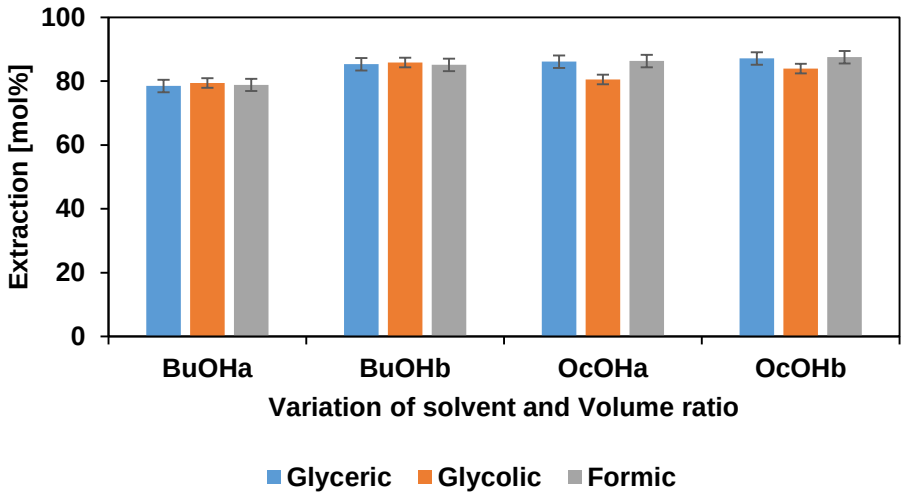

Figure 5-6. Percentages of extraction in salt form, using BuOH: Butanol and OcOH: Octanol; Temp: 35°C, stirring time: 20, stirring speed: 1000 rpm. Sol/Alc (v/v): a. 1-2 and b. 1-4.

The solvation is encouraged because like water and carboxylic acids, alcohols are part of the group of polar protic solvents. Therefore, high interaction forces take place: the ion-dipole interactions between alcohols-salts, and hydrogen bonds interaction between alcohols-carboxylic acids [22]. Datta *et al.* [23] found that lower polarity involves lower carboxylic acids extraction efficiency from aqueous solution.

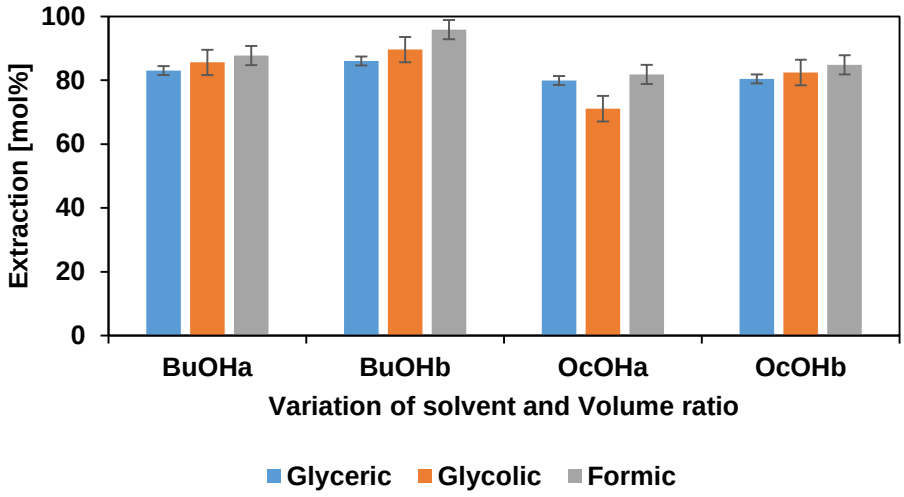

Figure 5-7. Percentages of extraction in acid form, using BuOH: Butanol and OcOH: Octanol; Temp: 35°C, stirring time: 20, stirring speed: 1000 rpm. Sol/Alc (v/v): a. 1-2 and b. 1-4.

When the mixtures were tested with butanol as a solvent, the carboxylic acids (glyceric and glycolic) extraction percentage presents an increase of 5 to 8% for both types of mixtures. This can be explained by the increase of the volume ratio, *i.e.*, an increase in the solvent involve a better extraction percentage. However, taking into account the amount of solvent used (v/v 1:4), the increase of extraction percentage obtained was not significant. Furthermore, when octanol was used in a volume ratio initial solution/extract (alcohol) of 1:2 and 1:4, the increase of extraction percentage of glycolic acid was of 5 and 9% in salt and acid form respectively. In contrast, no major differences in the extraction percentages of glyceric acid were observed. Although the recovery of the carboxylic acids can be improved by increasing volume of extractants, the cost for solvent recovery is increased at the same time, which should be taken into account in the economic feasibility of the process [24].

Considering the results obtained with the volume ratio 1:2, it can be inferred that butanol has better performance as a solvent in comparison with octanol for the mixture in acid form, mainly, a better extraction of glycolic acid (Butanol: 85%, Octanol:73%) is observed as seen in Figure 5-7.

When the mixture in salt form was tested, better performance was obtained with octanol, mainly, a better extraction of glyceric acid (Butanol: 78%, Octanol: 86%) can be observed under these conditions, see Figure 5-6. This can be explained by the affinity of these molecules according to their polarities. Table 5-4 shows the dielectric constants of butanol, octanol and formic acid. Butanol has similar polarity with this organic acids (ξ>17) allowing a great solvation [22]. Furthermore, considering the low relative polarity (ξ) of octanol and the decrease of the polarity of acids *via* the inductive effect of a positive ion like Na+, tend to have better solvation with this alcohol [25].

Table 5-4. Dielectric constants of Butanol, octanol and formic acids.

Compound	Dielectric constant [ξ]	Ref.
Formic acid	58.0	[26]
Glycolic acid	34.2	Calc.
Butanol	17.5	[27]
Octanol	10.3	[28]

Following the tests carried out in salt form *via* vacuum distillation for a water removal of 30 and 60%, respectively. Liquid-liquid extraction was implemented consecutively, with a view to evaluating the extraction percentage under these conditions. Only butanol was used like solvent. The extraction percentages obtained are shown in Figure 5-8.

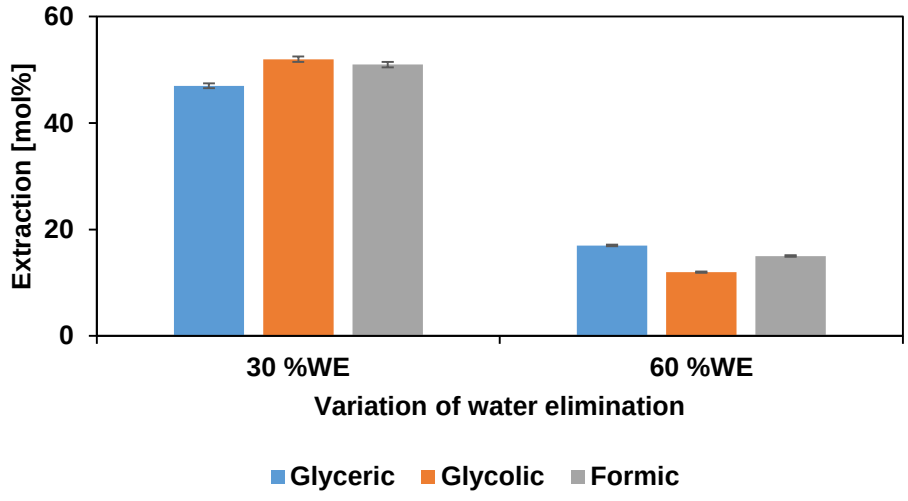

Figure 5-8. Percentages of extraction in salt form after vacuum distillation process. Solvent: Butanol, Temp: 35°C, stirring time: 20min, stirring speed: 1000 rpm, WE: water elimination.

As expected, the initial concentration of acids has a significant influence, since, in the case of water removal of 30wt%, the extraction percentages decreased around 30% for each acid in comparison with the mixtures without the pretreatment, see Figure 5 66. Likewise, with 60% of water removal, the extraction percentage decrease around 70% for glycolic and formic acid. Similar results were obtained by Kuma et al. [29] in the recovery of glycolic acid, this study concluded that the degree of extraction decrease when the acid concentration increases in the aqueous phase, disfavoring the extraction capacity. Therefore, distillation and liquid-liquid extraction is not a suitable consecutive configuration in the recovery of this carboxylic acids.

In order to analyze the performance of liquid-liquid extraction, the different partition coefficients of each carboxylic acid in each solvent (butanol-octanol) were calculated using equation 5.1.

$$K_D = \frac{([A]_1 * V_{org})}{([A]_2 * V_{aq})} \quad (5.1)$$

Table 5-5. shows the partition coefficients reported in the literature for some carboxylic acids and some binary mixtures using butanol and octanol as solvents. In general, low partition coefficient values (<1) were reported when the extraction was carried out for a single acid.

Table 5-6. Partition coefficients of organic acids using butanol and octanol as solvents [50].

Carboxylic acids	Butanol	Octanol
Acetic	-	0.49
Formic	-	0.29
Glycolic	-	0.08
Lactic	-	0.24
Propionic	-	1.80
Acetic -Glycolic	3.60	6.30
Propionic -Lactic	4.30	7.60

The results obtained are shown in Table 5-7. Partition coefficients obtained using initial mix-acid form. and Table 5-8. Partition coefficients obtained using initial mix-salt form. The minor differences found in partition coefficients values, with the same solvent, could be explained by the influence of some variables such as pH value, temperature, and acids concentration on these coefficients [30]. However, when a binary mixture was used, a significant increase in their coefficients was obtained (around 6 times), where octanol showed better distribution efficiency for

mixtures. In this sense, similar coefficient values were calculated in this study with both types of mixtures (in acid and salt form). Nevertheless, in this case, butanol shows better distribution efficiency in the mixture made up of glycolic, formic and glyceric acids. Munson *et al*. [31] concluded that the behavior encountered in any particular mixture seems to be a complex and difficult-to-predict combination of a number of factors, including the influence of various constituents on the degrees of acidity or basicity of the other constituents, preferential association between the components of a solvent mixture, the degree of solvation of a complexed form of the solute by the solvent mixture, and/or the ability of multiple solvent constituents to interact separately or synergistically with multiple functional groups on the solute molecule.

Table 5-7. Partition coefficients obtained using initial mix-acid form.

ACID	(K_D)			
	BuOH[a]	BuOH[b]	OcOH[a]	OcOH[b]
Glyceric	4.9	6.2	4.5	4.2
Glycolic	6.0	8.6	2.8	4.8
Glycerol	0.5	—	6.6	1.4
Formic	7.1	2.4	5.1	5.7

BuOH: Butanol, OcOH: Octanol. a: 1:2 Volume ratio, b: 1:4 Volume ratio

Table 5-8. Partition coefficients obtained using initial mix-salt form.

ACID	(K_D)			
	BuOH [a]	BuOH[b]	OcOH[a]	OcOH[b]
Glyceric	3.7	6.8	6.2	5.8
Glycolic	3.9	5.2	4.1	6.0
Glycerol	0.1	—	—	0.5
Formic	3.7	7.0	6.3	5.7

BuOH: Butanol, OcOH: Octanol; [a]: 1:2 Volume ratio, [b] 1:4 Volume ratio

5.2.5 Reactive extraction

The recovery of glyceric, glycolic and formic acids was carried out *via* reactive extraction using the two types of initial mixtures: acid and salt form. For this technique, organic solvent was used (butanol) in volume ratio 1:2. Tri-octylamine (TOA) was selected due to its promising extraction as an extractant [29][45], chemical (reactive extraction) equilibria were studied using 16 and 32 %

(v/v) TOA in 1-butanol at 35°C. Figure 5-9 shows the influence of increasing quantity of TOA in the reactive extraction for both types of mixture, in acid and salt form.

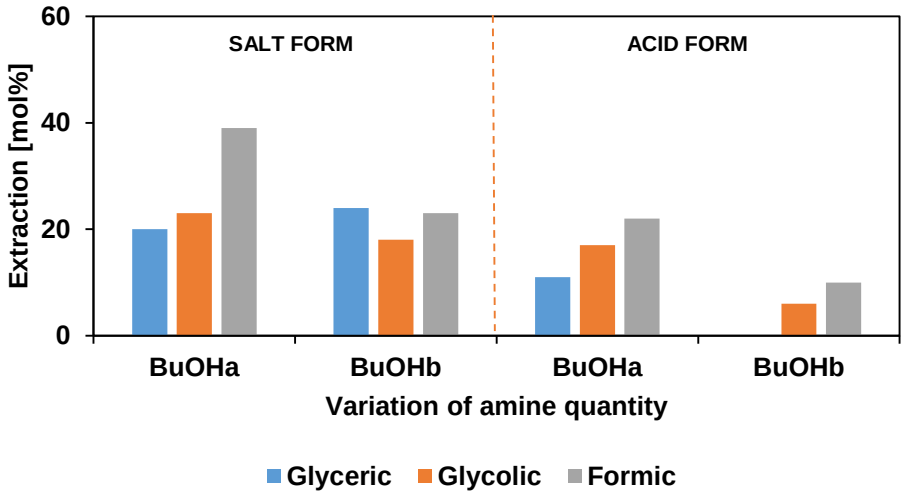

Figure 5-9. Percentages of extraction using butanol as solvent. BuOH. a: 16 mL TOA, b: 32 mL TOA. Temp: 35 °C, stirring time: 6h, stirring speed: 1000 rpm.

In general, low extraction percentages were obtained (<40%) under these conditions, mainly in the salt mixture (around 25%). Several factors tend to influence the values obtained such as pH and solvent used. Amine-based extraction works a low pH (<6) in order to convert the acid to its undissociated form for the transfer to the solvent [33, 46, 50,51].The extraction efficiency is inversely proportional to pH value, optimum pH value is before the pKa value of acid [50][15]. In this work the pH of mixture in acid and salt form were 6 and 13 respectively. In addition, organic-phase polarity has an important role in the mechanism of the interfacial reaction between the solute and the extractant [23][51]. A non-polar solvent involves the formation of a third-phase (emulsion), conversely, an appropriate polarity in the solvent improves the acid extraction [45]. Alcohols are usually used as modifiers in the organic phase for increase the polarity because this one exhibits a favorable effect on the solubilization of polar molecules, however, this increase in the polarity is limited by the adequate solvation of the amine used [29]. In this study butanol has a high polarity (ξ=17.5) in comparison with TOA (ξ=3.2), making difficult its adequate solvation and functioning [27, 52]. When a mixture in acid form was used, the amount of acid extracted from aqueous solutions increases with amine concentration around 20%. Similar trends were reported by Marti *et al*. [53] in the extraction of pyruvic acid with the extractant/solvent mixture of Trioctylamine/1-octanol. The extraction efficiency is raised with an increase in the TOA

composition at a lower level of acid concentration [54]. However, different behavior was obtained with the salt mixture, no influence was observed.

The partition coefficients of each carboxylic acid using TOA as an extractant in a concentration of 16 and 32%, and butanol as a solvent was calculated. Table 5-9. Partition coefficients *via* reactive extraction. summarizes the values obtained; coefficients lower than 1.7 indicate a low extraction percentage in the organic phase. Similar results were obtained in the recovery of lactic acid via reactive extraction by Wasewar *et al.* [37].They reported a partition coefficient of 0.9 using 30% TOA/1-octanol, the increase of TOA concentration to 90%, increase the partition coefficient to 1.2.

Table 5-9. Partition coefficients *via* reactive extraction.

	Partition coefficient (K_D)			
	SALT		**ACID**	
	BuOH[a]	**BuOH[b]**	**BuOH[a]**	**BuOH[b]**
Glyceric	1,0	1,4	0,5	1,7
Glycolic	1,2	1,0	0,7	1,1
Glycerol	---	—	—	—
Formic	1,6	1,3	1,0	1,4

5.2.6 Results and Discussion

Separation techniques such as simple and vacuum distillation, liquid-liquid and reactive extraction were carried out in order to recover glyceric, glycolic and formic acids from an aqueous mixture obtained from glycerol oxidation using 5% $Ag/CeO_{.75}ZrO_{.25}O_2$ as a catalyst. The conversion of glycerol was 85% and the selectivity obtained were 13, 33 and 36% for glyceric, formic and glycolic acids respectively. Two types of mixtures were tested, in salt form and in acid form.

The stability of this mixture was studied *via* atmospheric and vacuum distillation for the water removal percentages 30, 60 and 80%. For instance, water and volatile impurities are removed from non-volatile carboxylic acids with this technic; many researches have been conducted for concentrating carboxylic acids from aqueous solution. However, evaporation costs are high for dilute aqueous solutions due to the energy required to evaporate water. Kiss *et al.* [55] have noted that the separation of acetic acid and lactic acid from aqueous solutions by simple distillation is

difficult, requiring a column with many stages and a high reflux ratio, thus incurring high running costs.

In general, the mixture in salt form shows better stability in comparison with the mixture in acid form, *i.e.,* a molar percentage higher than 90% rest in the bottom of the column after the test, allowing a 60% of dewatering, using both techniques. This performance is due to the decreasing of the volatility of organic acids in presence of Na+ ions, reflecting the importance of the neutralization process. However, for a water removal of 80%, the concentration of the mixture in the salt form was limited by the solubility in the aqueous phase, it means, a precipitation around 45% is achieved. This was confirmed by the precipitation around 9% of each acid via centrifugation. Thus, according to the results, an acidification step should take place after the distillation stage in order to preserve the major quantity of compounds without degradation.

Liquid-liquid extraction was carried out using butanol and octanol as extractants. Their use as extraction solvents is favored for both types of mixtures. Despite the increase in the polarity resulting from the absence of protons, each carboxylic acid, and its carboxylate remain relatively soluble, high extraction percentages were obtained (>70%). The increase of molar ratio mixture/extractant improves the extraction efficiency of around 9%, nevertheless, although the recovery of the carboxylic acids can be improved by increasing volume of extractants, the cost for solvent recovery is increased at the same time, which should be taken into account in the economic feasibility of the process. Butanol showed better performance in the extraction of carboxylic acids (Butanol: 85%, Octanol: 73%), whereas octanol showed better affinity with the organic salt of the corresponding acids (Butanol: 78%, Octanol: 86%). This behavior was due to the polarity of the molecules which allows a better solvation. The initial concentration of acids has an important influence in the liquid-liquid extraction efficiency, an extraction decreases of around 30 and 70% was obtained for the mixtures with a dewatering of 30% and 60%, respectively. The degree of extraction decreases when the concentration of acid is increased in the aqueous phase, it means, disfavors the extraction capacity. Therefore, distillation and liquid-liquid extraction is not a suitable consecutive configuration in the recovery of these carboxylic acids.

Reactive extraction was carried out using butanol and TOA as solvent and extractant, respectively. Low extraction percentages were obtained (<40%) under these conditions, mainly in the salt mixture (around 25%) due to the pH used and the influence of the organic phase polarity. The

extraction efficiency is inversely proportional to pH value; optimum pH value is before the pKa value of acid. In this work, the pH of the mixture in acid and salt form were 6 and 13 respectively. In addition, organic-phase polarity has an important role in the mechanism of the interfacial reaction between the solute and the extractant, in this study butanol has a high polarity (ξ= 17,5) in comparison with TOA (ξ = 3.2), making difficult its adequate solvation and functioning. In this context, trying with another solvent, with a slight polarity as octanol or decanol might be an interesting approach for the process intensification, as well as studying the optimal conditions for the complex formation, particularly, the influence of pH, temperature, and type of amine.

5.2.7 Conclusion

After analyzing the different techniques and their efficiency in the process of eliminating water without affecting the stability of the acids, simple reactive distillation was chosen as the most promising technology. The study showed that it is convenient to carry out the elimination of water before the acidification process. The operating temperature of the single distillation column can operate at the temperature at the outlet of the glycerol oxidation reactor. The amount of water remaining in the solution is directly related to the efficiency and operating cost of the consecutive reactive distillation column and/or double-walled reactive distillation column, for this reason, it is considered as the best scenario for the start of the reactive distillation process a mixture subjected to the elimination of 60wt% of the initial amount of water.

5.2.8 Bibliography

[1] E. Skrzyńska, S. Zaid, J. S. Girardon, M. Capron, and F. Dumeignil, “Catalytic behaviour of four different supported noble metals in the crude glycerol oxidation,” *Appl. Catal. A Gen.*, vol. 499, pp. 89–100, 2015.

[2] S. Zaid and P. Fongarland, “GLYCEROL OXIDATION IN AQUEOUS PHASE BY USING SILVER-BASED CATALYSTS : KINETIC ANALYSIS AND MODELLING,” pp. 5–6, 1918.

[3] E. Skrzyńska, S. Zaid, A. Addad, J.-S. Girardon, M. Capron, and F. Dumeignil, “Performance of Ag/Al $_2$ O $_3$ catalysts in the liquid phase oxidation of glycerol – effect of preparation method and reaction conditions,” *Catal. Sci. Technol.*, vol. 6, no. 9, pp. 3182–3196, 2016.

[4] B. M. Pagliaro, M. Rossi, and M. Pagliaro, “Glycerol : Properties and Production,” pp. 1–18, 2008.

[5] F.-Z. S. ZAID, “Nouveau type de catalyseurs à base d’argent supportés pour l’obtention d’acide glycolique à partir du glycerol en phase liquid.” .

[6] C. R. Vitasari, G. W. Meindersma, and A. B. De Haan, “Glycolaldehyde co-extraction during the reactive extraction of acetic acid with tri-n-octylamine/2-ethyl-1-hexanol from a wood-based pyrolysis oil-derived aqueous phase,” *Sep. Purif. Technol.*, vol. 95, pp. 39–43, 2012.

[7] B. H. Gu, P. Zheng, Q. Yan, and W. Liu, “Aqueous two-phase system: An alternative process for recovery of succinic acid from fermentation broth,” *Sep. Purif. Technol.*, vol. 138, pp. 47–54, 2014.

[8] R. Kumar, S. M. Mahajani, H. Nanavati, and S. B. Noronha, “Recovery of lactic acid by batch reactive distillation,” vol. 1150, no. June 2005, pp. 1141–1150, 2006.

[9] S. Hakkinen, F. McNeill, and I. Riipinen, “Effect of Inorganic Salts on the Volatility of Organic Acids,” *Environ. Sci. Technol.*, vol. 48, pp. 13718–13726, 2014.

[10] A. Laskin *et al.*, “Tropospheric chemistry of internally mixed sea salt and organic particles : Surprising reactivity of NaCl with weak organic acids,” vol. 117, pp. 1–12, 2012.

[11] C. Ni, X. Wu, J. Dan, and D. Du, “Facile recovery of acetic acid from waste acids of electronic industry via a partial neutralization pretreatment (PNP) - Distillation strategy,” *Sep. Purif. Technol.*, vol. 132, pp. 23–26, 2014.

[12] J. Tyler and G. Dibdin, “Method involving separation from biological material by vacuum distillation,” *J. Chromatogr.*, vol. 105, p. 77, 1975.

[13] H. G. Brittain, Y. Gong, and D. Grant, “Principles of solubility,” in *springer*, no. August 2007, 2014, p. 466.

[14] T. Kurzrock and D. Weuster-Botz, “Recovery of succinic acid from fermentation broth,” *Biotechnol. Lett.*, vol. 32, no. 3, pp. 331–339, 2010.

[15] Y. K. Hong, W. H. Hong, and D. H. Han, “Application of reactive extraction to recovery of carboxylic acids,” *Biotechnol. Bioprocess Eng.*, vol. 6, pp. 386–394, 2001.

[16] Q. Z. Li *et al.*, “Recovery processes of organic acids from fermentation broths in the biomass-based industry,” *J. Microbiol. Biotechnol.*, vol. 26, no. 1, pp. 1–8, 2015.

[17] E. L. Ibarra-Montaño, N. Rodríguez-Laguna, A. Sánchez-Hernández, and A. Rojas-Hernández, “Determination of pKa Values for Acrylic, Methacrylic and Itaconic Acids by 1H and 13C NMR in Deuterated Water,” *J. Appl. Solut. Chem. Model.*, vol. 4, pp. 7–18, 2015.

[18] K. P. Johnston and J. B. Chlistunoff, “Neutralization of acids and bases in subcritical and

supercritical water: Acetic acid and HCl," *J. Supercrit. Fluids*, vol. 12, no. 2, pp. 155–164, 1998.

[19] E. Serjeant and B. Dempsey, *Ionisation constants of organic acids in aqueous solution*. 1979.

[20] H. M. Ijmker, M. Gramblička, S. R. A. Kersten, A. G. J. Van Der Ham, and B. Schuur, "Acetic acid extraction from aqueous solutions using fatty acids," *Sep. Purif. Technol.*, vol. 125, pp. 256–263, 2014.

[21] E. Alkaya, S. Kaptan, L. Ozkan, S. Uludag-Demirer, and G. N. Demirer, "Recovery of acids from anaerobic acidification broth by liquid-liquid extraction," *Chemosphere*, vol. 77, no. 8, pp. 1137–1142, 2009.

[22] A. Kovalenko, "Molecular theory of solvation : Methodology summary and illustrations," *Condens. matter Phys.*, vol. 18, no. 3, pp. 1–24, 2015.

[23] D. Datta, M. E. Marti, H. Uslu, and S. Kumar, "Extraction of levulinic acid using tri-n-butyl phosphate and tri-n-octylamine in 1-octanol: Column design," *J. Taiwan Inst. Chem. Eng.*, vol. 66, pp. 407–413, 2016.

[24] H. Fu, Y. Sun, H. Teng, D. Zhang, and Z. Xiu, "Salting-out extraction of carboxylic acids," *Sep. Purif. Technol.*, vol. 139, pp. 36–42, 2015.

[25] G. Roos and C. Roos, *Acids and Bases*. 2015.

[26] M. Mohsen-Nia, H. Amiri, and B. Jazi, "Dielectric constants of water, methanol, ethanol, butanol and acetone: Measurement and computational study," *J. Solution Chem.*, vol. 39, no. 5, pp. 701–708, 2010.

[27] S. H. Ha, N. L. Mai, and Y. M. Koo, "Butanol recovery from aqueous solution into ionic liquids by liquid-liquid extraction," *Process Biochem.*, vol. 45, no. 12, pp. 1899–1903, 2010.

[28] K. L. Wasewar and D. Z. Shende, "Reactive extraction of caproic acid using tri-n-butyl phosphate in hexanol, octanol, and decanol," *J. Chem. Eng. Data*, vol. 56, no. 8, pp. 3318–3322, 2011.

[29] D. Datta and S. Kumar, "Modeling Using Response Surface Methodology and Optimization Using Differential Evolution of Reactive Extraction of Glycolic Acid," *Chem. Eng. Commun.*, vol. 2, no. 1, pp. 37–41, 2014.

[30] G. H. Kim, S. J. Park, and B. H. Um, "Response surface methodology for optimization of solvent extraction to recovery of acetic acid from black liquor derived from Typha latifolia pulping process," *Ind. Crops Prod.*, vol. 89, pp. 34–44, 2016.

[31] C. L. Munson and C. J. King, “Factors Influencing Solvent Selection for Extraction of Ethanol from Aqueous Solutions,” *Ind. Eng. Chem. Process Des. Dev.*, vol. 23, no. 1, pp. 109–115, 1984.

[32] S. Kumar and B. Babu, “Separation of carboxylic acids from waste water via reactive extraction,” *Int. Conv. Water*, pp. 1–9, 2008.

[33] D. Datta, S. Kumar, and H. Uslu, “Status of the Reactive Extraction as a Method of Separation,” *J. Chem.*, vol. Volume 201, no. i, pp. 1–16, 2014.

[34] A. Qader and M. A. Hughes, “Extraction equilibria of acetic and propionic acids from dilute aqueous solution by several solvents,” *Sep. Sci. Technol.*, vol. 27, no. 13, pp. 1809–1821, 1992.

[35] W. Cai, S. Zhu, and X. Piao, “Extraction equilibria of formic and acetic acids from aqueous solution by phosphate-containing extractants,” *J. Chem. Eng. Data*, vol. 46, no. 6, pp. 1472–1475, 2001.

[36] J. M. Wardell and C. J. King, “Solvent Equilibria for Extraction of Carboxylic Acids from Water,” *J. Chem. Eng. Data*, vol. 23, no. 2, pp. 144–148, 1978.

[37] K. L. Wasewar, A. A. Yawalkar, J. A. Moulijn, and V. G. Pangarkar, “Fermentation of Glucose to Lactic Acid Coupled with Reactive Extraction: A Review,” *Ind. Eng. Chem. Res.*, vol. 43, no. 19, pp. 5969–5982, 2004.

[38] A. S. Kertes and C. J. King, “Extraction chemistry of fermentation product carboxylic acids,” *Biotechnol. Bioeng.*, vol. 28, no. 2, pp. 269–282, 1986.

[39] S. Kumar and B. V Babu, “Process Intensification for Separation of Carboxylic Acids from Fermentation Broths using Reactive Extraction,” *J. Futur. Eng. Technol.*, vol. 3, no. 3, pp. 19–26, 2008.

[40] S. T. Yang, S. A. White, and S. T. Hsu, “Extraction of Carboxylic Acids with Tertiary and Quaternary Amines: Effect of pH,” *Ind. Eng. Chem. Res.*, vol. 30, no. 6, pp. 1335–1342, 1991.

[41] H. Honda, Y. Toyama, H. Takahashi, T. Nakazeko, and T. Kobayashi, “Effective lactic acid production by two-stage extractive fermentation,” *J. Ferment. Bioeng.*, vol. 79, no. 6, pp. 589–593, 1995.

[42] D. H. Han and W. H. Hong, “Water-Enhanced Solubilities of Lactic Acid in Reactive Extraction Using Trioctylamine / Various Active Diluents Systems,” *Sep. Sci. Technol.*, no. December 2014, pp. 271–281, 1998.

[43] K. L. Wasewar, A. B. M. Heesink, G. F. Versteeg, and V. G. Pangarkar, “Equilibria and kinetics for reactive extraction of lactic acid using Alamine 336 in decanol,” *J. Chem. Technol. Biotechnol.*, vol. 1075, no. January, pp. 1068–1075, 2002.

[44] S. Uenoyama, T. Hano, M. Hirata, and S. Miura, “Extraction Kinetics of Organic Acids with Tri-n- octylphosphine Oxide,” *J. Chem. Technol. Biotechnol.*, vol. 67, pp. 260–264, 1996.

[45] D. Datta and S. Kumar, “Modeling and Optimization of Recovery Process of Glycolic Acid using Reactive Extraction,” *J. Chem. Eng. Appl.*, vol. 3, no. 2, pp. 141–146, 2012.

[46] B. Choudhury, A. Basha, and T. Swaminathan, “Stud y of Lactic Acid Extraction with Higher Molecular Weight Aliphatic Amines,” *J. Chem. Technol. Biotechnol.*, vol. 72, pp. 111–116, 1998.

[47] B. H. Um, B. Friedman, and G. P. Van Walsum, “Conditioning hardwood-derived pre-pulping extracts for use in fermentation through removal and recovery of acetic acid using trioctylphosphine oxide (TOPO),” *Holzforschung*, vol. 65, no. 1, pp. 51–58, 2011.

[48] A. Keshav and K. L. Wasewar, “Back extraction of propionic acid from loaded organic phase,” *Chem. Eng. Sci.*, vol. 65, no. 9, pp. 2751–2757, 2010.

[49] K. L. Wasewar, “Reactive Extraction : An Intensifying Approach for Carboxylic Acid Separation,” *Int. J. Chem. Eng. Appl.*, vol. 3, no. 4, 2012.

[50] S. Eda, “Recovery and Regeneration of Carboxylic Acids from Aqueous Solutions Using Process Intensification,” no. August, 2017.

[51] D. Datta, Y. S. Aşçı, and A. F. Tuyun, “Extraction Equilibria of Glycolic Acid Using Tertiary Amines: Experimental Data and Theoretical Predictions,” *J. Chem. Eng. Data*, p. acs.jced.5b00497, 2015.

[52] A. I. Galaction, L. Kloetzer, and D. Cascaval, “Influence of Solvent Polarity on the Mechanism and Efficiency of Formic Acid Reactive Extraction with Tri-n-Octylamine from Aqueous Solutions,” *Chem. Eng. Technol.*, vol. 34, no. 8, pp. 1341–1346, 2011.

[53] M. E. Marti, T. Gurkan, and L. K. Doraiswamy, “Equilibrium and kinetic studies on reactive extraction of pyruvic acid with trioctylamine in 1-octanol,” *Ind. Eng. Chem. Res.*, vol. 50, no. 23, pp. 13518–13525, 2011.

[54] S. Eda, “Recovery of Succinic acid by Reactive Extraction using using Tri-n-Octylamine in 1-Decanol : Equilibrium Optimization Using response surface method and kinetic studies,” *Int. J. Chem. Sep. Technol.*, vol. 2, no. 2, p. 13, 2016.

[55] A. A. Kiss, J. P. Lange, B. Schuur, D. W. F. Brilman, A. G. J. van der Ham, and S. R. A.

Kersten, “Separation technology–Making a difference in biorefineries,” *Biomass and Bioenergy*, vol. 95, pp. 296–309, 2016.

Chapter 6. General conclusions and perspectives

6.1 Conclusion

In the first part of this thesis, the existing processes for the recovery of carboxylic acids in highly diluted solutions were reviewed. Although in the literature there are no studies specifically related to the acids produced from the oxidation of glycerol (*i.e.* glycolic and glyceric acid), the results of the studies carried out with acetic acid can mainly be considered as possible recovery strategies. In general, the most studied processes found can be classified into membrane processes, ion exchange adsorption, reactive extraction, and reactive distillation. Membrane processes are flexible in terms of production quantity and achieve high levels of purity, however, they require pretreatment and present easy fouling, which implies a higher energy consumption, and thus raising its cost. On the other hand, ion exchange adsorption processes prove to be a reliable technology, but their high regeneration cost there is also their greatest obstacle. Reactive extraction processes are a promising option with several advantages such as the benefits of being able to use a solvent efficiently, produced in an environmentally responsible manner and the possibility of being reused. However, the required pH conditions make their implementation challenging. As the last strategy, one can consider the reactive distillation. Although it also has some disadvantages, it can be interesting due to the existing number of units at the industrial level. This technology allows better conversion and selectivity towards the desired products, making the acid recovery process highly efficient. Still, this technology requires some improvements in terms of energy efficiency. One of the possible improvements is the use of reactive divided wall columns. These have a more complex design due to the greater amount of freedom degrees compared with conventional columns.

Accordingly, in the present thesis, the reactive distillation system was chosen as the most suitable technology for the separation of the acids obtained from the oxidation of glycerol. In which, the esterification reaction is in charge of protecting the thermally sensitive acid function and of difficult separation to highly diluted aqueous conditions. The design of the technology requires preliminary information about the thermodynamics of the different compounds involved, the kinetics reaction in the presence of a heterogeneous catalyst, and the ability to adapt the solution and reduce the amount of water in the mixture. The glycolic acid was chosen as the reference acid to carry out

the different studies, propanol, butanol, and octanol were the alcohols chosen for the evaluation of the three different systems.

The second part consisted mainly of choosing at model capable of adequately predicting the thermodynamic behavior of the compounds present in each of the glycolic acid and alcohol reaction systems. The first step consisted of the determination of the parameters of the Antoine equation from the regression of the experimental data of P-T, this was carried out for the esters of the corresponding alcohols since no data was found in the literature. The second step consisted in determining the binary parameters of the NRTL and UNIQUAC models capable of reproducing the experimental data of T-x-y and T-x-x. It was also demonstrated that the parameters obtained with the UNIFAC model are incapable of adequately representing the experimental data. The validation and choice of the most suitable method were made from the comparison of experimental data and the prediction of ternary equilibrium between alcohol-ester-water*, i.e.,* BuOH-BG-Water. The NRTL model managed to better represent the binary and ternary LLE and VLE data in comparison with the UNIQUAC model. The NRTL model was also used to predict the SLE equilibrium between glycolic acid and the different compounds in liquid phase, the binary parameters were determined from the acid solubility data in the different compounds, *i.e.,* alcohols, ester and water. Calorimetric studies of glycolic acid at specific preheating conditions were additionally performed to ensure complete water removal. In order to validate the model, the obtained thermophysical properties were compared to results obtained from simulation with Aspen Plus® software. Correlations were found to predict the liquid and solid calorific capacity. No phase change phenomena were observed for glycolic acid. The obtained binary parameters are very useful for the modeling and designing reactive distillation process.

The third part consisted of the kinetic study of the esterification reaction of glycolic acid and the different alcohols: propanol, butanol and octanol. The first stage consisted of the study of the reaction using H_2SO_4 as homogeneous catalysis. From this part, the thermodynamic parameters such as standard enthalpy and standards entropy of the reaction were calculated. The second stage consisted of the evaluation and selection of the best catalyst. Amberlyst 36 proved to be the best performing catalyst. This catalyst was used for the kinetic study in the presence of heterogeneous catalysis. The results showed that for the case of propanol is the LH model that best describes experimental data, while for the case of butanol and octanol, it was the ER model that best represented the experimental data. The change in the kinetic model due to the change

in the length and size of the molecules involved was explained due to a possible steric hindrance effect. Activation energy, pre-exponential factor, and absorption coefficients data obtained can be used to model and simulate the reactive distillation process.

The fourth part consisted of the evaluation of different process strategies to eliminate the amount of water present in the initial mixture that represents between 90 to 95 wt% of the solution. The technologies evaluated were atmospheric distillation, and vacuum distillation, and liquid-liquid extraction. Tests were performed on actual glycerol oxidation samples before and after the acidification process. The results showed that the most suitable technology is a distillation, the process can preferably be performed before acidification. It is possible to decrease up to 60 wt% of the amount of initial mass by eliminating water in the initial solution, where at with this percentage, no precipitation effect of the salts of the acids was observed.

In general, the preliminary information necessary to carry out the study of recovery of glycolic acid using three different alcohols by reactive distillation was produced. The additional study of water elimination implies better energy saving and a decrease in the complexity of the mixture inside the reactive distillation column.

6.2 Perspectives

The success of the design of industrial processes depends to a great extent on the starting data, the thermodynamic data obtained experimentally and validated diminish the error in the design of the processes. In order to guarantee the quality of the results, appropriate equipment is required to determine VLE at both, constant pressure and constant temperature, especially to analyze cases when binary systems are reactive. In the literature, most of the thermodynamic data reported are only for well-known couples such as those formed by acetic, formic, and lactic acid. However, the lack of information on molecules such as glycolic acid, glyceric acid, among others, making the implementation of recovery strategies impossible. To continue working in the methodology of determination of balances SL, LL and VL is of great utility for the development of new technologies.

Carboxylic acid recovery processes based on distillation reactivate where the solution to be processed contains large quantities of water, requiring important attention in the catalysts development. Ion exchange resins, a catalyst used in most cases, have low stability, at high

temperature conditions and large amounts of water. New catalytic studies could be based on the possibility of developing materials resistant to operating conditions of high temperatures (>120°C) and in the presence of high quantities of water. Another important aspect is the development of catalysts with morphological characteristics suitable for use in a reactive distillation system, i.e. an adequate particle size that allows easy positioning within the reaction zone of the column.

Although the initial objective of the project was to of the design a conventional reactive distillation process, in this work it was suggested to carry out the design of a system of reactive divided wall columns. The objective is to be able to compare the benefits of implementing a conventional reaction distillation system or a reactive divided wall column system. The rigorous design of a process requires experimental data obtained from a representative pilot unit and simulations to validate the results obtained experimentally. For this purpose, it is suggested to design and build a RDWC pilot unit.

Conventional process simulators still do not have a module that represents the RDWC system. The studies presented in the simulation literature perform the simulation considering that an assembly of equipment is capable of representing the RDWC. The literature shows that the design, simulation, control and experimental data of an RDWC are still under investigation.

ANNEX A.

Approach of a conceptual design of reactive divide wall column by simulation in ASPEN PLUS

In recent years, research into industrial processes has been based on the improvement, not only in terms of efficiency, but also in relation to lower energy consumption and lower implementation costs. The method of process intensification aims to combine different operations that can be carried out simultaneously, the synergy of this step leads to more efficient processes. Reactive distillation (RD) is the result of the coupling of the separation and reaction process in a single unit. This technology has been widely studied and implemented at an industrial level. The RD allows to improve reaction yields, selectivity, thermodynamic limitations and the considerable reduction of energy, water and solvent consumption, and avoidance of hot spots by simultaneous liquid evaporation; and ability to separate close boiling components [1]. The design of this process is complex due to the interactions that must be considered related to heat and mass transfer phenomena in the system [2]. Usually, the design of the process can be done by simulation using different existing software such as Aspen Plus® and ProSim^{PLUS} or from experimental data obtained from a pilot plant, these two stages are complementary to validate the design of the process.

Within the overall framework of the project for the recovery of carboxylic acids obtained from glycerol oxidation, the reactive distillation process was chosen as a recovery and separation strategy through the esterification reaction. The UCCS provided kinetic and thermodynamic data for the different acids (*e.g*. glycolic and formic acid) involved in the esterification reaction with different alcohols (*e.g*. propanol, butanol and octanol). On the other hand, the LGPC was in charge of carrying out the experimental tests in the reactive distillation pilot unit and the validation of the results by simulation in ProSim^{PLUS}.

Reactive divide wall column (RDWC) has been presented as an intensification strategy of the reactive distillation process and the multi-component separation strategy is also called Petlyuk arrangements [3]. The addition of a wall inside the column allows the separation of high and low boiling point components, but also those of intermediate boiling points [4]. Among the main advantages of the implementation of a RDWC are the purity of the products recovered at the outlet

of the unit, the higher thermodynamic and energetic efficiency due to the reduction of the re-mixing effects; and fewer units of equipment compared to conventional systems [5]. These advantages are directly reflected in the cost of implementation and operation of the system. However, there are some drawbacks with operating the RDWC unit, *i.e.*, a single operating pressure along the column and the stability of the catalyst in the reaction zone, which restricts the possibility of modifying the operation of the column depending on the volatility of the compounds. From the operational point of view, the authors have reported a high complexity in the control of the system due to the inability to control internal flows [6].

The research reported in the literature for RDWC, has as main design criteria, for the analytical solution or by simulation, the minimum energy consumption in columns directly coupled to a multicomponent system at the input and output of the system. However, most of the work reported so far is mainly based on three-component mixtures. Researchers reported include short design methods, rigorous steady state simulations, dynamic control simulations, pilot experimental operation [7-17].

The RDWC is a promising technology, however, as it is a technology its application is not easy to address. The UCCS proposes the implementation of RDWC as an alternative of process intensification and improvement of the reactive distillation. The objective is to be able to compare the performance of the two technologies, the RD developed by LGPC and the RDWC proposed by UCCS. Aware of the complexity involved in the rigorous design of the RDWC system, a shortened method is proposed based on the methodology presented by Muller *et al*.[11] and Feng [15] in which, through preliminary simulation with the calculated thermodynamic data, values associated with separation efficiency are obtained that provide an initial approach to what would be a rigorous simulation of the RDWC system. This information is also the starting point for mathematical development.

A.1 Pre-simulation considerations

Plentyuk model consists of the arrangement of a series of conventional distillation columns representing the performance of an WDC[3]. Muller *et al.* [11] represents a simplified configuration of the complex configuration of the RWDC by decomposing the unit and preserving its behavior, therefore allowing a simpler approach of the process.

Muller *et al.* [11] describes the adaptation of the Petlyuk configuration taking onto account tree main assumptions, the first one states that the flows in the two zones (prefractionator and main column) can be calculated by the phase splits on the wall, the second one defines the approach made to reduce the four streams connecting the two columns to four heat exchangers , building the concept of prefractional and main column by the concept of thermal coupling, finally the last one describes the development of the three column arrangement taking on count that this one is only valid down the condition where the bottom products of the prefractional zone feeds the lower column on the top and the upper one by the bottom (see Figure A.10).

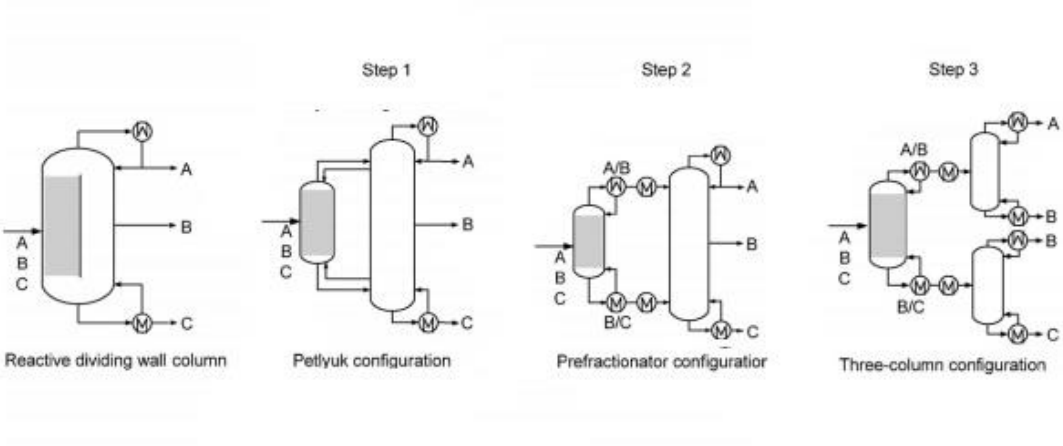

Figure A.10. Decomposition into simple column sequences (grey area: reactive zone) [11].

In order to carry out these simplifications, different design criteria must be considered. The main purpose is to minimize the inefficiency associated to the erroneous of the process design resulting from wrong criteria of the interlinking streams and trays [12]. Some authors agree on the following considerations: 1. constant relative volatility, 2. constant molar flow, 3. liquid and vapor interlinking streams are assuming at equilibrium, to development and design the columns. The systems were solved by different mathematical approaches as the FUGK and FUG method, which relates the expressions of mass and energy balance through the Fensky, Underwood, Gilliland and Kirkbride correlations. Where Fensky is used to calculated minimum number of stages at minimum reflux, which can be calculated by Underwood equation. The optimal stage numbers and fed stage are calculated by Gilliland correlation and Kirkbride equation, respectively. Ramirez-Corona *et al* [18] and Kai Ti Chu *et al* [9] explain and apply those methodologies on their research, in which they develop shortcut methods that allow an easier approach to procedure. However, other authors consider for the design of the system the minimum vapor flow (V_{min}), this model is based on a

graphical methodology obtained from the mass and energy balances. Halvorse et al. [7] presents its design strategy from a graphical model.

For this study, simulation approach, some of the assumptions mentioned before were adapted and applied as shown:

I. The system works at chemical equilibrium in the reactive part of the prefractional zone, and at thermodynamic equilibrium at the separation process, resulting on constant vapor liquid flow on each stage and by consequence the complete separation unit.

II. The constant pressure drop of the system remains constant; this means that for all the system was consider than the working pressure in the prefactionator column is equal to the top pressure of the main column system.

III. The operating temperature range of the column cannot be over 150°C, Amberlyst degradation temperature (See Table 4-6)

IV. The desired product (ester) is recovered at the bottom fraction of the main column.

V. The glycolic acid reaches its maximal conversion on the reaction section of the process.

VI. The heat transport phenomena at the dividing wall and the heat losses in the column's walls are negligible. Each stage of the unit (prefrac + main column) achieves the liquid-vapor equilibrium.

VII. The 3 columns are thermally coupled forming and representing the entire RDWC as one unique unit.

VIII. Finally, to reduce the computational effort and the number of interactions the number of stages of each column was fixed as 12.

The methodology approach in this study consisted in the adjustment of the work done by Muller *et al*.[11] and Feng [15], the authors set parameters such as the number of stages in the prefractionation zone to decrease the number of input variables for the design of the system.

A.1. Simulation procedure

The simulation of RDWC distillation was carried out using the simulator environment of Aspen Plus® (Version v8.8), a three column sequence model was chosen. This representation is divided in two principal sections, prefactionator and main column, the reaction takes place in the prefactionator zone while the separation process of the products is carried out in the main column which is subdivided into two distillation columns fed by the prefactionator outlet streams. The representation of the column arrangement was subdivided in different units depending on the characteristics of system and the reactive alcohol as shown in Figure A-11.

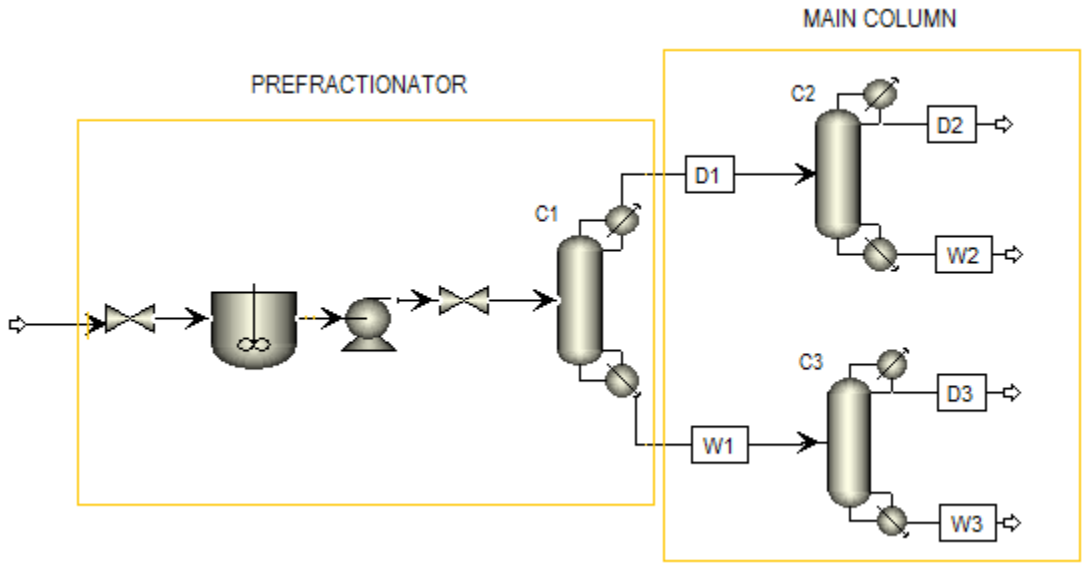

Figure A-11. Recreation of the RDWD column on Aspen

The simulation was sketched in an arrange of simple basic process units to ensure that the proposed model can be compatible with others process simulator programs that doesn't count necessarily with the reactive distillation system package such as ProSim^{Plus}, ChemCad, and Aspen Plus®.

The prefractional zone was simulated using a steady state model column (RAD-FRAC) for the separation process and a CSTR reactor for the reaction. The technical and operation parameters for the distillation column in the prefractional zone are listed in Table A-1.

Table A-1. Parameters and operation conditions.

Parameter	
Number of stages (N)	12
Mass Flow (kg/h)	100
HETP – Height equivalent to theoretical plate (m)	0.5
Reflux ratio	0.001
Catalyst	Ambelyst 36
Column Packing	Sulser BX
Reboiler type	Kettle
Condensator	Total

The number of stages in the simulation column is fixed at 12, the height equivalent to a theoretical stage (HETP = 0.5 m) reported for structured packaging [19]. The hydrodynamic conditions in the column were those presented in Aspen plus for BX type packages.

In addition to the latter parameters for the simulation was taken into account the thermal stability of the catalyst (<150°C) and the kinetic optimal temperature for the reaction (see Table 4-5). The operation pressure of each system was adjusted in order to satisfice the considerations posed before and therefore to guarantee optimal conditions of the reaction. The principal criteria to run the simulation was fixed to maximize the recovery of the main product on the final separation process.

In other to study the effect of the molar composition on the feed stream on the RDWD column operations three difference scenarios for each system reactions were proposed. The first one is at 1:3 molar ratio between the glycolic acid and the reactant alcohol, the second is a 1:5 ratio, to recreate a most accurate real life process and to establish the effect that has the presence of water in the feed stream a third scenario was proposed adding water to the first study case in 20 mol%.

A.2 Simulation results

A.2.1 Glycolic acid and butanol system

The separation process of the distillation column unit is based on the principle of the vapor pressure, at the same time is related to the volatility concept. As a result of the simulation, the operating pressure required for this system to meet the criteria mentioned in section 6.1 was 200

mbar. At these conditions, the glycolic acid and butanol case was represented by a column in the prefractionation zone and a single column in the main zone. This is due to the fact that in the upper zone the products of the top of the column, butanol and water can be separated by a simple decanting process being this an adjustments to the initial proposed model in Figure A-11 . The final scheme representation of the RDWC system in Aspen Plus® is shown on Figure A-12.

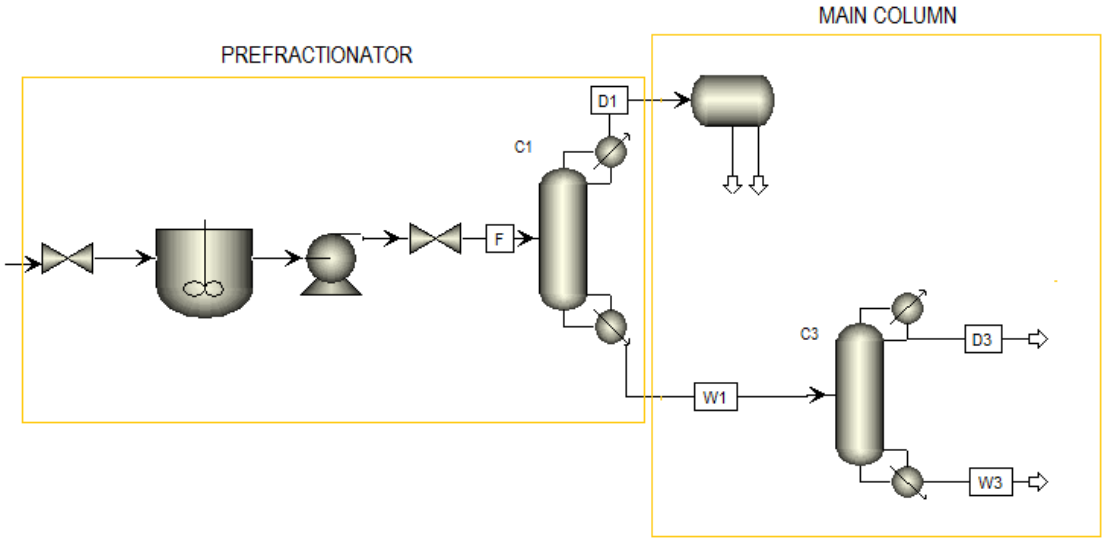

Figure A-12. RDWD column arrangement for complete compounds separation in presence of a heterogeneous azeotrope at the top of the prefractional column simulated by Aspen.

In the literature the impact of the number of stages and the feed location study are important parameters to optimize the unit, as the aim of this work is to get an approach to the initial parameter for the design, the Kirkbride equation establish a theorical approach for these parameters. Those variables were fixed as 12 for the number of stages and 6 as the number of the stage to the feed. Figure A-13 presents the temperature profile and the molar fraction profile on the prefactionator column of butanol in the column. Since the operation of the column is limited to a constant pressure, the different plates are in equilibrium, the graph shows the fraction of butanol in each of the stages.

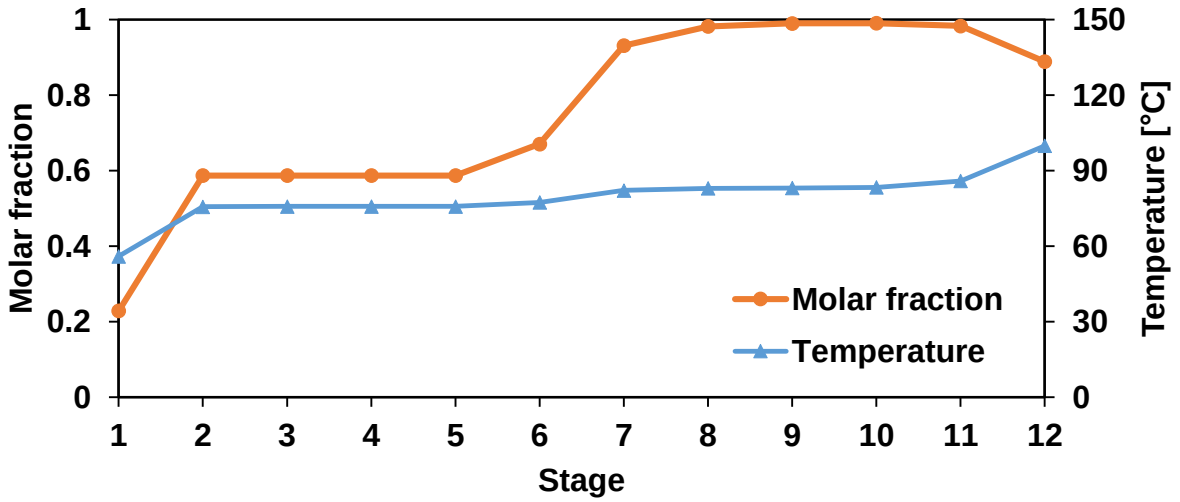

Figure A-13. Temperature and mol fraction profiles of butanol on the prefraction column.

As a result of establishing the operating parameters of the separation system the percentage of recovery of the ester at the bottom of the column was higher than 95%, the variation of the percentage of recovery when modifying the feed ratios can be considered negligible. However, the purity of the ester at the bottom of the column varied from 84 to 90 % with the increase of the acid alcohol ratio from R 1:3 to R 1:5, respectively. The presence of water in the lake system evidences an improvement in purity reached with 97% at the end of the process.

A.2.2 Glycolic acid and propanol system

For the glycolic acid and propanol system, the pressure was fixed at 400 mbar, this pressure condition allows to obtain a temperature around 70 °C in the prefactionator column. However, by simple distillation propanol cannot be separated since the distribution of the compounds at the top of the column, propanol and water, are in the concentration range of the homogeneous azeotrope for the binary system. The feed stream to the prefactionator system was established at the stage 6, the figure presents the temperature and molar fraction profiles of the ester along the prefactionator column. Figure A-14 presents the temperature profile of the prefactionator column and the concentration profile of propyl glycolate in the column.

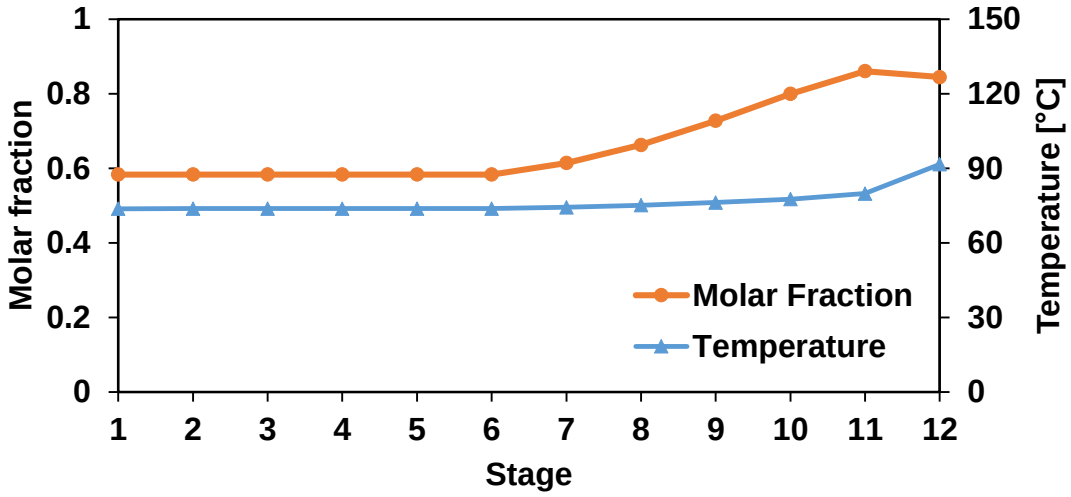

Figure A-14. Temperature and mol fraction profiles of propanol on the prefraction column.

As a result of setting the parameters at the initial proposed model shown in Figure A-11 it was observed that the ester is recover at the bottom of the column being 77% the minimum value of the three study cases and corresponding to the 1:3 molar ratio followed by a 93% for the 1:5 ratios and finally a 97% of recovery was archived in the system with water in the feed stream. On the other hand, the purity of the product is directly related to the alcohol excess and water presence in the feed stream, showing a 13% reduction in the purity compared to the R 1:3 scenarios where the maximal purity was obtained with a value of 99%.

A.2.3. Glycolic acid and octanol system

This system presented the less suitable profile and temperature range to carry out the reaction, even by decreasing the operation pressure to 200 mbar an adequate temperature to guarantee the integrity of the catalyst range was not achieved. Figure A-15 presents the temperature profile of the prefraction column and the concentration profile of octyl glycolate in the column.

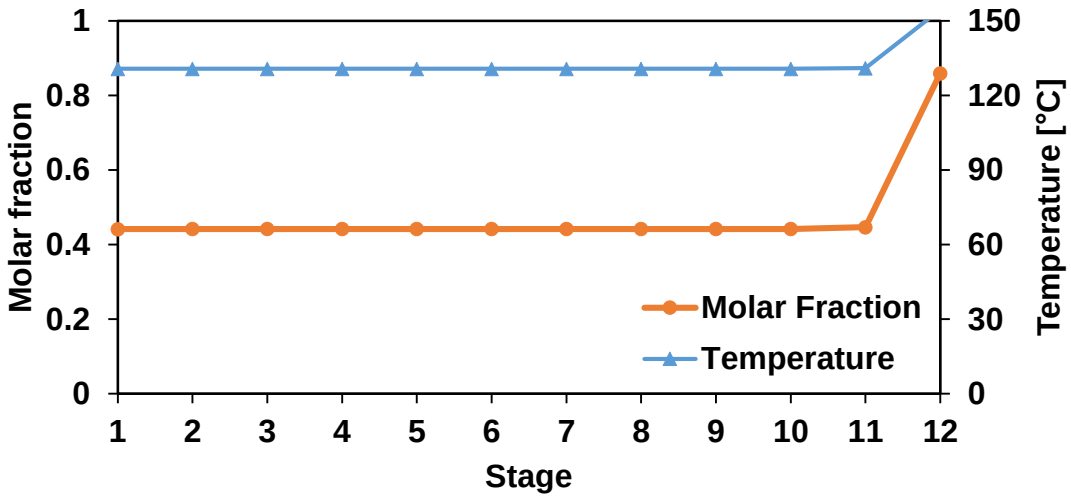

Figure A-15. Temperature and mol fraction profiles of octanol on the prefraction column.

The recovery of the ester in the bottom stream of the column for this system was higher than 93% in the three scenarios, the variation between them can be considered negligible. This system presents the lowest purity percentages compared to the results presented so far with percentages around 83%. However, an improvement in the purity percentage is seen when water is added to the inlet of the column.

A.3 Results and Discussion

The simulation of the RDWC for the separation and recovery of the esters of the different systems studied, showed the advantages of the implementation of the technology. As each of the three reactants alcohols and main products presents different thermodynamics behaviors the diagram proposed for the main column had to be adjusted to reach not only the maximal recovery of the main product but to achieve the complete separation of the compounds which can be recycled onto the process. The reactions systems with butanol and octanol as reactants forms a heterogenic azeotrope on the top of the prefactional system, due to the fact that those alcohols are not miscible with water, the separation of the compounds can be completed by a physical separation method as decantation. Figure A-12 shows the representative scheme for this scenarios.

Due to the formation of the heterogeneous azeotrope for butanol and octanol systems is possible to conclude that to achieve maximal recovery of the ester produced the reactive zone of the RDWD

column is located in the upper part of the separation unit. In the propanol case, the reaction zone must be located in the intermediate zone of the column because the upper part, the rectification part, is required to complete the separation of propanol.

The recovery percentages reached for the different systems are higher than 90% except for the case of propanol with an input molar ratio of R 1:3 as shown in Figure A-16.

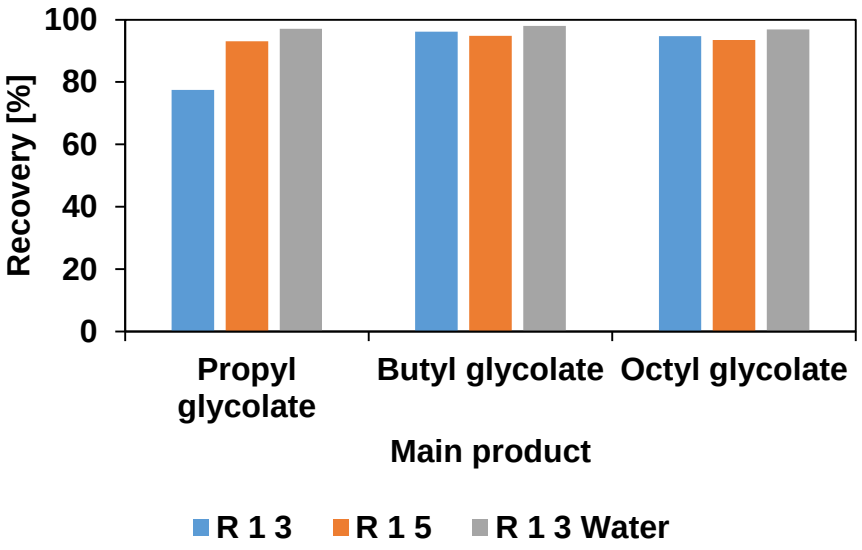

Figure A-16. Comparison of recovery percentage of ester for the different systems.

The stream composition at the bottom of the column represents the degree of purity of the recovered product, for all cases the percentage of purity is greater than 80%. Figure A-17 shows the comparison of the different purity percentages obtained. This allows to confirm that the different arrangements considered in each system evidences the viability of the implementation of the RDWC process.

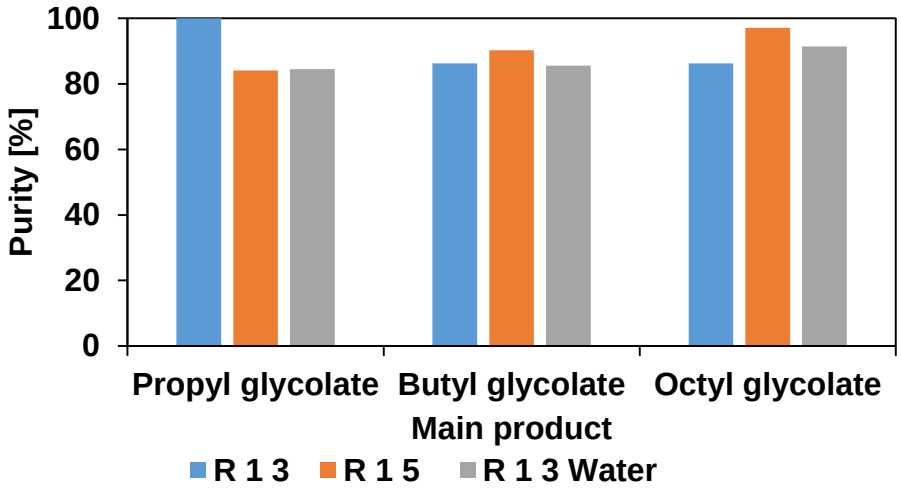

Figure A-17. Comparison of purity percentage of ester for the different systems.

However, the percentages of recovery and purity are not sufficient criteria to determine the viability of the technology. Energy consumption is a fundamental criterion when selecting the most suitable system. The energy calculations were considered based on the requirements of the equipment that conform the configuration that represents the RDWC, for a feed flow of 100 kg h^{-1}. It should be clarified that this calculation is an approximation. Figure A-18 shows the energy consumption for each of the systems. The systems made up of propanol and butanol have similar consumptions, while the consumption for the system made up of octanol is almost twice as high. It should be noted that for industrial implementation, operation under vacuum conditions represents an important energy consumption.

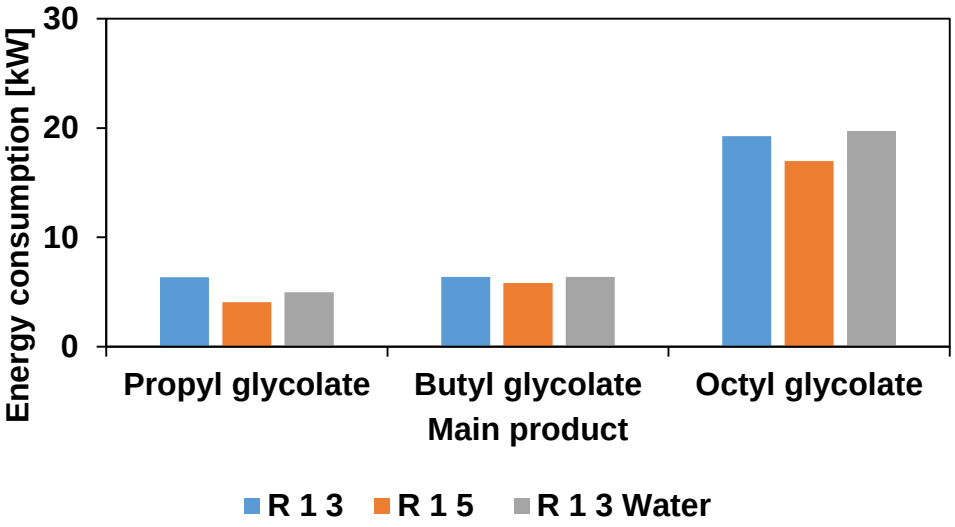

Figure A-18. Comparison of energy consumption of ester for the different systems

The simulation environment allowed to modify the operation pressure in order to meet the most important criteria, to work in the optimal thermal conditions for the catalyst in the prefractional zone for the octanol system this criterion was not able to be accomplished in a pressure comparable to the others systems this may suggest to discard this alcohol as a promising substrate to work with leaving only propanol and butanol as suitable options to be consider. However, butanol can be easily recovered compared to propanol, although this is not a definitive criterion.

A.4 Conclusion

The preliminary results of the evaluation of RDWC technology showed that this process intensification is a satisfactory technique to achieve in a simpler way the separation and recovery of the ester.

The results of the preliminary simulation are excellent data for the starting point of a more rigorous mathematically study and by simulation. The operating pressures, the concentration of the different stream, the relative volatility and the identification of the key components facilitate the design of the RDWC technology.

A.5 Bibliography

[1] I. Mueller and E. Y. Kenig, “Reactive distillation in a dividing wall column: Rate-based modeling and simulation,” *Ind. Eng. Chem. Res.*, vol. 46, no. 11, pp. 3709–3719, 2007.

[2] J. G. Segovia-Hernández, S. Hernández, and A. Bonilla Petriciolet, “Reactive distillation: A review of optimal design using deterministic and stochastic techniques,” *Chem. Eng. Process. Process Intensif.*, vol. 97, pp. 134–143, 2015.

[3] D. Petyluk, FB; Platonov, V.M.; Slavinskii, “Thermodynamically optimal method for separating multicomponent mixtures,” *Int. Chem. Eng.*, vol. 5, no. 3, pp. 555–561, 1965.

[4] A. Weinfeld, S. A. Owens, and R. B. Eldridge, “Reactive dividing wall columns : A comprehensive review,” *Chem. Eng. Process. Process Intensificatio*, vol. 123, no. September 2017, pp. 20–33, 2018.

[5] M. A. Schultz, D. G. Stewart, J. M. Harris, S. P. Rosenblum, M. S. Shakur, and D. E. O.

Brien, “Reduce Costs with Dividing-Wall Columns,” *Chem. Eng. Prog.*, vol. 95, pp. 64–71, 2002.

[6] M. M. Donahue, B. J. Roach, J. J. Downs, T. Blevins, M. Baldea, and R. B. Eldridge, “Dividing wall column control: Common practices and key findings,” *Chem. Eng. Process. Process Intensif.*, vol. 107, pp. 106–115, 2016.

[7] I. Halvorsen, “Minimum Energy Requirements in Complex Distillation Arrangements,” 2001.

[8] L. Sun and X. Bi, “Shortcut method for the design of reactive dividing wall column,” *Ind. Eng. Chem. Res.*, vol. 53, no. 6, pp. 2340–2347, 2014.

[9] K. T. Chu, L. Cadoret, C. C. Yu, and J. D. Ward, “A new shortcut design method and economic analysis of divided wall columns,” *Ind. Eng. Chem. Res.*, vol. 50, no. 15, pp. 9221–9235, 2011.

[10] N. Sotoudeh Chafi and B. Hashemi Shahraki, “A Method for the Design of Divided Wall Columns A New Mixture of Ionic liquids (the Combination of Chemical and Physical Absorption) to Capture CO2 from Flue Gas View project Carbon Dioxide Capture View project A Method for the Design of Divided Wall Columns,” *Chem. Eng. Technol.*, vol. 1, no. 9, pp. 1284–1291, 2007.

[11] I. Mueller, C. Pech, D. Bhatia, and E. Y. Kenig, “Rate-based analysis of reactive distillation sequences with different degrees of integration,” *Chem. Eng. Sci.*, vol. 62, no. 24, pp. 7327–7335, 2007.

[12] F. Z. Seihoub, H. Benyounes, W. Shen, and V. Gerbaud, “An Improved Shortcut Design Method of Divided Wall Columns Exemplified by a Liquefied Petroleum Gas Process,” *Ind. Eng. Chem. Res.*, vol. 56, no. 34, pp. 9710–9720, 2017.

[13] R. Delgado-Delgado, S. Hernández, F. O. Barroso-Muñoz, J. G. Segovia-Hernández, and A. J. Castro-Montoya, “From simulation studies to experimental tests in a reactive dividing wall distillation column,” *Chem. Eng. Res. Des.*, vol. 90, no. 7, pp. 855–862, 2012.

[14] A. A. Kiss and D. J. P. C. Suszwalak, “Enhanced dimethyl ether synthesis by reactive distillation in a dividing-wall column,” *Procedia Eng.*, vol. 42, no. August, pp. 581–587, 2012.

[15] J. Feng, “Design and Simulation of Reactive Dividing-Wall Distillation Column for Transesterification of Methyl Acetate with n-Propanol,” *Adv. Eng. Res.*, vol. 123, no. MSMEE, pp. 1127–1135, 2017.

[16] D. Kang and J. W. Lee, “Graphical design of integrated reaction and distillation in dividing wall columns,” *Ind. Eng. Chem. Res.*, vol. 54, no. 12, pp. 3175–3185, 2015.

[17] L. S. Harding and G. Fieg, “Energy minimum design and systematic analysis of the reactive dividing wall column,” *Chem. Eng. Trans.*, vol. 69, pp. 583–588, 2018.

[18] N. Ramírez-corona and A. Jiménez-gutiérrez, “Optimum design of Petlyuk and divided-wall distillation,” *Chem. Eng. Res. Des.*, vol. 88, pp. 1405–1418, 2010.

[19] A. Orjuela, A. Kolah, C. T. Lira, and D. J. Miller, “Mixed Succinic Acid / Acetic Acid Esterification with Ethanol by Reactive Distillation .,” pp. 9209–9220, 2011.

ANNEX B.

Quantum Calculations

Density Functional Theory (DFT) has proved very successful in describing the static electronic structure of molecules of considerable size, including such properties as bonding energies, potential surfaces, geometries, vibrational structure and charge distributions in the past two decades.

In quantum mechanics we learn that all information we can possibly have a bout a given system is contained in the system's wave function, Ψ [1]. Nonrelativistically, this wave function is calculated from Schrödinger's equation:

$$\hat{H}\Psi = E\Psi \qquad \text{(B.1)}$$

The Hamiltonian $\hat{H}$ is the total energy operator for a system and is written as the sum of the kinetic energy $\hat{T}$ of all the components of the system and the internal potential energy $\hat{V}$. Thus for a system of M nuclei and N electrons:

$$\hat{H} = \underbrace{-\frac{\hbar^2}{2}\sum_{\alpha}\frac{\nabla_\alpha^2}{M_\alpha}}_{\hat{T}_n} \underbrace{-\frac{\hbar^2}{2m_e}\sum_{i}\nabla_i^2}_{\hat{T}_e} + \underbrace{\sum_{\alpha>\beta}\frac{e^2 Z_\alpha Z_\beta}{4\pi\epsilon_0 R_{\alpha\beta}}}_{\hat{V}_{nn}} \underbrace{-\sum_{\alpha,i}\frac{e^2 Z_\alpha}{4\pi\epsilon_0 R_{\alpha i}}}_{\hat{V}_{en}} + \underbrace{\sum_{i>j}\frac{e^2}{4\pi\epsilon_0 r_{ij}}}_{\hat{V}_{ee}} \qquad \text{(B.2)}$$

$\hat{T}$ $\hat{V}$

Within the Born-Oppenheimer (B-O) approximation, we assume the nuclei are held fixed while the electrons move really fast around them. (note: $\frac{M_\alpha}{m_e} \approx 1840$.) In this case, nuclear motion and electronic motion are separated. The last two terms can be removed from the total hamiltonian to give the electronic hamiltonian:

$$\hat{H}_e = -\frac{1}{2}\sum_{i}\nabla_i^2 - \sum_{\alpha,i}\frac{Z_\alpha}{R_{i\alpha}} + \sum_{i>j}\frac{1}{r_{ij}} + \sum_{\alpha>\beta}\frac{Z_\alpha Z_\beta}{R_{\alpha\beta}} \qquad \text{(B.3)}$$

We completely define the problem. Solving the electronic Schrödinger equation using this will give the electronic structure of a molecular system at a fixed nuclear geometry.

$$E_e = \frac{\langle \psi_e | \hat{H}_e | \psi_e \rangle}{\langle \psi_e | \psi_e \rangle} \quad \text{(B.4)}$$

The total electronic wave function ψ_e is written as a Slater Determinant of the one electron functions, i.e. molecular orbitals, MO's :

$$\psi_e = \frac{1}{\sqrt{N!}} \begin{vmatrix} \phi_1(1) & \phi_2(1) & \cdots & \phi_N(1) \\ \phi_1(2) & \phi_2(2) & \cdots & \phi_N(2) \\ \cdots & \cdots & \cdots & \cdots \\ \phi_1(N) & \phi_2(N) & \cdots & \phi_N(N) \end{vmatrix} \quad \text{(B.5)}$$

MO's are written as a linear combination of one electron atomic functions or atomic orbitals (AO's):

$$\phi_i = \sum_{\mu=1}^{N} c_{\mu i} \chi_\mu \quad \text{(B.6)}$$

$c_{\mu i}$ and χ_μ are the MO coefficients and atomic basis functions, respectively. Note that increasing N centers lead to a higher quality of wavefunction but higher computational cost too. Ones of the most widely used basis sets are those developed by Dunning and coworkers, cc-pVNZ where N=D,T,Q,5,6,... (D=double, T=triples, etc.). The 'cc-p', stands for 'correlation-consistent polarized' and the 'V' indicates they are valence-only basis sets. They include successively larger shells of polarization (correlating) functions (d, f, g, etc.). More recently these 'correlation-consistent polarized' basis sets have become widely used and are the current state of the art for correlated calculations. Examples of these are:

- cc-pVDZ - Double-zeta
- cc-pVTZ - Triple-zeta
- cc-pVQZ - Quadruple-zeta
- cc-pV5Z - Quintuple-zeta, etc.
- aug-cc-pVDZ, etc. - Augmented versions of the preceding basis sets with added diffuse functions.
- cc-pCVDZ - Double-zeta with core correlation

The electronic Schrödinger equation 4 is intractable. However, many powerful methods for solving Schrödinger's equation have been developed. In chemistry, for example, one often uses methods based on systematic expansion of wave functions in Slater determinants. However, the problem with these methods is the great demand they place on one's computational resources: it is simply impossible to apply them efficiently to large and complex systems. It is here where DFT provides a viable alternative, less accurate perhaps, but much more versatile. In DFT, the ground state energy is expressed in terms of the total electron density ρ:

$$E[\rho] \equiv \frac{\langle \Psi | \hat{H} | \Psi \rangle}{\langle \Psi | \Psi \rangle} \qquad \text{(B.7)}$$

The ground state energy can be obtained variationally, the density that minimizes the total energy is the exact ground state density:

$$E[\rho] > E[\rho_0], \text{ if } \rho \neq \rho_0 \qquad \text{(B.8)}$$

If density is known, then the total energy is:

$$E[\rho] = T[\rho] + V_{ne}[\rho] + J[\rho] + E_{nn} + E_{xc}[\rho] \qquad \text{(B.9)}$$

where,

$$E_{nn}[\rho] = \sum_{A>B} \frac{Z_A Z_B}{R_{AB}}, \qquad \text{(B.10)}$$

$$V_{ne}[\rho] = \int \rho(r) V_{ext}(r) dr, \qquad \text{(B.11)}$$

$$J[\rho] = \frac{1}{2} \int \frac{\rho(r_1)\rho(r_2)}{r_{12}} dr_1 dr_2 \qquad \text{(B.12)}$$

If the density is known, the two unknowns in the energy expression are the kinetic energy functional $T[\rho]$ and the exchange-correlation functional $E_{xc}[\rho]$. To calculate $T[\rho]$, Kohn and Sham introduced the concept of Kohn-Sham orbitals which are eigenvectors of the Kohn-Sham equation

$$\left(-\frac{1}{2}\nabla^2 + v_{eff}(r)\right)\phi_i(r) = \varepsilon_i\phi_i(r) \qquad (B.13)$$

Here, ε_i is the orbital energy of the corresponding Kohn-Sham orbital, ϕ_i, and the density for an "N"-particle system is $\rho(r) = \sum_i^N |\phi_i(r)|^2$. The total energy of a system is:

$$E[\rho] = T_s[\rho] + \int dr v_{ext}(r)\rho(r) + V_H[\rho] + E_{xc}[\rho] \qquad (B.14)$$

T_s is the Kohn-Sham kinetic energy which is expressed in terms of the Kohn-Sham orbitals as :

$$T_s[\rho] = \sum_{i=1}^N \int dr \phi_i^*(r)\left(-\frac{1}{2}\nabla^2\right)\phi_i(r) \qquad (B.15)$$

v_{ext} is the external potential acting on the interacting system (at minimum, for a molecular system, the electron-nuclei interaction), V_H is the Hartree (or Coulomb) energy:

$$V_H = \frac{1}{2}\int dr dr' \frac{\rho(r)\rho(r')}{|r-r'|} \qquad (B.16)$$

and E_{xc} is the exchange-correlation energy.

The Kohn-Sham equations are found by varying the total energy expression with respect to a set of orbitals to yield the Kohn-Sham potential as:

$$v_{eff}(r) = v_{ext}(r) + \int \frac{\rho(r')}{|r-r'|} dr' + \frac{\delta E_{xc}[\rho]}{\delta\rho(r)} \qquad (B.17)$$

$v_{xc}(r) \equiv \frac{\delta E_{xc}[\rho]}{\delta\rho(r)}$ is the exchange-correlation potential.

The exchange-correlation potential, and the corresponding energy expression, are the only unknowns in the Kohn-Sham approach to density functional theory. There are many ways to approximate this functional E_{xc}, generally divided into two separate terms:

$$E_{xc}[\rho] = E_x[\rho] + E_c[\rho] \qquad (B.18)$$

Where the first term is the exchange functional while the second term is the correlation functional. Quite a few research groups have developed the exchange and correlation functionals which are fit to empirical data or data from explicitly correlated methods: PBE0 (PBEPBE), B3LYP, PBE, BP86, M06-2X, B2PLYP, B3PW91, B97-D, M06-L, CAM-B3LYP.

In the present work, all calculations were performed using Gaussian 03 program package [2]. The geometry of each compound was optimized using DFT method with B3LYP functional without any constraints (energy cut-off of 10–5 kJ mol^{-1}, final RMS energy gradient under 0.01 kJ mol^{-1} $Å^{-1}$). The calculations were performed in cc-pVTZ basis set. For the species having more conformers, all conformers were investigated. The conformer with the lowest electronic energy was used in this work.

In the case of DFT method, which does not provide enthalpies directly [3, 4], the total enthalpies of the species X, H(X), at temperature T are usually estimated from the expression:

$$\mathrm{H(X)} = \mathrm{E_0} + \mathrm{ZPE} + \Delta\mathrm{H_{trans}} + \Delta\mathrm{H_{rot}} + \Delta\mathrm{H_{vib}} + \mathrm{RT} \qquad \text{(B.19)}$$

where E_0 is the calculated total electronic energy of the molecular system under study. ZPE stands for zero-point energy resulting from the vibrational motion of molecular systems even at 0 K, this energy is calculated for a harmonic oscillator model as a sum of contributions from all i vibrational modes of the system:

$$\mathrm{ZPE} = \sum_{\mathrm{i}} 0.5\mathrm{hc}\tilde{\nu}_{\mathrm{i}} \qquad \text{(B.20)}$$

ΔH_{trans}, ΔH_{rot}, and ΔH_{vib} are the translational, rotational and vibrational contributions to the enthalpy. Finally, RT represents PV-work term and is added to convert the energy to enthalpy. The translational energy of an ideal gas at temperature T is given (in molar quantities) as:

$$\Delta\mathrm{H_{trans}} = \frac{3}{2}\mathrm{RT} \qquad \text{(B.21)}$$

As the spacing of rotational energy levels is much narrower than that of vibrational energy levels, an approximate formula for the contribution of rotational energy levels to the internal energy is:

$$\Delta H_{rot} = RT \qquad (B.22)$$

The last two formulas implies that at 0 K there is no contribution to the internal energy from translational and rotational motion, but that these energies increases linearly with increasing absolute temperature.

By far the largest contribution to the internal energy at room temperature stems from vibrational degrees of freedom which can be calculated according to:

$$\Delta H_{vib} = K_B \sum_i \Theta_i \left(\frac{1}{2} + \frac{1}{\exp\frac{\Theta_i}{T} - 1}\right) \qquad (B.23)$$

where Θ_i is the vibrational temperature:

$$\Theta_i = \frac{hc\tilde{\nu}_i}{K_B} \qquad (B.24)$$

A detailed account of how above thermochemical values are calculated in Gaussian 03 can be found in ref [5].

References

[1] Michael Springborg (1997). *Density-Functional Methods in Chemistry and Materials Science*, John Wiley & Sons.

[2] Frisch MJ, Trucks GW, Schlegel HB, Scuseria GE, Robb MA, Cheeseman JR, Montgomery JA, Jr., Vreven T, Kudin KN, Burant JC, Millam JM, Iyengar SS, Tomasi J, Barone, B. Mennucci, M. Cossi, G. Scalmani, N. Rega, G.A. Petersson, H. Nakatsuji, M. Hada V, Ehara M, Toyota K, Fukuda R, Hasegawa J, Ishida M, Nakajima T, Honda Y, Kitao O, Nakai H, Klene M, Li X, Knox JE, Hratchian HP, Cross JB, Adamo C, Jaramillo J, Gomperts R, Stratmann RE, Yazyev O, Austin AJ, Cammi R, Pomelli C, Ochterski JW,

Ayala PY, Morokuma K, Voth GA, Salvador P, Dannenberg JJ, Zakrzewski VG, Dapprich S, Daniels AD, Strain M-C, Farkas O, Malick DK, Rabuck AD, Raghavachari K, Foresman JB, Ortiz JV, Cui Q, Baboul AG, Clifford S, Cioslowski J, Stefanov BB, Liu G, Liashenko A, Piskorz P, Komaromi I, Martin RL, Fox DJ, Keith T, Al-Laham MA, Peng CY, Nanayakkara A, Challacombe M, Gill PMW, Johnson B, Chen W, Wong MW, Gonzalez C, Pople JA (2003) GAUSSIAN 03, Revision A.1, Gaussian, Inc., Pittsburgh;

[3] McQuarrie, D. A., & Simon, J. D. (1999). *Molecular thermodynamics*. Sausalito (California: University Science Books).

[4] Atkins PW (1998) *Physical Chemistry, 6th ed*. Oxford University Press, Oxford.

[5] Ochterski, J. W. (2000). *Thermochemistry in gaussian*. *Gaussian Inc*

ANNEX C
Brief review of thermodynamic definitions

In process engineering, thermodynamics is an essential part to understand the modifications a system undergoes due to heating, compression, expansion, mixing, separation or chemical reactions. It is important to understand the changes that can occur in multi-component mixtures due to variations in temperature, pressure and composition.

In general, phase equilibrium, physical and thermodynamic properties of both pure fluids and mixtures are ultimately governed by intermolecular forces. The greater the intermolecular forces, the more the behavior of the mixture moves away from the ideal, making it more difficult to model.

These deviations from ideality have been studied from the first and second principles of thermodynamics, where they are determined from relationships of the fundamental properties of thermodynamics such as temperature, pressure, volume and entropy, Gibbs energy in any closed or open system. The partial derivative of this last system with respect to the number of moles of species i, at constant conditions of T, P and the number of moles of the rest of species n_j, allow the definition of chemical potential of species i in the mixture:

$$\mu_i \equiv \left[\frac{\partial(nG)}{\partial n_i}\right]_{T,P,n_j} \tag{C.1}$$

In terms of the fundamental properties this expression can be written as:

$$d(nG) = (nV)dp - (nS)dT + \sum_i \mu_i dn_i \tag{C.2}$$

Equation 3.2 represents the fundamental expression of dissolution thermodynamics which relates the fundamental properties of single-phase multicomponent fluid systems of constant or variable mass and composition.

Applying the concept of chemical potential to a closed system with two phases in equilibrium, it can be considered that each of the phases is like an open system that exchanges matter with the other phase. Using equation 3.2 to each of the phases, and considering that the equilibrium P and T are uniform throughout the system, the conclusion is reached:

$$\mu_i^{\alpha} = \mu_i^{\beta} = \cdots = \mu_i^{\pi} \ (i = 1, 2, 3, \ldots, N) \tag{C.3}$$

The expression 3.3 indicates that the condition for the equilibrium between the phases of N components is that the chemical potential of each component is equal.

The complexity and nature of the mixture determines the thermodynamic models to be performed for the study of each system. The systems of less complexity or homogeneous mixtures can be represented from the models of ideal gas, ideal dissolution and Raoult's Law. These are simple mathematically and serve to represent with precision the behavior in the real systems. They basically consider that an ideal solution is a mixture model that results from assuming that the molecules of the different components are of the same size, and that the forces between the molecules (of the same component or of different components) are also equal. With this definition the ideal gas model is a particular case of ideal dissolution, in which volumes and intermolecular forces are zero.

More complex systems or heterogeneous mixtures cannot be represented in the same way. These systems have deviations from the ideality, which are often of great magnitude and do not allow the ideal model to be used for design and control purposes. Indeed, by introducing two auxiliary thermodynamic properties related to Gibbs' energy: fugacity coefficient and activity coefficient, it is possible to transform the ideal models and Raoult's Law into a general expression suitable for the treatment of liquid-vapor equilibrium of non-ideal real systems. These deviations are expressed from residual and excess properties. The residual properties are defined from the difference of the real value that possesses an extensive thermodynamic property of any of the mixture and the value that it would have if the fluid were an ideal gas at the same pressure, temperature and composition.

$$M^R = M - M^{ig} \tag{C.4}$$

and similarly for partial molar properties:

$$\overline{M^R} = \bar{M} - \overline{M^{ig}} \tag{C.5}$$

On the other hand, the excess properties are defined as the difference between the real value that possesses an extensive thermodynamic property of any of the mixture and the calculated value that would have an ideal dissolution at the same pressure, temperature and composition.[18].

$$M^E = M - M^{id} \tag{C.6}$$

and similarly for partial molar properties:

$$\overline{M^E} = \bar{M} - \overline{M^{id}} \tag{C.7}$$

Thermodynamically, it has been shown that the deviation of the ideal behavior of the liquid phase can be measured from the excess properties applied to the Gibbs function:

$$G^E = G - G^{id} \tag{C.8}$$

Multiplying this equation by the number of moles, n, and differentiating with respect to n_i, keeping T, P and n_j constant, the partial excess Gibbs energy is obtained:

$$\overline{G_i^E} = \bar{G}_i - \overline{G_i^{id}} \tag{C.9}$$

The partial molar Gibbs energy of the component i in a mixture, at constant temperature and pressure, can be represented in terms of fugacity from a pure state to the condition of dissolution to an arbitrary molar fraction x_i:

$$\bar{G}_i - G_i = RTln\frac{\hat{f}_i}{f_i} \tag{C.10}$$

On the other hand, the Gibbs energy of an ideal dilution can be calculated from the definition of chemical potential of the component i:

$$\bar{G}_i^{id} = \mu_i^{id} = G_i + RTlnx_i \tag{C.11}$$

From the difference of equations 3.10 and 3.11 the partial excess Gibbs energy of component i can be determined:

$$\bar{G}_i^E = RT\ln\frac{\hat{f}_i}{x_i f_i} \tag{C.12}$$

This expression gives rise to two new properties: the activity of the component i in the solution, a_i and the activity coefficient of the substance i in the solution, γ_i:

$$\hat{a}_i = \frac{\hat{f}_i}{f_i} \tag{C.13}$$

$$\gamma_i = \frac{\hat{a}_i}{x_i} = \frac{\hat{f}_i}{x_i f_i} \tag{C.14}$$

The function of Gibbs energy molar partial excess of component i at dissolution can be written as:

$$\bar{G}_i^E = RT\ln\gamma_i \tag{C.15}$$

The energy of Gibbs molar from the mixture as:

$$G^E = RT\ \sum_i x_i\, ln\gamma_i \tag{C.16}$$

In this way, also it is possible to obtain:

$$\frac{G^E}{RT} = \sum_i x_i\, ln\gamma_i \tag{3.17}$$

$$\sum_i x_i\, ln\gamma_i = 0$$

And finally the expression:

$$ln\,\gamma_i = \left[\frac{\partial(\frac{nG^E}{RT})}{\partial n_i}\right]_{P,T,n_j} \quad \text{(C.18)}$$

These expressions make it possible to relate the experimental data obtained from the vapor-liquid equilibrium with the activity coefficients that will be calculated later.

The expressions presented in the upper part allow to define the concept of equilibrium as the condition in which there are no changes in the macroscopic properties of a system with time. However, at the microscopic level, molecules that are in a phase at a given time can pass from one phase to another, provided that the flow of molecules is the same in both directions and there is no net transfer of matter between the phases.

With the expressions presented the equilibrium can be defined in terms of chemical potential or with the expression deduced for fugacity:

$$\mu_i^{\alpha} = \mu_i^{\beta} = \cdots = \mu_i^{\pi}\ (i = 1, 2, 3, \ldots, N)$$

$$\hat{f}_i^{\alpha} = \hat{f}_i^{\beta} = \cdots = \hat{f}_i^{\pi}\ (i = 1, 2, 3, \ldots, N)$$

Thus, for the specific case of vapor-liquid equilibrium of multicomponent systems, the equality of the fugacities remains of the form:

$$\hat{f}_i^{l} = \hat{f}_i^{v} \quad (i = 1, 2, 3, \ldots, N)$$

The choice of thermodynamic models for determining the fugacity and activity coefficients depends on the compounds and the pressure and temperature range of the process. For this, one can choose between equations of state, to model the vapor phase and models of activity coefficients, to model the liquid phase, or in its defect, the combination of the two.

The modeling of pure fluids and mixtures of non-polar molecules, such as hydrocarbons, is relatively easy to model as it is considered that only the physical forces of attraction and repulsion between molecules influence. The equations of state, the expansion of Redlich and Kister (1948) and the models of Margules (1895), van Laar (1910) and Wohl (1953), are functions that are commonly expressed as algebraic expressions of the molar fractions with arbitrary coefficients obtained by adjusting experimental data. Such expressions have as many terms and parameters as necessary to achieve appropriate representations of reality. The limitation of such models is that they can be successfully applied to binary systems, but they can be less accurate for multicomponent systems.

In the case of polar molecules such as organic acids, alcohols, bases and water, the presence of hydrogen bonds can lead to non-ideal behaviors such as vapor phase dimerization, azeotropes, phase separation. To model systems with these characteristics, a method of activity coefficient for liquid phase and special equations of state for vapor phase is usually chosen.

For the most part, the existing methods for the determination of activity coefficients consider the definition of local composition, where the interaction of molecule i with its environment or proximity is taken into account, also called interaction cell, the molecular orientations are not completely random since they depend on the differences between the size of the compounds and the intermolecular forces between them.

The energy of interaction between molecules i and j can be denoted as g_{ij}. Taking into account that x_{ij} represents the local molar fraction of molecule i in the cell centered on molecule j, for a binary system the requirements of equations 3.19 and 3.20 must be met in each cell:

$$x_{21} + x_{11} = 1 \tag{C.19}$$

$$x_{12} + x_{22} = 1 \tag{C.20}$$

Within the existing methods for the determination of the activity coefficients that consider the definition of local composition, we found Wilson's method (1964) who showed that Gibbs' energy in excess could be conveniently expressed through an algebraic function of the local composition and developed the equation that bears his name, using local volumetric fractions for the adjustment of two parameters. This equation is useful for dissolutions of polar or associated components (*e.g.*, alcohols) dissolved in non-polar solvents, mainly miscible mixtures. Orye and Prausnitz (1965) validated Wilson's equation by corroborating its usefulness for representing the equilibrium data of a wide variety of liquid mixtures. However, this model is not able to predict immiscibility and cannot represent maximums and minimums in the activity coefficients versus composition. Therefore, it is not applicable in immiscibility case.

Other models that use local compositions are Renon's NRTL (1968), Abrams' UNIQUAC (Universal Quasichemical) and Prausnitz (1975), the Heil equation that modifies the Wilson equation to represent equilibrium in polymeric solutions and UNIFAC, developed by Fredenslund, Jones and Prausnitz (1975), which calculates the activity coefficients from the contributions of the functional groups that are part of the molecules in solution, assuming, as Smith, Van Ness and Abbott (2001) say: "a liquid mixture can be considered as a solution of the structural units from which molecules are formed, rather than a solution of the molecules themselves" [7].

According to the properties of the molecules involved in the esterification reaction between glycolic acid and butanol, the reference reaction system, the models presented in detail are the following:

NRTL model

The NRTL (Non-Random-Two-Liquid) model was proposed by Renon and Prausnitz in 1968 and is an extension of the Wilson equation. It is applicable for the correlation of multicomponent systems in liquid-liquid, liquid-vapor and liquid-liquid-vapor equilibrium.

This model considers the Gibbs energy of excess for a liquid mixture as:

$$\frac{G^E}{RT} = \sum_i x_i \frac{\sum_j \tau_{ji} G_{ji} x_j}{\sum_k G_{ki} x_k} \tag{C.21}$$

Where $G_{ji} = \exp(-\alpha_{ji}\tau_{ji})$ and $\tau_{ji} = a_{ji} + \frac{b_{ji}}{T}$.

The new parameter included in the model is α, α_{ji} and α_{ij} are equivalent, dimensionless and represents the non-randomness of the mixture. The parameter is chosen considering the polarity, the miscibility and the degree of association of the components that make up the mixture. The values that can be taken range from 0.2 to 0.47 [7].

The expression of the activity coefficients for the general case of a multicomponent system is,

$$\ln \gamma_i = \frac{\sum_{j=1}^{N} \tau_{ji} G_{ji} x_j}{\sum_{k=1}^{N} G_{ki} x_k} + \sum_{j=1}^{N} \frac{x_j G_{ij}}{\sum_{k=1}^{N} x_k G_{kj}} \left(\tau_{ij} - \frac{\sum_{m=1}^{N} \tau_{mj} G_{mj} x_m}{\sum_{k=1}^{N} G_{kj} x_k} \right) \tag{C.22}$$

The G^E expression for the case of a binary system provides the following equation,

$$\frac{G^E}{RT} = x_1 x_2 \left[\frac{\tau_{21} G_{21}}{x_1 + x_2 G_{21}} + \frac{\tau_{12} G_{12}}{x_1 G_{12} + x_2} \right] \tag{C.23}$$

which, by differentiation, provides the expressions that make it possible to obtain the activity coefficients,

$$\ln \gamma_1 = x_2^2 \left[\tau_{21} \left(\frac{G_{21}}{x_1 + x_2 G_{21}} \right)^2 + \frac{\tau_{12} G_{12}}{(x_1 G_{12} + x_2)^2} \right]$$

$$\ln \gamma_2 = x_1^2 \left[\tau_{12} \left(\frac{G_{12}}{x_2 + x_1 G_{12}} \right)^2 + \frac{\tau_{21} G_{21}}{(x_2 G_{21} + x_1)^2} \right] \tag{C.24}$$

For modeling systems with more than two components, it is only necessary to know the binary parameters of each of the pairs present.

Its main disadvantage with respect to the Wilson and UNIQUAC models (which will be described below) is that it is an equation with three parameters and not two like the ones mentioned above.

UNIQUAC model

Abrams and Prausnitz in 1975 adopted the two liquid model and the local composition concept to develop the UNIQUAC (UNIversal QUAsi-Chemical) semitheoretical equation. This model states that the excess Gibbs free energy can be divided into two contributions: one that takes into account differences in the size and shape of molecules (combinatorial part) and a second in which energy interactions between them are considered (residual part).

The expression they propose for the Gibbs function of generalized excess for multicomponent systems takes the form:

$$\frac{G^E}{RT} = \sum_i x_i ln \frac{\varphi_i}{x_i} + \frac{z}{2}\sum_i q_i x_i ln \frac{\vartheta_i}{\varphi_i} - \sum_i q_i x_i \ln\left(\sum_j \vartheta_j \tau_{ji}\right) \quad \text{(C.25)}$$

Where $\vartheta_i = \frac{q_i x_i}{\sum_j q_j x_j}$ represents the surface fraction of the component i

$\varphi_i = \frac{r_i x_i}{\sum_j r_j x_j}$ the volume fraction of the component i

And $z = 10$ is the coordination number

Adjustable τ_{ji} parameters are expressed as:

$$\tau_{ji} = exp\left[-\frac{(u_{ji}-u_{ii})}{RT}\right] \quad \text{or} \quad \ln \tau_{ji} = a_{ij} + \frac{b_{ij}}{T} \quad \text{(C.26)}$$

Where u_{ji} is an interaction parameter between the j-i components. $(u_{ji} = u_{ij})$.

The r_i and q_i parameters of the pure components are respectively measured from the molecular volumes of Van der Waals and areas of the molecular surface. These parameters are calculated as the sum of the contributions of the functional groups forming the compound molecule.

$$r_i = \sum_k v_k^{(i)} R_k; \quad q_i = \sum_k v_k^{(i)} Q_k \quad \text{(C.27)}$$

Where $v_k^{(i)}$ is the number of type k groups in molecule i.

The activity coefficients for multicomponent systems are expressed taking into account the combinatorial part and the residual part:

$$ln\gamma_i = ln\gamma_i^C + \ln \gamma_i^R \quad \text{(C.28)}$$

In the particular case of binary systems the expression $\frac{G^E}{RT}$ is developed as follows,

$$\frac{G^E}{RT} = x_1\left[ln\frac{\varphi_1}{x_1} + \frac{q_1 z}{2}\ln\frac{\vartheta_1}{\varphi_1} - q_1\ln(\vartheta_1 + \vartheta_2\tau_{21})\right] + x_2\left[ln\frac{\varphi_2}{x_2} + \frac{q_2 z}{2}\ln\frac{\vartheta_2}{\varphi_2} - q_2\ln(\vartheta_1\tau_{12} + \vartheta_2)\right] \quad \text{(C.29)}$$

One of the main advantages of this model is the possibility of applying it to multicomponent systems starting from the binary parameter fairness, its capacity to describe the liquid-liquid equilibrium and the possibility of extending the results obtained taking into account the dependence with the temperature for a moderate interval of this parameter. Another important aspect of the model is that it serves as a basis for the development of the UNIFAC predictive method, the model consists in the calculation of the activity coefficients by means of the contributions of the different groups that constitute the molecules in a solution. Its main disadvantage is the complexity of its expression as well as the limitation it presents in the representation of the data, and the deviation of the results in comparison with the data obtained experimentally.

ANNEX D

The determination of the binary parameters of the NRTL model

```
clear
global a b c nc T gamma
nc = 4;
T =343.15;
x =[0.535150413 0.042538273 0.211155657 0.211155657];

% les paramètres d'interaction binaire sont à entrer dans les matrices a, b
% et c
% ordre des constituants 1. butanol / 2. acide glycolique / 3. ester / 4.
%water

a=[0 0 -18.2254 -2.0405; 0 0 0 0; 8.56337 0 0 -2.64357937; 13.1102 0
1.79258459 0];%BUTANOL
b=[0 554.8973 8273.01 763.869; 57.337   0 -181.3178 536.8455; -3848.5
1317.198    0   1013.13199; -3338.95 -298.0107  563.40161   0];%BUTANOL
c=[0 0.3 0.3 0.3  ; 0.3 0 0.3 0.3 ;0.3 0.3 0 0.2 ; 0.3 0.3 0.2 0 ];%BUTANOL

tau = a+b/T;
G  = exp(-c .* tau);


  for i=1:nc
    st(i)=sum( x(:) .* tau(:,i) .* G(:,i)); % x vecteur colonne des 4
concentrations
    s(i) =sum( x(:) .* G(:,i));
  end

S = st ./ s;

for i=1:nc
  g (i,:)=x(:)' .* G(i,:)./s;
end


for i=1:nc
  lng(i)=S(i)+sum(g(i,:).*(tau(i,:)-S));

end

gamma= exp(lng(:,i) );
```

ANNEX E

Experimental data of the VLE BG+BuOH.

Table E-1. T-x-y data for the system BG + BuOH at 1013.25 mbar.

T [°C]	x_{BuOH}	y_{BuOH}
189.39	0	0
178.49	0.049	0.317
169.34	0.094	0.536
155.69	0.160	0.733
151.79	0.204	0.761
147.54	0.222	0.800
136.24	0.435	0.902
135.04	0.491	0.901
133.58	0.483	0.918
132.37	0.470	0.909
127.09	0.598	0.948
125.76	0.679	0.957
125.27	0.661	0.961
124.36	0.716	0.963
123.39	0.717	0.954
121.69	0.718	0.966
121.62	0.765	0.969
120.75	0.830	0.979
119.21	0.879	0.980
117.02	1	1

Table E-2. T-x-y data for the system BuOH + BG at 700 mbar.

T [°C]	x_{BuOH}	y_{BuOH}
175.85	0	0
164.42	0.054	0.357
162.71	0.057	0.382
153.93	0.106	0.555
145.86	0.151	0.693
137.09	0.210	0.811
130.01	0.277	0.844
122.23	0.369	0.901
120.04	0.495	0.929
119.44	0.490	0.926
117.34	0.482	0.930
114.5	0.568	0.943
114.13	0.559	0.945
112.52	0.611	0.957
111.76	0.674	0.962
111.53	0.640	0.964
108.9	0.775	0.974
108.64	0.785	0.972
107.2	1	1

Table E-3. T-x-y data for the system BuOH + BG at 300 mbar.

T [°C]	x_{BuOH}	y_{BuOH}
147	0	0
140.52	0.024	0.268
137.7	0.047	0.346
120.27	0.139	0.673
108.24	0.258	0.857
104.09	0.338	0.886
101.55	0.395	0.911
99.33	0.470	0.936
97.27	0.501	0.941
95.44	0.540	0.942
95.16	0.569	0.947
90.65	0.648	0.961
91.72	0.7046	0.966
91.07	0.730	0.967
86.69	1	1

ANNEX F

The determination of the binary parameters of the NRTL model for SLE system.

```
clear all
close all

global t x y gamma_exp c V tau1 tau2 G1 G2 gamma_mod

multi ='C:\Users\JulianaAdmin\Desktop\SLE THERMO\Multi SLE.xlsx' ; %données du
multistart (modifier le chemin)

multistart=xlsread(multi,'Feuil1','A1:D300'); %(modifier la taille de la
matrice récupérer)

for j=1:1 %(nombre de vecteur initiaux à fixer)


% for j=1:70 %(nombre de vecteur initiaux à fixer)
%
%
% VV=multistart(j,1:4);
% V0=VV';

V0 = [0 1 0 1];

%minimisation des écarts
%GraphFlag=0 ;
lb=[0 -100000 0 -100000]';
ub=[0 100000 0 100000]';
options = optimoptions('lsqnonlin','Display','iter','FunctionTolerance',1e-
45,'StepTolerance',1e-45,'MaxIterations',4000,'MaxFunctionEvaluations',10000);
ecartHandle=@(V) toto(V);
%ecartHandle=@(V)activity(V,GraphFlag);
[V,resnorm,residual,exitflag,output,lambda,jacobian] =
lsqnonlin(ecartHandle,V0,lb,ub,options);

% end

end

V_optim = V ;

 hold on
plot(x,gamma_exp,'o')
plot(x,gamma_mod,'o')
hold off


unction ecart=toto(V)

global t x gamma_exp gamma_mod c y
```

```
ecart=[];

t=[303.15   306.15  309.15  316.15  321.15];
x=[0.282289894  0.298921123 0.306929622 0.3385257   0.379685065];
x=x';
y=[1-x];

dh=14923;
tf=353.15;
r=8.314;
cpl=@(t) -0.2122*t+302.01;
cps=@(t) 0.3251*t+26.615;
cpd=@(t)-0.5373*t+275.395;
cpdsurt=@(t) -0.5373+275.395./t;
m=dh/r;
n=[];
p=[];
% calcul des coefficients d'activité à partir des données expérimentales
for i=1:length(t)
ini =t(i)    ;
int1=integral((cpd),ini,tf);
int2=integral((cpdsurt),ini,tf);
n=[n ; int1];
p=[p ; int2];
end

o=log(x);
q=(m*(1/tf-(1./t))+(1./(r*t)).*n')-(1/r)*p'-o';
gamma_exp=exp(q');

%calcul à partir du modèle NRTL du coefficient d'activité du dans ?
%initialisation des paramètres d'intéraction :
c=0.3;

%V=[1;1;1;1];

gamma_mod=[];

for i=1:length(t)
tau1(i) = V(1)+V(2)/t(i);
tau2(i) = V(3)+V(4)/t(i);
G1(i)=exp(-c*tau1(i));
G2(i)=exp(-c*tau2(i));
calcul=exp(y(i)^2*(((tau2(i)*(G2(i)/(x(i)+y(i)*G2(i)))^2))+((tau1(i)*G1(i))/(y
(i)+x(i)*G1(i))^2)));
gamma_mod=[gamma_mod ; calcul];
end

ecart=[ecart; (gamma_mod-gamma_exp).^2];

end
```

ANNEX G

I. Identification and purity determination of propyl glycolate.

GC

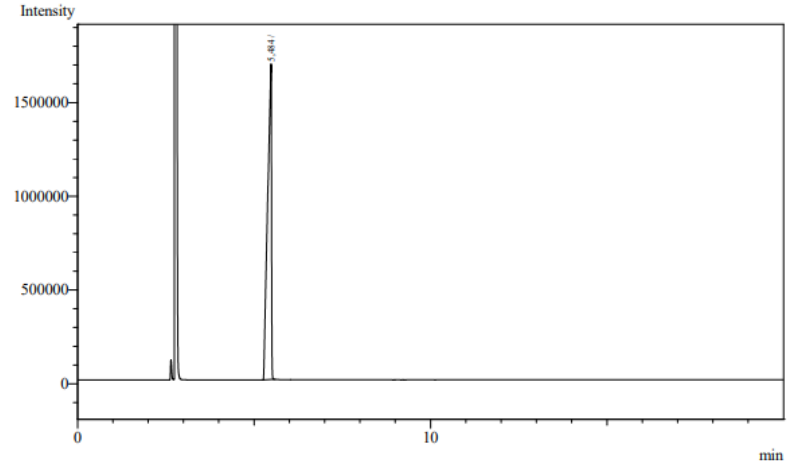

Peak#	Ret.Time	Area	Area%	Height	Height%
1	5,484	12497116	100,0000	1683703	100,0000
Total		12497116	100,0000	1683703	100,0000

GCMS

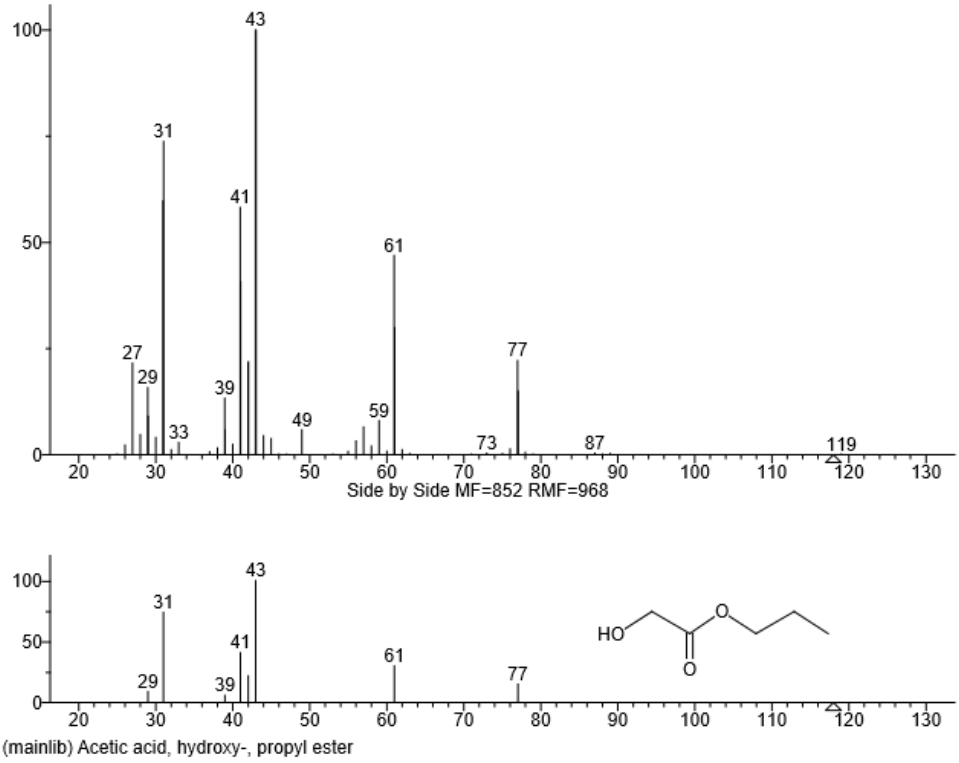

II. Identification and purity determination of octyl glycolate.

GC

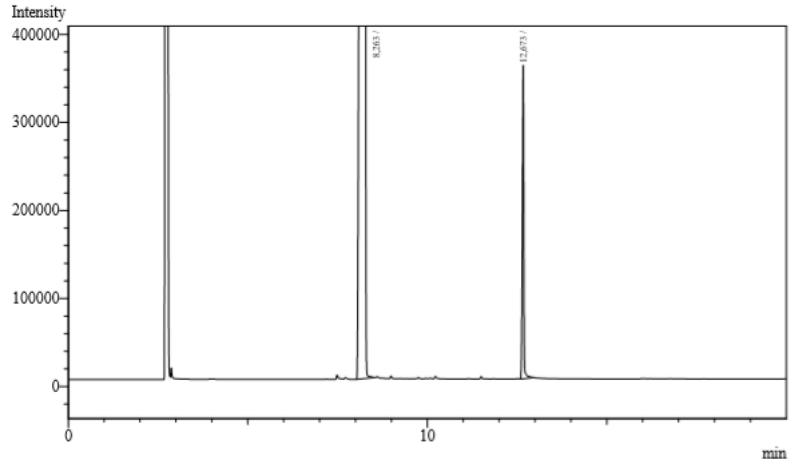

Peak#	Ret.Time	Area	Area%	Height	Height%
1	8,263	18829320	95,0748	2605004	87,9768
2	12,673	975423	4,9252	356009	12,0232
Total		19804743	100,0000	2961013	100,0000

GCMS

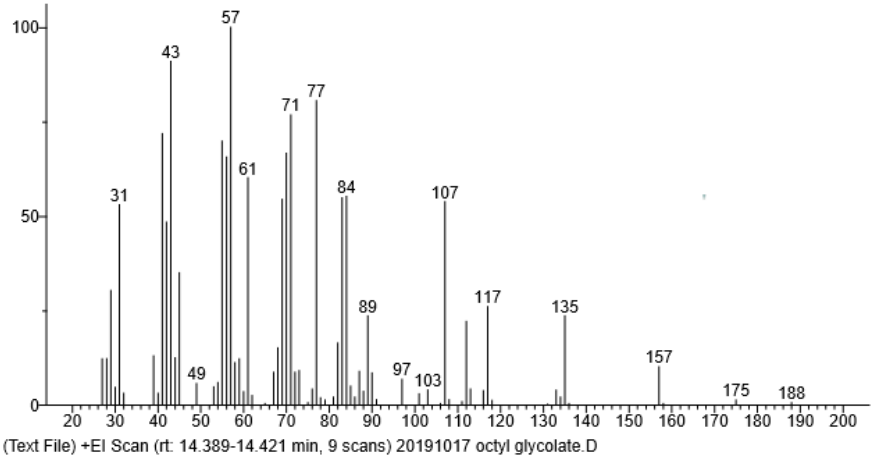

ANNEX H

Kinetic model code

```
clear all
close all
%--
% programme développé dans le cadre de du projet PIVERT Ester&Cat2
% dernier update : 2 avril 2019
% écrit par Clémence NIKITINE
% Ce programme permet d'optimiser les paramètre cinétique d'une réaction
% d'estérification, il demande en entrée : composition du mélange (molaire) en
% fonction du temps, la température
% la loi de vitesse est exprimée en activité (à entrée dans la fonction
EvalFun) et le modèle thermo utilisé
% pour calculer les activités est NRTL. Les cofficients d'interaction
% binaires doivent être entrée dans la fonction "NRTL"


global tspan t  activite_exp w_cata C ntot a  Nexp  T keq


% ordre des constituants 1. butanol / 2. acide glycolique / 3. ester / 4.
%water

%-- récupération des données expérimentales
name = 'C:\Users\JulianaAdmin\Desktop\TEST KINEC -2\Donne Matlab2.xlsx'; % nom
du fichier d'import / modifier le chemin
data = xlsread(name,'GA B Cat hete','A1:M200'); %àmodifier dès qu'on ajoute
une expérience ou si tu changes de feuille de sélection
ExpData=struct;
Nexp = max(data(:,1)) ; % nombre d'expériences à modifier selon le nombre de
cata testé
%--
%
 for i=1:Nexp
    ExpData(i).ChemName=[{'Butanol'} {'Acide Glycolique'} {'ester'} {'H2O'} ];
    j = find(isnan(data(5*i,:)));
    ExpData(i).t=data(5*i,3:j(2)-1);
    l = find(isnan(data(5*i+1,:)));
    ExpData(i).Conc = data(5*i+1:5*i+4,3:l(3)-1).';
    ExpData(i).w_cata=data(5*i+1,13);
    ExpData(i).T=data(5*i+1,12);
 end

% multi ='C:\Users\JulianaAdmin\Desktop\TEST KINEC -2\Multi KINETIC.xlsx' ;
%données du multistart (modifier le chemin)
%
% multistart=xlsread(multi,'Feuil1','A1:C50'); %(modifier la taille de la
matrice récupérer)

% for j=1:50 %(nombre de vecteur initiaux à fixer)
%
% kk=multistart(j,1:3);
```

```
% k0=kk';

% initialisation des paramètres cinétiques

k0=[20 60000]; % le nombre de paramètres à ajuster est fonction du modèle
cinétique utilisé
lb=[0 0]'; % la longueur des vecteur lb et ub doit être ajustée au nombre de
paramètres à ajuster
ub=[1000 100000]; % le nombre de paramètres à ajuster est fonction du modèle
cinétique utilisé

% k0=[20 60000 0.1 0.1 0.1 0.1]; % le nombre de paramètres à ajuster est
fonction du modèle cinétique utilisé
% lb=[0 0 0 0 0 0]'; % la longueur des vecteur lb et ub doit être ajustée au
nombre de paramètres à ajuster
% ub=[1000 100000 100 100 100 100]; % le nombre de paramètres à ajuster est
fonction du modèle cinétique utilisé

% k0=[20 60000 0.1 0.1]; % le nombre de paramètres à ajuster est fonction du
modèle cinétique utilisé
% lb=[0 0 0 0]'; % la longueur des vecteur lb et ub doit être ajustée au
nombre de paramètres à ajuster
% ub=[10000 100000 100 100]; % le nombre de paramètres à ajuster est fonction
du modèle cinétique utilisé

% k0=[20 60000 0.1 0.1 0.1 0.1]; % le nombre de paramètres à ajuster
estfonction du modèle cinétique utilisé
% lb=[0 0 0 0 0 0]'; % la longueur des vecteur lb et ub doit être ajustée au
nombre de paramètres à ajuster
% ub=[1000 100000 10000 10000 10000 10000]; % le nombre de paramètres à
ajuster est fonction du modèle cinétique utilisé

% k0=[20 60000 0.1]; % le nombre de paramètres à ajuster est fonction du
modèle cinétique utilisé
% lb=[0 0 0]'; % la longueur des vecteur lb et ub doit être ajustée au nombre
de paramètres à ajuster
% ub=[1000 100000 1000]; % le nombre de paramètres à ajuster est fonction du
modèle cinétique utilisé

%--

%option de l'optimiseur
options = optimoptions('lsqnonlin','Display','iter','FunctionTolerance',1e-
45,'StepTolerance',1e-45,'MaxIterations',4000,'MaxFunctionEvaluations',1000);

%optimisation
GraphFlag=0 ;
ObjFunHandle=@(k) ObjFun(k, ExpData,GraphFlag);
[k,resnorm,residual,exitflag,output,lambda,jacobian] =
lsqnonlin(ObjFunHandle,k0,lb,ub,options);


% end

%tracé des courbes
```

```
GraphFlag=1 ;
k_optim =k;%[13911815.2276487 44227.1546536450]
x0=C(1,:);
EvalFunHandle=@(t,x) ObjFun(k, ExpData, GraphFlag) ;
[F] = ObjFun(k_optim,ExpData,GraphFlag);


k_moins=k_optim(1)/k_optim(2)

% statistique
%calcul de la covariance / matrice de corrélation
J = jacobian;
covariance = full((J'*J)^(-1)) ;
corr=corrcov1(covariance)


Npar = 2; % nombre de parametres
J = full(jacobian);
varE   = resnorm/((5*3*Nexp)-Npar);       % error variance (from lsqnonlin) =
e'*e
stdE   = sqrt(varE) ;                % error std deviation
covP   = varE * [J.'*J]^(-1) ;       % parameter covariance matrix
covP = full(covP) ;
sigmaP = sqrt(diag(covP))       ;    % parameter stddev (approximate, linear)
corP   = covP ./ (sigmaP * sigmaP') ;% parameter correlation matrix

% %figure
% hold on
% z=[0 5];
% plot(z,z)
% plot(x,C,'o')
% hold off
%


function gam=NRTL(x,T);

global a b c nc
nc = 4;

% les paramètres d'interaction binaire sont à entrer dans les matrices a, b
% et c
% ordre des constituants 1. butanol / 2. acide glycolique / 3. ester / 4.
%water

% a=[0  -2.75314    30.7972 -1.7411;    1.95074 0   0   0;  4.92442 0   0
0.232903;   5.4486  0   -0.22445    0];%GLYCOLIC ACID PROPANOL
% b=[0  -192.6053   -10000  576.446;    1015.08 0   -90.3513    536.8455;   -
2463.23    693.907 0   -62.5368;   -861.1792   -298.0107   59.842
0];%GLYCOLIC ACID PROPANOL
% c=[0 0.3 0.3 0.3  ; 0.3 0 0.3 0.3 ;0.3 0.3 0 0.3 ; 0.3 0.3 0.3 0 ];%GLYCOLIC
ACID PROPANOL

% a=[0 0 -18.2254 -2.0405; 0 0 0 0; 8.56337 0 0 -2.64357937; 13.1102 0
1.79258459   0];%GLYCOLIC ACID BUTANOL
```

```
% b=[0 554.8973 8273.01 763.869; 57.337 0 -181.3178 536.8455; -3848.5
1317.198    0   1013.13199; -3338.95 -298.0107  563.40161   0];%GLYCOLIC ACID
BUTANOL
% c=[0 0.3 0.3 0.3  ; 0.3 0 0.3 0.3 ;0.3 0.3 0 0.2 ; 0.3 0.3 0.2 0 ];%GLYCOLIC
ACID BUTANOL

a=[0    0   -3.79301    -1.4468;    0   0   0   0;  3.20031 0   0   -0.896863;
5.9173  0   -1.44187    0]; %GLYCOLIC ACID OCTANOL
b=[0    660.5762    1385.68 741.9184;   -6.461  0   1036.3  536.8455;   -
835.782    -158.6741   0   55.3328;    798.3772    -298.0107   2532.02 0];
%GLYCOLIC ACID OCTANOL
c=[0 0.3 0.3 0.26  ; 0.3 0 0.3 0.3 ;0.3 0.3 0 0.2 ; 0.26 0.3 0.2 0 ];
%GLYCOLIC ACID OCTANOL

% a=[0  0   0   -1.7411;    0   0   0   0;  0   0   0   13.5628;    5.4486  0
-24.628 0];%FORMIC ACID PROPANOL
% b=[0  55.5879 59.5237 576.446;    19.9785 0   -658.942    -51.0942;
348.479 563.587 0   -4387.12;   -861.179    -74.0973    10000   0];%FORMIC
ACID PROPANOL
% c=[0  0.3 0.3 0.3;    0.3 0   0.1 0.205966;   0.3 0.1 0   0.2;    0.3
0.205966    0.2 0];%FORMIC ACID PROPANOL

% a=[0  0   2.06361 -2.0405;    0   0   0   4.5156; -1.5224 0   0 -2.6609;
13.1102 -2.5864 -10.1517    0];% FORMIC ACID BUTANOL
% b=[0  678.6229    11.769  763.869;    -208.1044   0   259.229868  -
1432.0835; 85.2739 161.594384  0   1556.15;    -3338.95    725.0173    5148.1
0];%FORMIC ACID BUTANOL
% c=[0  0.3 0.1 0.3;    0.3 0   0.3 0.3;    0.1 0.3 0   0.298851;   0.3 0.3
0.298851    0];%FORMIC ACID BUTANOL

% a=[0  0   -5.53363    -1.4468;    0   0   -17.5005    4.5156; 2.70778 4.8802
0   3.54945;    5.9173  -2.5864 11.0192 0];%FORMIC ACID OCTANOL
% b=[0  591.138 2672.58 741.918;    -263.94 0   10000   -1432.08;   -1118.99
-3314.14    0   22.2649;    798.377 725.017 -708.161    0];%FORMIC ACID
OCTANOL
% c=[0  0.3 0.3 0.26;   0.3 0   0.1 0.3;    0.3 0.1 0   0.338669;   0.26
0.3 0.338669    0];%FORMIC ACID OCTANOL

tau = a+b/T;
G  = exp(-c .* tau);


  for i=1:nc
    st(i)=sum( x(:) .* tau(:,i) .* G(:,i)); % x vecteur colonne des 4
concentrations
    s(i) =sum( x(:) .* G(:,i));
  end

S = st ./ s;

for i=1:nc
  g (i,:)=x(:)' .* G(i,:)./s;
end
```

```
for i=1:nc
  lng(i)=S(i)+sum(g(i,:).*(tau(i,:)-S));

end

gam=exp(lng);


end


function [err, ExpData]=ObjFun(k, ExpData, GraphFlag)

global tspan  t  C   activite Nexp  w_cata ntot T

%cette fonction est la fonction objective à minimiser

err=[];
 stockage=[];
 toto=[];
  for i=1:Nexp
       n=ExpData(i).Conc;
        tspan=ExpData(i).t;
        tdata=ExpData(i).t;
        w_cata= ExpData(i).w_cata;
        T=ExpData(i).T+273;
       ntot = sum(n(1,:));
       C=n/ntot;
       [m,o]=size(C);
        gamma_exp=[];

        for j=1:m
            z = C(j,:);
            [gam]=NRTL(z,T);
            gamma_exp=[gamma_exp;gam];
        end


    x0=C(1,:); %activité initiale pour résolution bilan matière


    EvalFunHandle=@(t,x) EvalFun(t,x,k) ;
   [t x] = ode45(EvalFunHandle, tspan, x0);


   if GraphFlag == 1

   tspan=[0 240];
   EvalFunHandle=@(t,x) EvalFun(t,x,k) ;
   [t x] = ode45(EvalFunHandle, tspan, x0);
     stockage=[stockage;x];
     toto=[toto;t];
%
     figure
```

```
    hold on
    plot(t,x(:,1))
    plot(tdata,C(:,1),'o')
    plot(t,x(:,2))
    plot(tdata,C(:,2),'o')
    plot(t,x(:,3))
    plot(tdata,C(:,3),'o')
    hold off

%       figure
%      hold on
%     z=[0 1];
%     z1=[0 1+1*0.15];
%     z2=[0 1-1*0.15];
%     plot(z,z)
%     plot(z,z1,'--')
%      plot(z,z2,'--')
%     plot(x,C,'*')
%      xlabel('x modèle')
%         ylabel('x expérimentale')
%         xlim([0 1])
%         ylim([0 1])
%       hold off
%       save('resultat1.dat','stockage');
%       filename='resultat1.xlsx';
%       xlswrite(filename,stockage);
     else
   err=[err; abs(C-x)];
   end
  end
end


function [F]=EvalFun(t,x,k)


global w_cata ntot a keq T
% ordre des constituants 1. butanol / 2. acide glycolique / 3. ester / 4.
%water


 %calcul gamma

 [gam]=NRTL(x',T);
    gamma_mod=[gam];
    activite=gamma_mod.*x';


% la loi de vitesse est à modifier selon le modèle utilisé
% il faut intégrer une loi de vitesse qui prend en compte la loi
% d'Arrhénius + la constante d'équilibre déjà déterminer.
% modèle de type LH ?

% keq=exp((-3696.2/T)+12.968); %GLYCOLIC ACID PROPANOL
```

```
% keq=exp((-2858.5/T)+9.4143); %GLYCOLIC ACID BUTANOL

keq=exp((-1968.4/T)+7.5192); %GLYCOLIC ACID OCTANOL

% keq=exp((-3650.3/T)+14.098); %FORMIC ACID PROPANOL

% keq=exp((-473.85/T)+3.7694); %FORMIC ACID BUTANOL

% keq=exp((-1630.9/T)+7.8223); %FORMIC ACID OCTANOL


ln_K= k(1)-k(2)/(8.314*T);
K=exp(ln_K);

%K=(k(1)*exp(-k(2)/(8.314*T)));

r=K*(activite(1)*activite(2)-(activite(3)*activite(4))/keq) ; %modèle pseudo-
homogène

% r=K*(activite(1)*activite(2)-activite(3)*activite(4)); %modèle pseudo-
homogène

% r=(K*(activite(1)*activite(2)-
(activite(3)*activite(4))/keq))/(1+k(3)*activite(1)+k(4)*activite(2)+k(5)*acti
vite(3)+k(6)*activite(4))^2; %modèle LHH
% r=(K*(activite(1)*activite(2)-
(activite(3)*activite(4))/keq))/(1+k(3)*activite(1)+k(4)*activite(4))^2;
%modèle LHH MODIFIE
% r=(K*(activite(1)*activite(2)-
(activite(3)*activite(4))/keq))/(1+k(3)*activite(1))^2; %modèle LHH MODIFIE
% r=(K*(activite(1)*activite(2)-
(activite(3)*activite(4))/keq))/(1+k(3)*activite(1)+k(4)*activite(2)+k(5)*acti
vite(3)+k(6)*activite(4)); %modèle ER
% r=(K*(activite(1)*activite(2)-
(activite(3)*activite(4))/keq))/(1+k(3)*activite(1)); %modèle  ER MODIFIE

% a=cat(2,a,activite);

% bilan matière sur les 4 espèces / la loi de vitesse est donnée ici en
% mol/s/g de cata
F(1)=-r*w_cata;
F(2)=-r*w_cata;
F(3)=r*w_cata;
F(4)=r*w_cata;


F = F(:);

end


function [R,sigma] = corrcov1(C,nocheck)
%CORRCOV Compute correlation matrix from covariance matrix.
%   R = CORRCOV(C) computes the correlation matrix R that corresponds to the
```

```
%   covariance matrix C, by standardizing each row and column of C using the
%   square roots of the variances (diagonal elements) of C.  C is square,
%   symmetric, and positive semi-definite.  The correlation for a constant
%   variable (zero diagonal element of C) is undefined.
%
%   [R,SIGMA] = CORRCOV(C) computes the vector of standard deviations SIGMA
%   from the diagonal elements of C.
%
%   See also COV, CORR, CORRCOEF, CHOLCOV.

%   R = CORRCOV(C,1) computes the correlation matrix R without checking that C
%   is a valid covariance matrix.

%   Copyright 2007 The MathWorks, Inc.


% Check square, symmetric, positive semidefinite.
% if nargin < 2
%     [T,p] = cholcov(C);
%     if p ~= 0
%         error(message('stats:corrcov:BadC'));
%     end
% end

[m,n] = size(C);
sigma = sqrt(diag(C)); % sqrt first to avoid under/overflow
R = bsxfun(@rdivide,C,sigma); R = bsxfun(@rdivide,R,sigma'); % R = C ./
sigma*sigma';

% Fix up possible round-off problems, while preserving NaN: put exact 1 on the
% diagonal, and limit off-diag to [-1,1]
t = find(abs(R) > 1); R(t) = R(t)./abs(R(t));
R(1:m+1:end) = sign(diag(R));
```